AD NUMBER

AD390357

LIMITATION CHANGES

TO:

Approved for public release; distribution is unlimited.

FROM:

**Distribution authorized to U.S. Gov't. agencies and their contractors;
Administrative/Operational Use; MAY 1968. Other requests shall be referred to Air Force Rocket Propulsion Lab., Edwards AFB, CA.**

AUTHORITY

AFRPL ltr 5 Feb 1986

AD NUMBER
AD390357
CLASSIFICATION CHANGES
TO: **UNCLASSIFIED**
FROM: **CONFIDENTIAL**
AUTHORITY
AFRPL ltr 5 Feb 1986

AD 390 352

AUTHORITY: AFRPL
ltr, 5 Feb 86

SECURITY MARKING

The classified or limited status of this report applies to each page, unless otherwise marked.
Separate page printouts MUST be marked accordingly.

THIS DOCUMENT CONTAINS INFORMATION AFFECTING THE NATIONAL DEFENSE OF THE UNITED STATES WITHIN THE MEANING OF THE ESPIONAGE LAWS, TITLE 18, U.S.C., SECTIONS 793 AND 794. THE TRANSMISSION OR THE REVELATION OF ITS CONTENTS IN ANY MANNER TO AN UNAUTHORIZED PERSON IS PROHIBITED BY LAW.

NOTICE: When government or other drawings, specifications or other data are used for any purpose other than in connection with a definitely related government procurement operation, the U.S. Government thereby incurs no responsibility, nor any obligation whatsoever; and the fact that the Government may have formulated, furnished, or in any way supplied the said drawings, specifications, or other data is not to be regarded by implication or otherwise as in any manner licensing the holder or any other person or corporation, or conveying any rights or permission to manufacture, use or sell any patented invention that may in any way be related thereto.

DISCLAIMER NOTICE

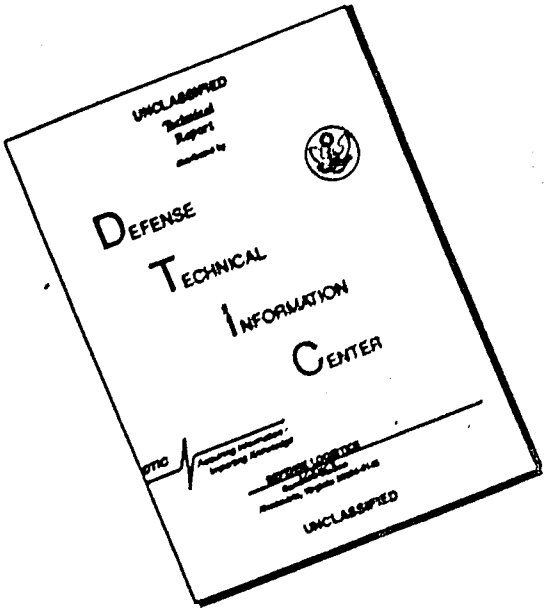

THIS DOCUMENT IS BEST QUALITY AVAILABLE. THE COPY FURNISHED TO DTIC CONTAINED A SIGNIFICANT NUMBER OF PAGES WHICH DO NOT REPRODUCE LEGIBLY.

AFRPL-TR-68-70

MAY 1968

(TITLE UNCLASSIFIED)

ADVANCED ROCKET ENGINE--STORABLE

Phase I Final Report, Supplement 1

Report 10830-F-1, Phase I, Supplement 1

R. Beichel, J. A. Gibb, R. A. Hankins, et al.

Prepared by

AEROJET-GENERAL CORPORATION
Advanced Storable Engine Program Division
Liquid Rocket Operations
Sacramento, California

In addition to security requirements which must be met, this document is subject to special export controls and each transmittal to foreign governments or foreign nationals may be made only with prior approval of AFRPL (RPPR/STINFO), Edwards, California 93523.

Prepared for

AIR FORCE ROCKET PROPULSION LABORATORY
Air Force Systems Command
United States Air Force
Edwards, California

0947

LEGAL NOTICE

"When U.S. Government drawings, specifications, or other data are used for any purpose other than a definitely related Government procurement operation, the Government thereby incurs no responsibility nor any obligation whatsoever, and the fact that the Government may have formulated, furnished, or in any way supplied the said drawings, specifications, or other data, is not to be regarded by implication or otherwise, or in any manner licensing the holder or any other person or corporation, or conveying any rights or permission to manufacture, use, or sell any patented invention that may in any way be related thereto."

(This page is Unclassified)

AFRPL-TR-68-70

MAY 1968

(TITLE UNCLASSIFIED)
ADVANCED ROCKET ENGINE--STORABLE

Phase I Final Report, Supplement 1

Report 10830-F-1, Phase I, Supplement 1

R. Beichel, J. A. Gibb, R. A. Hankins, et al.

Prepared by

AEROJET-GENERAL CORPORATION
Advanced Storable Engine Program Division
Liquid Rocket Operations
Sacramento, California

Prepared for

AIR FORCE ROCKET PROPULSION LABORATORY
Air Force Systems Command
United States Air Force
Edwards, California

19414T

FOREWORD

(U) This report delineates the technical accomplishments of the ARES Advanced Development Program, Phase I, of Project 682A, Contract AF 04(611)-10830. The period of performance was from 1 July 1965 through 31 January 1968. The work during this period was directed primarily toward demonstrating the practicality of advanced components and subsystems considered critical to the integrated engine module design. Analysis, design, fabrication, and test activities are summarized. All program accomplishments prior to 27 January 1967 were reported in an interim final report.(1) Also, related classified work was performed under Contract F04611-68-C-0008.(2)

(U) All work was performed by Liquid Rocket Operations of Aerojet-General Corporation for the Air Force Rocket Propulsion Laboratory at Edwards, California. Mr. R. Beichel is the Aerojet Program Manager, and Mr. C. D. Penn is the Air Force Program Manager.

(U) This technical report has been reviewed and is approved.

C. D. Penn
Program Manager
Liquid Rocket Division
Air Force Rocket Propulsion Laboratory
Edwards, California 93523

(1) Advanced Rocket Engine-Storable, Phase I Interim Final Report, AFRPL-TR-67-75, August 1967
(2) Throttling and Scaling Study for Advanced Storable Engines, Report AFRPL-TR-68-2, January 1968

Report 10830-F-1, Phase I, Supplement 1

UNCLASSIFIED ABSTRACT

(U) This report summarizes the Phase I work of ARES Program, Contract AF 04(611)-10830. The period of performance was from 1 July 1965 through 31 January 1968.

(U) The objective of this program was to demonstrate the engineering practicality and performance characteristics of a high chamber pressure, staged combustion engine. The program was to be conducted in two phases. Phase I was to demonstrate critical engine features by component testing. Demonstration of the assembled engine system was to be accomplished in Phase II.

(U) Phase I is now completed and all critical engine features have been demonstrated. This engine concept is ready to proceed into the Phase II program. Specific accomplishments of the Phase I program are as follows:

(1) Master layouts for two engine designs were established. One uses a turbopump with the shaft axis oriented perpendicular to the thrust axis, while the other uses a turbopump with the shaft axis oriented in line with the thrust axis.

(2) A master layout was established for a propulsion system utilizing 20 engine modules in a cluster, with all modules exhausting into a single large forced-deflection nozzle.

(3) Detail designs for all the engine components tested in this program were prepared.

(4) The primary injector and combustion chamber for production of the turbine drive gas were demonstrated.

(5) Performance and durability of the cooled thrust chamber and secondary injector combination were demonstrated.

UNCLASSIFIED ABSTRACT (cont.)

(6) The feasibility of lubricating turbopump bearings with the storable propellants used in the engine was demonstrated.

(7) Pump wear ring designs that permit high pump efficiency operation without need for high tolerances and with no risk of explosion hazard from pump rub were demonstrated.

(8) The weight and practicality of two types of multipurpose housings for the turbopump and primary combustion chamber assembly were demonstrated.

(9) Propellant flow control components and shutoff valves for the engine were demonstrated.

(10) A layout design of the engine evolved from the testing effort was prepared.

(11) Several supporting studies were completed that provide additional design criteria in such areas as nozzle aerodynamics, low-frequency stability, fluid flow characteristics of propellant and turbine drive-gas passages, and design changes required for conversion to advanced storable propellants.

Report 10830-F-1, Phase I, Supplement 1

TABLE OF CONTENTS

APPENDIX

TABLE LIST

FIGURE LIST

FIGURE LIST (cont.)

FIGURE LIST (cont.)

FIGURE LIST (cont.)

FIGURE LIST (cont.)

FIGURE LIST (cont.)

SECTION I

INTRODUCTION

(U) The objective of the ARES Program was to demonstrate in a two-phase effort the engineering practicality and performance characteristics of a high chamber pressure, staged combustion engine. The program was to be accomplished in two phases. Phase I was to demonstrate critical engine features and the demonstration of the assembled engine system was to be accomplished in Phase II. All critical component testing was accomplished using full-scale hardware operating at engine design conditions. The engine components tested were the cooled thrust chamber, integrated turbopump housing, propellant-lubricated bearings, pump wear rings, annular primary combustor, hydrostatic combustion seal, and controls. In addition, the Phase I effort included analysis, design, and test activity on several other aspects of the overall engine and of its unique components.

(U) All components tested, with the exception of the hydrostatic combustion seal, were successfully demonstrated. The hydrostatic combustion seal is not used in the finally selected engine configuration. Therefore this engine concept is ready to proceed into Phase II. The Phase I program, with the exception of the cooled thrust chamber demonstrations, hydrostatic combustion seal demonstrations, and final engine design was completed prior to 27 January 1967. At that time the program was extended for one year in order to solve a basic incompatibility problem between the injector and cooled thrust chamber and then to conduct the required cooled thrust chamber demonstration tests. Combustion seal demonstrations and final engine design were also to be completed. All program accomplishments prior to 27 January 1967 were reported in the Interim Final Report (Reference 1). This report contains the detailed results of effort accomplished in the Phase I extension program and a summary of the entire Phase I program.

(1) ARES, Phase I Interim Final Report, AFRPL-TR-67-75, August 1967.

SECTION II

SUMMARY AND CONCLUSIONS

A. ENGINE AND PROPULSION SYSTEM DESIGN

(C) ARES is a 100,000-lb-thrust rocket engine that uses N_2O_4/AeroZINE 50 propellants and embodies advanced features resulting in higher performance and lower weight when compared to conventional rocket engines. High performance results from use of the staged combustion cycle and high thrust chamber pressure (2800 psia). In this staged combustion cycle, nearly all of the oxidizer and 18% of the fuel are burned in the primary combustor to produce a 1200°F gas to drive the turbine. This gas then exhausts into the thrust chamber where it is combined with the remaining fuel. Use of this cycle permits high chamber pressure operation without any turbine drive losses which are characteristic in conventional engines using the gas generator cycle. The high chamber pressure permits use of a higher area ratio nozzle which further increases performance. The staged combustion cycle is best exploited in an engine which is highly integrated so that the turbine can exhaust directly into the thrust chamber. This also results in a significant weight savings. By using high strength materials such as Inconel 718, further weight savings result.

(U) The latest configuration of the ARES engine, incorporating the experience gained in the 10830 Phase I contract, is shown in Figure II-1 and is described in Section III of this report. The evolution of this engine through the Phase I program period is summarized below.

(U) At the initiation of the Phase I program, the engine was conceived in two basic configurations: T and Inline (see Figures II-2 and II-3). In both of these configurations, the turbopump is mounted on top of the engine. The rotating part is a single shaft on which a single-stage turbine, the oxidizer pump and the fuel pump are mounted. Shaft bearings are propellant lubricated.

II, A, Engine and Propulsion System Design (cont.)

Oxidizer is ducted through internal passages in the housing thus ensuring a cool running engine. The primary combustor and injector are integrated into the turbopump housing. The T engine uses a high pressure interpropellant combustion seal to isolate the fuel pump end. The Inline engine uses a low pressure vented cavity seal between pumps. The shaft rotating speed is 40,000 rpm for the T engine and 30,000 rpm for the Inline engine. The T engine was the prime candidate because of its more integrated design. The Inline configuration, incorporating a turbopump of more conservative design, was carried as a backup. Turbopump component testing was conducted on housings, bearings and pump wear rings that are applicable to both designs. The combustion seal is only used in the T engine. The primary combustor was sized for the T engine but need be only one inch greater in diameter for use in the Inline engine. Secondary injector, thrust chamber, controls, boost pumps and suction valves are interchangeable between engines.

(U) The final selection between these two engine configurations was made during the Phase I extension program period (27 January 1967 through 31 January 1968). The Inline configuration was selected because the turbopump housing for this configuration is significantly less expensive and its development posed less risk than the T-engine, particularly in view of the difficulties encountered with the combustion seal.

(U) Two thrust chamber cooling methods were evaluated in this program: regenerative and transpiration. At program initiation, regenerative cooling was the primary candidate because of the extensive background on this type of cooling. The transpiration-cooled chamber proved to be the most practical design during the Phase I program testing and was selected for use in the ARES engine.

(U) The final ARES engine configuration, shown in Figure II-1, uses the Inline turbopump and the transpiration-cooled chamber and is described in Section III.

II, Summary and Conclusions (cont.)

B. TURBOPUMP ASSEMBLY

1. General

(C) The ARES turbopump consists of a two-stage fuel pump, a single oxidizer pump, a single-stage turbine, and associated power transmission assemblies mounted in a housing. Propellant is ducted through the housing insofar as possible to minimize external plumbing and provide cooling for the housing. Thrust takeout is provided by a pad located on top of the housing ar the thrust chamber is mounted on the bottom of the housing. The primary combustor and injector are contained within the housing. Oxidizer pump discharge pressure is approximately 5800 psia. First-stage fuel pump discharge pressure is approximately 5500 psia, and second-stage fuel pump discharge pressure is approximately 6200 psia. Two turbopump configurations, T and Inline, were designed in this program. These are described below.

(C) The T turbopump (Figure II-4) consists of a two-stage fuel pump and a single-stage oxidizer pump at opposite ends of a common shaft, driven by a single-stage turbine located between pumps. The turbine is driven by oxidizer-rich gas provided by an annular primary combustor located between the oxidizer pump and the turbine. The bearings are lubricated by the propellants. Separation of fuel and oxidizer along the shaft is attained by a unique hydrostatic combustion seal which deliberately leaks a metered amount of fuel into the turbine exhaust. The entire package of rotating machinery and primary combustion chamber is enclosed in a high-pressure housing, which also acts as a thrust takeout member and as the propellant distribution medium from the pumps.

(U) The Inline turbopump (Figure II-5) has its shaft oriented along the thrust axis. The turbine is mounted on the lower end of the shaft

II, B, Turbopump Assembly (cont.)

and exhausts into the thrust chamber. The oxidizer pump is mounted in the center of the shaft, and the fuel pump is mounted on the upper end of the shaft. The turbine is driven by oxidizer-rich gas provided by an annular primary combustor located at the lower end of the housing. Bearings are propellant lubricated. Separation of the fuel and oxidizer along the shaft is attained by a low-pressure vented cavity seal located between the suction side of the two pumps. This seal is similar in concept to that used in the Titan I second-stage engine auxiliary turbopump assembly. No purge was used in that design, which is flight demonstrated. Propellants were LOX/RP-1. This type of seal has not been demonstrated with hypergolic propellants. Therefore, provision for a purge is provided if a purge is needed. The entire package is mounted in a high-pressure housing which also acts as the thrust takeout structure. Oxidizer distributed in the oxidizer pump housing provides cooling around the parts containing hot gas.

(U) A detailed design was prepared for the T turbopump. A layout design was prepared for the Inline turbopump with details of tested components. Critical component demonstration testing was accomplished on components for both turbopumps. This testing had the following objectives:

a. Demonstrate the feasibility of lubricating rolling contact bearings at 40,000 rpm (DN of 1.6 million) in both of the propellants.

b. Demonstrate the structural integrity of the turbopump housings under various imposed structural and vibrational loads.

c. Demonstrate successful operation of the hydrostatic combustion seal in simulated engine operating conditions.

d. Develop pump wear rings that will provide adequate pump efficiency by operating at very close clearances, but with minimum explosion hazard from pump rubbing.

II, B, Turbopump Assembly (cont.)

e. Design and test a purge seal to be utilized if the hydrostatic combustion seal is found to be not feasible.

2. Turbopump Housing Development

(C) Integrated turbopump and primary combustor housings were designed and tested for both the advanced T and the backup Inline turbopumps. The contract requires that the housings not weigh more than 350 lb, that they have a permanent axial deflection less than 0.020 in., and that the radial misalignment be less than 0.008 in. at 1.4 times nominal design pressure and thrust, applied simultaneously. Also, the housing cannot have a critical vibration mode in any axis of 667 $\pm$ 10% cps, either without internal pressure or when pressurized to 1.2 times design pressure under an excitation force of 1-g input. It is also important that the housing have a low-pressure drop across the propellant distribution passages, that it adequately cool itself with the propellant flow, and that it permit easy insertion and removal of the turbopump and primary combustor components.

(U) Analytical stress methods are not adequate to treat the three-wall structure used for the T configuration advanced turbopump. Consequently, single-wall, double-wall, and photoelastic models were built and tested to obtain necessary design data for the full-scale three-wall structure. This work indicated the actual stresses that would be encountered--generally lower than predicted by stress analytical models--and suggested design changes to optimize the configuration.

(C) One of the two full-scale models were electron-beam welded and one was plug welded. Manufacturing difficulties were experienced with both housings but refined welding and heat-treat methods solved these problems. Pressure testing was accomplished (1) with internal pressures simulating actual engine operating conditions, (2) with 50% design thrust load and no internal

II, B, Turbopump Assembly (cont.)

pressure, and (3) with combined thrust loads and internal pressures, both at 1.4 times nominal design values (140,000 lb of thrust and 8400-psi internal pressure). The T-housing tested together with test conditions is shown in Figure II-6. The housing weighed 300 lb as compared to a target weight of 350 lb. The weights of the primary injector and rotating components are not included.

(U) These tests and the subsequent vibration tests demonstrated the ability of the design to meet contractual requirements, and also indicated several desirable improvements that should be incorporated into the housing design if it were to be carried on into Phase II of the program. This housing would make greater use of castings and would have modified propellant passage design to improve cooling.

(U) The Inline housing test program was simpler because it is of more conventional design. Pressure testing accomplished under similar conditions to those in the T housing proved the structural integrity of the Inline housing. The Inline housing tested together with test conditions is shown in Figure II-7. This housing weighed 230 lb as compared to 300 lb for the T-engine turbopump housing.

3. Propellant-Lubricated Bearings

(C) The program objective was to demonstrate the feasibility of eliminating conventional lubrication systems for the turbopump bearings by use of propellant lubrication. The program requirements were to test both the ball and roller bearings for at least 12 min of operation with N_2O_4 and with AeroZINE 50 at rotating speeds of 40,000 rpm (DN of 1,600,000). During the 40,000-rpm tests, the tandem ball bearings were to be subjected to an axial load of 2,500 lb for 8 sec, and to 1500 lb for the remainder of the run. Roller bearings were to be subjected to 1000-lb radial load for 8 sec and to 500 lb for the remainder of the run.

II, B, Turbopump Assembly (cont.)

(C) The fuel (AeroZINE 50) generally proved to be a more severe environment for the bearings, cages, and races than was the oxidizer (N_2O_4). All rollers, for example, experienced definite end wear in AeroZINE 50, but only burnishing in N_2O_4; however, the amount of wear in AeroZINE 50 was not excessive for TPA life requirements. Ball bearings with tungsten-titanium carbide balls (designated K5H by Kennametal, Latrobe, Pa.) in 440C races proved to be the best design for AeroZINE 50 operation. Use of 440C for both the rollers and for the races was satisfactory for the radial bearings. A 25% glass-filled Teflon shrouded with stainless steel provided the best cages. The bearings as they appeared after demonstration testing together with demonstrated performance are shown in Figure II-8.

(U) The ball bearings were also successfully tested at 31,250 rpm with higher loads consistent with the Inline TPA operating conditions; 8 sec and 2200 lb for the remainder of the 12-min run.

4. Pump Wear Rings

(U) A wear-ring development program was conducted to evaluate the ARES wear-ring design. The objectives were to show that the design was satisfactory to limit internal leakage in the pump to a value consistent with the turbopump efficiency and thrust-balance requirements, and to do this safely and reliably in spite of intermittent rubbing in both N_2O_4 and AeroZINE 50. Secondary objectives were to establish insert materials for other close-running components, such as shaft labyrinths, inducers, and boost pumps.

II, B, Turbopump Assembly (cont.)

(U) One approach allowed intermittent rubbing of the impeller wear ring on compatible inserts; straight labyrinth seals were designed and tested with various combinations of insert materials and pressure retention mechanisms.

(U) The second approach allowed low-speed transient rubbing but prevented high-speed contact by maintaining a fluid film between the impeller rubbing surfaces and the seal itself. On the basis of this concept, hydrostatic face and journal seals were designed and tested.

(U) For oxidizer pump application, both the hydrostatic face seal and the straight labyrinth with Vespel SP-21 inserts limited flow through the wear ring to very low values at the required 4000-psi pressure differential. Both withstood intentional attempts at rubbing at 40,000 rpm without causing fire or explosion and were in reusable condition.

(U) The fuel pump is designed integrally with the thrust balancer in a manner that requires a straight labyrinth seal at the outside diameter of the fuel pump impeller. The optimum design of this labyringh seal requires operation at a clearance of 0.007 in. Two inert inserts of Kynar and Kel-F were satisfactorily designed and tested under simulated conditions. This included repeatable flow rate before and after rubbing at high speed and pressure differentials of 2250 psi. Kynar was selected for the fuel pump application on the basis of its slightly better properties after exposures to AeroZINE 50 in laboratory tests.

(U) On the basis of this program and analysis of the turbopump requirements, hydrostatic face seals were selected for the oxidizer-pump wear ring and straight labyrinths with pressure-relieved Kynar inserts were selected for the fuel pump wear ring. These designs are shown for the T turbopump in Figure II-9 and 10. Similar designs are used in the Inline engine.

II, B, Turbopump Assembly (cont.)

5. Hydrostatic Combustion Seal

(U) The T-engine requires a rotating shaft seal between the fuel pump and the oxidizer-rich turbine exhaust gas. A hydrostatic seal was adopted because the operating speed of 40,000 rpm imposes an excessive surface velocity of 600 ft/sec on rubbing contact seals. The seal maintains separation of the nonrotating seal face from the running ring with a fluid film of fuel, leaking from the pump and exhausting into the oxidizer-rich turbine exhaust. The seal and its adjacent parts are cooled by streams of oxidizer flowing through holes on each side of the seal.

(U) The Phase I program required a 60-sec demonstration of the seal under simulated engine operating conditions.

(U) Several tests were conducted in a two-dimensional tester to determine surface temperatures, feasible operating clearances, and optimum design configurations. The data from this program were then incorporated into full-scale seals which were initially tested without combustion in the separate propellants, both with and without shaft rotation. After solving some initial sequence problems, the seal operated successfully at design rpm with operating clearances of 0.001 in. and less. The seal demonstrated its ability to tolerate axial wobble several times larger than the nominal operating clearance.

(U) Seventeen hot rotating tests with propellants were then conducted for a total testing time with combustion of over 120 sec. The same seal was used for four of these tests, establishing that the seal is capable of restarts. The program was terminated prior to completion because of technical difficulties. This was one of the motivating factors in the selection of the Inline turbopump, which does not use this type of seal. The status of development at program termination is summarized as follows:

II, B, Turbopump Assembly (cont.)

Valid tests	15
Total testing duration	125 sec
Maximum duration	30 sec
Maximum duration refirable	10 sec
Number of tests, refirable seal	7
Maximum number of restarts	3

6. Purge Seal

(U) A purge seal design was developed as an alternative approach in case the hydrostatic combustion seal proved difficult to develop. The purge seal operates on the hydrostatic principle to avoid high rubbing contact velocities, but it uses an inert purge fluid instead of controlled fuel leakage as in the primary design.

(U) Initial cold rotating tests attained 40,000 rpm at less than design purge fluid flow, causing slight rubbing contact. Hot testing was then initiated with increased purge-fluid flow. Although as high as 55 sec of testing at 40,000 rpm was attained, problem-free operation was not achieved. This program was also discontinued with the selection of the Inline TPA.

C. THRUST CHAMBER ASSEMBLY

1. General

(U) The ARES thrust chamber assembly consists of two engine subsystems: the primary combustor assembly and the secondary combustor assembly. The primary combustor assembly produces the oxidizer-rich turbine drive gas and consists of an injector and combustion chamber. The secondary combustor assembly consists of a gas-liquid secondary injector, which unites

II, C, Thrust Chamber Assembly (cont.)

the turbine drive gas with the balance of the fuel, and a cooled secondary combustion chamber. When ARES engines are used in clusters in forced deflection or plug nozzles to provide a high-thrust engine, the expansion nozzle of the secondary combustion chamber is sometimes designed as a two-dimensional configuration to provide better nozzle performance. Evaluation of an uncooled two-dimensional nozzle to determine nozzle heat-transfer conditions was included as part of the Phase I program.

2. Primary Combustor Assembly

(U) The objective of the primary combustor program was to evaluate primary combustor injectors, to define performance characteristics and to obtain temperature profiles along the chamber wall and across the gas stream. Injector testing was to be conducted at off-design conditions to define the minimum injector pressure drop, the sensitivity to off-design mixture ratio operation, and finally to define inherent stability of the combustor by shocking it with a pulse gun. The goal of the program was to develop one injector configuration to the point where it could be used in conjunction with the turbopump housing for early Phase II testing.

(U) The success criterion for the primary combustor effort was that the temperature of the primary combustor exhaust gas, as measured by three thermocouples at the entrance to the turbine nozzle ring, could not exceed 1650°F, with the variation between each thermocouple not exceeding 400°F. Also, chamber pressure oscillations must not exceed ±5% of the average chamber pressure value and must not be divergent with time when measured during the steady-state portion of the test firings. Compliance with these conditions was to be demonstrated in three tests, each having a minimum duration of 1-sec steady state. The primary combustor must be in a refirable condition following the demonstration series.

II, C, Thrust Chamber Assembly (cont.)

(U) Three injector concepts, designated the pentad, quadlet, and full-flow configurations, were test evaluated during the program. These injectors were evaluated in a heavyweight workhorse housing which was designed to have the same interface dimensions and gas-passage configurations as the flight-weight modular TPA housing. This housing included extensive instrumentation to facilitate the evaluation of injector performance and operating characteristics.

(U) The test program consisted of 31 hot-fire tests. Development problems encountered during the test program included low-frequency feed system coupled instability, and minor erosion of the injectors and combustion chamber. Incorporation of five axial vanes to inhibit the instability together with two turbulators to provide mechanical mixing of the propellants solved both problems. The pentad injector proved to be the best injector.

(C) The primary combustor configuration developed during the test program met or exceeded all requirements. The average temperature obtained on the three required successful tests was 1340°F; the average chamber pressure was 4650 psia; the chamber pressure oscillations at steady state averaged 1.27%. The average mixture ratio during these tests was 11.63. The final injector and combustor chamber configurations which ultimately satisfied all contract work statement requirements are shown in Figures II-11 and 12. Demonstration tests are also summarized in Figure II-11.

3. Secondary Combustor Assembly

(C) The objective of the secondary combustor assembly program was to demonstrate the performance and durability of the cooled thrust chamber for the ARES engine. To accomplish this objective three tests, each of 20-sec duration, were to be conducted wherein a delivered sea-level specific

II, C, Thrust Chamber Assembly (cont.)

impulse of 280 sec (90% I_s) or higher had to be demonstrated at full-scale design conditions of 100,000-lb thrust and 2800 psia chamber pressure. The hardware also had to be refirable after each test.

(U) The program schedule (Figure VI-1) shows the major items of work in the accomplishment of the program. The first nine months were devoted to hardware design and fabrication. During this period, testing of residual hardware from a previous contract (Integrated Components Program, Contract AF 04(611)-8548) was also accomplished to obtain design data. The following eight months were devoted to test evaluation of ARES injectors and cooled chamber testing. At the conclusion of this test period, an incompatibility between the injector and cooled thrust chamber prevented the accomplishment of the program objectives. An injector redesign was required to solve this problem; as a result, the program was extended one year to allow development of a new injector. During the next eight months, redesign and test evaluation of several new injector concepts occurred which culminated in the selection of a new injector for resumption of cooled testing. The final four months of the program were devoted to cooled thrust chamber testing with the new injector; this effort resulted in the successful demonstration of secondary combustor performance and durability.

(C) As a result of the initial design effort, together with the results from residual hardware testing from the ICP program, two injector concepts were fabricated for test evaluation; these were designated the Fuel Swirl Rake and the Mark 125. These injectors are shown in Figures II-13 and 14, respectively. The Fuel Swirl Rake injector has 108 fuel elements, oriented as shown, through which fuel is injected in a swirling cone pattern. Oxidizer gas passes through from the backside of the injector and surrounds the fuel elements. The Mark 125 injector consists of 32 radial vanes which

II; C, Thrust Chamber Assembly (cont.)

introduce fuel through 20 tubes in each vane. These tubes are bent to evenly distribute the fuel over the face of the injeccor. Oxidizer is introduced from the back side of the injector and surrounds the fuel elements.

(U) Results of uncooled testing with these injectors showed that both were of relatively high performance, stable, and erosion-free. The performance of the Mark 125 was slightly higher than that of the fuel swirl rake, and on this basis, was selected for cooled chamber testing.

(U) Two cooled chamber concepts were test-evaluated: regenerative and transpiration. The regenerative chamber is shown in Figure II-15. This chamber is a double-pass design and consists of 96 tubes fabricated from Inconel 718 material. The tube bundle is reinforced by a fiberglass wrap. The regenerative coolant (N_2O_4) enters and leaves the chamber through the top flange. Five tests were conducted using this chamber. Results of this testing proved the mechanical integrity of the design; however, high performance was not achieved. Meanwhile, testing of the transpiration cooled chamber was proceeding with excellent results. Therefore, further testing of this regenerative cooled chamber was suspended.

(U) The transpiration cooled chamber is shown schematically in Figure VI-55. This thrust chamber uses the new TRANSPIRE concept in which thin photo-etched washers are used to meter precise amounts of flow uniformly to the chamber inner surface. The chamber is divided into 12 compartments, each of which has a separate coolant feed line. The details of the washer design are shown in Figure VI-58. The chamber consists of approximately 1300 washer pairs. Internal manifolding and flow distribution are accomplished by the pattern photoetched into a thick washer (0.020 in. thick in the chamber and 0.010 in. thick in the throat region). Flow rate control in each washer pair is provided by the pattern photoetched through a washer 0.001 in. thick.

II, C, Thrust Chamber Assembly (cont.)

(C) Testing with this chamber yielded very encouraging results. Thirty tests were conducted with two transpiration cooled chambers using the Mark 125 injector. During this testing, coolant flow rate was reduced selectively in the various compartments to increase performance. However, when flow rate was reduced below approximately 36 lb/sec, injector streaking caused chamber erosion. Maximum steady-state performance achieved was approximately 267 sec, which is approximately 86% of theoretical specific impulse, substantially below the required 280 sec. Analysis of test results revealed that the injector streaking was caused by two major effects. The fuel pattern at the wall was too coarse and unburned fuel existed too far down the chamber. Some of this fuel combining with the oxidizer coolant resulted in streaks that were observed as discoloration of the chamber wall after several tests. The other problem was that the bent injector tubes near the wall were spraying fuel on the wall. It was concluded that achievable performance with the Mark 125 injector in a cooled chamber would be inherently limited to the values achieved and that a new injector design was needed.

(C) Results of the transpiration cooled chamber testing were used in conjunction with latest analytical techniques to evolve new injector concepts. These concepts were evaluated analytically, by hydrotest of individual elements, and air testing of the gas circuit. The best concepts were then fabricated into full-scale hardware and hot tested. Thrust chambers specifically designed to evaluate compatibility were used in this testing, including film-cooled ablative chambers and transpiration cooled chambers with ablative throats. From this effort, the platelet injector was evolved. This injector consists of 88 platelet vanes as shown in Figure VI-6. Fuel is injected through the orifices at the trailing edge of each platelet while oxidizer gas enters from the back of the injector between platelets. Each platelet consists of two plates. The fuel distribution manifolding and

II, C, Thrust Chamber Assembly (cont.)

injector orifices are photoetched into each plate. The plates are then brazed together to form the platelet vane. These vanes are then brazed into the injector housing.

(C) Transpiration-cooled testing with this injector was resumed. Coolant was reduced selectively in the various compartments until required performance was achieved. A total of 46 cooled thrust chamber tests were conducted in this test series using three injectors and three cooled chambers. Of these, greater than 90% of theoretical specific impulse was achieved in four tests, one of which was of long duration (20 sec). Greater than 89% of theoretical specific impulse was achieved in 12 tests, 4 of which were of long duration. A total of 220-sec duration was accumulated during this 46 test series. Of this 107 sec, including four long duration tests, were accumulated on a single thrust chamber.

(C) During this testing, several factors that revealed areas for further performance improvement became evident. The most important of these were a mal-distribution of oxidizer-rich gas circumferentially around the chamber and a non-optimum chamber contour, both of which necessitated some overcooling of the chamber. Correction of these deficiencies would result in an approximate 2.7% specific impulse increase.

(C) The entire cooled test program was conducted with a low area ratio nozzle (20:1) in performance demonstration tests. Currently, the most promising application for the engine is in future spacecraft. Therefore, the test data were analyzed to determine what performance would result in a space engine. This is tabulated below for two nozzle area ratios which bracket the range of area ratios that would likely be used in an ARES space engine.

II, C, Thrust Chamber Assembly (cont.)

Nozzle Area Ratio	Equivalent Achieved Specific Impulse, sec	Available Specific Impulse with Known Improvements (3% Gain), sec
150	323	333
300	330	340

4. Uncooled Two-Dimensional Nozzle Evaluation

(U) The ARES engine module can be used singly or in clusters to provide thrust in multiples of 100,000 lb. Approximately eight or more engines can be arranged to discharge through a common nozzle to increase effective area ratio. With 8 to 12 engine clusters, superior nozzle performance results by using two-dimensional, nonaxisymmetric nozzles that are flared and flattened to distribute the gases evenly into the forced deflection or plug nozzle.

(U) The Phase I effort included a task to determine the temperature distribution in a two-dimensional nozzle using both uniform and tailored film coolant injection. A two-dimensional nozzle with an area ratio of 5:1 was fabricated and tested twice. The chamber consisted of an ablative liner enclosed in a heavy steel case. Thermocouples penetrated the chamber wall in axial rows along both the curved and the flat sides. The chamber configuration is shown in Figure II-16.

(U) The first test with uniform film coolant injection confirmed the fact that temperature distribution was uneven, with the higher temperatures occurring on the flat side of the nozzle. In the second test the film coolant at its injection point was directed in the main chamber to provide relatively greater amounts of coolant on the flat side of the nozzle. The thermocouple data indicated that this was an effective way to equalize the temperature distribution around the nozzle.

II, Summary and Conclusions (cont.)

D. CONTROLS

1. General

(U) The principal goal of this portion of the program was to develop the fuel and oxidizer valves for use in the engine testing. Four valves are used in the engine: two are the suction valves and are of the same design for fuel and oxidizer; the other two are the primary and secondary combustor fuel control valves. These control valves are similar in design but of different size.

2. Suction Valve

(U) A multiple purpose suction valve suitable for both propellants was designed for long-term storage and positive-shutoff operational use. It must have a response capability to open or close in less than 0.400 sec and must give unobstructed flow from the propellant line through the valve to the pump.

(U) The configuration that met all work statement requirements is a unique design in which a segmented ball gate lifts from the operational seal, and then rotates entirely out of the flow path. A metal foil seal, which acts as a long-term storage seal, is sheared during the initial lifting motion. In the reverse motion, the segmented ball gate rotates into the flow path and is then pushed linearly against a spring-loaded lip seal. This design, with its cam operating mechanism, is shown in Figure II-17.

(U) The operation of the valve after endurance cycling with both water and propellants met or exceeded contract requirements and there was no discernible internal or external leakage of either propellant. Test results and work statement requirements together with photographs of the valve are shown in Figure II-18.

II, D, Controls (cont.)

3. Fuel Controls

(U) Separate fuel control valves were developed for both the primary and secondary injectors. The primary combustor fuel control valve must accurately control the fuel flow rate to the primary combustor over a flow range of 25:1, and be able to repeat the flow for any preselected position. It must also have the capability to shut off 6,000 psi flow from any position in less than 0.025 sec.

(U) A rotary-sleeve valve configuration was selected to meet this requirement. Two of these valves were fabricated and tested. The tests verified the structural integrity of the design and demonstrated that all of the design criteria were met or exceeded. The flow constant (Kw) actually attained was 2.1, against a requirement of only 1.45. Thus, the valve gives more flow for a given ΔP than originally demanded and has the capability to accommodate lower inlet pressures than originally contemplated. The control range demonstrated was 80:1, versus a required range of 25:1.

(U) The secondary combustor fuel control valve is similar in concept to the primary control valve but it must handle approximately four times the flow. This valve also met or exceeded all contractual requirements and gave a control range of 75:1, versus a requirement of 25:1.

(U) Test results and operating charcteristics of these valves are shown in Figure II-19.

II, Summary and Conclusions (cont.)

E. SUPPORTING STUDIES

1. General

(U) Several studies and laboratory tests were conducted to provide specialized design data and to investigate matters relating to application and growth of the ARES engine concept. These are summarized below:

2. Fluid Dynamic Testing

(U) Analytical techniques cannot accurately predict pressure drop and flow distribution for some of the flow passages on the ARES "T" engine. Consequently, a program was undertaken to experimentally determine this information with air flow test models. Four full-scale models were built and tested to predict performance of the passages in the "T" configuration turbopump.

a. Oxidizer pump discharge down to the thrust chamber flange.
b. Thrust chamber flange up to the primary injector face.
c. Primary injector to the turbine inlet.
d. Turbine exhaust to the secondary injector face.

(U) The results of the air-flow testing gave sufficient information to confidently design all of the flow passages with the exception of the turbine exhaust to injector face passage. Additional effort is needed to optimize the design of this passage for uniform flow to the secondary injector. Design of this passage is more straightforward on the Inline engine.

II, E, Supporting Studies (cont.)

3. Subscale Nozzle Program

(U) When the ARES engine module is clustered into large single nozzles, discontinuities occur where the individual modules exhaust onto the common skirt. Also, in the forced-deflection nozzle, a base heat shield is needed to prevent base recirculation from damaging the bottom of the vehicle. In regions of flow discontinuities, experimental data were needed to optimize performance and determine heat transfer rates. Therefore, a subscale air flow test program was conducted to obtain design criteria for a 2-million-lb-thrust engine employing 20 100K modules exhausting into a single forced deflection nozzle skirt. The engine was designed for a vehicle approximately 18 ft in diameter. The first part of the program was to determine the performance potential of the nozzle and to evaluate the effect of various design parameters on the performance. The second part was to obtain heat transfer data in regions of the nozzle where flow conditions are such that purely analytical techniques would not be expected to apply.

(U) Some of the significant conclusions from this program are:

a. Forced-deflection and plug nozzles using 20 modules perform better with axisymmetric internal expansion sections (IES) than with contoured-wedge "two-dimensional" IES's.

(C) b. Ambient base bleed offers between 2.5% and 3.5% performance improvement over nonvented performance within the atmosphere.

(C) c. Throttling by module shutdown results in a performance (I_s) loss of only 0.5% down to 20% thrust under vacuum conditions for forced deflection nozzles employing either axisymmetric IES's or contoured-wedge IES's.

II, E, Supporting Studies (cont.)

(U) d. The heat-transfer coefficient in the region where the IES's flow onto the skirt is higher than would be predicted for a continuous wall with no discontinuities. The magnitude of the increase is strongly dependent on the IES geometry and spacing.

(C) e. Axisymmetric IES's result in the lowest heat-transfer rate of the cases tested.

(U) f. The heat transfer rate on the base heat shield at sea-level atmospheric conditions is approximately four times as high as at vacuum.

(U) g. The heat transfer rate inside the nozzle of a shutdown module is approximately the same as on the base heat shield.

4. Advanced Propellants

(U) A program was conducted to determine the changes necessary for the engine to be suitable for use with several advanced propellants--peroxide/Alumizine, Compound A/Hydrazine, and N_2O_4/Alumizine.

(U) The results of this study showed that conversion of the ARES module to the use of advanced propellants changes the flow schedule of the module significantly. However, boost pumps, suction lines, suction valves, and the primary combustor fuel valve can be used with no component design changes. The existing turbopump oxidizer housing is adequate for N_2O_4/Alumizine and for H_2O_2/Alumizine, but not for Compound A/N_2H_4. It can be made acceptable for Compound A/Alumizine if shaft speed is increased, if operating pressure of the secondary combustor is reduced, or if capability to accommodate a large-diameter pump impeller is provided.

II, E, Supporting Studies (cont.)

(U) The oxidizer impeller and the second-stage fuel impeller can be reworked from the ARES configuration to accommodate a specific propellant.

(U) Other major components are not acceptable because of the increased fluid flow to the secondary combustor. These components will have to be resized.

(U) The ARES turbopump can be used for the Compound A/N_2H_4 engine provided an oxidizer-rich cycle is used, thrust chamber pressure is reduced to 1600 psia, and throat area is increased 60%.

5. Analytical Models

(U) Several analytical models were developed to establish the engine steady-state and transient operation and to define its stability characteristics. To accomplish this, three engine simulation computer programs were developed:

(U) a. A steady-state program to establish the engine operating point, and the ability of the engine to regain the design point when perturbed.

(U) b. A transient program including water hammer effects to show the behavior of the engine during start, steady-state, and shutdown operations.

(U) c. A low-frequency analysis program for studying the system stability characteristics of the engine during steady-state operation.

II, E, Supporting Studies (cont.)

(U) Similar models were prepared for use with the component test hardware. These used basically the same equations, but their boundary conditions were varied to suit the particular test setup.

6. Reliability

(U) A reliability effort was conducted to assure that the engine will have high operational reliability. Most effort was concentrated in the areas of failure-mode analysis and design review, with limited effort devoted to such tasks as maintainability and reliability prediction.

(U) An initial task was to obtain applicable failure data from related programs. This task provided essential inputs for the failure mode analyses, maintainability reviews, reliability predictions, and various comparison studies. Data were obtained from the Titan II, Titan III, and Gemini programs on component failure modes, frequency of experienced failures, and the reliability of each component.

(U) Each component of the ARES engine was analyzed to identify the potential failure modes, the causes of those failures, and the anticipated effects of those failures on the engine. It is concluded that, even though effort must be directed toward the solution of some remaining design problems, greater emphasis must be placed in such nondesign areas as fabrication, assembly, inspection, transportation, checkout, cleaning, and testing. There are cases in which trapped propellants pose a potential safety hazard. The use of inert materials such as Kynar and Kel-F for inserts in the wear-rings removed all significant explosion hazards from main-stage or boost-pump rub.

II, Summary and Conclusions (cont.)

F. CONCLUSIONS

(U) 1. The practicality of all ARES critical components was proven in Phase I.

(U) 2. The ARES engine is ready for an engine demonstration program.

(C) 3. Engine performance of 90.3% of theoretical specific impulse was demonstrated by thrust chamber testing. By incorporating thrust chamber improvements identified during the test program, performance can be increased to approximately 93% of theoretical specific impulse.

(U) 4. The ARES engine is designed for 10:1 throttling, multiple restart capability, and reuse. Further demonstration of these features is needed. However, the only redesign anticipated is incorporation of throttlable primary injector to obtain 10:1 variable thrust capability.

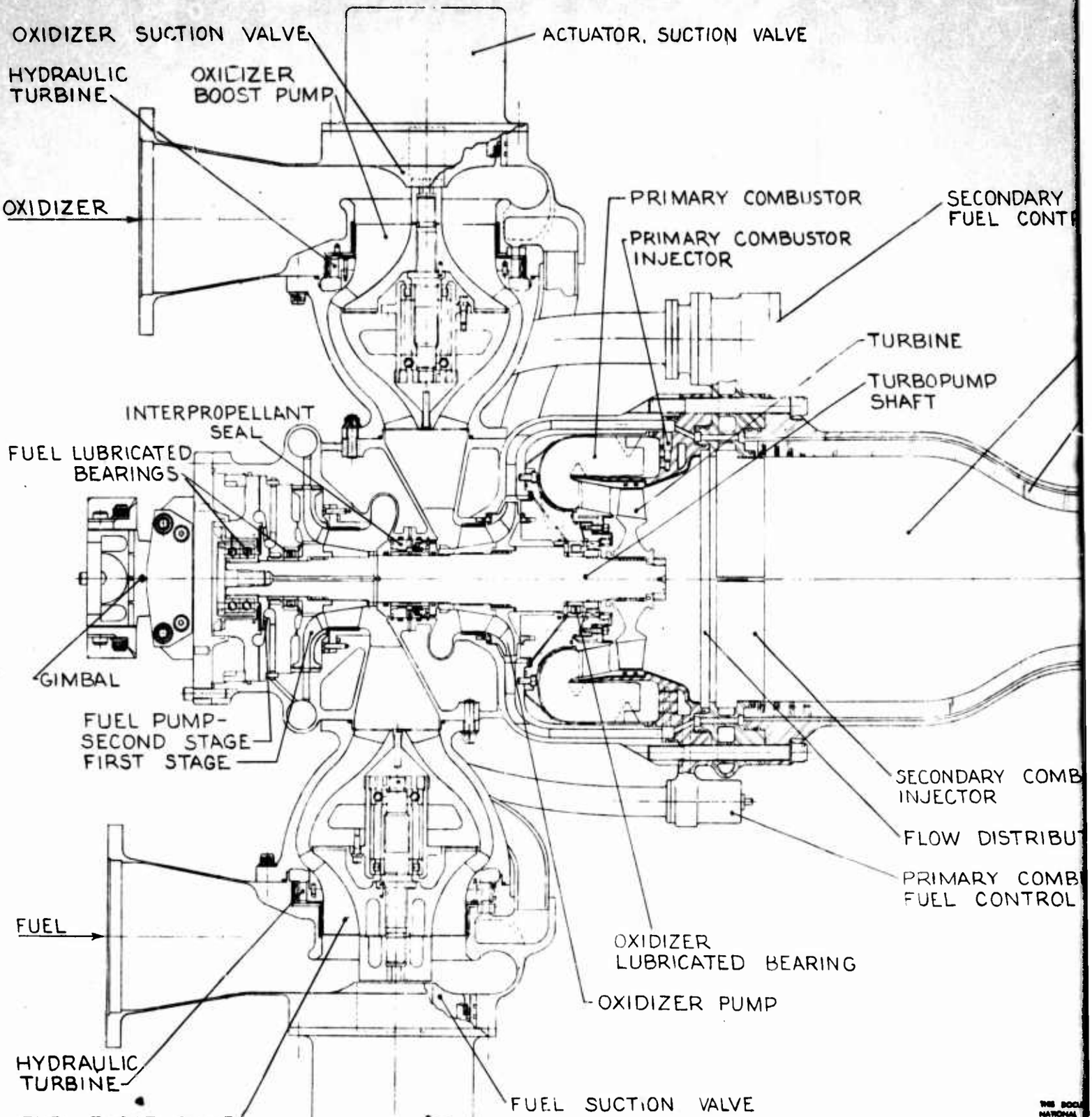

ION VALVE

RY COMBUSTOR

Y COMBUSTOR
OR

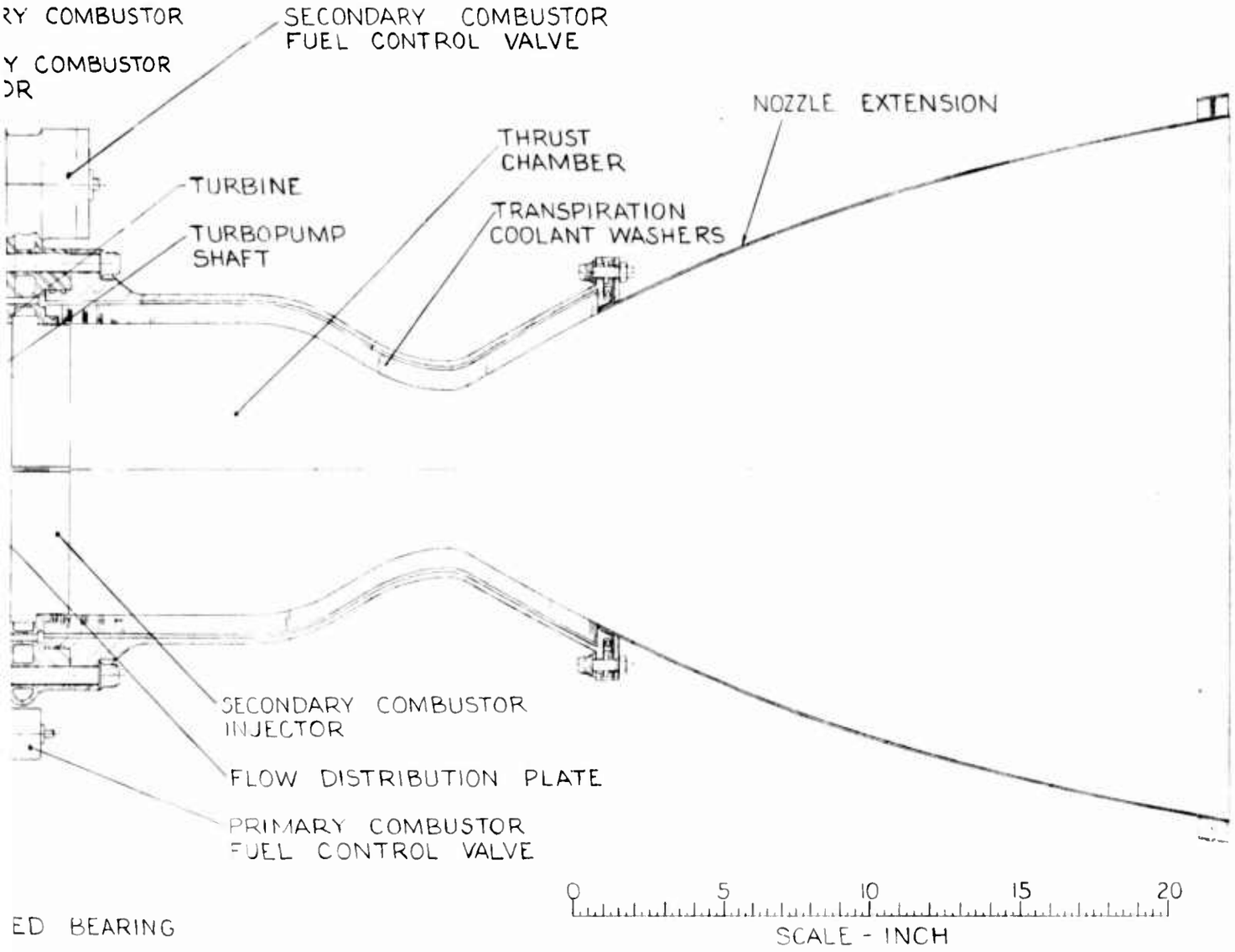

ED BEARING

PUMP

LVE

N VALVE

ARES Engine (U)

Figure II-1

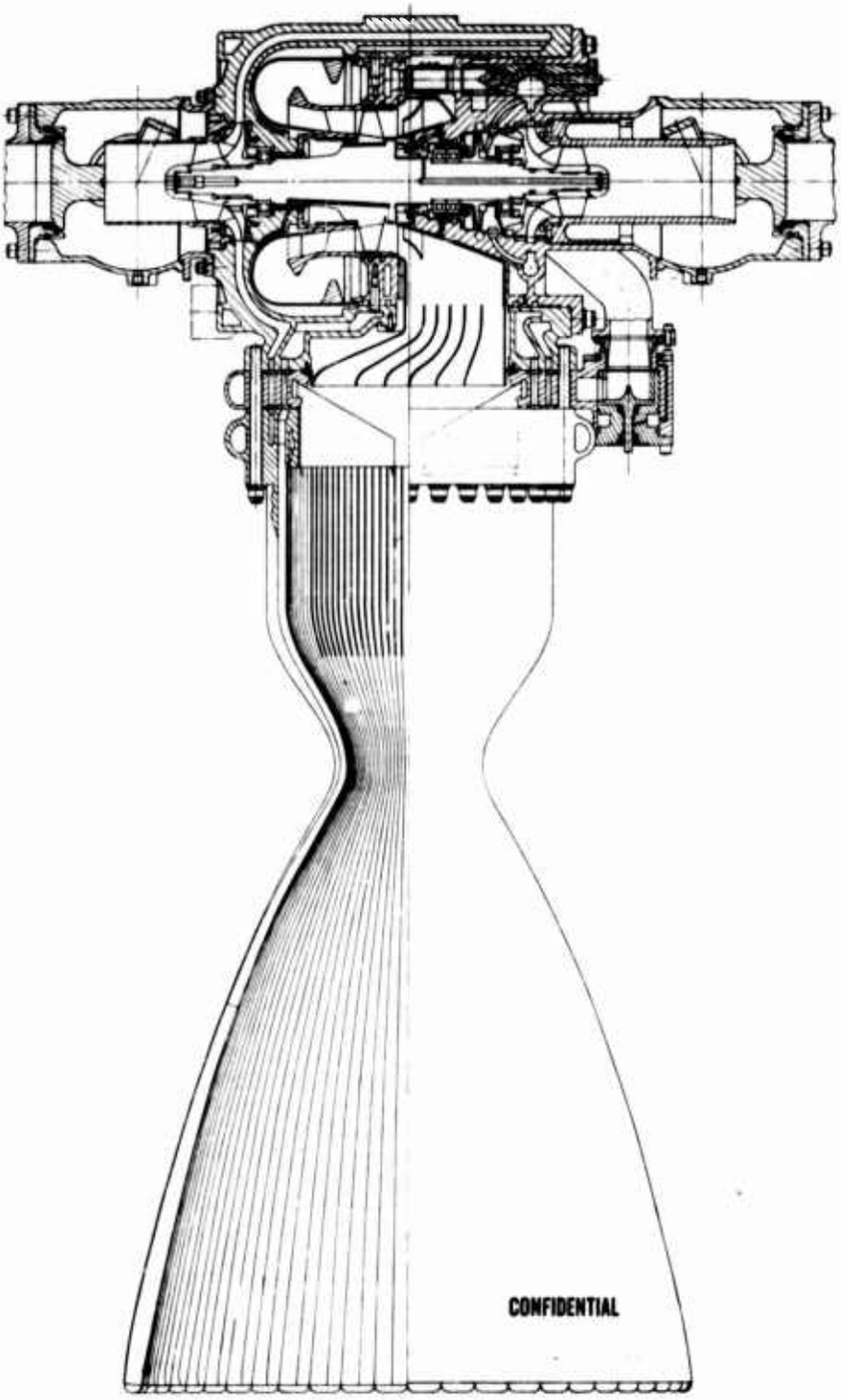

ARES "T" Engine--Regeneratively Cooled (U)

Figure II-2

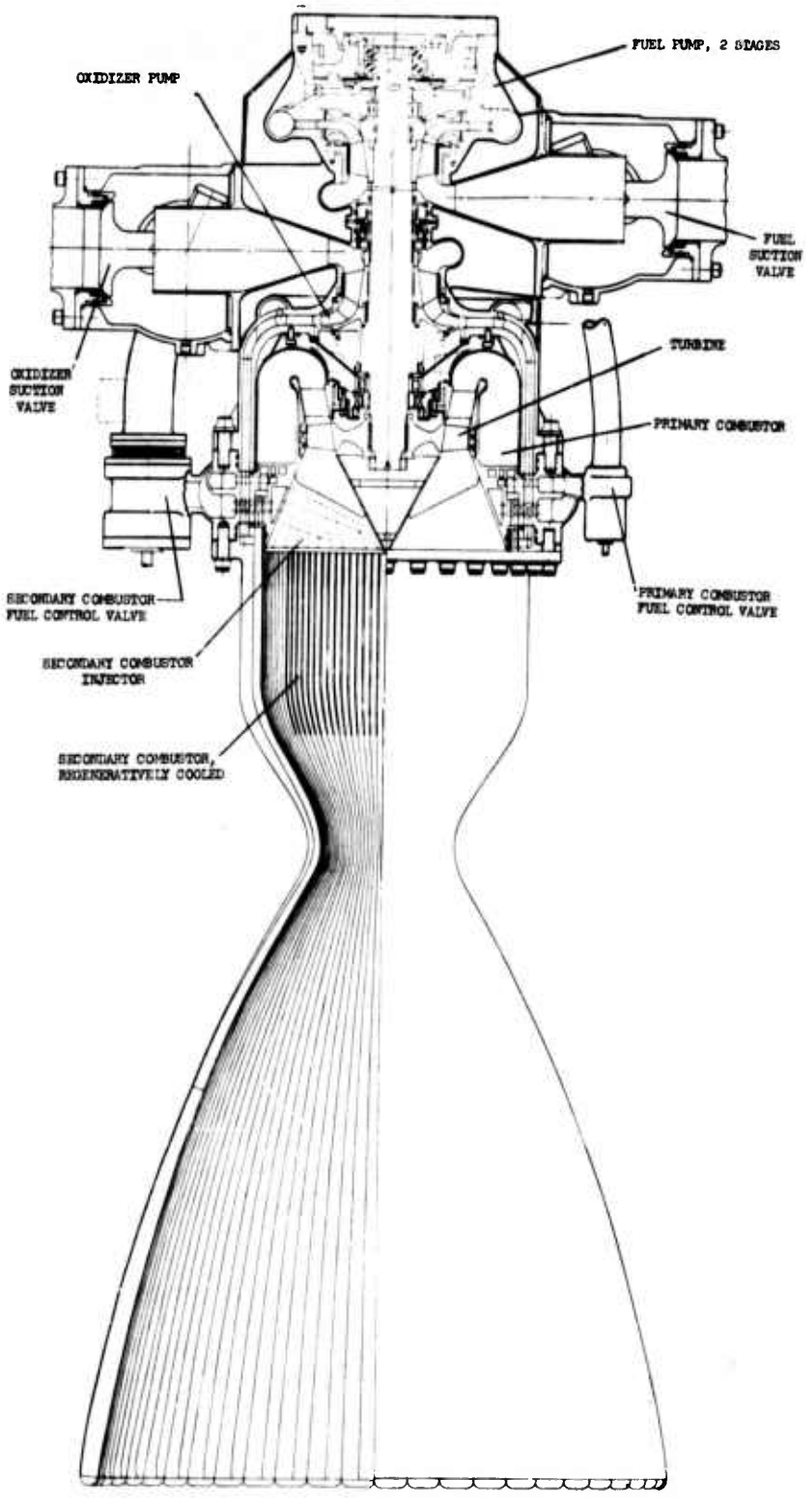

ARES Inline Engine, Regeneratively Cooled (u)

Figure II-3

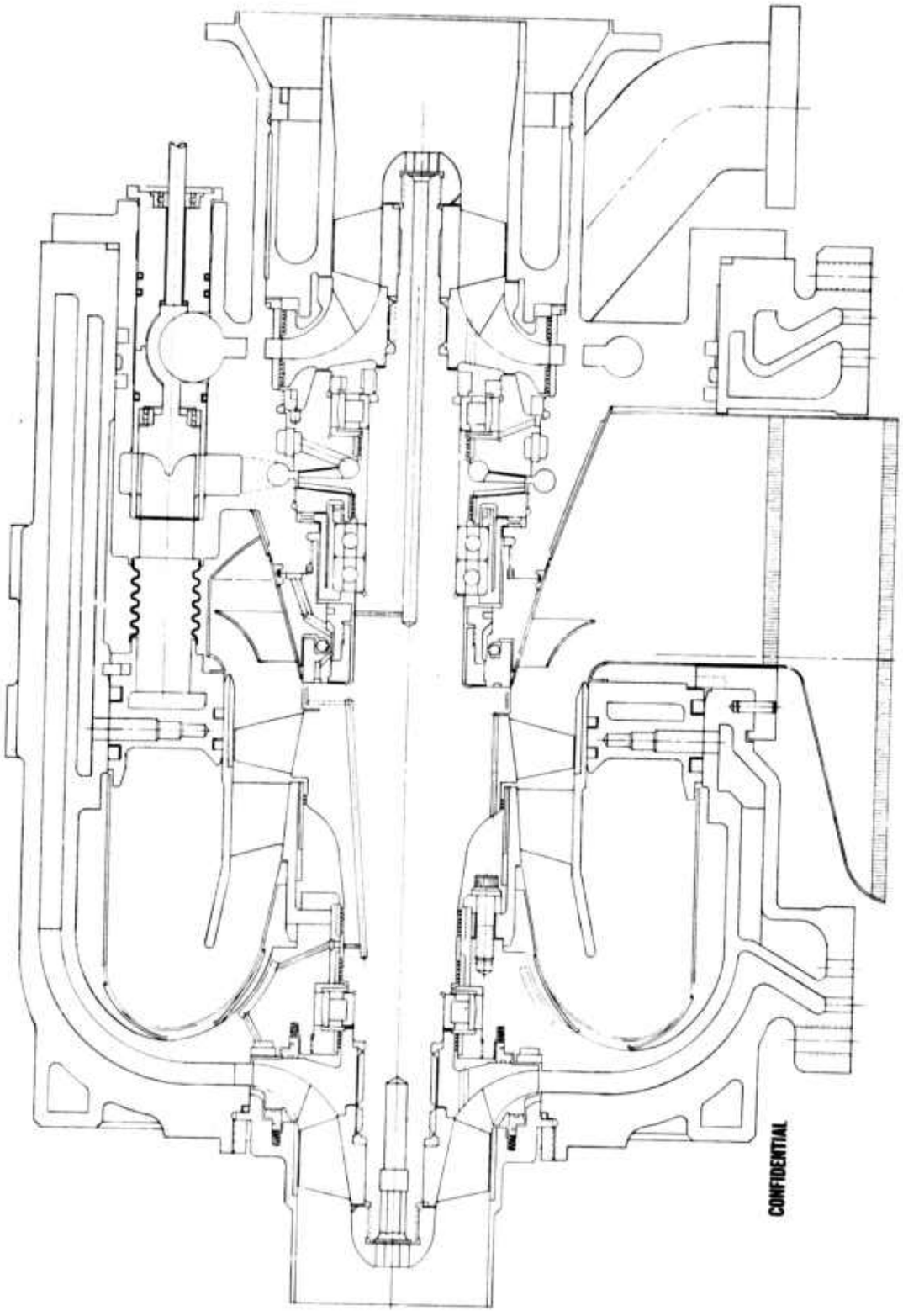

"T" Turbopump (U)

Figure II-4

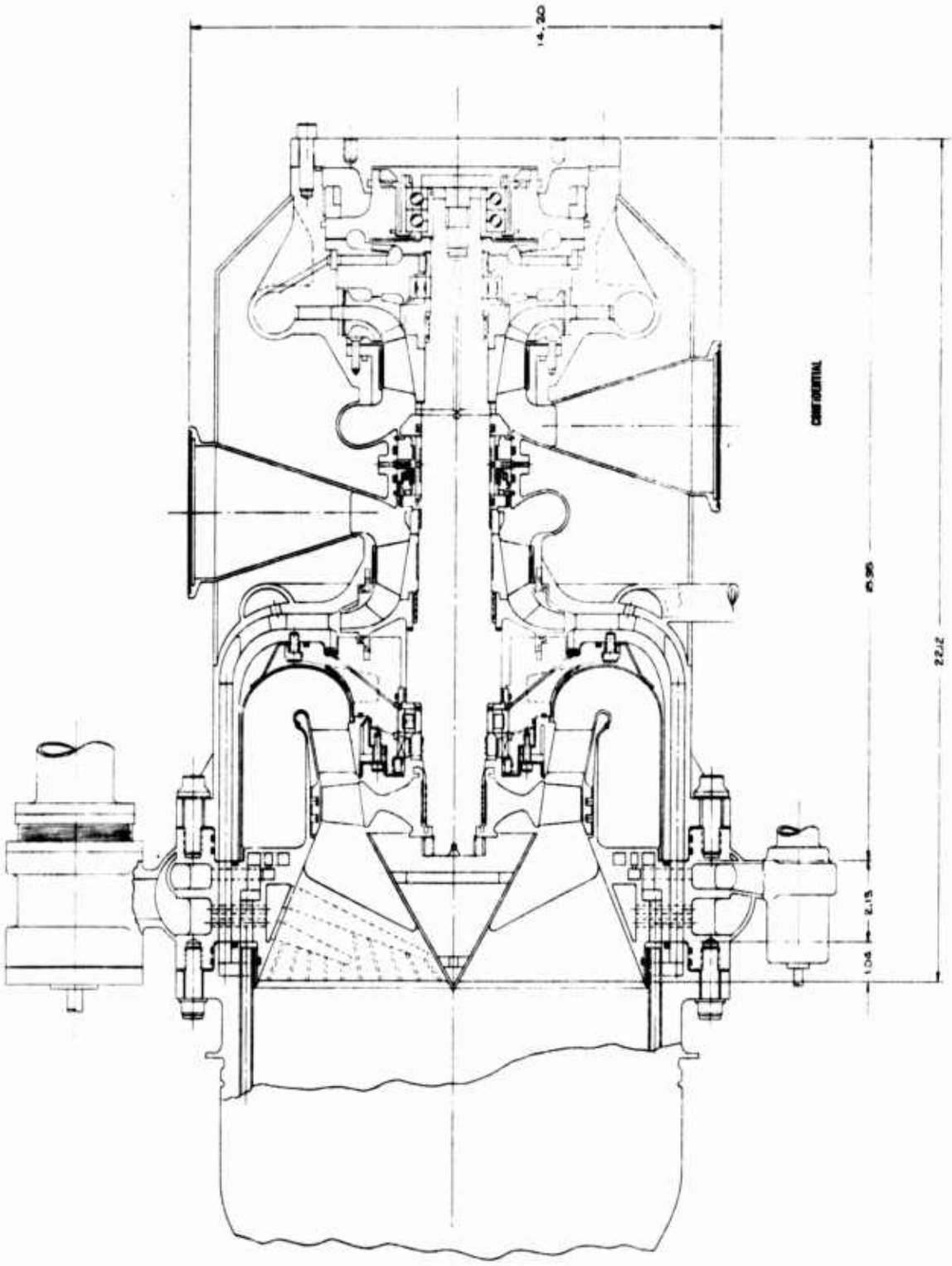

Inline TPA Cross Section (u)

Figure II-5

OBJECTIVES: Demonstrate by proof test at 1.4 x operating conditions. Maximum allowable weight is 350 lb.

TEST SUMMARY

Housing Weight, lb	300
Oxidizer Discharge Pressure, psi	8430
Oxidizer Return Pressure, psi	6850
Fuel Discharge Pressure, psi	5250
Turbine Exhaust Pressure, psi	4260
Thrust Load, lb	140,000
Roller Bearing Axial Deflection at Design Conditions, in.	0.021
Roller Bearing Radial Misalignment at Design Conditions, in.	0.0063
Housing Natural Frequency, cps	1500

"T" Engine TPA Housing Test Summary (U)

Figure II-6

OBJECTIVE: Demonstrate by proof test at 1.4 x operating conditions

TEST SUMMARY

Housing Weight, lb	230
Oxidizer Discharge Pressure, psi	8080
Turbine Inlet Pressure, psi	6250
Fuel Pump Discharge Pressure, psi	5250
Turbine Exhaust Pressure, psi	4210
Thrust Load, lb	140,000
Roller Bearing Axial Deflection at Design Conditions	0.022
Roller Bearing Radial Misalignment at Design Conditions	0
Housing Natural Frequency, cps	825

Inline TPA Housing Test Summary (U)

Figure II-7

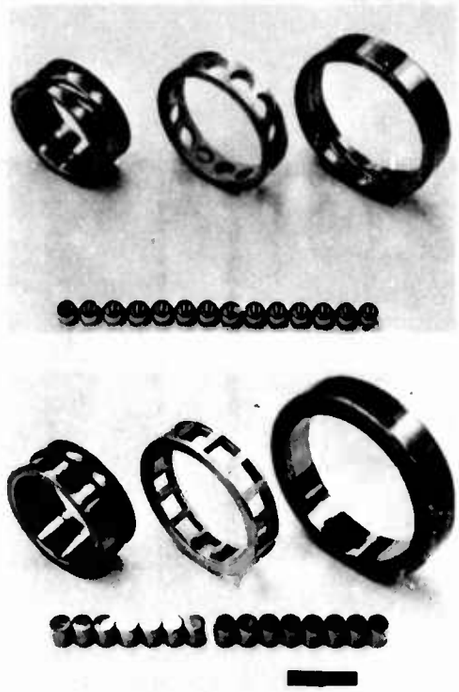

OBJECTIVE: Demonstrate at nominal load and speed for 12 min and peak loads for 8 sec

N_2O_4

	Speed, rpm	38,900	
	Duration, sec	791 (13 min, 11 sec)	
		Load, lb	Duration, sec
Axial,	Nominal	1500	739
	Peak	2500	52
Radial,	Nominal	500	759
	Peak	1000	32

AeroZINE 50

	Speed, rpm	40,000	
	Duration, sec	735 (12 min, 15 sec)	
		Load, lb	Duration, sec
Axial,	Nominal	1700	708
	Peak	2700	27
Radial,	Nominal	550	708
	Peak	1070	27

Bearing Test Summary

Figure II-8

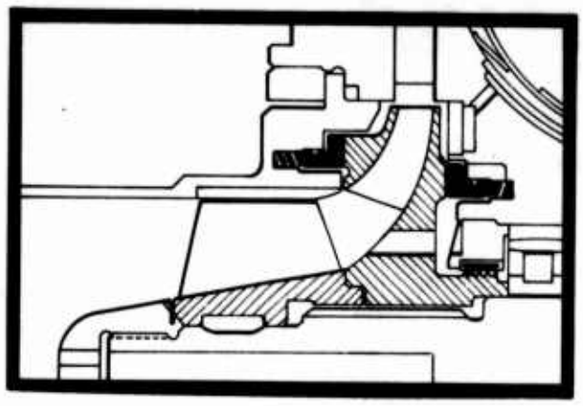

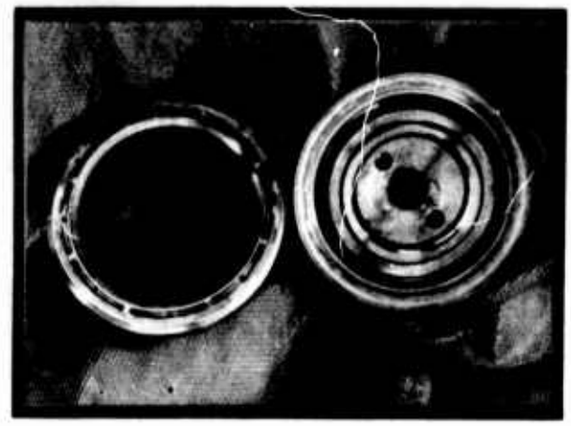

OBJECTIVE: Maintain close clearances needed for high pump efficiency at high pressure without change for pump rub. Maximum leakage: 53.8 gpm

Insert Material	Lynde LC-IC Flame-Spray over Stainless Steel
Axial Clearance, in.	0.0013
Axial Movement, in.	0.007
Pressure Across Seal, psi	4055
Leakage Flow, gpm	19.6*
lb/sec	3.8
Shaft Speed, rpm	40,000
Dry Rubbing	15,000 rpm for 6 sec

*This low leakage results in a pump efficiency increase of two points

N_2O_4 Wear Ring Test Summary

Figure II-9

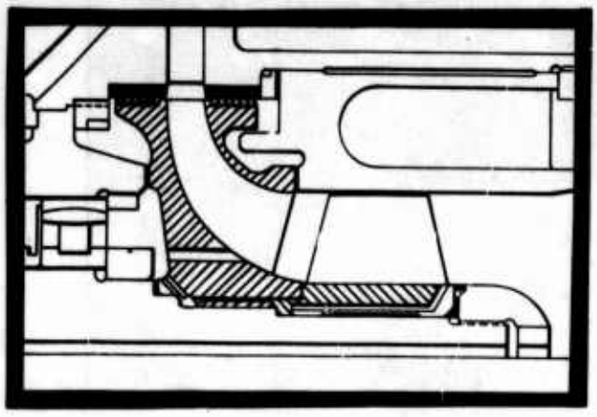

OBJECTIVE: Maintain close clearances needed for high pump efficiency at high pressure without chance for pump rub. Maximum leakage: 73 gpm

Insert Material	Kynar
Radial Clearance in.	0.006
Pressure Across Seal, psi	2300
Leakage Flow, gpm	32*
lb/sec	4
Shaft Speed, rpm	35,000
Amount of Rub, in.	0.010

*This low leakage results in a pump efficiency increase of three points.

AeroZINE 50 Wear Ring Test Summary

Figure II-10

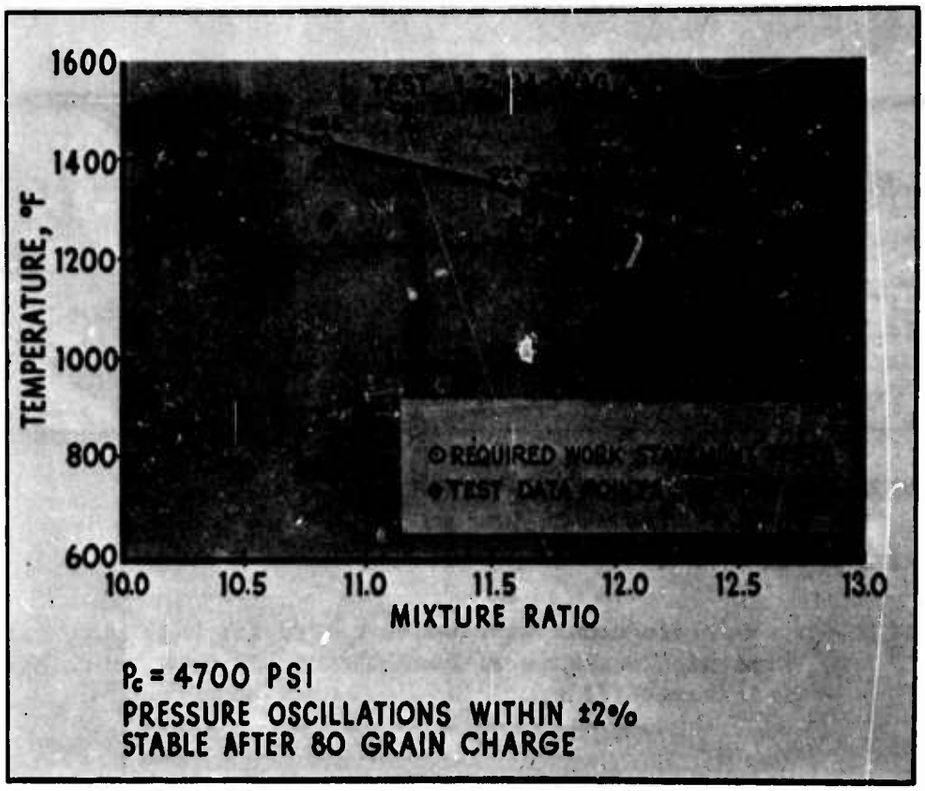

Requirement	Specified Value	Test Value
Exhaust Gas Temperature	1650°F max	1486°F max
Temperature Variation Between Three Thermocouples	400°F max	200°F max
P_c Oscillations from Average Value	±5% max	1.29% max
Steady-State Duration	1.0 sec, min	1.06 sec, min
Stability Pulse Test	None	80 Grain Charge 640 psi Peak-to-Peak 0.003 sec Duration

Primary Combustor Test Summary (U)

Figure II-11

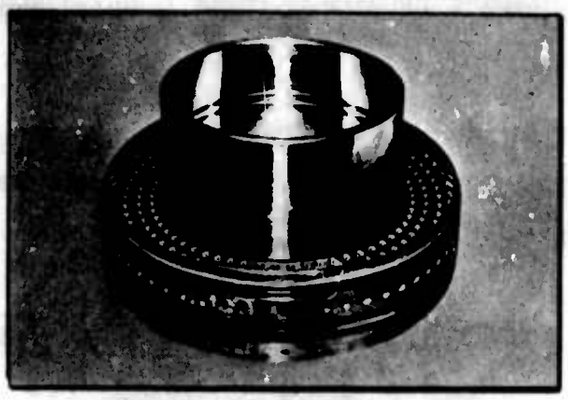

PRIMARY INJECTOR

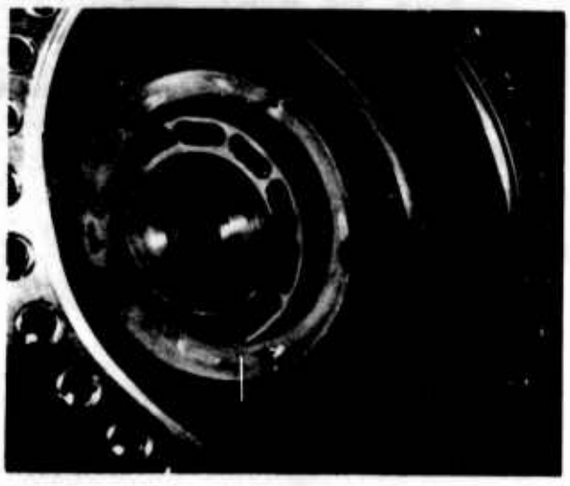

VIEW LOOKING TOWARD INJECTOR

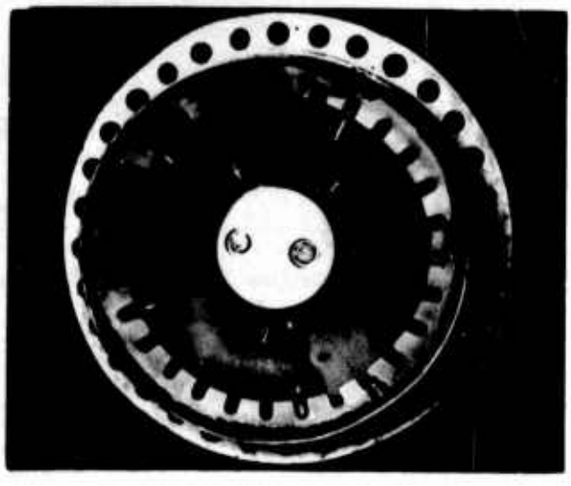

VIEW LOOKING TOWARD END CAP ASSY

Primary Combustor

Figure II-12

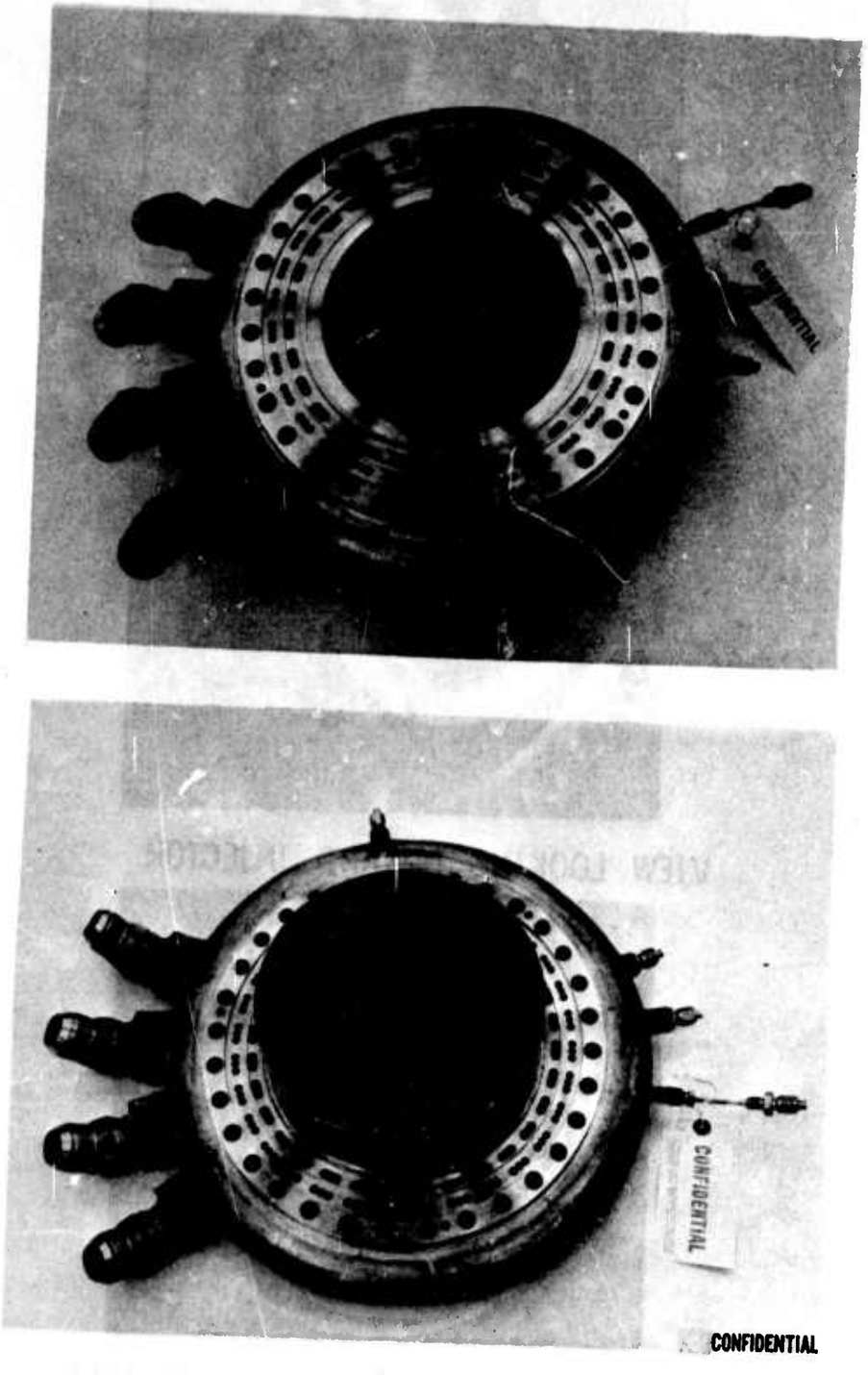

Fuel Swirl Rake Injector (u)

Figure II-13

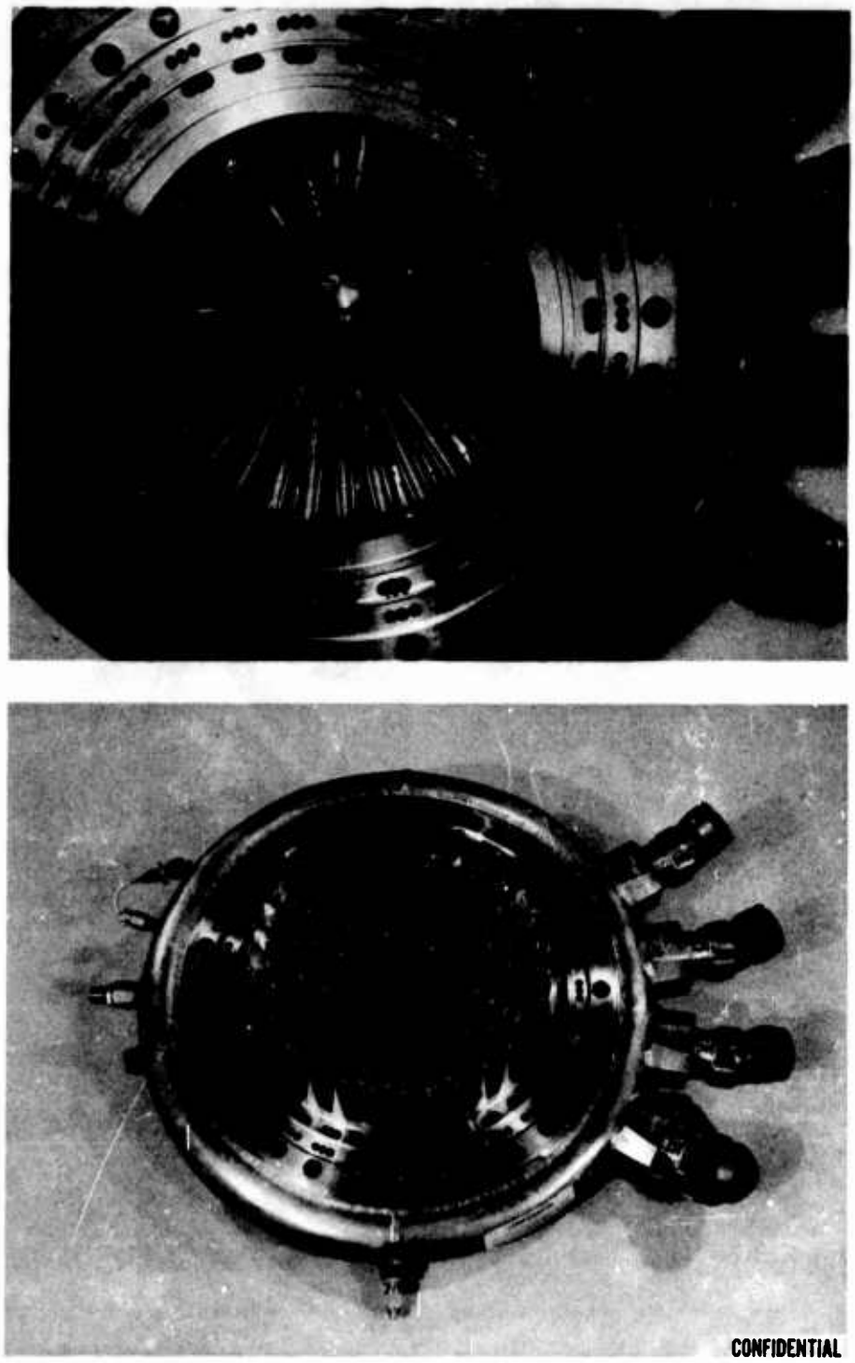

Modular Configuration--Mark 125 Injector (u)

Figure II-14

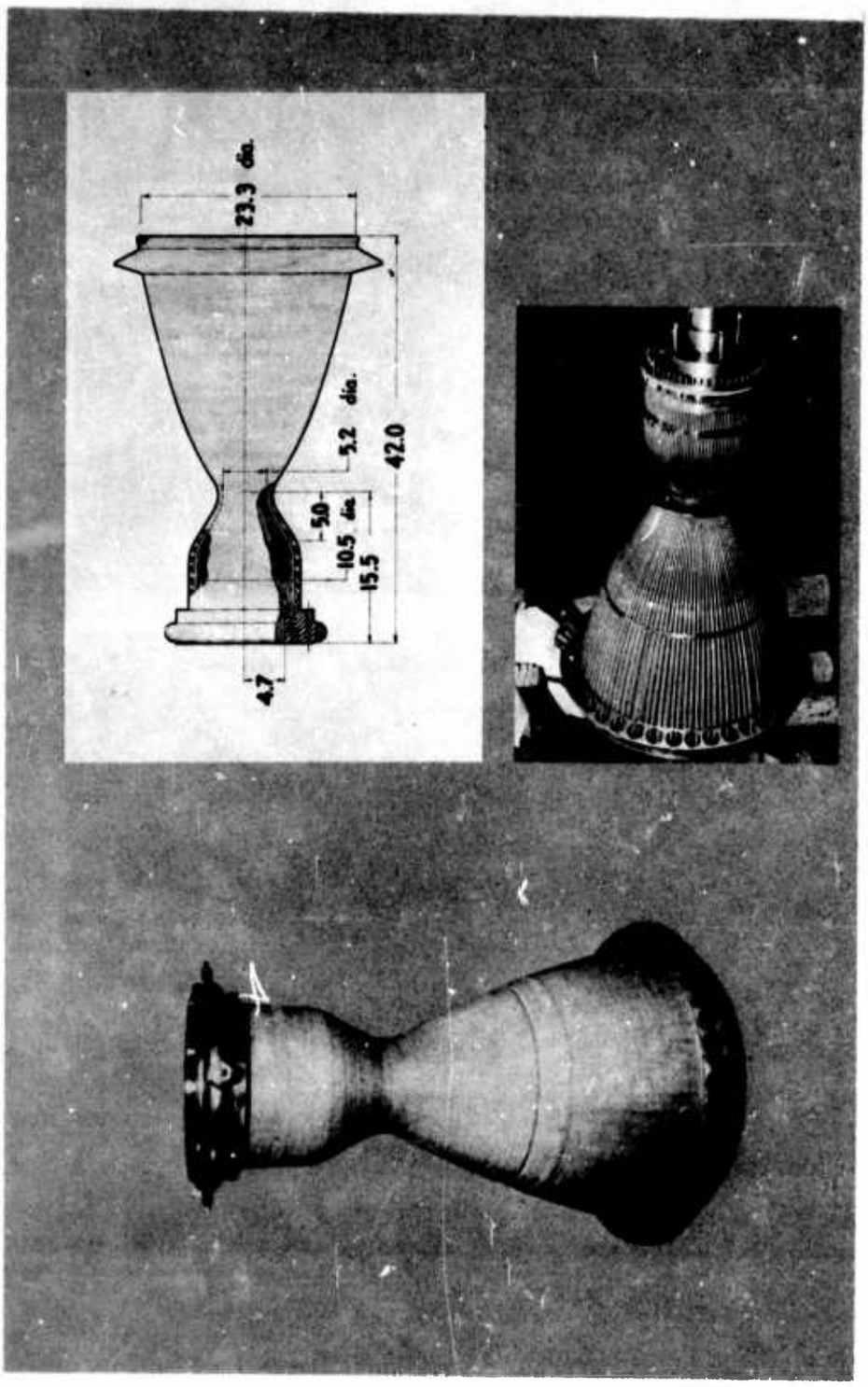

Regeneratively Cooled Combustion Chamber

Figure II-15

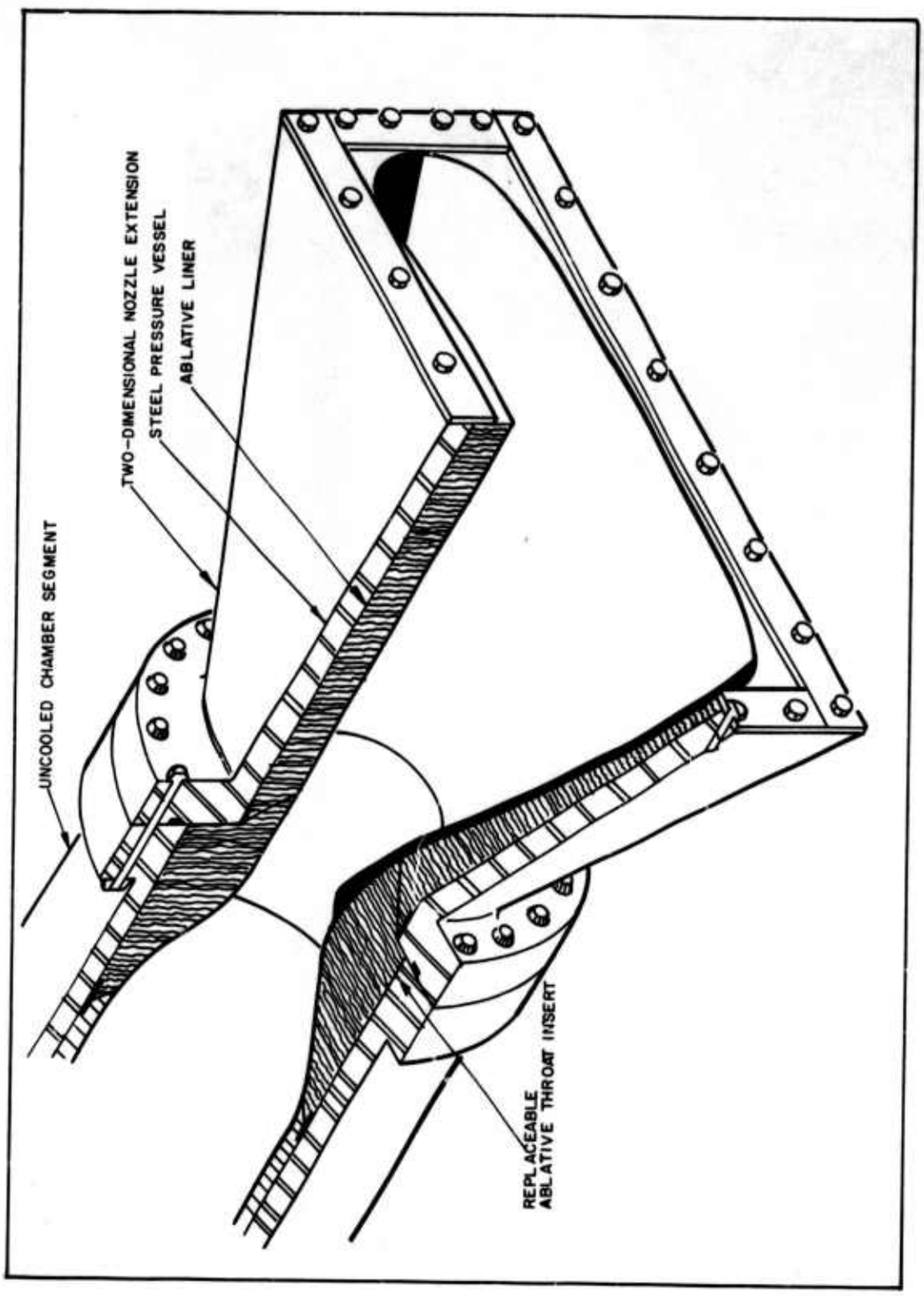

Two-Dimensional Nozzle Design

Figure II-16
Sheet 1 of 2

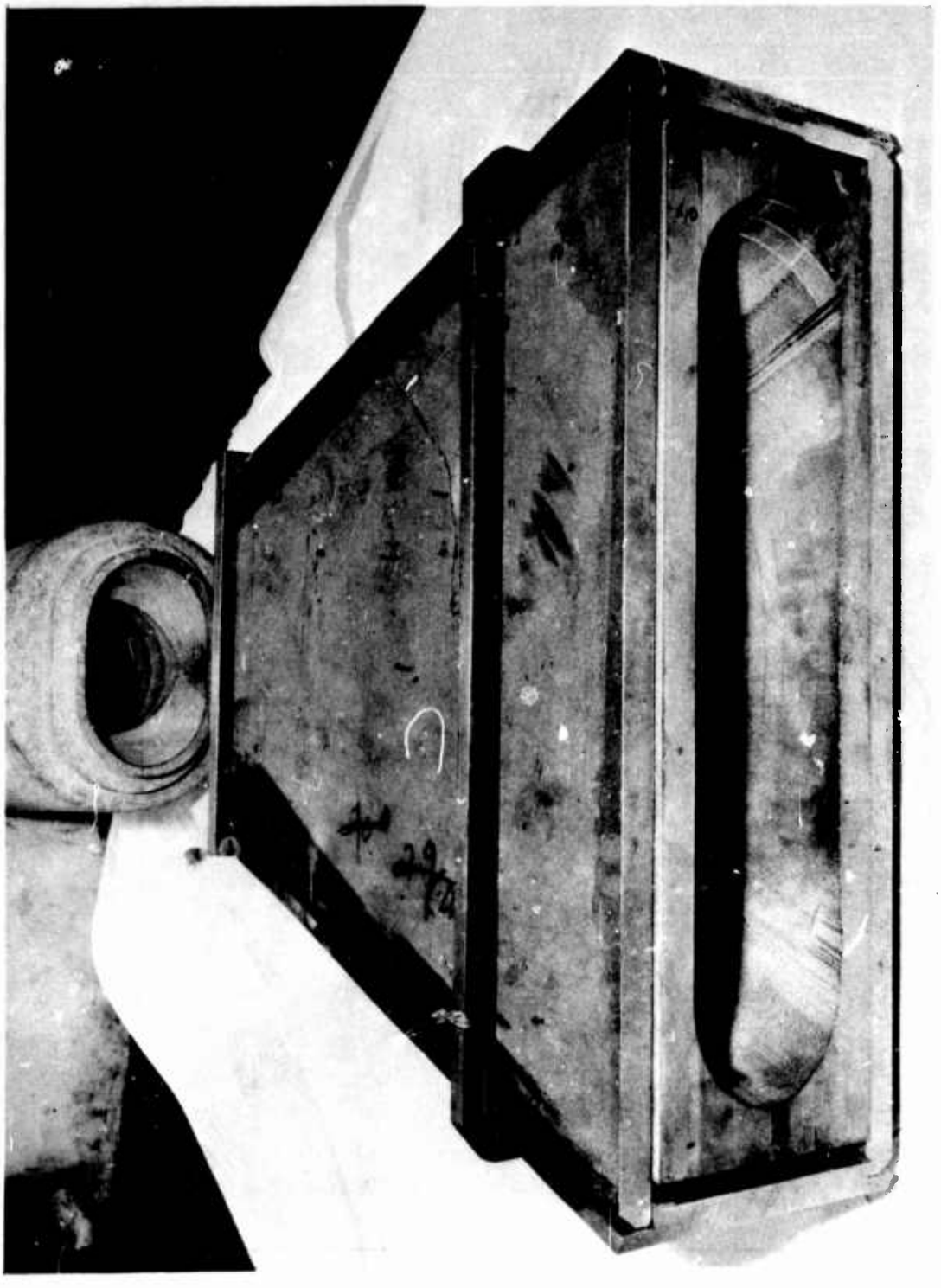

Two-Dimensional Nozzle Design

Figure II-16
Sheet 2 of 2

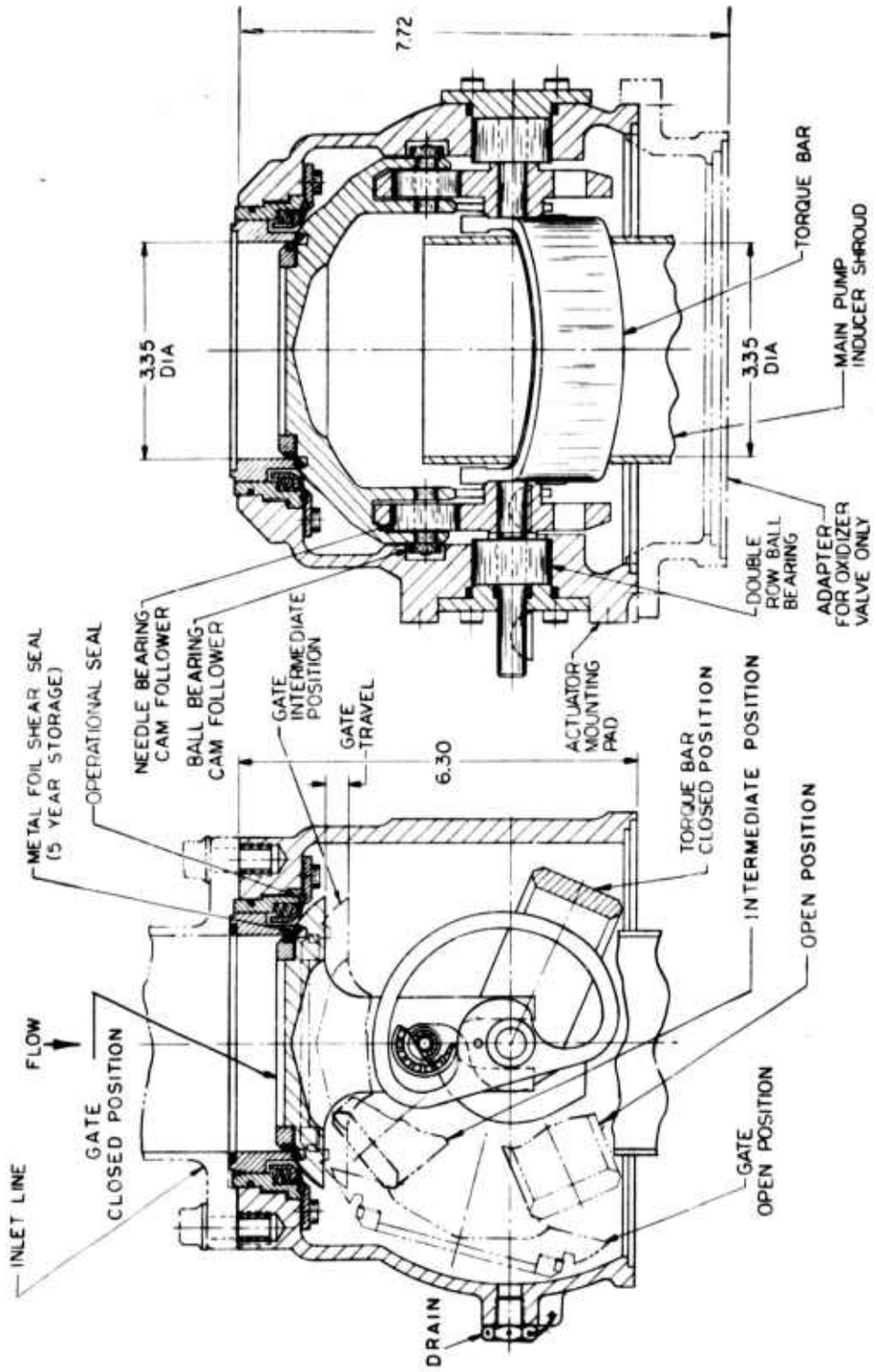

Suction Valve Configuration

Figure II-17

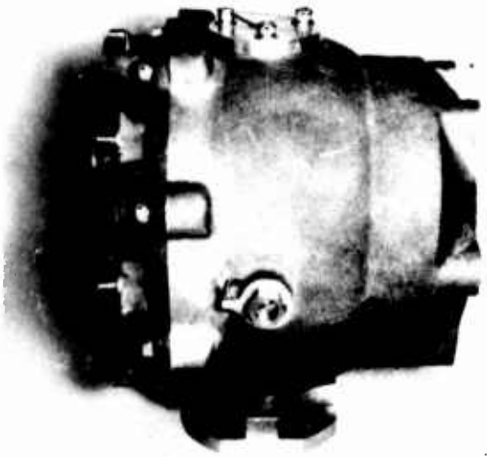

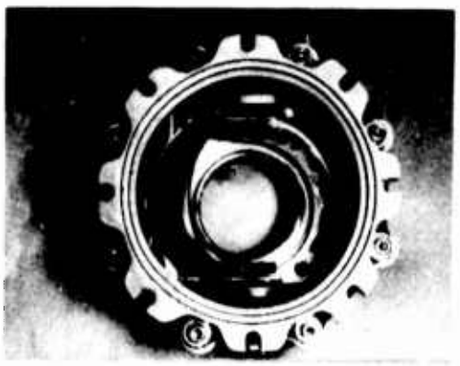

	Contract Requirement	Achieved
LEAKAGE		
Internal		
Storage Seal	10^{-4} cc/sec He	10^{-8}
Operational Seal	1 cc/min Fuel	None
	10 cc/min Oxidizer	
Shaft Seal	5 cc/hr	None
PROOF		
Oxidizer and Fuel	525	550
RESPONSE		
Open and Close	0.4	0.285
WEIGHT	None	15 lb

Suction Valve Test Summary

Figure II-18

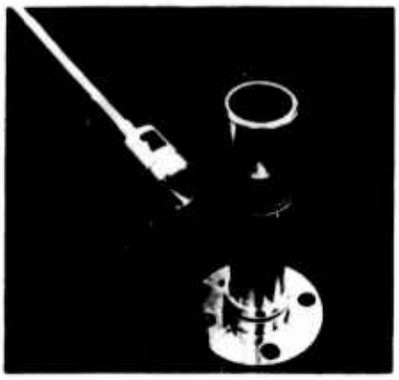

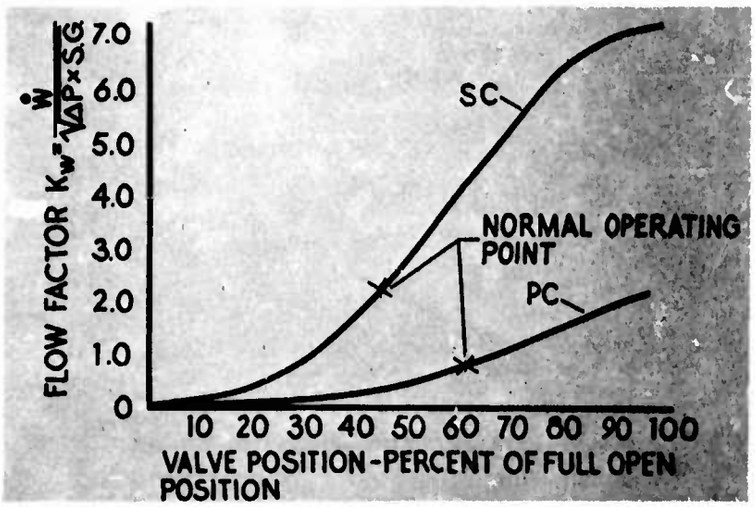

	P.C.	S.C.
Control Range	40:1	35:1
Pressure Drop, psi (Rated Flow)	120	125
Leakage, lb/sec (ΔP = 100 psi)	0.05	0.12
Response, sec (0 to Full Open)	0.025	0.025
	0.004	0.006
	6000	4000

Fuel Control Valve Test Summary

Figure II-19

SECTION III

ENGINE

A. OBJECTIVE

(C) One of the Phase I program objectives was to establish a layout design and predicted performance characteristic of a high chamber pressure, staged combustion rocket engine that would accomplish Phase II performance demonstration requirements at the target point or limits tabulated below:

	Target Design Point	Phase II Demonstration Range
Thrust, sea level, lbf	100,000	100,000 ± 5000
Chamber pressure, psia	2800	2800 ± 140
Sea level specific impulse, sec	285	283 (minimum)
Propellants	N_2O_4/A-50*	N_2O_4/A-50*
Mixture ratio, injector	2.2:1, nominal	2.2:1, nominal
Area ratio, nozzle (80% optimum bell contour)	20:1	20:1
NPSH, fuel, ft	43.0	43.0
NPSH, oxidizer, ft	30.0	30.0
Dry weight (including boost pump)	675	850 (maximum)

B. DESCRIPTION

1. Design

(U) The ARES engine layout incorporating the total experience gained in the Phase I program is shown in Figure II-1. The engine consists of a turbopump assembly, a thrust chamber assembly, fuel and oxidizer suction

*A-50, Aerojet-General Corporation trade name (AeroZINE 50) for 0.5 UDMH/0.5 N_2H_4 fuel blend.

III, B, Description (cont.)

valves, and boost pumps. The turbopump assembly includes the main pumps, the turbine, the primary injector and combustor, and the primary combustor fuel control valve. The thrust chamber assembly includes the secondary combustor, nozzle, secondary injector, and the secondary fuel valve.

(U) The turbopump is oriented with its shaft axis in line with the thrust vector. The turbopump is mounted on top of the thrust chamber, forming the central structure of the engine, with the engine thrust transmitted through the turbopump housing and gimbal to the airframe. The turbopump housing surrounds the annular primary combustor and is cooled by the large flow of oxidizer through the double wall. The turbine exhaust gas discharges directly to the thrust chamber injector.

(U) The primary combustor incorporates a 180-element pentad annular injector. The secondary combustor injector is of the platelet type: the fuel is introduced through photo-etched platelet pairs and the oxidizer-rich turbine exhaust gas passes between the platelets. The secondary combustor (thrust chamber), including the throat and a portion of the nozzle out to a 4:1 area ratio, is transpiration cooled, using platelet washers for metering the required amounts of oxidizer into the thrust chamber wall. The 20:1 area ratio nozzle extension is cooled primarily by a carryover of the transpiration coolant and is similar in design to the radiation-cooled nozzle on the Apollo engine.

(U) The turbopump shaft is supported in the housing by propellant-lubricated rolling contact bearings. The turbine is on the lower end of the shaft; the single stage oxidizer pump is on the center of the shaft, with the two-stage fuel pump on the top end of the shaft. Shrouded pump impellers with large running clearances are used to minimize the chance of pump rub. Wear rings are used to minimize back flow. An interpropellant seal is located

III, B, Description (cont.)

between the suction sides of the oxidizer pump and first-stage fuel pump to separate the propellants. The Titan I second-stage engine auxiliary turbopump assembly used a similar type seal which operated reliably in all Titan I flights even though propellants ignited occasionally in the seal cavity. Propellants were LOX/RP-1 which are not hypergolic. This type of seal has not been demonstrated with hypergolic propellants. Although complete design criteria for this seal using N_2O_4/AeroZINE 50 propellants are lacking, there is sufficient related data to give a high degree of assurance that it will perform satisfactorily under vacuum conditions without need for a purge.

(C) Ignition experiments with N_2O_4/AeroZINE 50 at low pressures were performed by Aerojet on Contract AF 04(611)-5959 in 1962 on the Ultra Low Chamber Pressure System Program (Reports SSD-TDR-62-37, Parts I and II). In this program, failure to ignite within 3 sec was observed at pressures below 3.6 psia. With excess oxidizer, the minimum ignition pressure was reduced to 1.5 psia.

(C) Similar experiments were performed by RMD on Contract AF 04(611)-9946 in 1965 on a program titled Hypergolic Ignition at Reduced Pressures (Report AFRPL-TR-65-105). In this program, one of the objectives was to determine ignition characteristics for impinging unconfined jets (no thrust chamber) using N_2O_4/AeroZINE 50 propellants. Ignition could not be achieved within 1/4 sec at pressures below 1.2 psia.

(U) Based on results from these three programs, it appears that N_2O_4/AeroZINE 50 propellants will not ignite at pressures below 1.2 psia and may not ignite at pressures up to 3.6 psia. An interpropellant seal, designed to operate below 1.2 psia in the region of propellant mixing, should operate without ignition occurring. Therefore, safe and reliable operation in space should be achievable. Provision for a purge has been included if needed for sea level operation.

III, B, Description (cont.)

(U) Fuel and oxidizer enter the engine through vertical inlets on each side of the turbopump. Each inlet consists of a suction valve, a hydraulically driven boost pump, and a 90-degree torus housing. The suction valve is integrated upstream of the boost pump and consists of a torus housing, a poppet, and a poppet actuator. The torus housing turns the propellant from the vertical engine inlet into the horizontal inlet of the boost pump. The suction valve poppet has a metal foil, long-term-storage seal that shears cleanly during the initial motion of the valve. The valve poppet has a spring loaded Teflon lip seal to seal the valve when the valve is closed after initial actuation.

(U) The primary and secondary combustor fuel control valves are of the rotary sleeve type and are pressure balanced to reduce actuation forces. The rotating sleeve is mounted on ball bearings to maintain close clearance between sleeve and housing, thereby controlling the leakage with minimum rubbing.

(U) All the valves were designed for use with conventional, ready-made, electrical or hydraulic actuators.

(U) The following engine components were demonstrated by testing similar designs during the Phase I program.

Cooled thrust chamber and injector
Primary combustor and injector
Turbopump housing
Propellant lubricated bearings

III, B, Description (cont.)

Pump wear rings
Turbine performance
Suction valves operational and storage seals
Fuel control valves

2. Cycle

(U) The ARES staged combustion cycle is shown schematically in Figure III-1. Propellants enter the engine through the suction valves and are pumped by the 8000 rpm boost pumps to a pressure of 100 and 170 psia, fuel and oxidizer, respectively, which is required for the 30,000 rpm main pumps. All of the oxidizer (N_2O_4) is then pumped to a pressure of 5800 psia in the main oxidizer pump with most of it continuing to the primary combustor injector. The fuel is pumped to a pressure of 5500 psia in the first-stage fuel pump. A portion of this fuel (20%) then enters the second-stage fuel pump where it is pumped to a higher pressure of 6200 psia and passes through the primary combustor fuel control valve to the primary injector. The oxidizer and fuel enter the primary combustor where they combine hypergolically to form a hot gas of 1150°F and 4900 psi chamber pressure. This oxidizer-rich gas passes through the turbine and is then exhausted into the thrust chamber. The major portion of the fuel flow from the first-stage pump is ducted through the secondary combustor fuel control valve to the main injector where it is injected into the thrust chamber. This fuel burns with the oxidizer-rich turbine exhaust in the thrust chamber at the 2800 psia chamber pressure.

(U) The boost pumps are driven by hydraulic turbines which use 8% of the respective propellant bled from the main pump discharge. This drive fluid is then exhausted into the boost pump discharge. In the main turbopump, oxidizer for bearing coolant is bled from the pump discharge, passed through the oxidizer bearings, and discharged into the turbine inlet where it provides

III, B, Description (cont.)

some turbine cooling. High-pressure fuel is used to cool the fuel pump bearings. Secondary combustor transpiration coolant, N_2O_4, is tapped from the oxidizer circuit at the primary injector.

(U) The two fuel control valves perform three functions: (1) propellant phasing is controlled during start and shutdown by sequencing both the primary and secondary fuel control valves, (2) engine thrust is established by the preset open position of the primary combustor fuel control valve (PCFCV), and (3) engine mixture ratio is established by the preset open position of the secondary combustor fuel control valve (SCFCV). No oxidizer control valve is required.

3. Operation and Performance

a. Design Point Operation

(U) The engine system was analyzed on the steady-state mathematical engine model to establish the internal pressure, flow, and temperature values. Consistent with minimum engine weight and turbine operating temperatures, an engine pressure schedule was established as shown in Table III-I. The predicted operating point of the engine that will deliver the target thrust and specific impulse is shown in Table III-II, with the parameters arranged to show the operating point of each major component.

b. Start and Shutdown

(U) The engine starts from tank pressure. No auxiliary start system is needed. Therefore, the engine is inherently restartable. The engine start and showdown transients have been predicted based on predicted component performance characteristics and current test stand suction pressure

III, B, Description (cont.)

(60 psia) capabilities. The predicted start and shutdown transients are shown in Figure III-2.

(U) The engine operating sequence to accomplish the predicted start transient is as follows:

(1) Pressurize propellant tanks to 60 psia.

(2) Open oxidizer suction valve.

(3) Open fuel suction valve approximately 0.5 sec later.

(4) Open primary combustor fuel control valve (PCFCV) to present amount (5% operating point K_w value) which allows fuel to flow to the primary combustor.

(5) Ignition occurs in the primary combustor.

(6) Open secondary combustor fuel control valve (SCFCV) to its full operating position.

(7) Ignition occurs in the thrust chamber.

(8) Continue opening PCFCV to the steady-state operating point.

(U) The shutdown operation is the reverse of the startup operation and ends with all engine valves closed.

c. Off Design Operation

(U) The Phase-I ARES engine was designed to achieve specified performance at full thrust. However, the engine can be throttled by varying the position of the primary fuel control valve while the secondary fuel control valve remains in its preset position. The mechanism by which the primary combustor fuel valve controls the thrust is as follows: increasing the resistance in this valve reduces the fuel flow to the primary combustor, which in turn reduces turbine temperature and, to a lesser extent, the turbine mass flow;

III, B, Description (cont.)

the reduction in turbine drive energy results in decreased turbopump speed, pump discharge pressures, propellant flow rate, and thrust. The engine system maintains nearly constant mixture ratio during throttling, because of the designed relationship between fuel and oxidizer pump heads almost exactly compensating for the other factors that influence engine mixture ratio. Throttling operation over a broad thrust range, such as 10:1, would necessitate incorporation of primary injector designed for deep throttling. Considerable effort on design of a throttleable ARES engine for use in space applications was accomplished on Contract F04611-68C-0008 (Report AFRPL-TR-68-2).

4. Weight

(U) Estimated engine weight and inertia values broken down by major component are tabulated shown in Table III-III. Also tabulated are estimated weight and inertia values of engine accessories including valve actuator and gimbal.

5. Materials

(U) A list of the materials for the components of the engine is shown in Table III-IV. Included in the list are the environmental and operational requirements for each part noted. Material selection was predicated on structural and chemical compatibility to the environmental conditions specified.

6. Application as a Spacecraft Engine

(U) Considerable effort has been expended over the past 1-1/2 years on designing ARES for use as a spacecraft engine. This work has been supported by both the Air Force and Aerojet. Air Force support was on Contract F04611-68C-0008 and was directed mainly towards throttling, restart, and design

III, B, Description (cont.)

of different size ARES engines (down to 25K thrust). Aerojet effort was directed mainly towards other operational features needed in a spacecraft engine, such as unlimited restart and space storage capability and reuse. Results of these studies are summarized briefly below.

a. Throttling

(U) Analytical engine studies (steady state and low frequency dynamics) have shown that the engine system can be throttled over a 10:1 range by use of the primary combustor fuel control valve only. The primary injector would probably be changed to accomplish this practically. A sufficient pressure drop exists for the secondary injector so that a change would probably not be required. Test verification of injector and thrust chamber throttling is needed.

b. Unlimited Restart

(U) The ARES starts from tank pressure and uses no third fluids; therefore, the engine has the potential for unlimited restart. Other factors that can limit restart are damage due to heat soak-back after shutdown and degradation of engine parts during coast periods by the action of propellants or other contaminants. Several features have been designed into the engine to minimize the amount of heat soak-back and thus minimize the detrimental effects of the heat left in the system. Thermal liners have been provided in all primary combustor and turbine exhaust passages to minimize the heat transfer to the thick housing parts. These thick parts are also cooled by passing propellant through them. The AeroZINE 50 pump is placed at the cool upper end of the TPA to eliminate the chance of heat soak-back from detonating any fuel that may be present in the fuel pump or fuel bearings after shutdown. Current studies indicate that heat soak-back will result in

III, B, Description (cont.)

a maximum temperature of the oxidizer bearing of approximately 300°F. The effect of this temperature on the oxidizer pump bearing must be determined experimentally. Temperature at the fuel pump end will rise to approximately 200°F. The secondary injector parts rise to a maximum of 300°F. Exposure of fuel to temperatures below 300°F does not result in spontaneous decomposition. The engine is isolated from the propellants after shutdown by suction inlet valves. Therefore, propellant rapidly leaves the engine after shutdown in space. Since there are no other fluids used in the engine, the chance for degradation of parts from exposure to contaminants is minimized.

c. Unlimited Space Storage

(U) The ARES is stored dry in space. Experience with Transtage indicates that after shutdown residual propellants leave the engine in a fairly short period of time: N_2O_4 leaves in a matter of a few seconds; AeroZINE 50 leaves in the order of 20 minutes. Propellant trapped between tight fitting components, such as bearing races and the housing or shaft, probably remains for significantly longer. How long propellant remains in these parts and its effect must be determined experimentally. However, materials used in the engine are compatible with the propellants in the absence of contaminants. Water combining with N_2O_4 results in the formation of acids which would attack engine parts. In vacuum, there is no water, so this is probably not a problem. AeroZINE 50 forms solid precipitates with many common lubricants that could plug vital engine parts; however, no lubricants are used in the engine. Precipitates formed by the action of N_2O_4 on the ferric metals in the engine are volatile in the absence of water.

d. Reuse

(U) The ARES engine has been designed with potential reuse in mind. It is recognized that component and engine system demonstrations are

III, B, Description (cont.)

needed to verify reuse; however, features have been designed into the engine specifically to enhance its reuse potential. The thermal liners in the primary combustor and turbine exhaust region combined with the cooled housing parts reduce thermal stress to the level needed for many cycle operations. The low turbine drive gas temperature reduces potential turbine life problems. Also, the turbine is an inherently low stress design because of the engine cycle. The thrust chamber nozzle is similar in design to that used on Transtage and Apollo. Transtage has demonstrated life of 439 sec with 205 restarts without failure of the nozzle extension. Conditions are somewhat different in the ARES engine, but the potential of long nozzle life and reuse is clearly indicated.

(U) Reuse and even long-term ground storage present several problems that do not exist in a space storage situation. The presence of water and N_2O_4 is the most severe condition. While experience indicates that the ARES engine materials are compatible with the propellants, contamination of N_2O_4 with water will cause corrosion. Therefore, cleaning procedures must be developed that will remove propellants from the engine. Then, as a further assurance, the engine should be isolated from moisture. One means of accomplishing this is by storing the engine with a cover over the nozzle exit. A desiccant can be placed inside the nozzle to absorb any residual moisture. Experience has shown that the bearings, which use the least corrosion resistant material in the engine, are not highly susceptible to corrosion even in the absence of a preservative, if cleaned and kept reasonably dry. Some of the bearings used for the ARES testing have been stored under uncontrolled conditions in a desk drawer for years without corroding.

TABLE III-I

ARES PRESSURE SCHEDULE (U)

Configuration: Mark I, Mod I (Inline TPA, Transpiration Cooled TCA)

Pressure, psia (Total Pressure Unless Otherwise Indicated)	Thrust Chamber Coolant	Primary Combustor and Hot Gas		Secondary Combustor Fuel
		Oxidizer	Fuel	
Boost Pump Inlet		36.3*	19.5**	
Boost Pump Discharge		171	93	
Main Pump Inlet		168	90	
Main Pump Discharge		5800	5500	
Second Stage Fuel Pump Inlet			5150	
Second Stage Fuel Pump Discharge			6150	
Manifold ΔP	125	0	50	100
Balancing Orifice ΔP	725	200		
Control Valve ΔP			500	1815
Manifold ΔP	50	100	100	100
PC Injector Inlet		5500	5500	
PC Injector ΔP		600	600	
PC Injector Face		4900		
ΔP to Turbine Inlet		125		
Turbine Inlet		4775		
Turbine P Total to Static		1790		
Turbine Pressure Ratio Total to Static		1.6		
Turbine Exit Static Pressure		2985		
Turbine Exit Total Pressure		3035		
ΔP to SC Injector		25		
SC Injector Inlet		3010		3485
SC Injector ΔP		125		600
Transpiration Cooling P (Ref. only)	2100			
SC Injector Face		2885		
ΔP to SC Plenum		85		
SC Chamber Pressure Ratio		1.03		
SC Chamber (P_c)		2800		

*Equivalent to 30 ft NPSH
**Equivalent to 43 ft NPSH

Table III-I

TABLE III-II

ARES OPERATING POINT

Configuration: Mark I, Mod I (Inline TPA, Transpiration Cooled TCA)

The parameters in this table define the target operating point for this engine configuration. This operating point is similar to the operating point predicted for the backup engine (Inline TPA) in the ARES Phase I Interim Final Report. Following are the changes in conditions:

1. Liquid injector pressure drops were increased to 600 psi to provide high stability margin at off-design conditions.

2. The ΔP of 850 psi originally allocated to the oxidizer regenerative-cooling jacket (not required with transpiration cooling) was distributed approximately as follows:

   a. 300 psi added to primary oxidizer injector ΔP to provide stability under throttled conditions (Report AFRPL-TR-68-2).
   b. 250 psi added to oxidizer housing and manifold ΔP to provide orificing for contingencies (balancing and tradeoff of ΔP with other components).
   c. 200 psi added to turbine inlet pressure to reduce turbine inlet temperature.
   d. 100 psi removed from oxidizer pump discharge pressure.

3. No change in turbine characteristics with the exception that the design point pressure ratio was increased from 1.5 to 1.6 to reduce turbine operating temperature.

4. No change in main pump characteristics, with the exception that the H_D and Q_D design point values were adjusted to the engine operating point values.

TABLE III-II (cont.)

5. No change in boost pump and turbine characteristics with the exception that the design point values were adjusted to the engine operating point values.

6. The ΔP between the boost pumps and the main pumps was reduced because the suction lines were eliminated.

7. Nominal $\dot{w}_{OFC}$ (transpiration coolant flow) was set at 18.6 lb/sec.

8. Fuel bypass flow (bearing coolant) of 1.25 lb/sec from second-stage pump discharge to first-stage pump suction has been added.

TABLE III-II (cont.)

Engine Assembly

Parameter	Symbol	Units	Value
Thrust	F	lb	100,000
Specific Impulse (Sea Level)	I_s	sec	285
Mixture Ratio*	MR	-	2.38
Efficiency, Specific Impulse	ηI_s	%	91.6
Oxidizer Weight Flow	$\dot{w}_{OSBP}$	lb/sec	247.1
Fuel Weight Flow	$\dot{w}_{FSBP}$	lb/sec	103.8
Total Weight Flow	$\dot{w}_T$	lb/sec	350.9
Fuel Suction Pressure	P_{FSBP}	psia	19.5
Oxidizer Suction Pressure	P_{OSBP}	psia	36.3

Secondary Combustor

Parameter	Symbol	Units	Value
Chamber Pressure, Plenum	P_{SC}	psia	2,800
Combustion Efficiency	η_c	-	96.3
Nozzle Efficiency	η_N	-	95.2
Mixture Ratio, Injector	MR_{SC}	-	2.20
Fuel Flow, Injector	$\dot{w}_{FSC}$	lb/sec	84.4
Gas Weight Flow to Injector	$\dot{w}_{GSC}$	lb/sec	247.9
Oxidizer Transpiration Cooling Flow	$\dot{w}_{OFC}$	lb/sec	18.6
Throat Area	A_{TSC}	$in.^2$	21.35

*Includes transpiration cooling.

TABLE III-II (cont.)

Secondary Combustor (cont.)

Parameter	Symbol	Units	Value
Area Ratio		-	20
Pressure Ratio (Sea Level)	R_{PSC}	-	190.5
Characteristic Length	L^*_{SC}	in.	35
Characteristic Velocity*	c^*_{SC}	ft/sec	5,481
Thrust Coefficient*	C_F	-	1.673

Primary Combustor

Parameter	Symbol	Units	Value
Chamber Pressure, Injector Face	P_{PC}	psia	4,918
Gas Temperature	T_{PC}	°F	1,156
Mixture Ratio	MR_{PC}	-	11.64
Oxidizer Flow	$\dot{w}_{OPC}$	lb/sec	226.2
Fuel Flow	$\dot{w}_{FPC}$	lb/sec	19.4
Propellant Total Flow	$\dot{w}_{TI}$	lb/sec	245.6
Characteristic Velocity	c^*_{PC}	ft/sec	2,332
Specific Heat Ratio	k_{PC}	-	1.2532
Molecular Weight	M_{PC}	lb/mole	34.1

*Based on geometric throat area and engine total flow.

TABLE III-II (cont.)

Secondary Combustor (cont.)

Parameter	Symbol	Units	Value
Area Ratio		-	20
Pressure Ratio (Sea Level)	R_{PSC}	-	190.5
Characteristic Length	L^*_{SC}	in.	35
Characteristic Velocity*	c^*_{SC}	ft/sec	5,481
Thrust Coefficient*	C_F	-	1.673

Primary Combustor

Parameter	Symbol	Units	Value
Chamber Pressure, Injector Face	P_{PC}	psia	4,918
Gas Temperature	T_{PC}	°F	1,156
Mixture Ratio	MR_{PC}	-	11.64
Oxidizer Flow	$\dot{w}_{OPC}$	lb/sec	226.2
Fuel Flow	$\dot{w}_{FPC}$	lb/sec	19.4
Propellant Total Flow	$\dot{w}_{TI}$	lb/sec	245.6
Characteristic Velocity	c^*_{PC}	ft/sec	2,332
Specific Heat Ratio	k_{PC}	-	1.2532
Molecular Weight	M_{PC}	lb/mole	34.1

*Based on geometric throat area and engine total flow.

TABLE III-II (cont.)

Main Turbopump - Pumps

Parameter	Symbol		Units	Value	
	Fuel	Oxidizer		Fuel	Oxidizer
Propellant Temperature	T_{FSM-1}	T_{OSM}	°F	78.8	79.8
Propellant Temperature	T_{FSM-2}		°F	93.8	
Propellant Specific Weight	γ_{FSM-1}	γ_{OSM}	lb/ft^3	56.0	89.4
Propellant Specific Weight	γ_{FSM-2}		lb/ft^3	56.5	
Shaft Speed	N_T	N_T	rpm	30,000	30,000
Total Suction Pressure	P_{FSM-1}	P_{OSM}	psia	90	168
Total Suction Pressure	P_{FSM-2}		psia	5,149	
Net Positive Suction Head	$NPSH_{FSM-1}$	$NPSH_{OSM}$	ft	224	244
Total Discharge Pressure	P_{FDM-1}	P_{ODM}	psia	5,500	5,818
Total Discharge Pressure	P_{FDM-2}		psia	6,170	
Head (noncavitating)	H_{FDM-1}	H_{ODM}	ft	13,897	9,102
Head	H_{FDM-2}		ft	2,598	
Weight Flow	$\dot{w}_{FSM-1}$	$\dot{w}_{OSM}$	lb/sec	110.6	266.2
Weight Flow	$\dot{w}_{FSM-2}$		lb/sec	20.7	
Volume Flow	Q_{FSM-1}	Q_{OSM}	gpm	886	1,337
Volume Flow	Q_{FSM-2}		gpm	164	
Ratio Pump to Engine Flow	$R_{\dot{w}FSM-1}$	$F_{\dot{w}OSM}$	-	1.065	1.078

TABLE III-II (cont.)

Main Turbopump - Pumps (cont.)

Parameter	Symbol		Unit	Value	
	Fuel	Oxidizer		Fuel	Oxidizer
Ratio Q/N	Q_{FSM-1}/N_T	Q_{OSM}/N_T	gpm/rpm	0.0295	0.0446
Ratio Q/N	Q_{FSM-2}/N_T		gpm/rpm	0.0055	
Specific Speed	N_{SFM-1}	N_{SOM}	$\frac{rpm\ gpm^{1/2}}{ft^{3/4}}$	697	1,777
Specific Speed	N_{SFM-2}		$\frac{rpm\ gpm^{1/2}}{ft^{3/4}}$	1,056	
Ratio $H/N^2 \times 10^6$ (noncavitating)	H_{FDM-1}/N_T^2	H_{ODM}/N_T^2	ft/rpm^2	15.44	10.11
Ratio $H/N^2 \times 10^6$	H_{FDM-2}/N_T^2		ft/rpm^2	2.89	
Efficiency	η_{FM-1}	η_{OM}	%	63.0	68.0
Efficiency	η_{FM-2}		%	55.0	
Shaft Power	SHP_{FM-1}	SHP_{OM}	hp	4,437	6,480
Shaft Power	SHP_{FM-2}		hp	180	
Suction Specific Speed	S_{FM-1}	S_{OM}	$\frac{rpm\ gpm^{1/2}}{ft^{3/4}}$	15,420	17,930
Suction Specific Speed	S_{FM-2}		$\frac{rpm\ gpm^{1/2}}{ft^{3/4}}$	315	

TABLE III-II (cont.)

Main Turbopump - Turbine

Parameter	Symbol	Units	Value
Pressure, Inlet Total	P_{TIT}	psia	4,784
Temperature, Inlet Total	T_{TIT}	°F	1,156
Pressure Ratio, Total to Static	R_{PT}	-	1,600
Static Back Pressure	P_{TES}	psia	3,654
Temperature, Exit Total	T_{TET}	°F	1,046
Gas Flow	$\dot{w}_{TI}$	lb/sec	245.6
Shaft Speed	N_T	rpm	30,000
Shaft Power	SHP_T	hp	11,097
Efficiency, Turbine	η_T	%	75.6

TABLE III-II (cont.)

Boost Pump - Pump

Parameter	Symbol		Units	Value	
	Fuel	Oxidizer		Fuel	Oxidizer
Propellant Temperature	T_{FSBP}	T_{OSBP}	°F	77	77
Propellant Specific Weight	γ_{FSBP}	γ_{OSBP}	lb/ft^3	56.1	89.5
Total Suction Pressure	P_{FSBP}	P_{OSBP}	psia	19.5	36.3
Net Positive Suction Head	$NPSH_{FSBP}$	$NPSH_{OSBP}$	ft	43.0	30.0
Shaft Speed	N_{FTBP}	N_{OTBP}	rpm	8,000	8,000
Total Discharge Pressure	P_{FDBP}	P_{ODBP}	psia	93	171
Head (noncavitating)	H_{FDBP}	H_{ODBP}	ft	188	218
Weight Flow	$\dot{w}_{FSBP}$	$\dot{w}_{OSBP}$	lb/sec	103.9	247.1
Volume Flow	Q_{FSBP}	Q_{OSBP}	gpm	831	1,239
Ratio Q/N	Q_{FS}/N_{FTBP}	Q_{OS}/N_{OTBP}	gpm/rpm	0.104	0.155
Specific Speed	N_{SFBP}	N_{SOBP}	$\frac{rpm\ gpm^{1/2}}{ft^{3/4}}$	4,545	4,966
Ratio H/N^2 (noncavitating)	$\frac{H_{FDBP}}{N_{FTBP}^2}$	$\frac{H_{ODBP}}{N_{OTBP}^2}$	$\frac{ft}{rpm^2}$	2.94×10^{-6}	3.40×10^{-6}
Efficiency, Pump	η_{FBP}	η_{OBP}	%	65.0	64.8
Shaft Power	SHP_{FBP}	SHP_{OBP}	hp	55	150
Suction Specific Speed	S_{FBP}	S_{OBP}	$\frac{rpm\ gpm^{1/2}}{ft^{3/4}}$	13,730	29,950

TABLE III-II (cont.)

Boost Pump - Hydraulic Turbine

Parameter	Symbol		Units	Value	
	Fuel	Oxidizer		Fuel	Oxidizer
Pressure, Inlet Total	P_{TITFBP}	P_{TITOBP}	psia	5,350	5,668
Temperature, Inlet Total	T_{TITFBP}	T_{TITOBP}	°F	93.8	94.9
Δ Pressure	ΔP_{TFBP}	ΔP_{TOBP}	psi	5,300	5,546
Static Back Pressure	P_{TEFBP}	P_{TEOBP}	psia	50	112
Flow, Turbine Drive	$\dot{w}_{FTBP}$	$\dot{w}_{OTBP}$	lb/sec	5.5	19.2
Shaft Speed	N_{FTBP}	N_{OTBP}	rpm	8,000	8,000
Shaft Power	SHP_{FTBP}	SHP_{OTBP}	hp	55	150
Efficiency, Turbine	η_{FTBP}	η_{OTBP}	%	40.5	49.9

TABLE III-III

ARES WEIGHT AND MOMENT OF INERTIA SUMMARY

Predicted Data, Calculated from Layout Drawing

Configuration: Mark I, Mod 1 (Inline TPA, Transpiration-Cooled TCA)

Component Assembly	Weight (Dry), lb	Moment of Inertia (Dry) About Gimbal, Slug ft^2
Turbopump	226.3	9.6
Primary Combustor, Injector, Valve and Line	63.6	6.0
Secondary Injector, Valve and Line	85.0	10.4
Thrust Chamber Assembly and Nozzle Extension	189.7	51.1
Boost Pumps (2)	36.0	1.7
Suction Valves and Propellant Inlet Housings (2)	62.0	4.0
Total	662.6	82.8

TABLE III-IV

ARES MATERIALS LIST

Configuration: Mark I, Mod I (Inline TPA, Transpiration-Cooled TCA)

Part	Material Surface Environment (Wall Temp, °F) Fuel	Oxid	Gas	Material (Alternates Shown in Parentheses)
1. Turbopump Housing	200°F	200°F	600°F	INCO 718
2. Turbopump Shaft	77	600	1000	INCO 718 (AM 355)
3. Turbine Nozzle	-	-	1200	Haynes 25 (713 C)
4. Turbine Rotor	-	600	1200	Forged Udimet 700 (Waspalloy)
5. Turbine Shaft Labyrinth	-	500	-	AM 355
6. Turbine Disc Nut	-	-	1000	AM 355
7. Turbine Exhaust Flow Distribution Plate	-	-	1200	Udimet 700 (Waspalloy)
8. Thrust Takeout Plate	77	-	-	AM 355
9. Fuel Pump, 1st Stage Impeller	77	-	-	17-4PH Cast, LC-1 Flame Plated
10. Fuel Pump, 1st Stage Backplate	77	-	-	AM 355, LC-1 Flame Plated Land
11. Fuel Pump, 1st Stage Inducer	77	-	-	Titanium 6Al-4Va
12. Fuel Pump, 1st Stage Inducer Housing	77	-	-	SS 347, LC-1 Flame Plated Land
13. Fuel Pump, 2nd Stage Impeller	100	-	-	AM 355
14. Fuel Pump, 2nd Stage Backplate & Retaining Nut	100	-	-	AM 355
15. Fuel Pump Labyrinth Inserts	100	-	-	Pressure Relieved Kynar
16. Fuel Pump Radial Bearing	200	-	-	SS 440C Rollers & Races, Glass-Filled Teflon Cages
17. Fuel Pump Thrust Bearing Sleeve, Retainers & Bolt	100	-	-	AM 355

TABLE III-IV (cont.)

Part	Material Surface Environment (Wall Temp, °F) Fuel	Oxid	Gas	Material (Alternates Shown in Parentheses)
18. Fuel Pump Thrust Bearings	200	-	-	SS 440C Races, K5H Balls, Glass-Filled Teflon Cages
19. Fuel Bearing Shaft Retaining Nut	77	-	-	AM 355
20. Interpropellant Seal	77	77	-	Carbon Stationary Ring, LC-1 Flame Plated, 440C Rotating Ring
21. Oxid Pump Impeller	-	200	-	17-4PH Cast, LC-1 Flame Plated Land
22. Oxid Pump Impeller Hydrostatic Seal	-	77	-	LC-1 Flame Plates SS 347
23. Oxidizer Pump Inducer	-	77	-	AM 355
24. Oxidizer Pump Inducer Nut	-	77	-	AM 355
25. Oxid Pump Radial Bearing	-	200	-	SS 440C Rollers & Races, Glass-Filled Teflon Cages
26. Oxid Pump Radial Bearing Retaining Nut	-	500	-	AM 355
27. Oxid Pump Inducer Insert	-	77	-	Graphite-Filled Vespo SP-21
28. Fuel Boost Pump Inlet Housing	77	-	-	SS 347
29. Fuel Boost Pump Discharge Housing	77	-	-	Al A356 Cast
30. Fuel Boost Pump Impeller	77	-	-	Al 7075-T73
31. Fuel Boost Pump Impeller Nut	77	-	-	Al 7075-T6
32. Fuel Boost Pump Shaft	77	-	-	AM 355
33. Fuel Boost Pump Bearing Housing	77	-	-	AM 355
34. Fuel Boost Pump Bearing	200	-	-	SS 440C Rolling Elements & Races, Glass-Filled Teflon Cages
35. Fuel Boost Pump Bearing Retaining Nuts	77	-	-	SS 347

TABLE III-IV (cont.)

Part	Material Surface Environment (Wall Temp, °F) Fuel	Oxid	Gas	Material (Alternates Shown in Parentheses)
36. Fuel Boost Pump Turbine Rotor	77	-	-	AM 355
37. Fuel Boost Pump Turbine Stators	77	-	-	AM 355
38. Oxidizer Boost Pump	-	77	-	Same materials as Fuel Boost Pump (Items 28 through 37)
39. Fuel Suction Valve Body	77	-	-	SS-17-4PH
40. Fuel Suction Valve Poppet	77	-	-	SS-17-4PH (AM 350)
41. Fuel Suction Valve Springs	77	-	-	SS-17-7PH
42. Fuel Suction Valve Poppet Seal	77	-	-	Teflon
43. Fuel Suction Valve Static Seals	77	-	-	Teflon
44. Fuel Suction Valve Shear Seal (Optional, Long-Term Storage)	77	-	-	SS 304L
45. Oxidizer Suction Valve	-	77	-	Same materials as Fuel Suction Valve (Items 39 through 44)
46. Primary Fuel Valve Body	100	-	-	Integral part of Primary Injector
47. Primary Fuel Valve Shaft	100	-	-	AM 350 (17-4PH)
48. Primary Fuel Valve Sleeve	100	-	-	SS-17-4PH (AM 350)
49. Primary Fuel Valve Bearings	100	-	-	440C
50. Primary Fuel Valve Dynamic Seals	100	-	-	Teflon
51. Primary Fuel Valve Static Seals	100	-	-	AS 4004 (Butyl)
52. Secondary Fuel Valve	200	-	-	Same materials as Primary Fuel Valve, except valve body is integral part of Secondary Injector

TABLE III-IV (cont.)

Part	Material Surface Environment (Wall Temp, °F) Fuel	Oxid	Gas	Material (Alternates Shown in Parentheses)
53. Primary Fuel Feed Line	100	-	-	MIL-T-6845 304
54. Secondary Fuel Feed Line	100	-	-	MIL-T-6845 304
55. Fuel Boost Pump Turbine Feed Line	100	-	-	MIL-T-6845 304
56. Oxidizer Boost Pump Turbine Feed Line	100	-	-	MIL-T-6845 304
57. Primary Injector	200	200	1200	SS 347
58. Adapter Turbopump/ Combustors	-	-	1200	INCO 718 (Hastelloy X)
59. Primary Combustor Liner	-	-	1200	Hastelloy X (René 62, INCO 718)
60. Secondary Injector	600	-	1200	SS 347
61. Secondary Combustor Washers	-	1625	-	SS 347 (Nickel)
62. Secondary Combustor Housing	-	300 Soakback	- -	Maraging Steel - 18% Nickel (Titanium)
63. Nozzle Extension, First Section	-	-	2200	Columbium (10 HF, 1 Ti)
64. Nozzle Extension, Second Section	-	-	1100	Titanium (5 Al, 2.5 Sn)

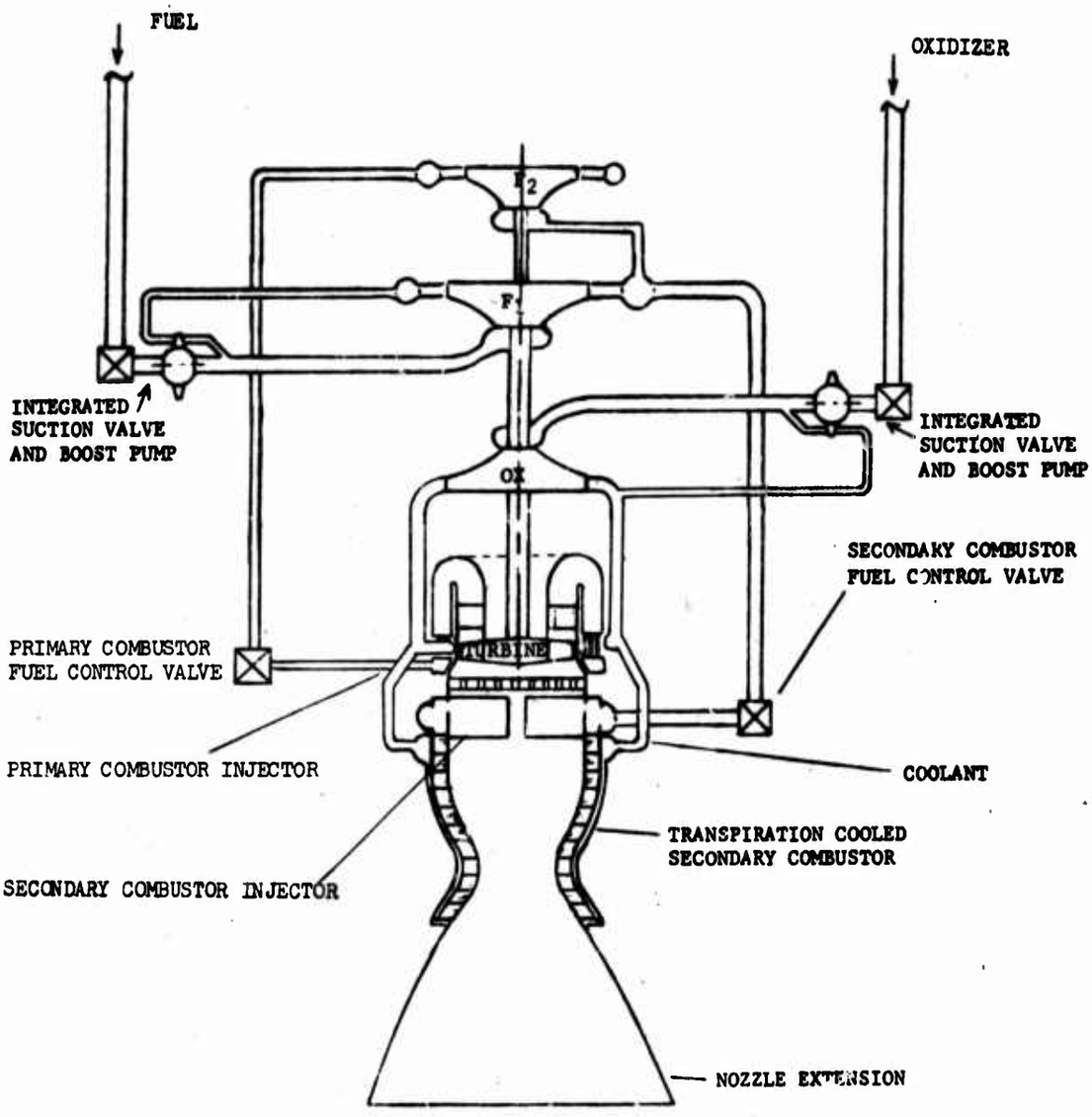

ARES Engine Schematic

Figure III-1

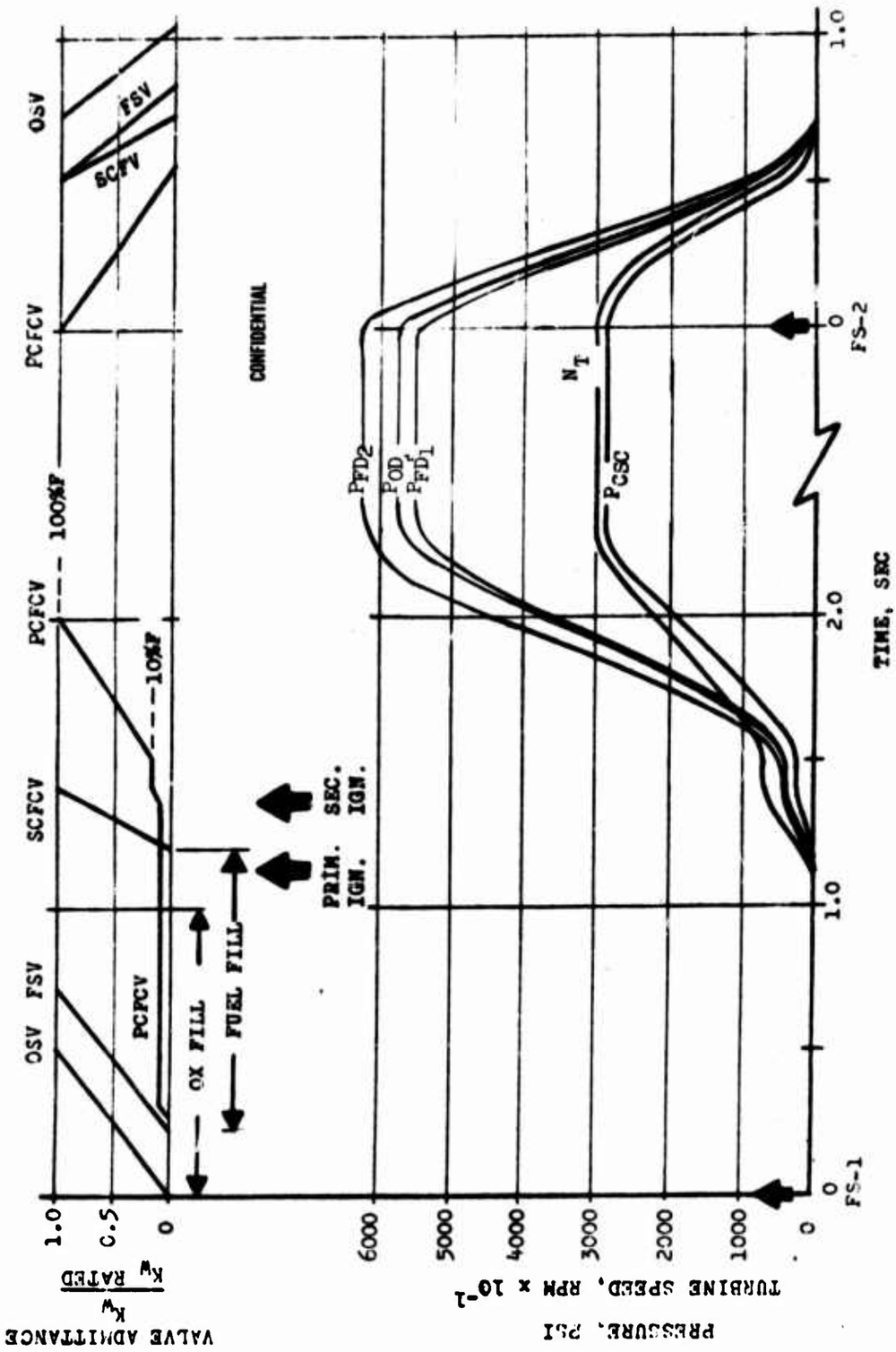

ARES Start and Shutdown (U)

Figure III-2

SECTION IV

TURBOPUMP ASSEMBLY

A. INTRODUCTION

(U) All Phase I effort relating to the TPA, with the exception of the hydrostatic combustion seal, was completed prior to the Phase I extension and is reported in the Interim Final Report. The Hydrostatic Combustion Seal Program was discontinued because of technical difficulties and the inline TPA was selected for the ARES engine. The inline TPA does not use the combustion seal.

(U) The results of that portion of the combustion seal program conducted during the Phase I extension are discussed in this section.

B. COMBUSTION SEAL PROGRAM

1. Background

(U) The ARES "T" engine configuration utilizes a seal between the fuel pump and the oxidizer-rich combustion gas, located just downstream of the turbine. The operating conditions are too severe to allow the use of a rubbing contact seal, however, the requirements for positive shutoff and possible restart necessitated the selection of a seal which would close tightly while inoperative. The combustion seal is a hydrostatic seal which was designed for this application. In operation, fuel is forced under pressure between the seal faces to prevent face contact. When shut down, the face contacts under spring load to provide a positive shutoff. When operating, part of the fuel between the seal faces discharges into the turbine exhaust where it is consumed in the oxidizer-rich gas. The remainder of the fuel flows inward to the fuel bearing cavity. Combustion of the fuel in the turbine exhaust region is controlled and metal parts protected by two streams of liquid oxidizer introduced upstream and downstream of the fuel entry, respectively.

IV, B, Combustion Seal Program (cont.)

(U) The ARES Phase I program included testing of the hydrostatic combustion seal, using a tester which provided oxidizer-rich gas, oxidizer and fuel under conditions expected in the ARES engine. The tester and seal are described in detail in the Phase I Interim Final report and is shown as installed in the test area in Figure IV-1. In order to simulate engine conditions with the tester, an intricate sequencing of a combination of pressures, flows, and speed was required. Several tests were terminated as a result of system malfunctions because of the complexity of the test setup.

2. Objective

(C) The prime objective for the hydrostatic combustion seal program was the demonstration of the prototype seal under simulated ARES engine operating conditions for 60 seconds. The seal had to be reusable at the completion of the test. All tests conducted in this program are summarized in Figure IV-2.

(C) The test condition goals were:

Operating pressure	3100 $\pm$ 600 psi	Gas Temperature	1100 $\pm$ 50°F
Pressurizing time	0.75 to 1.25 sec	Speed	40,000 RPM
Acceleration time	1.0 to 1.5 sec	Gas Velocity	200 to 250 fps

Duration: 60 sec including 50 sec at 40,000 RPM

3. Status Prior to Phase I Extension

(U) At the conclusion of Phase I, prior to the extension, 11 hot rotating tests had been completed on several seals (Tests 004-014 Figure IV-2). These tests are described in the Interim Final Report, the accomplishments are summarized as follows:

IV, B, Combustion Seal Program (cont.)

Hot Rotating Tests Completed:	11
Total Combustion Duration:	82.25 sec
Total Rotation Time:	
Over 30,000 rpm	29.65 sec
Over 35,000 rpm	21.25 sec
40,000 $\pm$ 500 rpm	4.1 sec

(U) At the conclusion of Phase I, it appeared that the seal and tester design had been optimized to the point that the only remaining task was to reach the program objective of 60 sec operating time. Phase I was extended in order that this could be done.

4. Phase I Extension Tests

(U) Beginning with Test 15, a total of six tests were conducted during the Phase I extension (Tests 015-020 Figure IV-2). The first three tests were terminated because of system malfunctions with no apparent hardware damage. Test 18, after 9.1 sec operation, was stopped because of a spike in chamber pressure. Posttest examination revealed damage to the rotating ring, seal face and burnoff shield. This apparently resulted from oxidizer penetration across the seal face during startup, which heated the rotating ring until it cracked, rubbed, and ignited in the oxidizer-rich atmosphere. The burnoff shield was redesigned so that the downstream oxidizer was deflected at an angle of about 45° outward, eliminating the tendency to force the seal effluent upstream. Test 19 far exceeded any previous duration, but terminated in an explosion after 29.7 sec. During Test 19, combustion just downstream of the seal face resulted in gradual burning of the seal stationary face and burnoff shield and eventually caused a bellows failure.

IV, B, Combustion Seal Program (cont.)

(U) Test hardware for Test 20, the final test, was significantly modified (Figure IV-3), so that upstream and downstream oxidizer streams were introduced to impinge immediately above the seal face, in the same manner as an annular triplet injector. Additionally, the conical portion of the rotating ring was removed. A further modification was incorporated to maintain a fixed gap between the upstream oxidizer supply housing and the rotating ring. The upstream oxidizer supply housing was also cooled and insulated to minimize thermal distortion. Test 20 was terminated after 4.7 sec, followed by an explosion resulting from a bellows failure. The pressure unbalance which stopped the test was a sudden decrease in chamber pressure and increase in seal pressurization pressure. At the same time, there was a disproportionate increase in outflow from the seal cavity, which could only have resulted from the evolution of gas at the seal face. The seal face was not severely burned, as would be expected with N_2O_4/AeroZINE 50 combustion, but the outer land was scored as if from rubbing. Apparently the AeroZINE 50 in the outer land of the seal face started decomposing during the test. The heat from this was sufficient to expand the seal face so that contact occurred during shutdown. After shutdown, and after the fuel was purged, oxidizer entered the seal bellows, contacted the residual fuel in the bellows torus, and burst the bellows, causing minor damage. There was no evidence of thermal damage to the exterior of the seal, aside from the effect of the explosion in the bellows.

5. Conclusions and Recommendations

(U) In two tests, the seal and running ring were eroded symmetrically and smoothly, back nearly to the fuel pockets. In three tests, there is evidence that the fuel decomposed within the seal faces. This is strong evidence of fuel rich burning near the surface. This probably resulted because the net oxidizer impingement angles were insufficient to hold burning off the surface. The relatively high velocity turbine exhaust oxidizer stream

IV, B, Combustion Seal Program (cont.)

probably aggravated this condition. Experimental development, wherein the relative momentum and injection angles of the propellants is varied, is needed to solve this problem.

(U) There were several instances of bellows failure. Initially, manufacturing problems were encountered. However, these appeared to be solved by the end of the program. Other bellows failures were directly attributable to other failures that occurred prior to the bellows failure. Therefore, it can be concluded that the bellows design is satisfactory.

(U) Flame plating on the seal face was observed to fail in a number of instances. Therefore, improved flame plating quality or an alternative process is needed to achieve an acceptable reliability level.

(U) The testing setup was designed to accurately simulate engine transient conditions. This resulted in an extremely complex hardware arrangement and contributed to several test malfunctions. Redesign of this test setup towards simplicity, even at the expense of accurately simulating the start transient, is strongly recommended if further feasibility testing is undertaken.

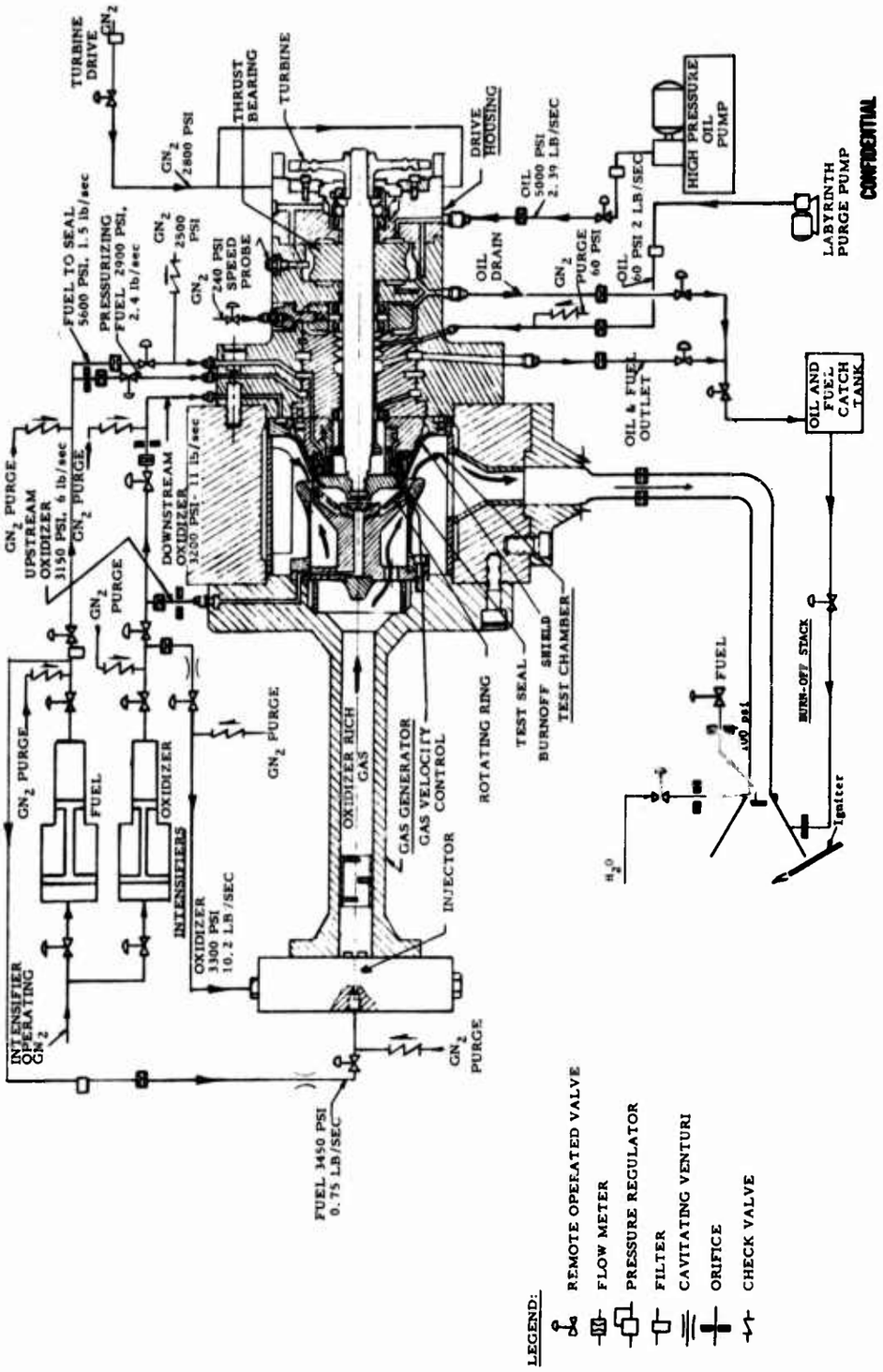

Flow Diagram, Hot Tests (u)

Figure IV-1

TEST NO	DATE	OBJECTIVE	DURATION, SECONDS FS_1 FS_2	RAMP	ROTATION TIME AT RPM 30,000	35,000+	40,700	PREBURNER FLOW LB/SEC FUEL	OXID	M/R	TEMP °F	PRESS PSI	SEALS FLOWS LB/SEC FUEL TOTAL FLOW	FUEL OUT FLOW	OXIDIZER UP STREAM	OXIDIZER DOWN STREAM	M/R	HOUSING TEMP °F	HOUSING PRESS PSI	COMMENTS	RATING
PREBURNER CHECKOUT																					
001	2-8	CALIB. OXID FLOW	73	0.7	NO SEAL USED			0	9.5	-	-	-	NO SEAL USED					-	-	CORRECTED CAVITATING VENTURI	SUCCESS
002	2-8	CALIB FUEL FLOW	18	0.9				0.88	0	-	-	-						-	-	LEAK IN SYSTEM	PARTIAL SUCCESS
003	2-8	CALIB FUEL FLOW	112	0.75				0.88	0	-	-	-						-	-	CORRECTED CAVITATING VENTURI	SUCCESS
004	2-17	HOT START AT 650PSI	4	0.7				0.8	10.5	13.1	1140	3600						1050	3600	SMOOTH OPERATION	SUCCESS
005	2-18	HOT START AT 250 PSI	.8	-				-	-	-	-	-						-	-	SAFETY SHUTOFF SET TOO LOW	PARTIAL SUCCESS
006	2-18	HOT START AT 250 PSI	10	0.7				0.45	9.4	20.9	550	2000						500	2000	OBSTRUCTION IN FUEL VENTURI NOZZLE	PARTIAL SUCCESS
007	2-18	HOT START AT 60 PSI	15	0.7				0.9	10.5	11.7	1300	3200						1150	3200	ALL OBJECTIVES REACHED	SUCCESS
SEAL DISTORTION																					
001	7-21	STATIC CHECKOUT	15.2	0.7	NO ROTATION			0.87	8.96	10.3	3200+	4740	1.54 (N_2O_4)		1.61	2.89	-	3200+	4100	OPERATED AT HIGH PREBURNER PRESSURE. COMBUSTION DAMAGE TO INJECTOR AND GAS SHROUD	PARTIAL SUCCESS
002	7-25	STATIC CHECKOUT	2.72	0.7				0.72	9.52	13.2	1100	2900	2.7 (N_2O_4)		2.24	4.11	-	1170		TEST TERMINATED BY FAULTY THERMOCOUPLE	PARTIAL SUCCESS
003	7-26	STATIC CHECKOUT	48.2	0.7				0.73	9.64	13.2	1100	3055	2.71 (N_2O_4)	0.95	2.24	4.12	-	1100	3100	FULL DURATION. ALL OBJECTIVES REACHED	SUCCESS
HOT ROTATING			FS1-RPM0																		
004	7-29	SHORT CHECKOUT	3.35	.3	0	0	0	0.72	8.9	13.6	1000	2760	3.5	3.5	2.50	4.20	1.7	3200+	3200	INTERPROPELLANT EXPLOSION DURING FILL. EXTENSIVE DAMAGE TO TEST CHAMBER. SPEED TO 20,000 RPM	FAILURE
005	9-16	SHORT CHECKOUT	5.5	.85	0	0	0	0.75	10.1	13.4	1100	3720	1.74	1.23	2.14	4.45	6.8	1508	3690	SHUTDOWN BECAUSE OF HIGH INTERNAL PRESSURE	PARTIAL SUCCESS

Figure IV-2
Sheet 1 of 2

Test Summary Sheet, ARES Hydrostatic Combustion Seal (u)

TEST NO.	DATE	DURATION, SECONDS					FLOW LB/SEC					SEALS					HOUSING		COMMENTS
		F_{O_2} RPM=0	PAMP	ROTATION TIME AT RPM 30,000+	25,000+	20,000	FUEL	OXID	M/R	TEMP °F	PRESS PSI	FLOWS LB/SEC FUEL TOTAL FLOW	FUEL OUT FLOW	OXIDIZER UP STREAM	OXIDIZER DOWN STREAM	M/R	TEMP °F	PRESS PSI	
006	9-17	6.3	.8	0.1	0	0	0.75	10.2	13.4	1085	3240	1.83	0.78	3.58	7.32	13.7	762	3200	RESTART. SHUTDOWN BECAUSE OF HIGH INTERNAL PRESSURE. RESIZED FUEL PRESSURIZING ORIFICE.
007	9-17	6.4	.8	0.3	0	0	0.75	10.1	13.4	1100	2950	2.0	0.69	3.50	7.75	14.0	820	2900	RESTART. SHUTDOWN BECAUSE OF LOW INTERNAL PRESSURE. RESIZED FUEL PRESSURIZING ORIFICE.
008	9-17	15.5	.8	9.6	7.25	0	0.75	10.2	13.4	1100	3070	2.15	0.82	3.60	7.30	12.7	940	3030	RESTART. SHUTDOWN BECAUSE OF BURNOFF AREA EROSION ATTRIBUTED TO FAULTY CHAMBER LINER. SLIGHT DAMAGE. ALL PARAMETERS OK EXCEPT SPEED WAS LOW.
009	10-14	6.0	.85	.05	0	0	0.75	10.2	13.4	1100	3080	1.5	0.47	2.88	5.93	14.7	900	3080	SHUTDOWN BECAUSE OF COMPUTOR MALFUNCTION. VISUAL HARDWARE INSPECTION, O.K. RESET COMPUTOR.
010	10-14	3.0	.85	0	0	0	0.74	10.2	13.8	1050	4800	2.8	1.1	3.05	5.87	8.0	2500	4800	RESTART. SEAL FACES SEPARATED DURING FILL DUE TO SURFACE CONTAMINATION. EXPLOSION DURING FILL. EXTENSIVE DAMAGE TO TESTER AND STAND.
011	11-12	10.3	.85	5.95	5.6	3.2	0.75	10.1	13.5	1100	3120	1.5	0.46	1.9	5.1	15.2	1000	3100	EVIDENCE OF FUEL DECOMPOSITION AT SEAL FACE. UNBALANCE VIBRATION ALSO DETECTED. TEST TERMINATED BY BELLOWS FAILURE
012	11-23	6.4	.75	3.45	2.1	0.9	0.75	10.0	13.3	1050	3020	1.6	0.52	0	5.45	10.4	1050	2880	ASSEMBLY ERROR CAUSED NO UPSTREAM OXIDIZER. BELLOWS FAILED FROM HIGH TEMPERATURE. SEAL AND TESTER DAMAGED. BURNOFF SHIELD FAILED BECAUSE OF HIGH TEMPERATURE.
013	12-18	9.2	.90	3.6	0	0	0.74	10.6	13.3	1080	3180	1.43	0.41	5.25	11.1	40	540	3150	NEW DESIGN BURNOFF SHIELD CRACKED AT SLOTTED TIP. NO DAMAGE. SHIELD REDESIGNED TO REPLACE SLOTS WITH RADIAL HOLES AT TIP.
014	1-19 1967	10.3	.95	6.6	6.3	0	0.77	10.2	13.3	1100	3370	1.7	0.43	5.9	10.1	37.2	600	3320	UPSTREAM VELOCITY CONTROL BOLT FAILED. SLIGHT COMBUSTION DAMAGE. SEAL REUSABLE. NEW SHIELD O.K. REDESIGNED VELOCITY CONTROL TO ELIMINATE BOLTS.
015	2-16	0	1.10	0	0	0	0.74	9.80	13.2	1050	3300	1.53	0.43	5.42	10.4	36.8	500	3250	TURBINE SPIN VALVE FAILED TO OPEN. NORMAL SHUTDOWN. RESTART AFTER INSPECTION SHOWED NO DAMAGE.
016	2-20	5	1.05	1.0	0	0	0.74	10.2	13.8	1050	3250	1.75	0.43	5.9	10.8	39.0	530	3200	VIBRATION OPENED LUBE OIL PRESSURE SWITCH. VISUAL INSPECTION OK. LEAK TEST INDICATED POSSIBILITY OF FLAME PLATING FAILURE, PURGE CORRECTED IT. REPLACED FAULTY SWITCH.
017	2-23	5.5	1.0	4.0	3	0	0.74	10.2	13.8	1050	3250	1.75	0.43	5.9	10.8	39.0	530	3200	COMPUTER MISRANGE CAUSED MALFUNCTION SHUTDOWN. SEAL EXTERNALLY CHECKED FOR LEAK. LEAK APPARENT, BUT DISAPPEARED AFTER GN_2 PURGE. NO VISUAL INSPEC.
018	2-24	9.1	1.0	5.3	5.1	2.7	0.75	10.2	13.4	1040	3230	1.50	0.43	6.1	10.5	38.6	546	3160	TEST TERMINATED BY EMERGENCY SHUTDOWN WHEN CHAMBER PRESSURE SPIKED. ROTATING RING, UPSTREAM DIFFUSER, SEAL FACE DAMAGED. EVIDENCE OF RUB. NO TESTER DAMAGE.
019	4-6	29.7	1.0	25.7	25.5	24.3	0.78	10.2	13.1	1140	3300	1.50	0.43	6.0	11.3	40.7	600	3240	DOWNSTREAM OXIDIZER SUPPLY WAS MOVED TO .080 IN. BEHIND SEAL FACE. COMBUSTION STARTED IMMEDIATELY BEHIND SEAL FACE. HEATED AND CRACKED ROTATING RING, DESTROYED OUTLET EDGE OF SHIELD, AND CAUSED BELLOWS RUPTURE. MODERATE TESTER DAMAGE. EVIDENCE OF FUEL DECOMP. IN SEAL FACE. SHUTDOWN BECAUSE OF PRESS. UNBALANCE. DURING SHUTDOWN, OXIDIZER ENTERED SEAL. RUPTURED BELLOWS. TESTER UNDAMAGED.
020	5-26	5.6	1.0	2.2	2.0	1.6	.77	10.0	13.0	1150	3600	1.60	0.46	8.6	10.7	45.0	650	3500	

Test Summary Sheet, ARES Hydrostatic Combustion Seal (u)

Figure IV-2
Sheet 2 of 2

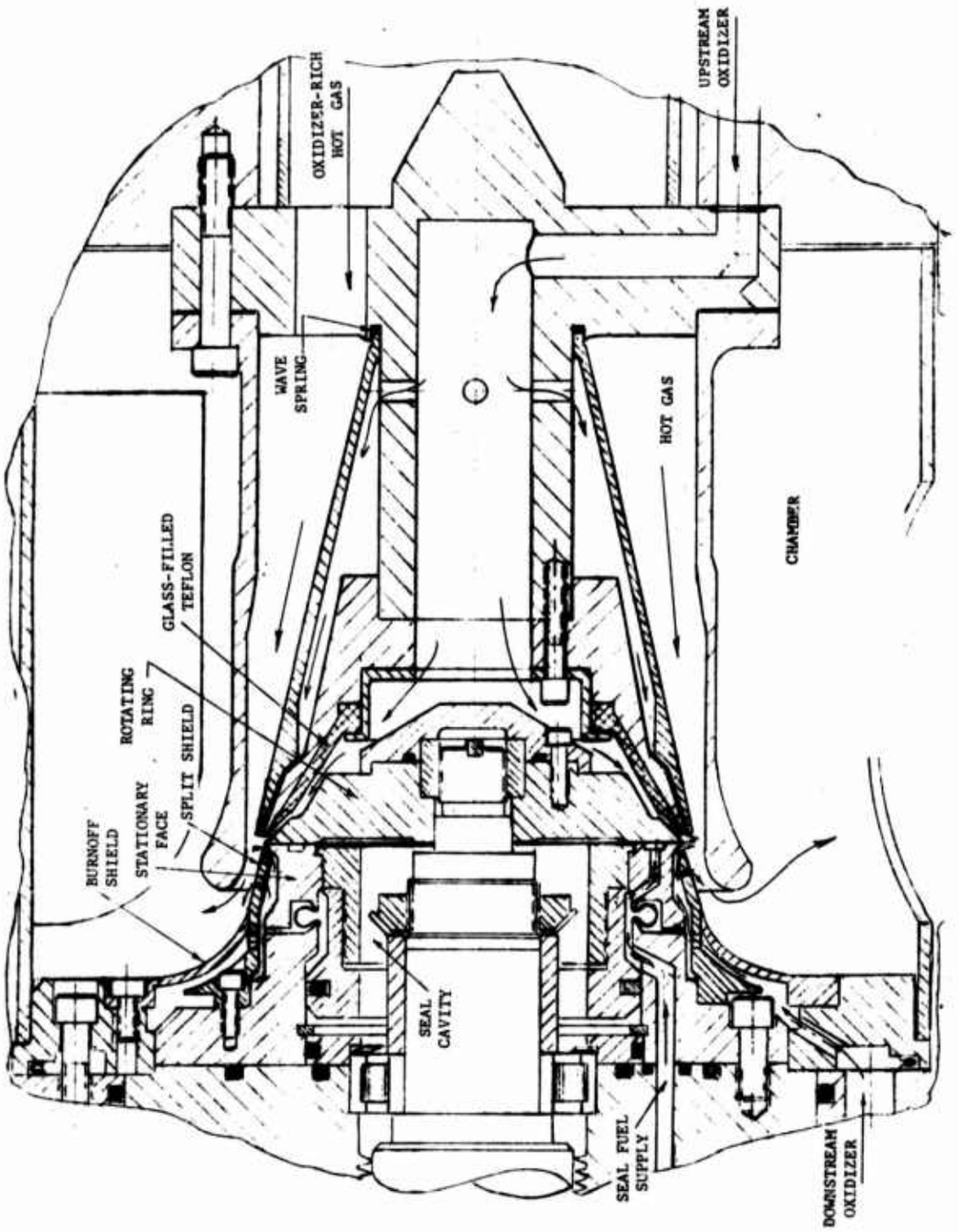

Hardware Configuration for Test 20

Figure IV-3

SECTION VI

SECONDARY COMBUSTOR PROGRAM

A. OBJECTIVE

(C) The objective of the secondary combustor program was to demonstrate a minimum delivered sea-level specific impulse of 280 sec during each of three or more tests of 20-sec minimum duration, and with the following conditions:

Thrust:	100,000 $\pm$ 5000 lb
Chamber Pressure:	2800 $\pm$ 140 psia
Area Ratio:	20:1 (80% bell nozzle contour)
Propellants:	N_2O_4/0.5 hydrazine - 0.5 UDMH

(U) The injector used in these tests had to achieve a minimum duration of 0.5 sec of steady-state operation in an uncooled thrust chamber with steady-state chamber pressure oscillations not exceeding $\pm$ 5% of the average chamber pressure value. Also, the injector had to be capable of refire without repair.

VI, Secondary Combustor Program (cont.)

B. SUMMARY

(U) The Phase I TCA program was initiated in July 1965 and successfully concluded in January 1968. A program schedule showing the major items of work is given in Figure VI-1.

(C) The first nine months of the program were devoted primarily to the design and fabrication of test hardware, of which the secondary injectors and cooled chambers were the major components. Also during this period, residual hardware from the preceding exploratory development program, "Integrated Components Program," Contract AF 04(611)-8548, was tested to provide design data for the ARES configuration hardware. This hardware was designed for operation at 2770 psia chamber pressure and 100,000-lb thrust, virtually the same as the ARES specification. The test program consisted of 13 valid test firings, nine for injector evaluation and four for regeneratively cooled chamber evaluation.

(C) Testing with the ARES secondary injectors was initiated in March 1967. Twenty-four tests were conducted with two injectors, designated the Fuel Rake and Mark 125. These tests culminated with the selection of the Mark 125 injector for cooled chamber testing. Testing with cooled chambers started in August 1966; two cooling concepts were evaluated, including the regenerative and transpiration cooling systems. The transpiration-cooled chamber proved to be the better of the two and testing with the regenerative chamber was discontinued after five tests. Thirty tests were conducted with the transpiration-cooled chamber, during which the transpiration coolant was selectively reduced in an effort to optimize performance. The required Phase I performance and duration requirements were not attained at this time because of an incompatibility problem with the Mark 125 injector. When coolant flow was reduced to about 36 lb/sec, at which point performance was at approximately 86% I_s, chamber burnout repeatably occurred. Fuel from the

VI, B, Summary (cont.)

injector impinging on the chamber wall was the cause of the problem. It was concluded that a redesign of the injector pattern would be required before the performance and durability requirements could be demonstrated.

(U) A one year extension to the Phase I program was granted to complete the thrust chamber objectives. All effort up to this time was reported in detail in the ARES, Phase I Interim Final Report[1]. The technical effort performed during the extended Phase I period, which commenced on 1 February 1967, is reported here.

(C) The extended Phase I effort centered upon the development of a nonstreaking secondary injector. Two modifications to the Mark 125 injector and two new injector concepts were test-evaluated during this period. One of the new concepts, designated the Impinging Platelet Injector, successfully achieved the established performance and compatibility criteria and was selected for cooled chamber testing. One of these injectors was used in 41 tests for a total accumulated duration of 197 sec. The injector development effort is fully discussed in Section VI,B, of this report. In support of the secondary injector program, two supporting studies of major significance were performed: (1) an analytical study in support of the streak-free injector design effort (2) and a laboratory air-flow test program which led to several improvements in the engine test system. These efforts are discussed in detail in Section VI,E, of this report.

(C) Using the impinging platelet injector, testing was resumed with the transpiration cooled chamber. A total of 46 tests were conducted with three chambers, including six tests of 20-sec duration and a total accumulated duration of 220 sec. At the conclusion of the test series, four tests had been conducted above the contractually required performance level of 90% I_s,

(1) ARES, Phase I Interim Final Report, AFRPL-TR-67-75, August 1967

VI, B, Summary (cont.)

one of these a 20-sec duration test. The highest performance level achieved was 281 sec, which is 90.3% I_s. In addition, three additional tests of 20-sec duration were conducted at a performance level of approximately 89% I_s. Shortage of cooled hardware prevented the demonstration of two additional 20-sec duration tests at the 90% I_s level. The cooled chamber program is discussed in detail in Section VI,D.

VI, Secondary Combustor Program (cont.)

C. SECONDARY INJECTOR PROGRAM

1. Introduction

(C) The objective of the Secondary Injector Program was to develop a high performance, stable, mechanically sound injector suitable for use with the modular cooled secondary combustor chamber. The success criteria for this effort, as defined in the contractual work statement, was that the injector selected for test with cooled thrust chambers must have achieved a minimum duration of 0.5 sec of steady-state operation in an uncooled thrust chamber with steady-state chamber pressure oscillations which shall not have exceeded ±5% of the average chamber pressure value. Additionally, the hardware must be in refirable condition at the conclusion of the test.

(U) The Mark 125 secondary injector was developed during the basic Phase I period of the ARES program. This injector had high performance and good stability characteristics, and satisfied all secondary injector requirements prior to cooled chamber testing as set forth by the contractual work statement. Subsequent testing with the transpiration-cooled chamber revealed a compatibility problem between the injector and the chamber. When the transpiration coolant was reduced in successive steps to increase secondary chamber performance, a streaking condition became evident on the chamber wall which, during two tests, progressed to metal erosion and subsequent destruction of the transpiration-cooled chambers. The streaks were caused by direct impingement of fuel from the injector tubes onto the chamber wall. It was concluded that because of this streaking problem, attainment of the required performance level with the Mark 125 injector was not possible, and that the injector must be changed before the Phase I requirement could be completed.

VI, C, Secondary Injector Program (cont.)

(U) The basic development task during the extended Phase I period was to develop an injector which would be compatible with the transpiration-cooled chamber while still maintaining high performance and good stability characteristics. Two parallel approaches were pursued to solve this problem. The first was to modify the Mark 125 injector to eliminate the impingement of fuel on to the chamber wall; the second was to test new injector concepts designed specifically for optimum injector and chamber compatibility. This effort was successfully concluded with the development of a new injector, termed the Impinging Platelet Injector. Using this injector and the transpiration-cooled chamber, operation at the contractually required performance level was demonstrated in each of four tests, one of which was of 20-sec duration. A summary of the extended Phase I effort is given in Section VI,C,2. Details of the injector designs and supporting test hardware are discussed in Sections VI,C,3 and VI,C,4. The development test program performed and the test results are given in Section VI,C,5.

2. Summary

(U) The Mark 125 injector developed during the basic Phase I program is shown in Figure VI-2. Testing with this injector yielded substantial data and general insight relative to performance and compatibility characteristics of high pressure staged-combustion injectors. Also, during this same time period, new mathematical models were developed by Aerojet in which the performance and compatibility characteristics of a rocket injector are scientifically defined and in a form so that they can be analyzed quantitatively. Using these new analytical techniques, the experience gained with the Mark 125 injector, and a mechanical design study of new injectors, a redesign of the ARES secondary injector to eliminate the previously encountered compatibility problem was initiated. A complete discussion of the analytical effort is given in Section VI,E,1.

VI, C, Secondary Injector Program (cont.)

(C) From this combined study, two modifications to the Mark 125 injector and two new injector concepts were selected for test evaluation in the extended Phase I program. Both modifications to the Mark 125 injector were directed at eliminating the impingement of fuel on the chamber wall. The first consisted of removing the outer three rows of tubes from each vane and replacing them with a much larger number of smaller axially directed tubes. The new tube assembly had the appearance of a miniaturized candelabra, and the injector became known as the Mark 125 candelabra design. A photo of this injector is shown in Figure VI-3. The second modification to the Mark 125 injector consisted of replacing the outer three rows of tubes with a single row of axially directed tubes. In this design the size and number of tubes remained equal to that of the original design. This injector, shown in Figure VI-4, was known as the Mark 125 3 ORST configuration (3 Outer Rows Straight).

(C) The first new injector concept, designated the WARP injector, is shown in Figure VI-5. This injector incorporates a face plate to precisely control the oxidizer gas flow distribution at the plane of fuel injection. In the face plate are drilled approximately 750 holes, the downstream sides of which are machined into the shape of divergent cones. Fuel is injected through axially directed tubes located in the center of each hole; the oxidizer gas flows through the face plate in the annular spaces between drilled holes and the fuel tubes. The cones in the face plate are made to overlap at their bases, leaving no flat face area for gas recirculation.

(C) The second new injector concept, shown in Figure VI-6, is called the Platelet injector. The injector consists of 88 vanes, 1/8 in. thick, arranged into eight symmetrical groups of 11 vanes each. Uniform propellant distribution is achieved by locating the longest vane in each of eight groups radially and the remaining vanes in each group parallel to it, so that a constant-width oxidizer gas passage remains between vanes. Each vane is composed of a left hand and right hand 1/16-in. platelet, which are brazed

VI, C, Secondary Injector Program (cont.)

together to form the finished vane. The inner sides of each platelet have matched chemically etched passages which form the internal fuel circuit when the halves are joined together. The fuel circuit passages were designed in two alternative injection patterns. In the first design, all fuel exits from the vanes in an axial direction, giving a showerhead pattern. In the second design, the exit orifices are arranged in pairs which impinge at an included angle of 60 degrees. The fuel is impinged upon itself as it leaves the vane, which causes the fuel streams to break up into a fine fuel fog.

(C) The injector evaluation test program was initiated 14 March 1967 and concluded 11 October 1967. Twenty-seven tests were conducted during this period, of which all yielded valid data. The test program included one test with the Mark 125 candelabra injector, four tests with the Mark 125 3 ORST injector, five tests with the WARP injector, eight tests with the showerhead platelet injector, and nine tests with the impinging platelet injector. Nominal chamber pressure and mixture ratio for all tests were 2800 psia and 2.2, respectively. A cumulative summary for all testing is shown on Figure VI-7. A nomenclature list of the tabulated quantities is given in Figure VI-8. A representative oscillograph showing the major test parameters is given in Figure VI-9.

(C) Structural problems were encountered during testing with the Mark 125 candelabra and WARP injectors. With the former, approximately 30% of the candelabra elements failed on the first test and testing with this concept was discontinued. In the initial tests with the WARP injector, the joint between the face plate and its support ring failed; this joint was subsequently redesigned and proven satisfactory. However, erosion around the periphery of the face plate occurred, which would have to be corrected by additional development effort. At this time the platelet injectors were operating very satisfactorily, so no further effort was performed with the WARP injector. Testing with the Mark 125 3 ORST design indicated that the fuel impingement problem

VI, C, Secondary Injector Program (cont.)

with the basic Mark 125 had been corrected; however, the fuel pattern was still considerably coarser than with the Platelet designs, which gives the fuel a greater chance to burn with the transpiration coolant before being completely vaporized. On the basis of the success with the Platelet injectors, work was also terminated with this injector.

(C) Both the showerhead and impinging platelet injectors were structurally sound, stable, and high performing. The performance and compatibility of both injectors was evaluated in a special test series designed specifically for that purpose. Uncooled ablative-lined chambers with steel exit nozzles were used for performance evaluation; film-cooled ablative chambers and a special chamber transpiration-cooled in the cylindrical section with a film-cooled ablative throat section were used for the compatibility evaluation. The impinging injector proved to have higher performance and better compatibility characteristics, which is primarily attributed to the better fuel atomization produced by the impinging fuel jets. On the basis of the results of this test program, the impinging platelet injector was selected for cooled chamber testing.

(U) Concurrent with the injector test program, an air-flow laboratory program was performed to determine the oxidizer gas distribution at the plane of fuel injection. For this study, the engine system beginning with the primary combustion chamber and extending through the secondary injector was mocked up in the air flow test laboratory using full-scale hardware. Initial results disclosed that the oxidizer gas entering the secondary injector was highly skewed and cored. This was largely caused by the unsymmetrical turbulators in the primary combustion chamber (which are used to promote mixing). Replacement of these turbulators with ones of symmetrical cross-section eliminated the skewing problem; however, the radial gas distribution was still uneven. The program was therefore directed toward the development of flow distribution devices for tailoring the radial flow distribution to the desired

VI, C, Secondary Injector Program (cont.)

condition. The final configuration selected was a pressure drop plate installed at the secondary injector inlet, with holes selectively sized to give the proper gas distribution entering the injector. As a result of this effort, the test engine was modified to incorporate the symmetrical turbulators and flow distribution plate. A complete discussion of the air-flow test program is given in Section VI,E,2.

(U) While the oxidizer gas distribution was greatly improved by incorporation of the changes discussed above, all maldistribution has not been eliminated. As the gas passes through the injector, it is redirected because of the body and vane designs such that it is not circumferentially uniform at the plane of fuel injection. With the platelet injector, this results in relatively low oxidizer gas flow in the eight long vane areas, producing local hot zones in eight circumferential locations around the chamber wall. A redesign of the injector has been made which should completely eliminate this problem; however, the Phase I program time schedule did not permit incorporating this improvement into the test hardware. As a result, some over-cooling of the entire transpiration-cooled chamber was required in the transpiration-cooled chamber test program to provide sufficient cooling for these eight hot zones. Considerable reduction in chamber cooling requirements is anticipated when the injector is changed to correct this problem.

(C) The success criteria for the secondary injector program, as defined in the contractual work statement, was that the injector selected for testing with the cooled thrust chamber must have achieved a minimum duration of 0.5 sec of steady-state operation with steady-state chamber pressure oscillations not exceeding $\pm 5\%$ of the average chamber pressure. Also, the injector must be in refirable condition following the test. These requirements were fulfilled in Test 1.2-16-WAM-019 with the Impinging Platelet injector. In this test, the injector operated at steady-state for 0.94 sec at an average chamber pressure of 2711 psia. Chamber pressure oscillations during the test

VI, C, Secondary Injector Program (cont.)

did not exceed ±1.07% of average chamber pressure. The injector was in perfect condition following the test.

(C) The durability of the Impinging Platelet injector was conclusively proven in the subsequent cooled chamber test program. By the conclusion of that program, a single injector (SN 3), had been used in 41 tests with a total accumulated duration of 197 sec. Five of these tests were of 20-sec duration.

3. Injector Design

(U) At the conclusion of the basic Phase I period, the compatibility of injectors with cooled chambers was recognized as the only known thrust chamber problem remaining to be resolved to complete ARES Phase I contractual requirements. Testing with the Mark 125 injector had provided considerable data and general insight relative to the performance and compatibility aspects of high-pressure staged-combustion injectors. Concurrently with this testing, new mathematical models were developed by Aerojet in which injector performance and compatibility can be quantitatively analyzed. Using these new analytical techniques, together with the experience gained with the Mark 125 injector and a mechanical design study of new injectors, a redesign of the ARES secondary injector was initiated.

(U) As a result of this effort, two modifications to the Mark 125 injector, and two new injector concepts were selected for detail design and test evaluation. These injectors were commonly known as the Mark 125 candelabra injector, the Mark 125 3 ORST injector, the WARP injector, and the platelet injector. Design descriptions for each of these injectors are given in this section. The analytical study performed in conjunction with the mechanical design effort is presented as a consolidated discussion in Section VI,E,1.

VI, C, Secondary Injector Program (cont.)

a. Modifications to the Mark 125 Injector

(1) Candelabra Configuration

(C) The basic Mark 125 injector is shown in Figure VI-2. The "Candelabra" modification consisted of removing the outer three rows of tubes from each vane and cutting each vane back 0.300 in. from the trailing edge in the area where tubes had been removed. Tee-shaped manifolds were made from 0.093 in. dia x 0.016 in. wall tubing. To each tee manifold, six 0.062 in. dia x 0.016 in. wall injection tubes were attached. These welded tube assemblies had the appearance of miniaturized candelabras. One of these assemblies was installed in each of the three outer holes in each vane. Figure VI-3 illustrates this installation. A refined fuel pattern and axially injected fuel near the chamber wall were the principal improvements of this modification over the original design. The height of the tee manifolds was staggered so as to produce minimum gas flow restriction to the 0.062-in.-dia injection tubes. The fuel injection velocity from the 576 0.062-in.-dia tubes was 81 ft/sec while that from the remaining 544 0.093-in.-dia tubes was 126 ft/sec.

(2) Mark 125 3 ORST Configuration

(C) The Mark 125 3 ORST injector was made from the Mark 125 candelabra injector. This modification consisted of removing the three candelabra assemblies from each vane and installing three 0.093-in.-dia x 0.015-in. wall axially oriented tubes. These tubes were bent and spaced in a manner to produce a row of 96 equally-spaced tubes at a 9.30 in. in diameter. This modification attempted to place a uniform sheet of axially injected fuel further away from the chamber wall and to overcome the structural inadequacy of the candelabra design. Figure VI-4 illustrates this modified injector pattern.

VI, C, Secondary Injector Program (cont.)

(U) During the test program this injector was further modified to support all tubes structurally to eliminate tube breakage during hot-fire testing. The support was accomplished by weaving 0.040-in.-dia weld wire around and near the tip of the tubes of each vane. This wire was then brazed where it contacted each tube. The reinforced Mark 125 3 ORIT injector is shown in Figure VI-10.

b. WARP Injector

(C) The WARP injector was designed to correct two known problems with the Mark 125 injector: (1) fuel impingement on the cylindrical chamber wall; and (2) the inability to precisely control the oxidizer flow over the fuel injection area. The first problem was corrected by directing all fuel in an axial direction. Uniform oxidizer gas distribution was insured by using a pressure drop type plate with a oxidizer gas hole for every fuel injection point. Fuel is injected through axially directed tubes located in the center of each hole; the oxidizer gas flows through the face plate in the annular space created by the fuel tube within the drilled oxidizer hole. The exit of the oxidizer holes are machined as overlapping cones, leaving no flat plate area on the face for gas recirculation.

(C) The WARP injector was designed and fabricated in three configurations, designated WARP I, WARP II, and WARP III. The WARP I was designed on the basis of requiring a minimum amount of fabrication lead time. The undesirable feature resulting from this approach was a fuel manifolding system known to be unsuitable for a final design should the injector concept be found satisfactory. The WARP II design provided an improved fuel-tube support structure to the WARP I design. In the WARP III configuration, the fuel manifolding system was redesigned to eliminate the undesirable features of the WARP I and II designs.

VI, C, Secondary Injector Program (cont.)

(U) The design details for each configuration are presented in the following paragraphs.

(1) WARP I Injector

(C) The WARP I injector consisted of a face plate, supporting cylinder for the face plate, fuel injection tubing and body-fuel manifold assembly. The face plate, made of Inconel 718, had 753 oxidizer gas holes arranged in 13 rows. Figure VI-5 shows the WARP I design. Seven-hundred fifty-three equal length 0.093-in.-dia by 0.020-in. wall fuel injection tubes are routed from the inner fuel manifold to each of the oxidizer gas holes, as shown in Figure VI-11. The tubes were brazed at the fuel manifold end and tack welded to the ID side of the oxidizer gas hole at the face plate end. The tubes were directed axially and the injection velocity was 132 ft/sec.

(2) WARP II Injector

(C) The only difference between the WARP I and WARP II configurations was in the method of attaching the fuel injection tubes to the face plate. To obtain the more desirable characteristic of centering the fuel injection tube in the oxidizer gas hole, grooves were cut on the upstream side of the face plate in such a manner as to leave a ridge of metal across each gas hole. Figures VI-12 and VI-13 show the upstream and downstream side of the face plate, respectively. A hole was drilled in this ridge into which a short SS 347 tube was inserted and tack welded. The SS 321 stainless-steel fuel injection tube was pushed through this support tube and brazed in place.

(3) WARP III Injector

(C) In the WARP III injector design the fuel manifolding system was completely changed. The long individual fuel tubes were replaced

VI, C, Secondary Injector Program (cont.)

by 32 Mark 125 type radial vanes, from which relatively short S-shaped tubes were attached. The design was made so that Mark 125 injectors could be reworked into the WARP III configuration by milling away the old tubes and the trailing portion of the vanes. Because of the vane design, it was necessary to reduce the number of fuel elements from 753 used in the WARP I and II injectors to 713 elements. Also, the wall thickness of each tube was increased from 0.015 to 0.020 in. to improve the structural soundness of the tubes. A photo showing the WARP III injector without the face plate installed is shown in Figure VI-14. The injector shown had been test-fired several times with the face plate removed, and is in sub-standard condition; however, it serves to illustrate the fuel manifolding system. A face view of an assembled new injector is given in Figure VI-15.

c. Platelet Injector

(C) The platelet injector is composed of 88 vanes, 1/8-in. thick, arranged into eight symmetrical groups of 11 vanes each as pictured in Figure VI-6. The 11 vanes vary in length from 0.850 to 4.500 in. Uniform propellant distribution is achieved by locating the longest vane in each of the eight groups radially and the remaining vanes in each group parallel to it, so that a constant 0.175-in.-wide oxidizer passage remains between each vane. The radius of the leading edge of each vane is such so as to decrease oxidizer gas boundary turbulence, whereas the trailing edge of each vane has been chamfered to minimize the area exposed to the combustion zone.

(C) The vanes are secured to the injector manifold ring by a TIG weld joint around the inlet of each vane. Additional strength is obtained by furnace brazing the joint to achieve a solid braze fillet around each vane where it departs from the inlet manifold. One-inch long spacers are brazed between the vanes approximately 1 in. above the trailing edge of each vane. These spacers not only assure a constant space between the vanes, but also

VI, C, Secondary Injector Program (cont.)

increase the resonant frequency of the vane, thereby minimizing the possibility of vane flutter.

(U) Within each octant, the vanes vary in height as well as length, as can be seen in a view of the upstream side of the injector in Figure VI-76. The longest vane is also the highest; vane height decreases as the vanes become shorter. In addition, all vanes slope downward in the direction toward the injector center. The net result is an ungulated surface which repeats eight times around the injector circumference. The selection of this geometry is a result of the injector body design, which has an 8.5-in. diameter at the inlet end (turbopump interface), transitioning to 9.5-in. at the outlet end (thrust chamber interface). The injector body design was based on the original T-engine interfaces, and was used without change throughout the program. Because of the tapered injector wall caused by this diameter change, it was necessary to vary the vane height to provide sufficient oxidizer gas flow to the short vane areas. The subsequent test program showed that the design overcompensates for this condition, providing too much flow to the short vane areas; this became a major problem in the performance optimization program with transpiration-cooled chamber (see Section VI,C,5,b(4)). This aspect of the injector design should be changed for the final engine design. The injector body diameter should be constant throughout its length, and all vanes should be of equal height and flat over their full length. With this modification, the oxidizer gas velocity and direction will remain constant throughout the injector, and the flow distribution exiting from the injector will be identical to that entering.

(U) Each vane is composed of left hand and right hand 1/16-in. platelets, which are brazed together to form the finished vane. The inner sides of each platelet have matched chemically etched passages which form the internal fuel circuits when the halves are joined together. Brazing was accomplished by first spot-welding narrow strips of 0.001-in.-thick

VI, C, Secondary Injector Program (cont.)

Palniro-1 gold braze alloy to the lands of one side of each vane pair. The vane halves were then accurately aligned and held in place by spot welding small pieces of 0.002-in.-thick stainless-steel foil to at least three edges of the assembled vane. Vanes thus assembled were then placed between platens and furnace-brazed at 2050°F. Post-braze X-rays were taken of each vane to assure that a uniform braze bond was achieved on all lands and that no braze runoff constricted any portion of the etched fuel circuit.

(U) The fuel circuit passages were designed in two alternate configurations, designated the showerhead and impinging patterns. Each of these is discussed in the following paragraphs.

(1) Showerhead Pattern

(C) In the showerhead pattern, each platelet has a 0.015-in.-deep fuel flow circuit etched into one side so that when the opposing sides are brazed together, a very accurate fuel flow circuit is achieved. The top half of Figure VI-16 shows two typical showerhead platelet halves. A photo of vane halves and an assembled vane is shown in Figure VI-17. To assure proper distribution within the vane, inlet lands are spaced in such a way that the longest fuel flow path has the same resistance as the shortest path. A common manifold at the end of the inlet lands assures further uniform distribution. Flow is then directed through a high pressure drop flow control zone. Flow is controlled by etching the passages on one side only of the two platelet halves to a depth of 0.015 in. Upon leaving the flow control passage, the high velocity (160 ft/sec) fuel enters a common diffusion zone prior to entering the 0.275 in. long 0.030 in. x 0.060 in. injection orifices. Fuel is injected in discrete streams from the trailing edge of the vane at 50 ft/sec through a total of 2464 individual orifices. The primary combustor oxidizer gas passes between the vanes at 125 ft/sec.

VI, C, Secondary Injector Program (cont.)

(2) Impinging Pattern

(C) The impinging pattern platelet injector is identical in construction to the showerhead platelet injector with the exception of the configuration and depth of the photo-etched fuel circuit within the vanes. Whereas the showerhead injector has 2464 orifices, the impinging pattern is composed of 3696 orifices. These orifices are arranged in pairs which impinge at an included angle of 60 degrees and are smaller in size (0.030 x 0.020 in. as compared to 0.030 x 0.060 in. in the showerhead). The reduction in fuel orifice area allows the fuel injection velocity to be increased from 46.7 to 93.5 ft/sec, thereby increasing the atomization of the impinging fuel. The increase in injection velocity, however, increases the pressure drop of the vane across the injection orifices. Thus, to obtain the same total pressure drop through the vanes as in the showerhead design, approximately 275 psi, the flow control passage is etched on both the left and right hand side to a combined depth of 0.020 in. instead of 0.015 in. as in the showerhead pattern. The lower half of Figure VI-16 shows both the left and right hand side of a typical impinging pattern vane.

(C) Test results with the showerhead and impinging patterns showed the impinging design to be superior in both performance and compatibility. The showerhead injectors, of which two units were fabricated, were still in excellent condition and capable of further testing after the test evaluation was completed. To provide a backup for the impinging design, a design study was performed to determine methods to improve the performance and compatibility of the showerhead platelet injector design. Two promising methods were selected, and each of these were incorporated on the two showerhead platelet injectors. Each design increased the velocity of the oxidizer gas at the trailing edge of the platelet vanes, directed the oxidizer gas into the fuel stream at slight impingement angles, and eliminated the oxidizer gas core that was thought to exist between sheets of injected fuel.

VI, C, Secondary Injector Program (cont.)

(C) The first design, called the photoetched strip design, consists of brazing metal strips to the beveled trailing edge on each side of the 88 platelet vanes. These photoetched metal strips were scalloped to reduce the available oxidizer gas flow area and thus increase the velocity of the oxidizer gas into the fuel streams at a 9 degree impingement half angle. Narrow gaps of 0.020 in. exist between the edges of adjacent strips and permit some oxidizer gas to escape between the strips to prevent gas recirculation. Figure VI-18 illustrates this design.

(C) The second design, designated the rod type, consisted of a rod suspended midway between adjacent vanes and placed flush with and parallel to the trailing edge of each vane. These 88 rods, 0.156 in. in diameter, were suspended from special vane separators that were brazed to the sides of the vane. The rods forced the oxidizer gas to flow into the fuel streams at high velocity, approximately 200 ft/sec. Some oxidizer gas turbulates around the downstream side of the rods. Figure VI-19 illustrates this design.

4. Supporting Test Hardware

(U) The test evaluations of the ARES secondary injectors were made using uncooled and partially cooled chambers. The oxidizer-rich gas entering the secondary injector was generated by a primary combustor assembly developed on a previous program, and represents the major item of supporting test hardware in addition to the secondary chambers. Descriptions of the chambers and the primary combustor are given in this section.

a. Combustion Chambers

(U) To evaluate the performance and compatibility characteristics of injectors, three types of uncooled and partially cooled chambers were used. These included an uncooled chamber, an instrumented ablative chamber,

VI, C, Secondary Injector Program (cont.)

and a trans-ablative chamber. The uncooled chamber was used to provide baseline thrust chamber performance data, the instrumented ablative chamber to provide heat transfer data to aid in preliminary evaluation of injector compatibility characteristics, and the trans-ablative chamber to evaluate the compatibility of injectors on the transpiration-cooled chamber wall in the area of fuel injection where both previous chamber burnout failures in the basic Phase I program had occurred.

(1) Uncooled Chamber

(U) The uncooled chamber is shown in Figure VI-20. It is composed of a chamber segment and a nozzle segment which are removable from each other. The chamber segment is of heavy wall-steel construction with a two-piece ablative liner. The ablative liners are both fabricated of compression-molded high silica Refrasil material type 2230 (Western Backing Corporation). One piece is used in the convergent and throat section while the other is used in the cylindrical section. The two-piece liner construction permits easy replacement of eroded throat sections and salvage of cylindrical sections for additional testing. Eroded throat sections are then reworked into cylindrical sections making maximum use of ablative materials. The chamber has a 9.500-in.-dia cylindrical section, a 5.214-in.-dia throat, and a 30 degree convergence angle. Chamber L* is 32 in.

(U) The expansion nozzle segment consists of a steel pressure vessel with a Rockide-coated steel liner. It is attached to the chamber segment at an area ratio of 2:1 and extends to an area ratio of 12:1. Testing with ablative-lined expansion nozzles in the basic Phase I program resulted in severe roughening of the liner wall, which caused a considerable performance loss because of the increased friction. The precise determination of this loss was very difficult because the roughness varied considerably from test to test. Therefore, the ablative expansion nozzle liner was replaced

VI, C, Secondary Injector Program (cont.)

with a steel liner, the walls of which remain smooth and allow accurate determination of injector performance.

(2) Instrumented Ablative Chamber

(U) The instrumented ablative chamber is shown in Figure VI-21. It is identical in design to the uncooled chamber, except for the expansion nozzle liner and the addition of thermal instrumentation. In this chamber, performance evaluation was not a primary objective; therefore the steel exit liner was replaced with a more durable ablative liner. The replacement liner is of tape-wrapped construction, 1/2 in. thick.

(U) Thirty fast response 0.040-in.-dia Chromel/Alumel thermocouples are located in the cylindrical section of the chamber. These thermocouples are arranged into six groups of five thermocouples per group. The groups are equally spaced around the chamber diameter and each group is located at a different axial station. An oxidizer film-coolant injection ring is used in conjunction with the chamber and injects coolant just ahead of the first thermocouple station.

(3) Trans-Ablative Chamber

(U) The trans-ablative chamber is shown in Figure VI-22. The forward portion of the chamber is composed of a flange and three transpiration-cooled chamber washer compartments identical in design to the corresponding compartments of the transpiration-cooled chamber. The aft end of each washer compartment contains an instrumented thermocouple washer with six flush mounted thermocouples.

(U) A film-coolant injection manifold is used downstream of the third compartment. The film coolant from this manifold cools the

VI, C, Secondary Injector Program (cont.)

exposed metal flange portion of the ring and the ablative material in the cylindrical, convergent, and expansion section of the nozzle. This manifold is also used to support the transpiration washer compartments with the necessary compressive load. The ablative portion of the chamber downstream of the film-coolant ring uses conventional ablative uncooled chamber components.

b. Primary Combustor Assembly

(U) The primary combustor assembly used during this program was designed and developed during the Integrated Components Program, Contract AF 04(611)-8548. An adapter was used to connect the small diameter primary chamber (5.0-in. dia) to the ARES secondary injector (9.5-in. dia). A photograph of the primary combustor assembly is presented in Figure VI-23. The following paragraphs briefly describe each of the major components.

(1) Primary Injector

(U) The primary injector is shown in Figure VI-24. The injector has 28 elements for each propellant. The oxidizer element is a 60 degree impinging triplet with an impingement distance of 1.4 in. The fuel element is a 50 degree cone spray element centered within the oxidizer triplet. The space between oxidizer streams prior to their impingement allows fuel to disperse outside the injection element, thereby preventing a "hot core" element of the type caused by a restricting gas-boundary layer. The design oxidizer injection velocity is 87.6 ft/sec; the fuel is introduced in a hollow cone spray and its true velocity is unknown. Pressure-drop across the injection elements is 200 psi for both circuits.

(U) The injector incorporates a porous injector face and convergent wall. The percentage of the total oxidizer flow rate through

the porous wall is 3%, which is sufficient to cool the wall while not significantly disturbing the mixture-ratio balance across the injector face.

(2) Primary Combustion Chamber

(U) The primary combustion chamber is a cylindrical chamber of 5 in. inside diameter, 24 in. in length, and composed of two identical sections 12 in. long. In the forward chamber section, three turbulators are used to promote gas mixing and ensure delivery of a homogeneous gas to the secondary injector. Figure VI-25 illustrates these turbulators. Each turbulator is quarter moon-shaped, tapered at the upstream side and abrupt at the downstream side. The elements are staggered at 180 degrees and positioned approximately 2-in. downstream from one another.

(U) During the course of development testing, it was determined that a uniform distribution of oxidizer-rich gas was not being introduced to the secondary injector. Extensive air-flow testing was conducted in the Aerophysics Laboratory to evaluate various flow distribution devices that would uniformly distribute the oxidizer flow. This air-flow testing is discussed in detail in Section VI,E,2, of this report. The final design, which proved to be satisfactory for testing, is shown in Figure VI-26. This design consists of three concentric rings located in the upstream chamber section at the same axial locations as the previous moon-shaped turbulator devices. The through-flow area of the three concentric rings matched the through-flow area of the moon-shaped turbulators. A perforated pressure-drop plate is inserted into the primary combustor adapter to further promote homogeneous and uniform flow to the secondary injector. This perforated plate is very similar in hole arrangement to the WARP II face plate shown in Figure VI-13. The holes are through holes and are not coned.

VI, C, Secondary Injector Program (cont.)

(3) Primary Combustor Adapter

(U) The adapter design is shown in Figure VI-27. It is a cone-shaped part approximately 17 in. long and is fabricated from stainless steel. It was originally designed to permit passage of oxidizer coolant from the secondary injector to the secondary regeneratively cooled chamber and then return the coolant to the primary combustor injector. When the transpiration cooled chamber is used, the oxidizer coolant still flows through the adapter but it is turned around in the transpiration-chamber adapter flange and does not pass into the chamber. The adapter also provides a thrust-take-out ring which connects the thrust chamber to the existing test stand interface.

5. Development Test Program

(U) The objective of the extended Phase I injector test program was to evaluate the performance and compatibility characteristics of candidate secondary injectors, and to perform all development work necessary to provide a high performing, stable, and streak-free injector for testing in conjunction with the transpiration-cooled chamber.

(U) The test program was intiated 14 March 1967 and concluded 11 October 1967, during which period 27 tests were conducted. Two modifications to the Mark 125 injector, together with two new injector concepts, were evaluated in the test program. A cumulative summary of all tests is shown in Figure VI-7. The new Impinging Platelet injector proved to be the best injector, and satisfied all technical requirements prior to cooled chamber testing.

VI, C, Secondary Injector Program (cont.)

(C) All injector testing was performed at a nominal chamber pressure of 2800 psia using the 100,000-lb-thrust staged-combustion test engine. A description of this engine and its operating characteristics is presented in Section VI,C,5,a. The detailed test program performed is discussed in Section VI,C,5,b. Finally, the evaluation of the test data, including both performance and heat transfer aspects, is discussed in Section VI,C,5,c.

a. Test System

(1) Engine Description

(U) The secondary injector test program was performed using the ARES staged-combustion test engine installed on Test Stand H-2 at Aerojet-General's Liquid Rocket test area in Sacramento, California. A schematic of this engine system is shown in Figure VI-28 with a photo of the actual test hardware in Figure VI-29. (This photo shows the pumps and cooled chamber installed, which were used in cooled chamber testing; however, all other hardware is identical.) Engine propellants are supplied at high pressure from pressure intensifiers located above the test engine. The complete intensifier-fed staged-combustion engine is described on Aerojet Drawing 1122831. This drawing references by a dash numbering system all configurations of secondary combustor hardware test-fired and/or designed in the ARES Phase I program. Using this drawing, together with other drawings referenced therein, the detail design of all components can be obtained. All drawings are permanently retained in the Aerojet drawing system file.

(U) The high-pressure oxidizer is supplied to the primary combustor through a control valve used for propellant phasing and termination. In cases where oxidizer film coolant is required, propellant is tapped off upstream of this valve through a separate control valve to the coolant injection system. Eighty percent of the high-pressure fuel flows directly to

VI, C, Secondary Injector Program (cont.)

the secondary injector through a control valve and balancing orifice. The remaining 20% flows to the primary combustor through a control valve for propellant phasing.

(U) Pressure intensification is accomplished using single stroke positive displacement pumps. The pumps are double-piston devices with a large gas piston and a smaller liquid piston on a common shaft. Gas-to-liquid piston area ratio is 5:1, giving a maximum of 6250-psi propellant pressure from the 1250-psi nitrogen gas supply pressure. A single stroke of the piston yields 5 sec of run time at engine design conditions.

(U) In operation, the gas-side pressure is sensed and its value compared with a programed value in a computer. The computer evaluates both the proportional error and integral error between the sensed pressure and the programed pressure, and signals operation of a gas-side flow control valve to correct the pressure accordingly. This system can control to any desired time-base pressure profile for flow rates of 10 to 280 lb/sec of oxidizer and one to 105 lb/sec of fuel.

(U) The sequence of engine operations is established by valve timing and intensifier phasing to obtain the following requirements in order: (1) priming of the film coolant circuit, (2) oxidizer lead to the primary combustor, (3) primary ignition, and (4) secondary ignition on a rising pressure schedule.

(U) Actual operation is accomplished by first purging the propellant circuits downstream of the propellant control valves prior to flow initiation. Propellant is then bled into the control valves using high- and low-point drain valves to remove entrapped air pockets. With the intensifier initial position set and valve actuation pressures established at the required level, the engine start program is signaled (FS_1). At this time the

VI, C, Secondary Injector Program (cont.)

valves are signaled open at required rates and the oxidizer and fuel pressure rise programs initiated following a slight delay. All rates are verified correct by pretest engine "functional" sequence checks. A representative oscillograph showing the start transient and steady-state portions of a test is shown in Figure VI-9.

(U) Several protective measures are included in the engine operation sequence to reduce the possibility of error or malfunction of the operating system. These malfunction detection systems operated in several cases, saving test hardware. With the addition of a solid-state computer, several parameter "window" shutdown signals were used. Parameters such as coolant flow, mixture ratio, and pressure levels were sampled during the test and compared to desired values and allowance tolerances. If the limits were exceeded, a shutdown was initiated.

(U) Shutdown is initiated by simultaneous closing of the primary and secondary fuel valves. The valves closing rates are set to give a slight primary fuel lag. When the fuel valves are approximately 80% closed, closing of the primary oxidizer valve and the oxidizer film coolant valve is initiated. The residual oxidizer in both circuits is purged automatically when the system decays to 800-psi chamber pressure. Fuel is purged from the engine several minutes after the test when all oxidizer has been expelled.

(U) Aerojet's transient analysis engine simulation program was used to establish valve timing and intensifier phasing necessary for the start and shutdown requirements. The program was constantly updated to reflect changes in injector volumes and combustion characteristics. In addition, the program was used to evaluate the results of malfunction shutdowns experienced and to establish the malfunction signal requirements necessary to prevent engine damage.

VI, C, Secondary Injector Program (cont.)

(3) Instrumentation

(U) The engine instrumentation can be classified into five categories: pressure, temperature, flow, thrust, and throat area. All instruments were calibrated to National Bureau of Standard Specifications and have accuracies as quoted in Aerojet Technical Memorandum TM-125D.(1)

(a) Pressure

(U) Pressure measurements were made using both low-frequency and high-frequency pressure transducers. The low-frequency transducers, which were of the strain-gage type giving acceptable gain to 1000 cps, were used for all engine parameters needed for balance, performance, sequence, and failure analysis. A schematic of the engine is given in Figure VI-28 with the location and nomenclature of instruments depicted. High-frequency transducers were used primarily for evaluation of dynamic response of engine components and during failure analyses where pressure response was of major concern. High-frequency transducers of three manufacturers were used: Photocon, Kistler, and Microsystem. All these transducers have natural frequencies in excess of 20,000 cps. A schematic defining the nomenclature of the high-frequency transducers is given in Figure VI-30. The injector and chamber configurations prohibited the installation of flush-mounted transducers for measuring chamber pressure; as an alternative, a flush-mounted Microsystem transducer was located in the fuel injector manifold and a flush-mounted Photocon in the primary combustor L* barrel.

(1) Technical Memorandum No. 125, Revision D, Revised Estimate of Instrumentation Accuracy for Performance Calculations, Contract AF 04(647)-521, 5 September 1963, Aerojet-General Corporation, Sacramento, California

VI, C, Secondary Injector Program (cont.)

(b) Temperature

(U) All temperature measurements were made using Chromel-Alumel thermocouples. Primary use of these measurements was in the determination of propellant specific gravities and primary combustor gas temperature. A schematic showing the location of all thermocouples is included in Figure VI-28.

(c) Flow

(U) Propellant flow rates were determined using a positive displacement measuring system installed on each pressure intensifier. The heart of the system consists of a mylar tape on which evenly spaced blips have been previously recorded. This tape is mechanically tied to intensifier piston shaft and moves linearly with the piston during a test. As the piston is displaced, the tape is drawn between two accurately positioned recorder heads and the time recorded for a blip to pass from one head to another. From these signals, the rate of piston travel over any time interval is accurately established. Knowing the piston area, together with the propellant density and compressibility characteristics, the propellant flow rate in lb/sec is then calculated.

(U) While the total oxidizer and fuel flow rates were accurately determined using the tape measuring system described above, it was necessary to determine the fuel flow split between the primary and secondary injectors, and in film-cooled tests, the oxidizer flow spit between the primary injector and the film coolant circuit. Therefore, the primary injector fuel flow and oxidizer film coolant flow were separately measured using 2-in. rotor flowmeters meanufactured by the Potter Aeronautical Corporation. These meters are turbine-type devices from which cycles of rotation determine the volumetric flow rate. Figure VI-28 shows the location of these meters in their respective circuits.

VI, C, Secondary Injector Program (cont.)

(U) Potter flowmeters were also installed on the primary oxidizer and secondary fuel circuits. These meters were 4-in.-dia and served as a backup flow measurement system for intensifier tests. With the conversion to the pump-fed system in the cooled chamber program, these meters were used exclusively to establish the flow rates, since the tape system can be used only in conjunction with the intensifiers. Figure VI-28 also shows the location of these meters in the respective circuits.

(d) Thrust

(U) The thrust measurement system consists of four parts: (1) a secondary force reference system (standard-cell) to calibrate the test stand force reading against actual measure values, (2) two redundant strain-gage force transducers to measure the millivolt output during test, (3) a mechanical thrust transfer system which allows the engine thrust to be transmitted with repeatable errors through the test stand to the transducer installation, and (4) a strain-gage recording system (MilliSADIC) to enable digital output of the data. The average of the two strain-gage readings was used to establish the thrust level for each test.

(e) Throat Area

(U) Throat area measurements were made using calibrated micrometers referenced to a linear reference standard. Four throat diameters were measured on each test at the following locations: 12:00, 1:30, 3:00, and 4:30 o'clock. The average of these measurements was used for calculation of the throat area and nozzle area ratio.

VI, C, Secondary Injector Program (cont.)

b. Detailed Test Program

(U) The tests conducted during the extended Phase I development testing program can be grouped into the following series: (1) Modified Mark 125 Injector Evaluation, (2) WARP Injector Evaluation, (3) Showerhead Platelet Injector Evaluation, and (4) Impinging Platelet Injector Evaluation. Each of the series is grouped in the discussion below. This section deals with the mechanical integrity, erosion characteristics and compatibility of the respective injector configurations. The performance and heat transfer aspects are discussed in Section VI,5,c. The test data and results for all tests are summarized in Figure VI-7, with a nomenclature list given in Figure VI-8. The final two tests listed in the test summary were not part of the injector evaluation program but were performed in conjunction with the checkout of the turbopumps installed for cooled chamber testing. Since these tests were performed using film-cooled ablative chambers, the data are comparable with those obtained in the injector evaluation tests and are therefore included in the summary.

(1) Modified Mark 125 Injector Evaluation--Tests 1.2-16-WAM-002 through -005, and -026

(U) The objective of this test series was to evaluate three modifications to the basic Mark 125 injector, including the "candelabra" configuration, the 3 ORST configuration (96 axial tubes around periphery), and the structurally reinforced 3 ORST configuration. These modifications are discussed in detail in Section VI,C,3,a. The injectors are shown in Figures VI-3, VI-4, and VI-10.

(U) Five tests were conducted, three of which were with uncooled ablative chambers using Rockide-coated steel nozzles, one with the instrumented film-cooled ablative chamber and one with the transpiration-ablative chamber. These chamber configurations are discussed in Section VI,C,4.

VI, C, Secondary Injector Program (cont.)

(U) The first test in the series, Test 1.2-16-WAM-002, was performed to evaluate the "candelabra" configuration. A 32-in. L* ablative chamber with a 9.5-in.-dia cylindrical section and a Rockide-coated steel nozzle were used in this evaluation. The test duration was 1.964 sec and design chamber pressure and mixture ratio were obtained. Postfire inspection revealed that approximately 30% of the candelabras had broken off either totally or in part. Also, all tubes which feed the center section of the injector were broken off. Localized erosion was noted on several vanes where tubes had broken close to the vane attachment point. The posttest condition of the injector is shown in Figure VI-31.

(U) Review of the test records showed that start transient on this test was very rough. This occurred as a result of a redistribution of resistances in the secondary fuel circuit from that employed in previous tests, a change made to improve the peripheral filling characteristics of the secondary injector inner manifold. The bulk of the resistance was moved from an orifice at the fuel valve exit to the inner fuel manifold inlet, which results in less metering of the fuel flow at the valve during the manifold fill time. Thus, at manifold fill the secondary fuel flow was at a higher rate, which results in a higher ignition pressure. This increased pressure rise rate produced a rapid cessation of fuel flow and caused the fuel system to relax and become responsive to system oscillations. This condition was verified by the fact that attenuation of the oscillations occurred upon reinstatement of fuel pressure and flow. This condition was corrected on future tests by reducing the fuel intensifier pressure rise rate during manifold fill and increasing it rapidly following fill. This reduces the fill flow rates and gives a greater stiffness to the fuel circuit following secondary ignition.

VI, C, Secondary Injector Program (cont.)

(U) Although the rough transient undoubtedly contributed to the large number of candelabra failures, it was concluded that even under normal conditions the candelabra structure would be marginal. Except for the inner row of tubes feeding the injector center, the basic Mark 125 tubes (which have experienced structural failure in the past) were in good condition following the test. Therefore, the candelabra configuration Mark 125 injector was dropped from further consideration.

(U) Three tests were conducted to evaluate the Mark 125-3 ORST injector configuration. The first two tests (-003 and -004) were performed with uncooled ablative chambers having Rockide-coated steel nozzles. Both tests were nominally of 2-sec duration and no injector damage was sustained on either test. Performance could not be evaluated on the first test because the ablative chamber used for this test had previously been fired to the extent that the chamber diameter and throat dimensions were no longer within specifications. A new chamber was used for the second test, which yielded a valid performance data point.

(U) Following the structural and performance evaluations of the Mark 125-3 ORST injector, the compatibility characteristics of the injector were evaluated during a test in which a film-cooled instrumented ablative chamber was used (Test -005). This chamber had five rows of five thermocouples located axially along the chamber wall to evaluate the temperature profile in the chamber. Test duration was 3.5 sec; postfire inspection of the chamber revealed extensive chamber ablation in the convergent and throat section. A discussion of the temperature profile obtained is given in Section VI,C,5,c,(2).

(U) The final test of this series evaluated the Mark 125-3 ORST injector with reinforced tube supports designed to prevent tube structural failure during test. The chamber used for this test was the

VI, C, Secondary Injector Program (cont.)

transpiration-ablative chamber, thereby allowing a compatibility evaluation of the cylindrical portion of the chamber. Test duration was 3 sec. The injector sustained no damage and the cylindrical portion of the chamber showed no evidence of streaking, indicating acceptable compatibility. Since the tube failure problem appears to be dependent on test cycling, this one test is an incomplete evaluation of the modification. Because of the success obtained with the impinging platelet injector design, no further effort was performed with the Mark 125 injector.

(2) WARP Injector Evaluation--Tests 1.2-16-WAM-001, -006, -011 through -013

(U) This test series evaluated the WARP I and WARP III injectors (Figures VI-5 and VI-15). The first test, of 2-sec duration, was made with the WARP I injector in an uncooled ablative chamber. Posttest inspection showed excessive damage to the injector. The weld which attached the injector face plate to the cylindrical face plate support was ruptured over the entire circumference. Both face plate and fuel injection tubes were severely eroded. Microscopic examination of the failed weld indicated a lack of weld penetration in some areas. Also, the start transient was very rough (similar to that obtained with the candelabra injector on Test -002). Because of the rough transient and the lack of weld penetration, the failure could not be conclusively attributed to the joint design.

(U) Testing was resumed with the WARP III injector, which had the same face plate support joint (Test -006). Again the injector face plate failed in much the same manner as the WARP I face plate in Test -001. The start transient during this test was smooth and the weld joint had been properly made. It was therefore concluded that the joint design was inadequate and would have to be redesigned.

VI, C, Secondary Injector Program (cont.)

(U) A new WARP III injector with a new design joint was evaluated in Test -011. No structural damage to the injector or face plate occurred. However, erosion occurred about the outer periphery of the face plate. At this time, a parallel effort was being conducted in the Aerophysics Laboratory to determine the primary combustor gas flow distribution to the secondary injector and chamber. Subsequent results showed that there was low primary oxidizer flow in the outer periphery of the injector which could cause recirculation of the combustion gases and erosion. It was therefore concluded that, with proper primary oxidizer gas distribution, the WARP injector would most likely operate satisfactorily. However, because of the success with the platelet injector, further evaluation of the WARP injectors was suspended.

(U) Two additional tests (-012 and -013) were performed with the WARP III injector with the face plate removed. The purpose of these tests was not an evaluation of the WARP injector concept but was an evaluation of the engine system modifications resulting from the Aerophysics Laboratory air flow test program. The injector was used solely as a workhorse unit to evaluate gas flow distribution devices installed upstream of the injector. These included three symmetrical turbulator rings extending one inch from the wall and having a triangular cross section with a right angle apex. The rings were located on 4-in. centers. To avoid possible core effects downstream of the last ring, an aerodynamic spud was installed in the center of the gas stream. These devices proved to provide proper mixing of the primary combustion gases (subsequent testing proved that the aerodynamic spud was not required). Thermocouples in the primary combustor measured within 100°F of each other, indicating a uniformally mixed exhaust gas. No injector damage was sustained on either test.

VI, C, Secondary Injector Program (cont.)

(3) Showerhead Platelet Injector Evaluation--Tests 1.2-16-WAM-007 through -010, -014, -015, and 1.2-13-WAM-015 and -016

(U) The showerhead platelet injector was evaluated in this test series. Eight tests were performed, of which six were with the basic showerhead platelet injector design and two with showerhead platelet injectors modified in an attempt to improve compatibility and performance. The basic injector is shown in Figure VI-6; the two modifications tested are shown in Figures VI-17 and VI-18.

(U) In the first three tests, the basic showerhead platelet design was evaluated in an uncooled ablative chamber having a Rockide-coated steel exit nozzle. The injector's performance was satisfactory; however, the posttest condition of the ablative chamber indicated that the compatibility of the injector with the chamber wall was questionable. Small streaks adjacent to the trailing edge of each vane were noted in the cylindrical portion of the ablative chamber. In addition, eight heavy streaks were present which started in the convergent section and continued through the chamber throat. The post-test condition of the chamber is shown in Figure VI-32.

(U) In the next test (-010), the injector was tested with a film-cooled ablative chamber with 36 lb/sec N_2O_4 film coolant introduced at the top of the chamber. The purpose of this test was to further investigate the compatibility aspects of the injector-chamber configuration (compatibility characteristics of an injector show up more clearly with this setup than with an uncooled chamber, since any fuel-rich areas combine with the oxidizer film cooling, producing marked color variations and streak patterns on the ablative chamber wall). Test results again indicated incompatibility in both the cylindrical and throat sections of the chamber.

VI, C, Secondary Injector Program (cont.)

(U) Concurrently with this test program, the laboratory test evaluation of the oxidizer gas distribution entering the secondary injector was being performed in the Aerophysics Laboratory (see Section VI,E). Results of that program clearly showed a nonuniform gas distribution with the test system in which the injectors were being evaluated. On the basis of the results of the laboratory air flow test program, the staged-combustion test engine was modified to improve the primary combustor gas distribution. The three unsymmetrical turbulators were replaced by three symmetrical turbulators; the injector was modified by adding vane extenders to which a screen was attached; and a 4° diffuser cone with an inlet screen was installed in the adapter just upstream of the secondary injector.

(U) With the modification to the test engine completed, testing was resumed with the showerhead platelet injector on Test -014. This was an uncooled test using an ablative chamber with a Rockide-coated steel exit liner. Performance was approximately 1% higher than that previously obtained with the old flow distribution system. Also, compatibility was improved, although the eight streaks in the throat region were still prominent.

(U) The compatibility evaluation was then continued in Test -015 by testing the injector with an instrumented ablative chamber in which 36 lb/sec film cooling were introduced. A discussion of the temperature profile obtained is given in Section VI,C,5,c,(1). It was concluded that the showerhead platelet injector would probably prove incompatible with a transpiration-cooled chamber; however, no tests were ever made to confirm this suspicion. Because of the availability of the impinging platelet injector and its inherently finer distribution of fuel over the injector face, the program was directed to evaluation of that injector.

VI, C, Secondary Injector Program (cont.)

(U) As a backup approach, two modifications of the showerhead platelet injector, designed to improve compatibility and performance, were test-evaluated. These modifications, which included the addition of bars and rods to the trailing edge of the injector vanes for oxidizer directional control, are discussed in Section VI,C,3. The bar configuration was evaluated in Test -015 and the rod configuration in Test -016. Both modifications improved performance slightly; however, the bars and rods sustained extensive erosion and proved unsuitable. Posttest pictures of these injectors are shown in Figures VI-33 and VI-34. Because of the injector failures, no assessment of compatibility could be made.

(4) Impinging Platelet Injector Evaluation--Tests 1.2-16-WAM-016 through -024

(U) This test series evaluated the impinging platelet injector. A total of nine tests were performed including one uncooled test, three tests with film cooled ablative chambers, and five tests with transpiration-ablative chambers. The successful completion of this test series resulted in the selecting of the impinging platelet injector for use with the transpiration-cooled thrust chamber.

(U) Because of the evidence of incompatibility in the test series using the showerhead platelet injector, a basic compatibility evaluation with the impinging platelet injector preceded the base performance evaluation using an uncooled chamber. The series was initiated with Test -016 which employed the symmetrical turbulator system and 4° diffuser cone with screen installed during the previous series. However, no vane extenders or screen were used at the inlet of the injector. Posttest inspection of the hardware showed the screen at the inlet of the diffuser cone was dislodged. The ablative chamber showed good compatibility in the cylindrical section; however, the eight streaks previously noted with the showerhead pattern were present in the throat region.

VI, C, Secondary Injector Program (cont.)

(U) Because of the low reliability of welded screens, it was decided to replace the diffuser cone and screen with a pressure drop plate located just upstream of the injector. The selected plate was a WARP III face plate with a biased flow pattern to give high oxidizer flow at the injector periphery (see Section VI,E for details). Using this new plate, Test -017 was performed at a film coolant flow rate of 36.6 lb/sec. Excellent wall compatibility between the injector and the chamber was obtained. However, heavy local ablation just below the throat was noted. It is theorized that the high oxidizer flow at the outer periphery allowed unburned fuel to pass through the throat and to combust supersonically downstream of the throat, causing the erosion. The heavy peripheral oxidizer flow also resulted in a high mixture ratio distribution performance loss; performance on this test was almost 2% lower than that previously achieved.

(U) The pressure drop plate was then modified by selectively chamfering the holes in the center portion of the plate, which reduced the entrance losses to these holes and thereby allowed more oxidizer through this section of the plate. This configuration was tested in Test -018 with a film coolant of 37.1 lb/sec. Performance returned to that value obtained in the original configuration; also, there was no evidence of the heavy erosion in the throat area as occurred in Test -017. Evidence of the eight streaks in the convergent and throat section aligned with the long vanes were present, much the same as in previous tests. Postfire inspection of the diffuser plate revealed that the plate had bowed approximately 0.170-in. and that several small cracks were present between holes. The plate was therefore replaced by another WARP face plate which was also available from an unassembled WARP II injector kit. Concurrently, design and fabrication of a new, stronger plate was initiated.

VI, C, Secondary Injector Program (cont.)

(C) The base performance of the impinging platelet injector, using the new WARP type pressure drop plate, was determined in Test -019. This test was performed using an uncooled ablative chamber with a steel nozzle and was of 2.5-sec duration. Delivered sea level specific impulse during this test was 286.3 sec (93.3% of theoretical) which was considered to be sufficiently high for use with the transpiration-cooled chamber in meeting the Phase I performance requirements. No hardware damage occurred during the test. Compatibility in the cylindrical chamber section appeared excellent; the condition of the convergent and throat section was comparable to that experienced in previous tests.

(U) The contractual work statement requirements for the secondary injector prior to cooled chamber testing were achieved in Test -019. The success criteria for the secondary injector was that the injector selected for testing with the cooled thrust chamber must have achieved a minimum duration of 0.5 sec of steady-state operation with steady-state chamber pressure oscillations not exceeding $\pm$5% of the average chamber pressure. Also, the injector must be in refirable condition following the test. In Test -019, the injector operated at steady-state for 0.94 sec at an average chamber pressure of 2711 psia. Chamber pressure oscillations during the test did not exceed $\pm$1.7% of average chamber pressure. The injector was in perfect condition following the test. A plot of chamber pressure during the data period of this test is shown in Figure VI-35.

(U) With acceptable performance and compatibility levels indicated, the test program proceeded to the final compatibility evaluation, which was made with a chamber transpiration cooled in the cylindrical portion and ablative-film cooled in the convergent and throat section.

VI, C, Secondary Injector Program (cont.)

(U) The trans-ablative chamber was installed and balanced for a total coolant flow of 55 lb/sec of which 10 lb/sec was to be injected through the transpiration compartments, the remaining 44 lb/sec to be injected through a film-coolant ring located just downstream of transpiration compartment 3. The test (-020) proceeded without incident to its scheduled duration of 2.5 sec. Transpiration wall condition was excellent with no heat marks noted. Erosion was noted in the ablative throat section in line with the long vane areas of the injector. The heat-transfer evaluation of the data obtained in this and subsequent tests is described in Section VI,C,5,c,(2).

(U) In the next three tests, the transpiration coolant was incrementally reduced to 7.12 lb/sec transpiration coolant. During the final test a fuel leak was incurred in one of the platelet injector vanes at the manifold attachment point. The fuel combined with the transpiration coolant and caused erosion down the chamber wall, which resulted in a strip nearly 3-in. wide and 1/4-in. deep at the end of the transpiration-cooled section (Figure VI-36). Also, a slight amount of burning occurred on the film coolant ring. The hardware was removed from the test stand and repaired. The eroded section of the transpiration-cooled chamber section was restored by grinding out the burned section and then electro-polishing to open up the pores in the chamber wall.

(U) Testing was resumed in Test -024 with the repaired injector and chamber. Also, fabrication of the new stronger pressure drop plate had been completed and this plate was used in place of the WARP type plate. Because of the uncertainty of the operation of the repaired hardware and the new plate, the transpiration coolant flow rate set for this test was increased to 9.25 lb/sec. The test was of 3-sec duration; no hardware damage occurred. The cylindrical portion of the chamber, as in all previous tests, was in excellent condition with no evidence of streaking. Therefore, it was decided to proceed with the evaluation of the full transpiration-cooled chamber.

VI, C, Secondary Injector Program (cont.)

(U) In all of the tests described in this section, the first impinging platelet injector fabricated, SN 3, was used. Subsequently, in cooled chamber testing, two additional injectors, SN 4 and SN 5, were also tested. Injectors SN 4 and 5 proved to be approximately 1% higher in performance than SN 3. This is believed to be the result of a better pattern obtained through more precise control on the injector element dimensions and to the fact that approximately 50 sets of orifices in SN 3 had been plug-welded closed to eliminate skewed streams issuing from those elements.

(U) Although the compatibility of the impinging platelet injector is excellent with the transpiration-cooled cylindrical chamber section, it obviously is not perfect in the convergent and throat section as evidenced by the eight streaks which occur in line with the long vane areas. This condition indicates a nonhomogeneous combustion process over the injector face which should be corrected in an engine development program. The streaking results from nonuniform presence of oxidizer at the plane of the fuel injection, i.e., the trailing edge of the vanes. Using the results of the air flow program performed in the Aerophysics Laboratory, the test engine was modified to have relatively uniform oxidizer flow at the inlet of the injector. However, because of the different vane heights, together with the injector diameter varying from 8.5-in.-dia at the top to 9.5-in.-dia at the bottom, the oxidizer gas distribution changes as it passes through the injector. (See discussion, Section VI,C,3,c.) This condition can be corrected by redesigning the injector to have a uniform diameter throughout its length and by redesigning the vanes so that all are of equal height. With these corrected, the oxidizer gas will pass through the injector with no change in velocity and should exit with the same distribution as that which enters the injector. Because of insufficient time to make these corrections in the present program, the transpiration-cooled chamber has had to be overcooled in the convergent portion of the chamber to be compatible with the injector. By making the corrections

V, C, Secondary Injector Program (cont.)

noted above, overall system performance can be increased since the overcooling of that part of the chamber will not be required.

c. Test Data Evaluation

(1) Performance

(U) The test data obtained during the secondary injector program were evaluated using the performance interaction theory, described in detail in Report AFRPL-67-75, Advanced Rocket Engine--Storable, Phase I Interim Final Report, Part 2, Section VI,A,5,a,(1). The delivered specific impulse for each test was determined through direct measurements of thrust, volumetric propellant flows, and propellant temperatures (from which specific gravities were determined). The difference between the delivered specific impulse and the theoretical specific impulse is the total performance loss of the system; the interaction theory provides a method for understanding the component parts of this loss and assessing their magnitudes. Performance losses which occur in injector testing are those due to: (1) nozzle friction, (2) nozzle geometry, (3) mixture ratio distribution, (4) energy release, and (5) film coolant, if used.

(U) The secondary injector program included 27 tests, in which four basic injector configurations were test-evaluated. Both uncooled and film-cooled tests were performed to provide performance and compatibility data. In addition, the program also investigated six different primary gas distribution devices, which were used to tailor the oxidizer gas distribution across the injector face. A summary of all test data is given in Figure VI-7. A nomenclature list of the symbols used in the figure and throughout the section appears in Figure VI-8. The performance summary gives the calculated quantities of specific impulse and performance losses, together with the data necessary

to make these calculations. Component specifications and other historical information are also included.

(U) The mixture ratio distribution loss and the energy release loss determine the inherent performance level of an injector. The magnitudes of these losses, however, are influenced by the primary oxidizer gas distribution at the injector inlet and therefore change with different primary gas distribution devices. The combinations of the injectors and gas distribution devices tested in the program, together with their calculated mixture ratio distribution (MRD) and energy release (ERL) losses, are shown in Figure VI-37. In tests where film cooling was used, the film cooling loss (FCL) is also shown. The highest performance was obtained with the impinging platelet injector using a drilled plate for primary gas distribution control. This combination also indicated relatively good compatibility characteristics.

(U) Each of the five component performance losses, as related to specific injector and primary gas distribution devices tested in this program, is discussed in the following paragraphs.

(a) Nozzle Friction Loss (NFL)

(U) The nozzle friction loss for each test was determined using the extended Frankel-Voishel analysis[1] for smooth wall friction losses. It was established early in the Phase I program that ablative exit nozzles in uncooled testing were not satisfactory for precise determination of the nozzle friction loss because of the severe roughening of the nozzle during test. Therefore, smooth steel-wall exit nozzles were used in all

(1) Frankel, F., and Voishel, "Friction in the Turbulent Boundary Layer of a Compressible Gas at High Speeds," NACA TM 1032, 1942.

VI, C, Secondary Injector Program (cont.)

uncooled tests where performance evaluation was a primary test objective. In film-cooled tests, the roughening is not as severe; furthermore, the gas velocity at the wall is substantially reduced because of the film coolant boundary layer, which decreases the importance of roughness in the friction loss calculation. Therefore, ablative exit nozzles were used during some film-cooled tests. The nozzle friction losses (NFL) for all tests are shown in Figure VI-7.

(b) Nozzle Geometry Loss (NGL)

(U) A 15-degree half-angle exit nozzle was used in all tests. Variances from test to test in the calculated NGL are caused by changes in injector mixture ratio and the test area ratio. A tabulation of these losses appears in Figure VI-7.

(c) Mixture Ratio Distribution Loss (MRD)

(U) Mixture ratio distribution loss results from nonideal flow of the primary combustor gas across the secondary injector face and/or from nonuniformly introduced fuel. Since the test program encompassed a number of devices for primary combustor gas control, the mixture ratio distribution loss varied according to the devices used on any particular test. With one exception, the MRD losses listed in the test data summary (Figure VI-7) were determined using the results of air flow tests with the gas control devices in conjunction with the secondary injector. With the mass flow distribution determined in the air flow tests, the MRD loss was calculated using the stream tube analysis technique. The one exception to this procedure was the determination of the MRD loss for the original primary gas distribution system, i.e., unsymmetrical turbulators and multihole orifice plate. This original system produced a very unbalanced flow with a predominantly fuel-rich zone around the

VI, C, Secondary Injector Program (cont.)

periphery of the injector, and a heavy oxidizer-rich core through the center of the injector. In film-cooled tests, the outer fuel-rich zone burned with the oxidizer film cooling, eliminating the otherwise expected loss. In uncooled tests, the oxidizer-rich center core underwent turbulent mixing with the fuel-rich periphery in the convergent section of the chamber, again diminishing the performance loss. For this reason, the MRD loss of the original system was determined by using engine test data together with calculated values of nozzle friction loss, nozzle geometry loss, and the analytically predicted energy release loss. (Normally, the energy release loss is the parameter determined from data using calculated values of NFL, NGL, and MRD.) Data from Tests 1.2-16-WAM-007 through -010, which were performed with the showerhead platelet injector, were used for the MRD loss calculation. Subsequent testing with the showerhead platelet injector using another gas distribution system showed agreement of the showerhead platelet injector ERL to be within 0.5% of the predicted value.

(d) Energy Release Loss (ERL)

(U) The energy release loss for each injector was determined from uncooled tests by subtracting calculated losses of NGL, NFL, and MRD from theoretical specific impulse, and then subtracting delivered specific impulse from the remaining quantity. The resulting ERL's are summarized for each injector in Figure VI-37. During the injector design analysis study, energy release loss for each of these injectors had been predicted, as shown in Figure VI-84. Pertinent comments relative to the ERL for each injector are given in the following paragraphs.

1 Mark 125-3 ORST Injector

(C) Experimental ERL's of 3.7 and 2.6% were obtained with the Mark 125-3 ORST injector in Tests 1.2-16-WAM-003 and -004, respectively. The discrepancy of 1.1% is substantially larger than has been

VI, C, Secondary Injector Program (cont.)

normally experienced; however, no error in recorded parameters could be found in a detailed review of the test data. The predicted ERL of this injector was 4.2%, which tends to support the data of Test -003 as being correct. Furthermore, a subsequent test performed with the WARP injector with the face plate removed (see Paragraph 2 below), a configuration very similar to the Mark 125-3 ORST injector, produced an ERL of 3.6%, which again substantiates the data of Test -003. However, because of the low statistical sample available, the ERL of the Mark 125-3 ORST injector used in subsequent film-cooling tests was taken as the average of the ERL's determined in the two uncooled tests, or 3.2%.

2 WARP Injector

(C) No steady-state performance data were obtained with WARP injectors because of structural problems with the face plates. Two tests were made with the face plate removed, Tests 1.2-16-WAM-012 and -013, from which an ERL of 3.6% was calculated. With the face plate removed, this WARP injector is very similar to the Mark 125 injector except that all tubes are directed axially. The predicted ERL was again 4.2%, which agrees within 0.6% of the experimental value.

3 Showerhead Platelet Injector

(C) The ERL for the showerhead platelet injector which appears in Figure VI-37 for Tests 1.2-16-WAM-007 through -010 is the predicted value calculated during the design analysis study (see Section VI,E,1). As previously discussed, this was necessary because of the inability to determine the MRD loss from air flow data with the original primary combustor gas distribution system. In subsequent Test 1.2-16-WAM-014, the showerhead platelet injector was tested with a notched screen used for gas mixture ratio control. Using the MRD loss calculated from air flow test results

VI, C, Secondary Injector Program (cont.)

with this screen, the injector ERL was calculated to be 2.3%, a 0.5% difference from the predicted value. The latter established value is believed to be the true representation of the showerhead platelet injector ERL loss. However, with the original primary gas distribution system, the injector ERL could truly have been 2.8% because, with the cored condition of the primary gas, the heat transfer to the fuel is reduced which decreases its vaporization rate.

(C) Performance improvement devices (PID) were installed on the showerhead injectors during Tests 1.2-13-WAM-015 and -016. These devices decreased the injector ERL from 2.3% to 1.4 and 1.6% for the two configurations tested. This improvement occurred because of better mixing caused by heavy recirculation patterns generated by these devices.

4 Impinging Platelet Injector

(C) An ERL of 1.9% was established for the impinging platelet injector on the basis of data from Test 1.2-16-WAM-019. This ERL is in disagreement by 1.5% with the analytically predicted value of 0.4%. It is believed that this difference is primarily caused by incomplete mixing of the highly vaporized fuel stream with the oxidizer. This effect is normally insignificant when the fuel vaporization is incomplete but can become the rate-controlling mechanism when vaporization approaches 100%. This implies that even though the fuel is vaporized, unless the atmosphere immediately surrounding the fuel vapor contains oxidizer, no combustion will take place. For the impinging platelet injector, it is thought that the spacing between the fuel vanes allows some of the oxidizer to pass into the combustion chamber in striated streams without properly mixing with the atomized fuel.

VI, C, Secondary Injector Programs (cont.)

(e) Film Cooling Loss (FCL)

(C) The film-cooling losses were determined by subtracting all the losses previously described from the difference between test and theoretical specific impulse. Normalized, these losses correlate as shown in Figure VI-38. The slope of the resulting curve is approximately 0.5% specific impulse loss per percent of film coolant, which is the same result obtained during the basic Phase I film-cooling evaluation. Of the eleven film-cooled test data points, three do not fit the correlation: Tests 1.2-16-WAM-005, -015, and -023.

(U) In Test -005, a very incompatible condition prevailed with all thermocouples overscaling past 2500°F. This condition resulted from burning of film coolant with the injector exhaust products, which results in a lower coolant loss. The transpiration portion of the trans-ablative chamber burned during Test -023, consuming coolant and thereby reducing the film coolant loss. Data from Test -015 reflect a high film coolant loss in comparison to the other tests. Detailed review of this test has revealed no abnormalities in engine operation or test data. It is concluded that this deviation is greater than would be expected with normal data scatter, indicating some of the test data are in error.

(2) Heat Transfer

(U) Two test hardware configurations capable of providing heat transfer data were used to define the compatibility characteristics of new injectors in the extended Phase I effort prior to cooled chamber testing. The first was an instrumented ablative chamber with film cooling introduced at the forward end of the chamber. This hardware was residual from the film-cooled chamber development program of Phase I and was intended to provide visual

VI, C, Secondary Injector Programs (cont.)

evaluation of compatibility through examination of the streak and erosion patterns on the ablative chamber liner. In support of this evaluation, temperature measurements from sheathed chromel-alumel thermocouples provided an approximate measure of the compatibility in the cylindrical portion of the chamber. The trans-ablative chamber was used as a refined means to acquire a quantitative measure of compatibility in the cylindrical chamber region. This chamber used the same cooling mechanism as the fully transpiration-cooled chamber and eliminated the risk of destroying a complete chamber assembly.

(U) Both the instrumented ablative chamber and trans-ablative chamber proved useful in evaluating the injector-chamber compatibility characteristics. Injectors were screened for gross incompatibility with the instrumented ablative chamber and those showing promising compatibility characteristics were further evaluated using the trans-ablative chamber. This effort culminated in testing with the impinging platelet injector, which proved compatible with the trans-ablative chamber. With this result, testing with the transpiration-cooled chamber was initiated.

(U) The heat transfer data obtained in the test series using the two compatibility chambers are discussed in the following paragraphs.

(a) Instrumented Ablative Chamber

(U) The instrumentation for this series consisted of groups of five thermocouples in close proximity to each other at each of six axial locations in the cylindrical portion of the chamber. The hardware, together with a figure showing the thermocouple locations, are described in Section VI,C,4 of this report. Valid test data were acquired on three injectors and a total of five different test configurations.

VI, C, Secondary Injector Programs (cont.)

(U) Approximate steady-state values for each temperature measurement in the series of tests are tabulated in Figure VI-39 together with predicted temperatures for each group of thermocouples at film coolant flow rates of 35 and 40 lb/sec. Wide variations in any one group of temperatures are attributed to instrumentation, but similar variations in several groups indicate irregularities in the combustion process.

(U) The first test (1.2-16-WAM-005) was performed using the 3 ORST modification of the Mark 125 injector. The thermocouple data, summarized in Figure VI-39, exhibited excellent correlation of temperatures within each thermocouple group and approximated the expected temperature difference between groups. However, all temperatures were substantially higher than the theoretical predicted temperatures, which indicates some burning of the film coolant with the fuel. A posttest picture of the hardware showing the very uniform marking of the cylindrical section is shown in Figure VI-40.

(U) Test -010 of this series was the initial compatibility test with the showerhead platelet injector. Despite the very short duration of this test due to a malfunction shutdown, the condition of the hardware and the thermocouple data showed a compatibility problem. Thermocouple readings 0.50 in. from the injector face ranged from 350°F to burnout, or more than 2500°F for these chromel-alumel junctions. Figure VI-39 shows further wide variations in temperature within each group of readings. The conditions of Row E of thermocouples (all burned out) indicate a serious presence of liquid fuel almost 5 in. from the injector face. Postfire examination of the hardware showed distinct irregularities in both erosion and marking.

(U) The showerhead platelet injector was re-evaluated in Test -015 in conjunction with a notched screen to improve the oxidizer gas distribution across the face of the injector. Examination of the thermocouple

VI, C, Secondary Injector Programs (cont.)

data and the posttest condition of the hardware show some improvement in compatibility. Note that in Test -010, which used the original gas distribution system, all thermocouples in Row E burned out, whereas in Test -015, using the notched screen, all temperatures but one were in the vicinity of the predicted values. However, the generally high temperatures recorded in the test compared to the theoretical values show burning of the fuel with the film coolant. This is also indicated by the condition of the chamber wall which shows relatively heavy ablation in line with each injector vane. The best steady-state data were in Rows A, C, and D, which exhibited temperature variations from 100% (Row D) to 600% (Row A). Rows B, E, and F in the upper two quadrants of the chamber showed the effect of some perturbation on local heat flux and never truly reached steady-state although the values in the figure are approximations to the steady-state values. Figure VI-41 shows the erosion pattern in the cylindrical portion of the chamber with several areas extending well into the convergent section.

(U) The first compatibility test with the impinging platelet injector, Test 1.2-16-WAM-016, was conducted with a 4° screened diffuser cone installed upstream of the injector. It was determined on posttest examination that the diffuser cone screen had failed early in the test (see Section VI,C,5). Apparently because of this perturbation, all thermocouples responded to a severe increase in heat flux with half of them burning out and only six of the remainder exhibiting true steady-state temperature measurements. There was no apparent pattern to the location of these six thermocouples (A-1, -2, -3, B-2, -4, and C-5). The hardware reflected the condition indicated by the thermocouples, having a number of severe and irregular eroded areas.

(U) The final test in this series with valid thermal data was also conducted with the impinging platelet injector. This test utilized a drilled plate (see details in Section VI,C,5) in lieu of all

VI, C, Secondary Injector Programs (cont.)

other gas distribution devices. A seventh row of thermocouples (Row G) was added at the entrance to the convergent section of the nozzles for this test. The compatibility of this configuration was the best achieved, with both the cylindrical and the convergent portions of the chamber showing a minimum of streaking. This is shown in Figure VI-42 where the even changes in color take place one-third to one-half of the distance to the convergent section. The thermocouple data partially substantiate this observation, with more measurements being within theoretical limits on this test than any other. Eight thermocouples, however, either burned out or were invalid. Because there was no apparent relation between these burnouts and the chamber markings, some of these failures can be attributed to the short life of this type of instrumentation. Particularly notable is a comparison between the Row D temperatures in Tests -015 and -017, which were conducted at approximately the same coolant flow rate. The values are reduced from a range of 1000 to 1800°F on Test -015 to a range of 600 to 1000°F on Test -017.

(b) Trans-Ablative Chamber

(U) The means of evaluating the compatibility of this system consisted of the temperature measurements acquired with a single instrumentation platelet at the aft end of each of the three compartments. Six thermocouples of the same type used on transpiration chambers SN 001 and 002 in Phase I of this contract were installed in each instrumentation platelet. Each thermocouple was brazed in an eloxed slot with the depth of the junction subsequently determined precisely by X-ray measurement. The instrumentation in the trans-ablative chamber exactly represents the conditions which will exist in the fully transpiration-cooled chamber except in the case of compartment 3. In this instance, the instrumentation platelet is directly adjacent to the aft flange (see discussion in Section VI,C,4,c) through which 40 to 50 lb/sec of film coolant is injected. The effect of this coolant within

VI, C, Secondary Injector Programs (cont.)

0.050 in. of the instrumentation platelet is to greatly attenuate the temperature effects of coolant reduction in that compartment. The trends should still be evident, however.

(U) In the first four tests of the series (1.2-16-WAM-020 through -023, see discussion above), twelve of the possible eighteen thermocouples were usable and valid. Two of these were in compartment 1, four in compartment 2, and six in compartment 3. A tabular summary of the measured temperature values is presented as Figure VI-43. This figure also shows the depth of each thermocouple junction from the gas-side surface.

(U) Figures VI-44, VI-45, and VI-46 show the temperature measurements in each compartment, corrected to the true surface value, as a function of the compartment coolant flow rate. Also shown are the analytically predicted temperatures. The flow rate for each test is indicated on the predicted temperature curve. The model used to predict the theoretical surface temperature of each compartment as a function of the coolant flow rate differs slightly from that used in Phase I of this contract. The reasons for this change, together with a discussion of the use of the model, follows in the Cooled Chamber Program section. A detailed description of the model is presented as Appendix 1 of this report.

(U) The experimental data, in general, show two things: some degree of normal data scatter and test-to-test variation; all data significantly below theoretical predictions. This second fact is attributed to a combination of effects. First, the injector was used in conjunction with an oxidizer gas distribution plate which intentionally provided an excess of oxidizer gas to the outer periphery of the chamber to improve the compatibility of the injector/chamber combination. This oxidizer-rich gas provides cooling in addition to the transpiration coolant, but is not considered

VI, C, Secondary Injector Program (cont.)

in the analytical temperature prediction. Second, the analytical model is conservative to the extent that it assumes the presence of complete and uniform stoichiometric combustion at the injector face and neglects any coolant carryover from one platelet to the next.

(U) As coolant flow was reduced in successive tests, the chamber showed increasing degrees of dark brown or heat marks with the darkest marks under or in line with the long vane areas of the injector. Generally, the chamber under the vane intersections appeared the coolest. This evidence is verified by the thermocouple data as indicated in the following paragraphs. Figure VI-47 shows the extent of the discolorations looking from the film coolant flange up to the injector face.

(U) The trans-ablative chamber was damaged during Test -023 when an injector vane failed. The chamber was subsequently repaired by grinding at electro-polishing; however, the thermocouples had to be destroyed in the repair process. Therefore, in the final two tests of the series, Tests -024 and -026, no meaningful thermal data were obtained.

(U) The coolant flow rate in compartment 1 was varied between 2.4 and 2.6 lb/sec during the test series, too narrow a range to establish a trend of wall temperature vs coolant flow rate. The temperatures measured in these tests, shown in Figure VI-44, varied from 300 to 600°F. Because of the small change in flow rate from test to test, the temperature spread is attributed to normal data scatter. The recorded temperature values were all substantially below the theoretical values; this is attributed to the low heat load due to the excess oxidizer cooling from the injector and to incomplete combustion.

(U) The initial coolant flow rate tested in compartment 2 was 3.72 lb/sec. This flow rate corresponds to a theoretical

VI, C, Secondary Injector Program (cont.)

wall surface temperature of about 1300°F. Figure VI-45 shows that the measured temperatures varied from 560 to 975°F or approximately from 355 to 770°F below that value predicted by the analytical model. Subsequent reductions in coolant flow rate, eventually to a value of 1.89 lb/sec, produced equivalent thermocouple data. Test 1.2-16-WAM-023 resulted in temperatures from 385 to 940°F below the predicted value of 1870°F. It can be seen from the figure that the measured temperatures, over a very wide range of coolant flow rates, parallel those predicted. The consistently high temperatures, TCSC-9 and -12, are diametrically opposed to each other in the long vane areas while TCSC-11 is at the vane intersections. TCSC-10 is at an intermediate location. These data clearly show a marked nonuniformity associated with the basic injector pattern. It is noted, however, that even in the hottest areas of the chamber the analytical model is somewhat conservative. More discussion of the comparison between the model and the experimental data are included in Section VI,D,4, Cooled Chamber Program.

(U) The compartment 3 data, shown in Figure VI-46, show similar trends to those discussed above for compartment 2 but with the temperatures greatly attenuated because of the proximity of the instrumentation to the film coolant flange. Qualitatively, the physical appearance of compartment 3 indicated heat flux conditions similar to those experienced in compartment 2.

VI, Secondary Combustor Program (cont.)

D. COOLED CHAMBER PROGRAM

1. Introduction

(C) The objective of the Phase I Cooled Chamber Program was to demonstrate high performance and structural integrity of a full-scale cooled combustion chamber and nozzle. The success criterion for this effort, as specified in the contractual work statement, was that the cooled thrust chamber must demonstrate a minimum delivered specific impulse at sea level of 280 sec during each of three or more tests each of 20-sec minimum duration. At the conclusion of each test, the thrust chamber must be in refirable condition.

(U) Two cooling concepts were evaluated in the basic Phase I Cooled-Chamber Development Program: (1) regenerative cooling supplemented with film cooling and a thermal-barrier coating, and (2) transpiration cooling. The two cooling systems represented alternative approaches; either concept could be used to satisfy program performance and duration requirements.

(U) The cooled test program was initiated on 4 August 1966 with the transpiration-cooled chamber. Testing with the regeneratively cooled chamber began on 4 November 1966. Thirty tests were performed with two transpiration-cooled chambers, and five tests were performed with three regeneratively cooled chambers. This testing demonstrated the feasibility of the transpiration chamber concept. The required performance was not achieved, however, because of the incompatibility problem associated with the Mark 125 injector which became apparent during the transpiration cooling test series. Fuel streaks from the injector reacted with the oxidizer transpiration coolant on the chamber wall on two occasions, resulting in burnout of the chambers. The streaking condition was aggravated by a 1-in. (diametral) transition section in the chamber where its diameter changed from 9.5 to 10.5 in., which promoted recirculation of the combustion gases.

VI, D, Cooled Chamber Program (cont.)

(C) In the transpiration-cooled chamber test series, the lowest transpiration coolant flow rate attained without chamber burnout was 36.6 lb/sec (Test 1.2-12-WAM-022). The measured sea-level specific impulse during this 3-sec test was 267.6 sec. Performance obtained with the regeneratively cooled chamber was significantly lower, the maximum obtained being 237 sec. This performance was low for two reasons: (1) the injector used in the test series had a large mixture ratio distribution loss, and (2) no significant amount of film cooling reduction was achieved before the chambers were damaged. Based on the relative success with the transpiration-cooled chamber, no further effort was performed with regeneratively cooled chambers.

(U) Because of the incompatibility problem, testing with cooled chambers was temporarily suspended. The basic Phase I program concluded with the following recommendations: First, develop a compatible high performing injector. This effort should include both improvement of the fuel distribution of the Mark 125 injector, as well as evaluation of new injector concepts designed for better inherent compatibility. Second, the transpiration-cooled chamber diameter should be changed to a constant 9.5 in., thereby removing gas recirculation tendencies near the injector-chamber interface. Third, a backup approach should be pursued whereby the cylindrical portion of the chamber is replaced by a 9.5-in.-dia regeneratively cooled tube bundle section, which may be less sensitive to injector combustion irregularities. (No regeneratively-cooled chamber burnouts had occurred in this region of the chamber.) The regeneratively cooled L* section would be used in conjunction with a transpiration-cooled convergent and throat segment.

(U) These recommendations formed the approach for the Extended Phase I program, which culminated with the successful demonstration of high performance and durability using the transpiration-cooled chamber in conjunction with the newly developed impinging platelet injector.

VI, D, Cooled Chamber Program (cont.)

(U) The specific results and accomplishments of the Cooled Chamber Program during the extended Phase I period are reported in this section. A program summary is given in Section VI,D,2. Details of the cooled chamber design and supporting test hardware are discussed in Sections VI,D,3. The development test program performed and the test results are given in Section VI,D,4.

2. Summary

(U) The transpiration-cooled test program was resumed following the successful development of the Impinging Platelet Injector. Three chambers were fabricated for testing during the extended Phase I program. These chambers were identical in design to those used in the basic Phase I program with two exceptions: (1) the 10.5-in.-dia-to-9.5-in.-dia transition section in the forward end of the chamber was changed to a constant 9.5 in.-dia throughout the cylindrical section; (2) one of the three new chambers incorporated an improved method of thermocouple installation, which resulted in extending the thermocouple life considerably.

(U) The two chamber failures in the basic Phase I program with the Mark-125 injector both occurred in the cylindrical chamber region. While the cause of the problem was attributed to a streaking condition of the injector, a backup chamber program was pursued in the extended Phase I program wherein the cylindrical portion of the chamber was to be replaced by a regeneratively cooled tube bundle (a configuration which could be less sensitive than the transpiration cooled chamber to injector combustion irregularities). The regeneratively cooled section would be used in conjunction with a transpiration cooled convergent and throat section; this concept was termed the "composite chamber". Two regenerative L* sections were fabricated; a photo of one is shown in Figure VI-48. However, because of the success achieved with the full transpiration cooled chamber, no testing was conducted with the composite chamber.

VI, D, Cooled Chamber Program (cont.)

(C) The extended Phase I transpiration cooled test program was initiated on 5 October 1967 and concluded on 22 January 1968. During this period, 46 tests were performed with three transpiration cooled chambers. A cumulative summary of all tests is shown in Figure VI-49. Test data and performance information are given in Figure VI-50. The approach used in the test program was to first operate the cooled chamber at the maximum coolant flow rate and then to selectively reduce the coolant flow in the 12 chamber compartments until the required performance level of 90% I_s was achieved. Three tools were available to aid in establishing the optimum coolant flow rate in each chamber compartment: temperature data obtained with thermocouples located between each compartment; visual examination of heat marks on the cooled chamber wall; and chamber burnout. Most tests were performed at test durations of 1.5 to 4.0 sec; however, some tests of 20 sec duration were included to confirm durability at specific performance levels.

(U) The performance of the transpiration cooled chamber as a function of transpiration coolant flow rate is shown in Figure VI-51. The figure shows two correlations, which represent the difference in performance obtained with two different Impinging Platelet injectors. SN-3 injector was the first Impinging Platelet injector fabricated in the program and had an imperfect pattern, which penalized performance approximately 1%. Improved fabrication techniques on subsequent injectors eliminated this problem. Data points enclosed in square boxes depict 20 sec duration tests. These tests were performed with the uncooled nozzle extension removed, which made direct measurement of delivered specific impulse impossible. Therefore, for these tests, performance was established using the measured coolant flow rate during the test and the performance vs coolant flow rate correlation established by the short duration tests.

VI, D, Cooled Chamber Program (cont.)

(C) The contractual work statement required the demonstration of three short duration tests at a delivered specific impulse of 280 sec (90%) and three 20 sec duration tests at a flow rate not exceeding that used in the performance demonstration test series. In addition, tolerances were placed upon chamber pressure and thrust for these tests. The three short duration tests were successfully completed using chamber SN-5 and injector SN-3. During these tests a maximum performance level of 281 sec I_s (90.3%) was achieved, at a coolant flow rate of 25.2 lb/sec. Using chamber SN-4 and high performing injector SN-4, one 20 sec duration test was performanced in which a delivered specific impulse of 90.5% I_s was achieved at a coolant flow rate of 28.2 lb/sec. (The performance of this test was determined from the correlation established in short duration tests.) The remaining two required long duration tests were not performed due to hardware limitations. The specific requirements for the demonstration test series, together with the values achieved in the test program, are shown in Figure VI-52.

(U) The flow rate distribution in each of the 12 chamber compartments for the long duration high performance test is shown in Figure VI-53. The measured temperature range recorded for each compartment for all tests in which performance was 89% or higher is shown in Figure VI-54. Two facts are evident from these curves: (1) approximately half of the total coolant flow is introduced into compartments 5 and 6 and (2) the measured temperatures of the chamber are substantially below values normally considered safe (the design temperature was 1900°F).

(U) Overcooling of compartments 5 and 6 was necessary because of a local hot zone which existed in the immediate vicinity of the intersection of these two compartments. By increasing the number of compartments in this section of the chamber, the flow can be better tailored to local flow

VI, D, Cooled Chamber Program (cont.)

requirements which will result in a substantial reduction of total flow required. As for the apparent overcooling of the entire chamber, while the measured temperatures give the average wall temperature, they do not reflect localized hot zones on the chamber wall. Because of the injector body design, a nonuniform circumferential distribution of the oxidizer gas was created as it passed through the injector, which resulted in localized hot streaks down the chamber wall. To protect these hot zones, overcooling of most of the chamber wall was required.

(C) By changing the injector body design and the number of compartments in the convergent chamber region, it is estimated that the transpiration coolant flow can be reduced to approximately 15 lb/sec, which would yield average wall temperature of 1600°F. This 10 lb/sec flow reduction over the current flow rate requirement would result in a performance increase of 2.7% including 0.8% for elimination of MRD loss. It is, therefore, concluded that the transpiration cooled chamber used with the impinging platelet injector has an inherent performance capability of 93% I_s, or 290 sec.

3. Cooled Chamber Design

a. Transpiration-Cooled Chamber

(U) The ARES transpiration-cooled combustion chamber was designed early in the Phase I program. Two such chambers were originally fabricated and test fired with the Mark-125 injector during the basic Phase I program. By the time the injector-chamber compatibility problem had been identified, the initial two chambers had sustained erosion damage to the extent that most of the individual washer compartments were not salvageable. However, all other chamber components were reusable. Additional washers were

VI, D, Cooled Chamber Program (cont.)

ordered to fabricate four more transpiration chambers. These washers were obtained and three complete chamber assemblies were built. The fourth set of new washers was retained as spares. With the exception of the chamber diameter change from 10.5 to 9.5 in., and a minor modification in the method of installing thermocouples into the instrumentation washer, all transpiration chambers, SN 001 through SN 005, were of identical design.

(U) The following paragraphs describe the transpiration-cooled chamber design.

(U) The ARES transpiration-cooled combustion chamber, shown in Figures VI-55 and VI-56, is a workhorse design. The chamber is composed of 12 individual compartments, as shown in Figure VI-57, which are housed in a 1-1/2-in.-thick steel shell forming a cylinder with a diameter of about 18 in. Each compartment is manifolded individually to allow external control of gross pressure drop and flow rate. Thus, coolant flow rate may be varied within the compartments from test to test in an effort to achieve optimum operation. Special instrumented washers, each containing six high-response thermocouples, are located between compartments to measure surface temperatures.

(U) Each compartment is composed of a stack of "washer pairs," as shown in Figure VI-58. These pairs consist of a 0.001-in.-thick flow-control washer and a flow-diffusion washer, 0.010 in. thick in the throat region and 0.020 in. thick in the chamber region. The passages in the flow-control washer are etched through the 0.001-in. thickness, whereas the channels in the flow-diffusion washers are 0.0025 in. deep.

(U) Precise metering of the coolant is achieved in the flow-control channels. The flow-diffusion channels provide peripheral distribution of the coolant and allow the coolant to diffuse into the chamber through the thermal influence zone. All heat is exchanged in the thermal

VI, D, Cooled Chamber Program (cont.)

influence zone; coolant flow into this zone is controlled by the previously mentioned flow-control channels and is independent of the heat input. Coolant flow within the washer passages is confined to the laminar region, permitting accurate flow-control predictions to be made.

(U) As mentioned previously, each compartment's total flow rate can be regulated externally. However, the flow rate within the washer pairs themselves is further controlled by the manner in which they are assembled. Because flow rate is directly proportional to flow channel length in the laminar flow regime, the washers were designed to be assembled in six possible positions, each providing a different channel length and, hence, different flow rate.

(U) The aft flange and the aft retainer are designed as an integral unit. The forward end of the chamber incorporates a 1/4-in. plate which extends from the chamber ID to the retainer OD. Both the 1/4-in. plate and the aft flange are keyed to their respective adjacent retainers by means of a shear ring in addition to the two dowel locating pins, which are used to locate all retainers in the entire assembly. An adapter flange was designed for the forward end of the transpiration-cooled chamber to permit installation to the secondary injector. The entire chamber is held in compression by 32 high-strength studs 5/8 in. in diameter.

b. Composite Chamber

(U) As a result of the two transpiration-cooled chamber burnouts that occurred with the Mark-125 injector, it was decided to attack the injector-chamber compatibility problem from two directions. One of these was injector modification and fabrication of two new injectors. This is discussed in Section VI,C,3. The second approach was to design and fabricate

VI, D, Cooled Chamber Program (cont.)

a new cooled combustion chamber assembly that would not be as sensitive to injector hot streaks as the transpiration-cooled chamber had been. It was known from past test experience that transpiration chamber burnout had originated in the cylindrical section of the chamber. This fact, combined with past test experience and heat transfer analysis work on regeneratively cooled combustion chambers, were the deciding factors prompting selection of the composite combustion chamber.

(U) The composite combustion chamber, shown in Figure VI-59, is a segmented combustion chamber design. It consists of a forward adapter flange that incorporates film cooling, a regeneratively cooled cylindrical L* segment, a convergent and throat segment that can be either a completely transpiration-cooled section or a film-cooled ablative section, and an ablative expansion nozzle section.

(U) It should be remembered that the composite chamber assembly was a second approach or a backup design for the totally transpiration-cooled chamber. In the course of development testing, the transpiration-cooled chambers performed so well that the actual testing of the composite chamber was not required. The transpiration-cooled chambers did not prove to be sensitive to burnout in the cylindrical sections when tested with the impinging platelet injector.

(U) Because the design and fabrication of the composite cooled chamber represented a substantial amount of work in the cooled chamber program, a brief discussion of each of the chamber components is presented below.

VI, D, Cooled Chamber Program (cont.)

(1) Adapter Flange

(U) The composite combustion chamber uses an adapter flange that was originally designed for the transpiration-cooled chamber. This adapter attaches the 17.500-in.-dia bolt circle of the regeneratively cooled L* segment to the 13.200-in.-dia bolt circle of the injector body. The adapter has been modified to incorporate a film coolant system with orifices located to inject film coolant on the crown of each tube in the regenerative L* section.

(U) The film coolant circuit consists of four 0.375-in.-dia tubular inlets to a common manifold feeding 248 orifices, each orifice being 0.020 in. in diameter. The film coolant circuit was designed to flow 5 lb of coolant per second with the capability of flowing a maximum of 10 lb/sec. The exit velocity at a flow rate of 5 lb/sec is 400 ft/sec. This velocity was set to match the calculated velocity of the hot oxidizer gas at this station in the chamber.

(2) Regeneratively Cooled L* Segment

(U) The regeneratively cooled L* segment was a double pass oxidizer-cooled tube bundle design composed of 248 straight and round 0.125-in.-dia by 0.010-in. wall tubes 6.0 in. long made from Type 347 stainless steel. No special forming was required on the tubes except at each end where the tubes were hand swaged to transition from round cross-section to square cross-section to facilitate welding. The hydraulic flow circuit was designed so that the incoming coolant would enter the chamber at the aft end and circulate around the tube bundle through a common manifold. The coolant would then flow up through 124 tubes toward the injector and then turn around in a common manifold and flow back through the remaining 124 down tubes

VI, D, Cooled Chamber Program (cont.)

into a common outlet manifold. The design provided for the absolute minimum of uncooled surfaces in the zones where coolant entered, turned around and left the coolant tubes. The tube bundle was supported by a thick-walled steel housing to provide the necessary flange connections to mating part interfaces, and hydraulic manifolding as well as to contain the high chamber pressure of the system. The regeneratively cooled chamber segment is shown in Figures VI-48 and VI-60.

(U) The heat-transfer analysis performed to verify the adequacy of this design is discussed in Section VI,D,5,b. Calculations showed that 25% of the total engine oxidizer flow would be required to satisfactorily cool the L* segment. Therefore, 55 lb/sec of oxidizer was used as the design coolant flow rate. This flow rate resulted in a coolant velocity of 100 ft/sec in the coolant tube and a total calculated L* segment pressure drc of 920 psi.

(3) Convergent and Throat Segment and Expansion Nozzle

(U) As noted previously, two combinations of convergent and throat segments were available for the composite chamber. One configuration simply used the transpiration-cooled chamber, Compartments 4 through 13. The desig of the transpiration-cooled chamber is discussed in Section VI,D,3,a. The second configuration consisted of a transition section and an ablative convergent and throat section. It was planned to use this ablative configuration when making initial checkout tests on the cooled L* segment. When the ablative convergent and throat section is used, a transition section is necessary to adapt the 9.783-in.-dia of the cooled L* segment to the 9.625-in.-dia of the film-cooled flange of the ablative nozzle. The transition section is a transpiration-cooled section made from Compartment 1 of the

transpiration-cooled chamber. The ablative convergent and throat section as well as the expansion nozzle are the conventional design and are discussed in Section IV,C,4.

4. Development Test Program

(C) The objective of the extended Phase I cooled chamber test program was to demonstrate the performance and durability of the transpiration-cooled chamber in conjunction with the impinging platelet injector. The success criteria for this effort was that the cooled chamber must demonstrate a minimum specific impulse at sea level of 280 sec during each of three tests of 20 sec minimum duration.

(C) The test program was initiated on 5 October 1967 and concluded on 22 January 1968, during which period 46 tests were conducted. The program concluded with the successful demonstration of the required performance during each of three short duration tests and one long duration test of 20 sec. Three additional 20 sec duration tests were demonstrated at the 89% performance level.

(C) All testing was performed at a nominal chamber pressure of 2800 psia using the pump-fed 100,000-lb-thrust staged-combustion test engine. A description of this engine and its operating characteristics is presented in Section VII,D,4,a,below. The detailed test program performed is discussed in Section VII,D,4,b. The evaluation of the test data, including both performance and heat transfer aspects, is discussed in Section VII,D,4,c.

VI, D, Cooled Chamber Program (cont.)

a. Test System

(1) Staged-Combustion Test Engine

(U) The cooled chamber program used the same staged-combustion test engine as was used in the secondary injector program except for the high-pressure propellant feed system (the basic test engine is described in Section VI,C,5,b,(1), above). Test durations up to 20 sec were required in the cooled chamber program, which precluded the use of the intensifiers with their 5-sec test duration limitation. Therefore, at the beginning of cooled chamber testing, high-pressure turbopumps were installed to supply high-pressure propellants to the engine. The turbopumps used were developed under the Integrated Components Program, Contract AF 04(611)-8548. These turbopumps are direct driven, with Titan II first-stage turbine components on one end, and specially designed pump components on the other end. The common shaft is supported in the center by two roller bearings and by two match-ground ball bearings. The pump impellers are of the mixed flow type with axial inlets and radial exits, and run inside a close fitting shroud. The bearings are lubricated with oil in a nonrecirculating system. A cross section through one of these pumps is shown in Figure VI-61. A single liquid oxygen/RP-1 gas generator is used to supply the gas energy for driving the turbines. The power split between the oxidizer and fuel turbines is accomplished by orificing the fuel turbine inlet.

(C) The ICP turbopumps were designed for a maximum discharge pressure of about 4000 psia at flow rates corresponding to a 100K thrust engine. The ARES transpiration-cooled chamber, on the other hand, was designed for integration into the ARES engine, which has a pump discharge pressure of about 6000 psia. This necessitated using the oxidizer high-pressure intensifier to supply the transpiration coolant flow and using

VI, D, Cooled Chamber Program (cont.)

the turbopumps to supply the flow to the primary and secondary combustors. The oxidizer intensifier is sufficiently large to allow a 20-sec test firing when it is supplying coolant flow at 40 lb/sec or below. A schematic of the test engine used in cooled chamber testing is shown in Figure VI-62. A photo of the actual engine is shown in Figure VI-29.

(U) The pump-fed staged-combustion test engine is completely described in Aerojet Drawings 1129668 and 1127831. Drawing 1129668 shows the turbopumps and their associated gas generator drive system, while Drawing 1122831 describes the rest of the engine. All test hardware configurations fire-tested and/or designed in the program are called out on these drawings by a series of dash numbers. The final configuration used for the cooled chamber performance and durability demonstrations is described by Drawing 1122831-179. The major assemblies and subassemblies of this final configuration are listed in a basic parts list, given as Figure VI-63. All drawings are available in the Aerojet drawing system.

(2) Engine Operation

(U) The criteria for operation of the pump-fed engine system was the same as for the intensifier engine system, i.e., (1) establishment of film coolant flow, (2) establishment of primary oxidizer flow, (3) primary ignition, and (4) secondary ignition on a rising pressure schedule.

(U) Preliminary steps required in order to prepare the engine system for each test included the following: the purge pressure regulators were adjusted; ullages were adjusted in the generator propellant storage vessels, surge bottles, and oxidizer intensifier. All propellants were bled in up to the control valves and pressures set on each vessel. The pump lubrication system was started and its operation verified prior to arm switch.

VI, D, Cooled Chamber Program (cont.)

(U) Arm switch signaled on all engine purges, and fire switch signaled the film coolant valve open. This valve was initiated open for several seconds prior to sequencing of the remainder of the engine controls to prime the transpiration coolant circuit. Thereafter, the gas generator valve and the thrust chamber valves were signaled open, while the intensifier pressure program was initiated at the desired rate. The control valves opened at such a rate that primary oxidizer lead, primary ignition, and secondary ignition occurred in succession. On shutdown, valve closing signals and rates were interlocked to preclude deadheading the pumps on shutdown, and to maintain primary mixture ratio above 12.0. The intensifier was vented following cessation of engine fuel flow.

(U) With turbopump testing, additional malfunction shutdown circuits were added to protect the test hardware. Upper and lower limits were placed upon film coolant flow rate and primary mixture ratio; oxidizer discharge pressure had to be higher than fuel discharge pressure by a preset amount, turbine inlet temperature had a maximum value, etc. The significance of these shutdown criteria lies in the fact that in one test, shutdown without hardware damage occurred only because the malfunction detection system shut down the engine quickly.

(3) Instrumentation

(U) The instrumentation system used for the cooled program was identical to the injector program, see Section VI,C,5,b,(4), with one major addition. This addition was the inclusion of the 12 transpiration chamber compartment flow readings measured by individual metering orifices. A schematic of the pump-fed engine system showing the metering orifice system of the transpiration chamber is shown in Figure VI-62. Pressure transducers on the upstream and downstream side of the orifices allow calculation of the

VI, D, Cooled Chamber Program (cont.)

individual weight flows. A flowmeter installed just upstream measures total coolant flow; this flow measurement was used for the performance calculation instead of the sum of the compartment flow since it is the more accurate measurement.

VI, D, Cooled Chamber Program (cont.)

b. Detailed Test Program

(C) The extended Phase I transpiration-cooled test program encompassed 46 tests using three transpiration-cooled chambers. The primary objective of the test program was to demonstrate the required performance level (90% I_s) and durability (20-sec duration) of the cooled thrust chamber. The approach followed in achieving this objective was to first operate the cooled chamber at maximum coolant flow rate and then to selectively reduce the coolant in each of the 12 chamber compartments until the required performance was achieved. To minimize hardware loss, a three-step test plan was adopted and generally followed throughout the test program. The first test at any specific flow rate was of very short duration, approximately 1.5 sec, and has as its objective the identification of any erosion or potential erosion before major hardware damage was sustained. (Almost all erosion experienced in the program occurred during the start transient prior to this time.) If the posttest condition of hardware appeared satisfactory, a test of 2.2 to 4.0 sec duration was performed to determine chamber performance. This was followed by a 20-sec test with the uncooled skirt extension removed to demonstrate durability. The long-duration tests were not performed with each coolant reduction, but only after a significant performance gain over that previously demonstrated had been made.

(U) A cumulative summary of all tests, including test objectives and results for each test, is tabulated in Figure VI-49. Detailed test and performance data are shown in Figure VI-50. The individual compartment flows for each test are shown in Figure VI-64. Summary test data for each compartment, including the flow rate range and the differential pressure from the compartment leading edge to trailing edge, are given in Figure VI-65. Also included in this figure are physical descriptions of each compartment, including dimensions, number of platelets and number of flow indexing positions.

VI, D, Cooled Chamber Program (cont.)

(U) The flow rates in each compartment were controlled by a balancing orifice located at the compartment inlet. The proper orifice selection required knowledge of the flow characteristics of each compartment. These were theoretically predicted at the beginning of the program and modified during the course of the test program as test data became available. The established flow characteristics of each compartment are shown in Figure VI-66. Differences between recorded values and theoretical laminar flow predictions are a result of three factors: (1) measurement errors at high flow rates with large hole size, low Δp orifices as evidenced in compartments 1, 9, and 12; (2) leakage past the primary metering zones where platelet compression was low as seen in compartments 7 and 10; (3) modifications to the primary metering zone flow restriction by machining a bypass as done in compartments 5, 6, and 8.

(U) The test program consisted of four test series, each of which is discussed in detail in this section. Series I included the testing with chamber SN 3, Series II with chamber SN 4, and Series III with chamber SN 5. Series IV encompassed testing with two reworked chambers in an effort to complete two remaining durability demonstration tests.

(U) During the course of the test program, chamber burnout occurred in several instances as coolant flow was reduced. These burnouts occurred predominantly in two areas: (1) in compartment 6 just below the intersection of compartments 5 and 6, and (2) in the exit nozzle section. The only other significant problem with test hardware during the program was the failure of a seal located between the injector and the upstream adapter. This seal failed on several occasions with resulting injector damage. A consolidated discussion of the failure investigations performed for the chamber burnouts and injector seal failures follows the discussion of the individual test series.

VI, D, Cooled Chamber Program (cont.)

(1) Test Series I, Tests 1.2-16-WAM-025, 1.2-13-WAM-005 through -014

(U) This test series consisted of 11 tests with impinging platelet injector SN 3 and transpiration-cooled chamber SN 3. Initial testing centered on evaluating the compatibility of the impinging platelet injector with the fully cooled transpiration chamber. (The compatibility of the cylindrical portion of the chamber had been previously evaluated in the injector test program.) The first test, 1.2-16-WAM-025, was scheduled for 1.15 sec or 50% of design chamber pressure at the maximum possible transpiration coolant flow rate. Posttest inspection of the chamber showed very dark heat marks in the convergent section near the intersection of compartments 5 and 6, as shown in Figure VI-67. To allow additional flow capability in this chamber region, the chamber was removed from the test stand and modified by machining a portion of the primary metering grooves in compartment 5 and 6 platelets, which increased their flow capability to approximately three times their former values. Following this modification, Test 1.2-13-WAM-005 was performed with the same test objectives as for Test 1.2-16-WAM-025. The chamber wall was in perfect condition following this test with no evidence of heat marks. Testing was then continued to determine thrust chamber performance at the maximum coolant flow rate condition (49 lb/sec), followed by evaluation of chamber durability with a 17.25 sec duration test. The chamber was in excellent condition following these tests.

(U) Transpiration coolant flow was then reduced in three incremental steps to 41.5, 36.1, and 31.3 lb/sec. During Test -014, which was a short-duration test at the lowest flow rate, the chamber experienced minor erosion starting approximately 0.25 in. below the intersection of compartments 5 and 6. A photograph of the damage in the convergent section is shown in Figure VI-68; nozzle damage is shown in Figure VI-69. This chamber was subsequently repaired by grinding out the eroded area and restoring the porous wall surface by electro-polishing.

VI, D, Cooled Chamber Program (cont.)

(2) Test Series II, Tests 1.2-13-WAM-017 through -027

(C) Testing was continued with transpiration chamber SN 4 and injector SN 4. The initial test was performed at maximum coolant flow rate of 50 lb/sec to confirm the hydraulic flow characteristics of this new chamber. A series of three flow cutbacks was then performed, which culminated in the attainment of a sea-level specific impulse of 89.5% (278.5 sec) at 30.8 lb/sec coolant flow. This test was followed by a successful durability demonstration test of 20.5 sec duration (Test 1.2-13-WAM-024). The coolant flow rate during the first 10 sec of this test gradually decreased from an initial 30 lb/sec to 28.1 lb/sec, after which it remained constant for the final 10 sec. The corresponding sea-level specific impulse for the steady flow value is 90.5% I_s.

(U) The next test, 1.2-13-WAM-025, was planned to confirm this performance value by conducting a short duration test using the 20:1 area ratio uncooled nozzle extension. In order to obtain a flow rate of 28.1 lb/sec early during the test (to provide a 1-sec steady-state data sample), the engine was rebalanced by slightly increasing the resistance in the coolant circuit. Unfortunately, minor erosion occurred in compartment 6 during the start transient, as shown in Figure VI-70, and the test was terminated prematurely. The damage was repaired on the test stand by electro-polishing the eroded area. In subsequent Test 1.2-13-WAM-027, in which the coolant flow rate was 30.25 lb/sec, gross nozzle erosion was experienced at 3.5 sec after FS_1. Also, the injector seal failed during the shutdown transient of this test, with resulting injector damage. The chamber and seal failures are discussed in detail in Paragraph VI,D,4,b,(5).

VI, D, Cooled Chamber Program (cont.)

(3) Test Series III, Tests 1.2-13-WAM-028 through -046

(C) This test series was performed with transpiration chamber SN 5 and injectors SN 5 and SN 3. Nineteen tests were performed, including three 1-sec steady-state duration tests at a performance level above the contractually required 90% I_s and three 20-sec duration durability demonstration tests at the 89% I_s level.

(U) The first test was a short-duration hydraulic balance checkout test of new transpiration chamber SN 5 using injector SN 5. With the hydraulic characteristics defined, coolant flow was reduced to 35 lb/sec in the next test. A malfunction detection system sensed a slow opening primary combustor oxidizer valve and terminated the test prematurely at 0.934 sec. On shutdown, the injector seal again failed, damaging the injector in a manner similar to that experienced in Test 1.2-13-WAM-027.

(C) Testing was resumed with injector SN 3 at the same balance point used for the previous test. Three flow reductions followed in which the flow was reduced to 29.7 lb/sec, at which flow the performance was 89% I_s. Two additional tests at this balance were performed to verify performance. Three long-duration 20-sec tests were then conducted to certify the durability of the cooled thrust chamber at the 89% performance level. The established performance for these tests were 89.3, 89.1, and 89.1% I_s.

(C) The flow reduction program continued with cutbacks being made in compartments 5, 6, and 7 until the total coolant flow was 25.3 lb/sec. At this flow rate, thrust chamber performance of 90.3% I_s was achieved, which is above the 90% I_s requirement. Two repeat tests were made at this balance to conclusively demonstrate operation at this performance level. The performance obtained in both repeat tests was 90.2%.

VI, D, Cooled Chamber Program (cont.)

(C) A durability demonstration at the 90% performance level was then attempted in Test 1.2-13-WAM-046, a scheduled 20-sec duration test. The test was terminated prematurely at 11.38 sec by a malfunction detection system sensing a rapidly increasing transpiration coolant flow. Posttest hardware inspection indicated severe burning in the nozzle section, as shown in Figure VI-71. Review of the test films subsequently showed that burning was initiated after approximately 7 sec of operation. The cause of failure of this test is considered identical to that which occurred in Test 1.2-03-WAM-027; see Paragraph VI,C,4,d,(5).

(4) Test Series IV, Test 1.2-13-WAM-047 through -051

(U) With the failure of chamber SN 5, no additional good quality chambers were available for testing. However, chambers SN 3 and SN 4 had been repaired and were in firable condition. The defect in both of these chambers was that in one circumferential location, the chamber convergent and throat sections were oblong where metal had been removed by previous erosion. In an effort to complete the remaining two durability demonstration tests, the test program was continued with these chambers.

(U) Initial tests utilized reworked chamber SN 4 and injector SN 3. Three tests were performed at coolant flow rates of 33.5, 31.5, and 29.3 lb/sec. In the last test, erosion occurred in compartment 6 adjacent to the repaired area, as shown in Figure VI-72. Posttest analysis disclosed no adverse flow conditions. Flow in both compartments 5 and 6 was well above previously demonstrated safe operating levels. Since the failure occurred adjacent to the repaired area, it was concluded that the marginal convergent section compatibility condition during the start transient (see paragraph VI,D,4,d,(5)) was aggravated by boundary layer disruption from the repaired area.

VI, D, Cooled Chamber Program (cont.)

(U) The test series was resumed using reworked chamber SN 3 which was previously damaged during Test 1.2-13-WAM-014. The repair of high performing injector SN 4 had been completed at this time and this injector was reinstated in the test program. Two tests were performed at coolant flow rates of 33.5 and 31.5 lb/sec. During the second test, a leak developed between the two halves of one of the injector vanes, resulting in liquid fuel being sprayed onto the transpiration-cooled chamber wall. This initiated chamber burning in compartment 1, which then extended down the entire chamber as shown in Figure VI-73. It was decided at this time that the remaining test hardware was of such substandard condition that continued testing was not warranted. Therefore, the test program was concluded.

(5) Failure Investigations

(U) During the test program several instances of chamber erosion and injector vane failures were experienced. Chamber erosion occurred in two locations: the chamber convergent section, and the nozzle divergent section. Injector vane failures occurred in the lower half of the injector as installed in the horizontal test firing facility.

(U) Overheating of the chamber's convergent section was first encountered on Test 1.2-16-WAM-025. This short-duration test to 50% of design chamber pressure produced heat marks in the convergent section between compartments 5 and 6 (see Figure VI-67). This location is where rapid turning of the combustion gas occurs and corresponds to where significant erosion started in ablative chambers during the injector test program. Evidently, the remaining unvaporized fuel in the combustion gas is impacted into the chamber wall at this point. To provide sufficient cooling for this local zone, the primary metering grooves of compartments 5 and 6 were modified to allow approximately three times their former flow capability. The resulting increased flow

VI, D, Cooled Chamber Program (cont.)

on subsequent tests eliminated the problem, as evidenced with the completion of nine successive tests without chamber erosion. The heat marks did reappear during the tests but to a lesser extent than experienced on Test 1.2-16-WAM-025. For this reason, cutbacks in compartments 5 and 6 were not made until the latter portion of the test program.

(U) On the third cutback of compartments 5 and 6, Test 1.2-13-WAM-014, chamber erosion occurred which started at the forward end of compartment 6. Failure analysis concluded the erosion occurred because of excessive flow reductions in compartments 5 and 6 (a reduction of 2.5 lb/sec, or 17% from the previous test value). In subsequent tests, higher flow rates were maintained in these compartments.

(U) Testing was resumed with chamber SN 4 with eight satisfactory tests being completed without reducing the flow in compartments 5 or 6. On Test 1.2-16-WAM-025, slight erosion was again experienced in compartment 6, but at a 45% greater flow (in compartments 5 and 6) than the burnout condition of Test 1.2-13-WAM-014. It was determined that in this instance the start transient was primarily responsible for the problem. Test data analysis showed cavitating flow was being experienced during the start transient in the primary metering grooves of compartment 5, which reduced the carryover cooling to compartment 6 during the flow recompression phase as back pressure was provided to the coolant by rising chamber pressure. This condition was present on all tests prior to this time and was probably a contributor to the previously experienced erosions. The condition was aggravated during this test due to an abnormally low pressure rise rate during the transient. This required the chamber to operate for a longer than normal period of time in the cavitating condition. Correction was made in subsequent tests by maintaining the pressure rise rate to previously demonstrated acceptable values. With the rise rate kept at a sufficiently high level, the cooled chamber program was completed with no further occurrences of this convergent section problem.

VI, D, Cooled Chamber Program (cont.)

(U) On the second test after the eroded area had been repaired (Test 1.2-13-WAM-027), the transpiration chamber experienced heavy erosion in the nozzle section, compartments 8 through 12. This failure is attributed to marginal operation of the nozzle section in the hot streak zones caused by the secondary injector. This condition is evident in the photograph of Figure VI-74, taken after Test -024. In this marginal condition small changes in operating conditions make the nozzle heat transfer critical. A contributing factor is the basic mechanical design of the chamber, which allows small movement of the washer compartments within the retainers. Even a very small movement can trip the boundary layer from laminar to turbulent flow, which increases the heat transfer to the already marginal streak condition on the wall. This effect has been evidenced in the high-speed movies, where burning has been seen to initiate and extinguish prior to initiation of continuous burning. Such a condition could occur if a compartment were moving into and out of the boundary layer. With careful attention given to nozzle flow cutbacks beyond those demonstrated in the test preceding Test 1.2-13-WAM-027, the development program continued using replacement chamber SN 5. Eighteen satisfactory tests followed. On Test 1.2-13-WAM-046, gross nozzle erosion was again experienced. Cause of failure is considered identical to that which occurred in Test -027.

(U) Injector vane failures occurred three times during the program, Tests 1.2-13-WAM-027, -029, and -049. In all instances, a seal which isolates liquid oxidizer passing through the injector body from the combustion zone failed during the shutdown transient, allowing gross quantities of liquid oxidizer to leak into the chamber following the test. Some of this oxidizer then entered the lower injector fuel vanes through the injection orifices. When the fuel was purged from the outer manifold, approximately 2 min following the test, it combined with the oxidizer, producing detonations within the injector vanes. A subsequent investigation revealed that the sealing surfaces had become warped during long-duration tests; this warping then allowed the seal to extrude from its sealing groove. Corrective action was to remove the hardware from the stand and remachine the metal surfaces to proper condition.

VI, D, Cooled Chamber Program (cont.)

c. Test Data Evaluation

(1) Performance

(U) Cooled-chamber performance analysis was conducted in the same manner as for the Secondary Injector Program, i.e. using the Performance Interaction Theory. Specific impulse measurements were obtained in each test using continuous measurements of thrust, volumetric flow rates, and propellant temperature and pressure for specific gravity determination. The difference between delivered and theoretical impulse was divided into five parts for assessment of component performance losses. The applicable component performance losses were (1) nozzle friction (NFL), (2) nozzle geometry (NGL), (3) mixture ratio distribution (MRD), (4) energy release (ERL), and (5) transpiration coolant (TCL).

(U) The transpiration-cooled chamber was cooled from the plane of the injector face down to an area ratio of 4:1; at this point an uncooled steel nozzle extension was attached and increased the overall area ratio to 20:1. The uncooled nozzle extension was used on all short-duration tests in which performance evaluation was the test objective. From these data, the relationship between delivered specific impulse and transpiration-coolant flow rate was established, as previously shown in Figure VI-51. For long-duration tests, the uncooled nozzle extension was removed, since the heat transfer rates were sufficiently high to cause metal erosion after about 4-sec of operation. For these tests, delivered specific impulse was established using the measured transpiration coolant flow during the test, together with the performance correlation of Figure VI-51.

(U) The component performance loss analysis was conducted only for tests in which specific impulse was directly measured,

VI, D, Cooled Chamber Program (cont.)

i.e., those with the uncooled-nozzle extension attached. The complete tabulation of the losses for these tests, together with measured specific impulse at sea-level and vacuum conditions, is included in the performance summary of Figure VI-50. Component specifications, historical information, and data necessary to make loss calculations are also given in the figure. A nomenclature list of the tabulated quantities is given in Figure VI-8. A discussion of each component loss follows in the ensuing paragraphs.

(a) Nozzle Friction Loss (NFL)

(U) Nozzle friction loss was calculated using the extended Frankel-Voishel analysis* for the 20:1 area ratio, 80% Bell nozzle contour. These losses are tabulated in seconds of vacuum specific impulse in Figure VI-50. This loss is a constant for all tests since the influence parameters of chamber pressure, mixture ratio, and area ratio were maintained as near-constants throughout the entire test series.

(b) Nozzle Geometry Loss (NGL)

(U) The 80% Bell nozzle contour had an exit half angle of 9.63 degrees. The resulting nozzle geometry loss for each test is also tabulated in Figure VI-50. The slight test-to-test variances in this loss are caused by changes in exhaust velocity, which varies slightly with transpiration-coolant flow rate.

(c) Mixture Ratio Distribution Loss (MRD)

(U) Mixture ratio distribution losses resulted from two effects: (1) non-uniform oxidizer flow across the fuel injector vanes and (2) a difference in the effective fuel injector diameter of

*Frankel, F., and Voishel, "Friction in the Turbulent Boundary Layer of a Compressible Gas at High Speeds," NACA TM 1032, 1942.

VI, D, Cooled Chamber Program (cont.)

different injectors tested. The portion of the loss attendant with the non-uniform oxidizer flow was determined to be 2.2 sec vacuum specific impulse during the Secondary Injector Test Program, which used a 12:1 area ratio nozzle and a drilled plate for oxidizer gas distribution. With the 20:1 area ratio nozzle used in cooled chamber testing, this loss increases to 2.3 sec. The same drilled plate was used throughout the cooled-chamber program.

(C) Injectors SN-3, SN-4, and SN-5 were used for cooled-chamber testing. Following the injector test program (which used SN-3 injector exclusively), but prior to cooled chamber testing, the outermost fuel doublets in each of the two longest vanes in each injector octant of SN-3 injector were plug-welded closed in an effort to reduce the hot streaks in the long vane areas caused by the maldistribution of oxidizer gas. In addition, following a pattern check of this injector, a substantial number of other outboard fuel doublets were plugged to prevent direct impingement of fuel on the chamber wall (caused by imperfectly flowing doublets). As a result of these modifications, the effective fuel injection diameter of SN-3 injector was approximately 9.17 in. vs the design value of 9.35 in., a 3.62% diameter reduction. This smaller effective diameter increased the gap area about the injector periphery and accounted for an additional 3.3 sec mixture ratio distribution loss. Injectors SN-4 and SN-5 were not modified in this manner and did not experience this additional loss.

(d) Energy Release Loss (ERL)

(C) An energy release loss of 5.9-sec vacuum specific impulse was established for the Impinging Platelet injector in the Secondary Injector Program. The values of energy release loss for cooled chamber testing are tabulated in Figure VI-50, and reflect slight changes

VI, D, Cooled Chamber Program (cont.)

resulting from effects of area ratio, injector mixture ratio, and chamber pressure. Changes in characteristic length (L*) from test-to-test were assumed to have no influence on energy release loss, since the distance from the injector face to the throat (L') remained constant as throat area measurements varied (see Section VI,E,1 for further discussion on this subject).

(e) Transpiration-Cooling Loss (TCL)

(C) The transpiration-cooling loss was determined by subtracting all the losses previously discussed from the difference between test and theoretical specific impulse. Twenty-nine transpiration-cooled tests yielded valid transpiration-coolant loss data. These are tabulated in seconds of vacuum specific impulse and percent of theoretical vacuum specific impulse in Figure VI-50. A correlation of the percent cooling loss vs percent coolant flow is given in Figure VI-75. The resulting performance loss slope is 0.65% specific impulse loss per percent coolant flow. This is in general agreement with results obtained from early transpiration chamber testing with SN-1 and SN-2 chambers, in which a 0.6% specific impulse loss per percent coolant slope was established.

(2) Heat Transfer

(U) The primary objective of the thermal instrumentation during this test program was to evaluate the surface temperatures at many points in the chamber. The resulting data, in combination with coolant-flow measurements in each compartment, was to provide a guide to selective coolant-flow reduction until the desired chamber performance was achieved. A secondary objective was to acquire data which would support or improve the analytical design model to strengthen future design efforts.

VI, D, Cooled Chamber Program (cont.)

(U) In the extended Phase I effort three transpiration-cooled chambers were tested, Chambers SN-3, SN-4, and SN-5. SN-3 was residual from the basic Phase I program and had brazed thermocouples which had proved to be very short lived. The cause of this instrumentation weakness was identified early in the Phase I extension. During the brazing process, an amalgam was formed between the braze (Nioro) and the sheathing of the thermocouple (304 SS). In a laboratory experiment, this amalgam was severely attacked by nitric acid fumes with the result that continuity of the thermocouple junction was lost within two days. This same phenomenon accounted for the loss of the brazed thermocouples in the chamber a short time after exposure to N_2O_4. To improve the integrity of the thermocouples for subsequent chambers, further laboratory tests were conducted. As a result of these tests, the thermocouple installation technique was modified for the next two cooled chambers. For chambers SN-4 and SN-5, slots were eloxed into the platelets as before, after which the junctions were welded to the gas-side surface and ground smooth. The thermocouples were staked at several locations back along the slot to eliminate or minimize any coolant flow bypassing part of the primary or secondary metering grooves. The depth of the thermocouple junction from the surface was measured by X-ray after grinding as had been done on previous chambers.

(U) Assembly of Chamber SN-4 resulted in sufficient mismatching of chamber compartments to require smoothing of the gas-side surface prior to test. This was accomplished by blending the discontinuities with a grinder, followed by electro-polishing of the entire gas-side surface. The effect of this polishing was to completely negate the validity of the thermocouple depth measurements and in a number of cases to completely remove the weld to the gas surface. This permitted coolant to flow around the remaining junction and invalidate the results.

VI, D, Cooled Chamber Program (cont.)

(U) The experience acquired on Chamber SN-4 led to extremely careful assembly of Chamber SN-5 with the result that 53 of the original 66 thermocouples were available for use at the initiation of testing. The improved method of installing by welding increased the life of the thermocouples sufficiently that substantial meaningful heat transfer data acquired on the extended Phase I program was provided by this chamber.

(U) The approach used in the various development test series was to selectively reduce the coolant flowrate in steps until the desired performance was attained. Two combustion phenomena, however, limited the flow reduction program in the various compartments. The first was a dynamic incompatibility in the convergent section of the chamber, caused by the impingement of incompletely burned fuel against the wall where the gases are turned rapidly. Figure VI-53 shows most clearly the influence of this effect. This figure shows the flow distribution summary for Chamber SN-4 on Test 1.2-13-WAM-024, which was conducted for 20 sec at a performance level slightly higher than the Phase I goal. It can be seen that 14.5 lb/sec, or more than half of the 28.2 lb/sec total coolant, is distributed to Compartments 5 and 6 in the convergent section of the chamber. Figure VI-67 shows the heat marks that necessitated this high coolant flowrate. This photograph was taken after Test 1.2-16-WAM-025, the first test on Chamber SN-3. The mechanical measures taken to increase the flow capability in Compartments 5 and 6 as a result of that test were discussed in Section VI,D,4,6. This indication of very hot areas all the way around the chamber at the instrumentation platelet of Compartment 5 continued to be seen throughout the test series and was most evident on the short duration tests. The failures of Chambers 3 and 4 on Tests 1.2-13-WAM-014 and -025, respectively, are directly attributed to this effect and were both on scheduled durations of 1.5 sec.

VI, D, Cooled Chamber Program (cont.)

(U) The second phenomenon limiting the flow reduction program was the non-uniform combustion characteristic of the impinging platelet injector. The most important contributor to this non-uniformity is a maldistribution of oxidizer-rich gas circumferentially around the chamber caused by the back side injector geometry (Figure VI-76), (see discussion Section VI,C,3,). The evidence that the flow was not uniform is graphically illustrated by the exhaust pattern of alternate hot and cool zones shown in Figure VI-77, a photograph of the steady-state portion of Test 1.2-13-WAM-035. This was a 2-sec test with 29.7 lb/sec of transpiration cooling. Figure VI-78, a photograph of the expansion section of the chamber after Test 1.2-13-WAM-038, also shows evidence of this non-uniform exhaust pattern.

(U) The effect of this phenomenon is to require extra coolant in each compartment to cool the high-temperature zones, while the majority of the compartment remains relatively cool. Figure VI-54 summarizes the steady-state temperature data for Chamber SN-5 from Tests 1.2-13-WAM-035 to -045. All of these tests were conducted with between 25 and 30 lb/sec of cooling at high performance levels. The bands of temperature in each compartment represent the majority of the thermal data on this chamber with only the highest temperatures which are attributable to the injector streaks not shown. This figure shows the operating conditions over a large number of highly successful tests and clearly indicates the potential of significant coolant flow reductions in the various compartments if the injector/chamber incompatibility can be successfully eliminated or minimized. It should be pointed out that the highest measured temperature on any successful test including all hot spots was 1681°F, while observation of the chamber indicated that there were a number of locations in the chamber operating under hotter or more adverse conditions than that measured. This verifies the validity of the original approach of designing to a capability of a 1900°F uniform wall temperature.

VI, D, Cooled Chamber Program (cont.)

(U) One other fact is evident from Figure VI-54. Compartments 5 and 6, which are flooded with cooling to protect the interface between these compartments from the incompatibility previously discussed, show very low steady-state temperatures. This evidence in combination with the fact that hardware inspection of this zone revealed adverse wall discolorations indicates this incompatibility occurs at times other than steady state. Movie reviews also verify this fact, where in Test 1.2-16-WAM-025 burning is observed during engine start. A complete discussion of the start transient characteristics, which allow this high temperature condition to exist, is presented in section VI,D,4,b,(5), Cooled Chamber Detailed Test Program Failure Investigations.

(U) A tabular summary of the steady-state surface temperatures resulting from the testing of Chamber SN-5 is presented in Figure VI-79. These surface temperatures are generated from the measured temperature by use of a multiplication factor which is a function of the depth of the thermocouple junction from the gas-side surface. The basis of this factor is the one-dimensional fin conduction model described in Appendix 1. There is no empirical verification of this portion of the heat transfer model due to the non-uniformities of the combustion process, so it is used only for those thermocouples that are a maximum of 0.010 in. from the surface. The depth of each junction is noted on the figure.

(U) Figure VI-80 shows the analytical temperature prediction as a function of the coolant flow rate for Compartments 1 through 12. The details of the analytical design model are presented in Appendix I. This approach differs slightly from that used in the basic Phase I program, in that a boundary layer mixing model is used for film cooling rather than the previously used Hatch & Papell model. The reasons for this change are two-fold. First and foremost, this model provided a truer representation of the experimental data acquired in Phase I of this program, in that there

VI, D, Cooled Chamber Program (cont.)

is now no location in the chamber where the predicted temperatures fall below those measured in that test series. Second, this version of the heat transfer model provided excellent correlation of surface temperature measurements acquired on similar chambers at lower chamber pressures[1]. The new model also lends itself to simple programming for an IBM 1130 computer and as such allows rapid data evaluation and correlation.

(U) This model, as utilized to develop these predicted design temperature curves for each compartment, is conservative to ensure the success of the original design. It assumes that complete and uniform combustion exists throughout the chamber and that no carryover of transpiration-coolant effectiveness exists from one platelet to the next. Additionally, a multiplying factor of 1.5 was applied to the hot-gas heat transfer coefficient calculated by the Bartz equation for the cylindrical portion of the chamber. This multiplying factor is decreased with contraction ratio to a value of 1.0 at the chamber throat.

(U) Prediction curves are shown for both the leading and the trailing edge for those compartments where the theoretical temperature varies. In addition, a prediction for the instrumentation platelet is shown for Compartments 6 through 11, where the compartment platelets are 0.010 in. thick and the instrumentation platelets are 0.020 in. The various predictions reflect the effect of changes in heat flux, the flow distribution within the compartment due to the various indexing positions utilized and the changes in internal pressure drop due to the gradient in the gas-side pressure. In the compartments where only one prediction is shown, a constant theoretical temperature exists throughout the compartment.

---

(1) Blubaugh, A. L., and Fisk, E. J., Demonstration of an Advanced Transpiration-Cooled Thrust Chamber, TR No. AFRPL-TR-67-198, 31 October 1967 (Confidential).

VI, D, Cooled Chamber Program (cont.)

(U) Figure VI-80, pages 1 through 10 also shows the experimental data acquired on Chamber SN-5 for Compartments 1 through 10, respectively. In general these figures all show the wide range of temperatures characteristic of the combustion process. The Compartment 8 temperature data are not plotted because flow rate measurements of this compartment were not sufficiently precise for heat transfer evaluation. The flow measuring orifice was removed for this series of tests to allow the maximum possible coolant to this compartment. The resulting temperatures, however, are tabulated in Figure VI-79. Compartments 9 and 10 show a particularly wide range of temperatures for a very small range of coolant flow rates. These measurements differ from those in other compartments, however, in that they each have only one valid thermocouple. The temperature range, therefore, is not attributable to geometric effects or the combustion process. In both of these compartments, however, Figure VI-79 shows a trend toward increasing temperatures with each successive test. This trend can be attributed only partly to the small decreases in compartment flow rate. A significant contribution to this effect must be the carryover of transpiration-coolant effectiveness from the compartments immediately upstream. This, to a large extent, verifies the observations on film cooling effectiveness in the expansion region of the nozzle made during film cooling studies on both the basic Phase I effort and the Integrated Components Program, Contracts AF04(611)-8017 and -8548.

(U) The data from Compartment 3 was selected for some correlation studies because of the number of data points and the wide range of both temperature and flow rate covered. Neglecting the effect of incomplete and non-uniform combustion, there are two factors which can be modified analytically: the presence of carryover from the two upstream platelets and the multiplying factor on the Bartz gas-side heat transfer coefficient. Figure VI-81 again shows the experimental data from Compartment 3 but this time with the range of correlations as well as the design prediction. It can be seen that the use of carryover in the model changes the slope of the curve

VI, D, Cooled Chamber Program (cont.)

and closely approximates the slope of the experimental data while the magnitude of the multiplying factor affects only the level of the curve. It can be seen that a multiplying factor of 0.75 accurately covers the high side of the data range presented in Figure 4 and a value of 1.75 conservatively predicts the highest temperatures measured in the hot areas.

(U) Several conclusions resulting from the evaluation of the heat transfer data are enumerated here.

1. Despite the limitations imposed by incompatibilities and hot spots, the feasibility and high-performance capability of the transpiration-cooling concept has been successfully demonstrated.

2. Elimination of both the dynamic incompatibility and the non-uniform combustion would conservatively result in a reduction in the coolant requirement to 15 lb/sec for a uniform wall temperature of 1600°F. It is estimated that this reduction would result in an improvement in performance of 3% I_s.

3. The circumferential maldistribution of oxidizer gas can be corrected by using an injector body with the same diameter at the upstream and the downstream end and platelet vanes of equal height. Further, sensitivity to any hot spots can be reduced by the use of alternative platelet materials, either with higher conductivity to distribute the heat or with higher temperature capability.

4. The overcooling in Compartments 5 and 6 can be reduced by making these compartments into three or four to minimize the area requiring extra coolant. Additionally, a change to a conical chamber contour with an injector whose elements focus parallel to the chamber wall will eliminate this incompatibility.

VI, Secondary Combustor (cont.)

E. SUPPORTING STUDIES

1. Injector Design Analysis Study

a. Introduction and Summary

(U) At the beginning of the extended Phase I contract period, an extensive analytical study was intiated to supply design data for improving performance and compatibility of the ARES secondary injector. Specifically, this effort encompassed:

(1) Providing analytical rationale for compatible chamber design including injector interaction.

(2) Improving performance and compatibility by modifying existing injectors.

(3) Providing analytical selection criteria for the design of new injectors.

(U) These tasks were accomplished by using two Aerojet-developed models (vaporization and compatibility) described in Sections VI,E,1,b and VI,E,1,c below, respectively. The vaporization model predicts the inherent inefficiencies of the combustion process from injection mechanics alone and is a valuable tool in assessing the potential merit of candidate injectors. Major injector parameters considered in this analysis include drop size (which is determined by the number of injection elements), drop atomization, and relative velocity of the oxidizer and fuel streams. This model is also used to predict the inherent efficiency of an injector through the calculation of its energy release loss (ERL). This loss is commonly expressed at % ERL, which is the derived ERL (in seconds) divided by the theoretical specific impulse.

VI, E, Supporting Studies (cont.)

(U) To establish the utility of the vaporization model in the ARES program, experimentally determined energy release losses for the Mark 125 injector, from the Phase I ICP residual hardware program were compared to analytically derived ERL's for the same injector over a range of chamber L*. The experimental ERL's were determined as follows: friction, geometry, and mixture ratio distribution losses were calculated, and the sum of these losses subtracted from the theoretical specific impulse. The difference between the remaining quantity and the measured specific impulse is the experimental energy release loss. Figure VI-82 shows the ERL of the Mark 125 injector as a function of L*. Note the excellent analytical correlation of 0.5%.

(U) In addition to the injector parameters considered by the vaporization model (i.e., drop size, drop atomization, and relative velocity), four more parameters are evaluated in the compatibility model, including impingement of fuel on the chamber wall, the net directional momentum of the combustion products as they leave the plane of the injector, the distribution of fuel over the injector face, and the distribution of the oxidizer gas over the injector face. These parameters were treated qualitatively in this program; the approach used was to design into candidate injectors the most ideal condition for each parameter.

(U) From the results of the study, together with a concurrent injector mechanical design study, two modifications to the basic Mark 125 injector and two new injector concepts were selected for fabrication and test evaluation. The Mark 125 injector modifications included the candelabra and the three ORST configurations (see Section VI,C,3,a). The first new injector concept, designated the WARP concept, was designed in three configurations (see Section VI,C,3,b). The second new concept was the platelet injector, designed in two configurations (see Section VI,C,3,c). The performance and compatibility characteristics for each of these injectors is shown in Figure VI-83. This figure illustrates calculated energy release loss for each

VI, E, Supporting Studies (cont.)

injector, together with relative ratings for each of the performance and compatibility parameters. Theoretically, all showed improvement over the basic Mark 125 injector; the test program subsequently showed the impinging platelet injector to be superior to all designs considered.

b. Vaporization Model

(U) The combustion mechanism can be subdivided into four basic components: propellant atomization, propellant vaporization, turbulent mixing, and chemical reaction. Each mechanism interacts with the others and contributes to the observed inefficiencies of the rocket engine. For many rocket engines it can be further shown that the rate-controlling process is that of vaporization. That is, the atomization, mixing, and reaction processes are fast compared to the vaporization process. Therefore, an injector/chamber design that maximizes vaporization must also maximize performance. This is not to say that vaporization is the only performance decrement of a rocket engine but rather that high performance can only be obtained with high vaporization rates.

(U) The vaporization model treats performance loss as a mass defect, i.e., the performance loss is due to propellants in liquid phase existing in the chamber throat. The assumption made here is that only vaporized propellant can contribute to the useful energy of the system. The potential chemical energy retained in the liquid phase is unavailable to the combustion mechanism and is proportional to the amount of mass unvaporized.

(U) The basic vaporization model used for these analyses was developed by Priem and Heidmann[1] and modified by Beltran[2] and Aerojet.

(1) Priem, R. J., and Heidmann, M. F., Propellant Vaporization as a Design Criteria for Rocket Engine Combustion Chambers, NASA TR-R-67, 1960.

(2) Beltran, M. R., et al., Analysis of Liquid Rocket Engine Combustion Instability, TR No. AFRPL-TR-65-254, January 1966.

VI, E, Supporting Studies (cont.)

The Beltran modification accounts for the decomposition reaction of hydrazine-base fuels. The Aerojet contribution added impingement angle, momentum, and element type effects to the basic atomization model.

(U) The model as developed by Priem solves the combined energy, momentum, and mass transfer processes acting on a statistically defined droplet distribution. The propellant distribution is defined by mass median drop radius and a standard deviation of drop sizes about this mean. This generalized drop is a function of the following injection mechanics and propellant properties: element type, injection velocity, impingement angle, velocity ratio, and propellant transport properties.

(U) Once the initial atomized drop size is known, the model postulates a sequence of logical interacting physical mechanisms which results in a prediction of droplet vaporization within the combustion chamber. A computer program is then utilized to simultaneously solve heat transfer, mass transfer, and aerodynamic momentum transfer (drag) effects between the combustion gas and the liquid droplet. Part of the heat input to the droplet raises the temperature of the liquid drop, part provides latent heat of vaporization, and the remainder goes to superheat the vapor phase. However, the heat transfer rate is not an independent variable. It must be solved simultaneously with interacting mass transfer and aerodynamic drag effects. A few of the more significant interactions follow.

(U) Heat flux is influenced by drop size, differential gas-liquid velocity, chamber pressure, thermal properties of the liquid/vapor combustion gas mixture, and vapor mantle thickness surrounding the droplet. Mass transfer rate from the above heat input is calculated by considering variables such as the propellant vapor pressure for the liquid drop temperature and propellant vapor phase diffusion into the combustion gases. The vaporized propellant

VI, E, Supporting Studies (cont.)

is then assumed to react instantaneously and produce combustion gases. The cross-sectional area of the chamber (chamber contour) and mass of reacted (vaporized) gases then determine the gas velocity at every axial location between the injector face and nozzle throat.

(U) At the injector face, the droplet is initially assumed to travel at its injection velocity. Thereafter, depending upon the droplet and gas velocities, droplet size, droplet drag coefficient, and gas properties, the acceleration of the droplet within the gas stream due to aerodynamic drag is calculated to determine its trajectory and chamber residence time available for vaporization. Analyses show that small drops will completely vaporize within the allowable length of the combustion chamber, but the large drops may reach the throat without vaporizing and thus be expelled without releasing their available chemical energy. Therefore, useful thrust can be obtained only from the vaporized mass at the corresponding vaporized mixture ratio. The degradation in overall engine performance due to unvaporized propellant is then attributed to energy release loss.

c. Compatibility Model

(U) The injector-chamber compatibility model enables qualitative evaluation of wall chemical and gas dynamic forces. The model used on this program graphically characterizes the element spray pattern, including its thermal and chemical composition, and the dynamic lateral movement of the resultant combustion gases. This is accomplished by application of two interrelated models, which are described in the following paragraphs.

(U) The chemical and thermal environment on the wall of a combustion chamber is a function of the overall mixture ratio distribution and the spray-fan distribution from individual injector elements. The model assumes that propellant vaporization is the rate-controlling mechanism for

combustion. On the basis of this assumption, the analysis is performed in the following sequence: first, the energy release potential is determined for each element as a function of its mass flow rate, operating mixture ratio, and atomization efficiency; next, the spray area of each element is assigned a value based on the energy release potential of that element, and the characteristic spray shape is determined by the element configuration. The elements are assigned a characteristic shape and mixture ratio distribution within the spray. Oxidizer-rich and/or fuel-rich zones can be readily evaluated by graphically overlapping the individual spray areas on the injector face.

(U) Gas dynamic forces on the wall of a combustion chamber result from non-axial flow of gases in the chamber, which in turn result from non-uniform mass and mixture ratio distribution across the injector face, or unevenly distributed combustion in the chamber. The Aerojet dynamic force model allows evaluation of the magnitude and direction of this non-axial flow, so that critical zones along the combustion chamber wall may be identified and design changes specified to minimize the gas dynamic forces in these zones. The input information required to apply the gas dynamic force model is as follows: (1) mass and mixture ratio distribution across the injector face, (2) resultant momentum and direction of effluent from each element, and (3) energy release profile as a function of axial distance. This information can be readily determined for a given injector/chamber design. The gas dynamic force model is then applied by assuming that each element forms a stream tube of combustion gases, which is represented by a geometric shape characteristic of the element design. The cross-sectional area of each stream tube is a function of the mass flow rate within the stream tube and the relative degree of vaporization achieved by the propellants. The stream tube initiates at the physical location of each element on the injector face and then moves to a new position determined by the chamber pressure profile and energy release profile. This movement is represented by a vector from the

VI, E, Supporting Studies (cont.)

center of the original location to the center of its relaxed location. The magnitude and direction of this vector represents the gas dynamic force effect.

d. Specific Application of Models

(1) Chamber Diameter Evaluation

(U) One of the hardware design changes made at the initiation of the extended Phase I program as part of the effort to eliminate the injector-chamber compatibility problem was to change the chamber diameter from the previous 10.5 to 9.5 in. (The previous contour was 9.5 in. in diameter at the injector face but transitioned downstream of the injector to the 10.5 in. in diameter.) The diameter change was made on the basis that with the previous contour a net outward radial flow of combustion gas occurred, which permitted the possibility of entrained unvaporized fuel impacting upon the chamber wall. This contour change resulted in the chamber characteristic length (L*) being decreased from 38.35 to 35.47 in. A study was made to determine the effect of this contour change upon performance. The WARP I injector was used in this analysis; however, the results are representative of any of the injectors. Chamber length was found to be the primary factor determining energy release loss, and the effect is shown in Figure VI-84. Length is a measure of droplet residence time according to the one dimensional vaporization model, and increasing the length increases the amount of propellant vaporized. For given chamber lengths, variations in chamber diameter between 7.0 and 10.5 in. affect ERL less than 0.3%. As seen by Figure VI-84, the vaporization analysis reveals that slightly higher performance could be expected from the smaller diameter chamber. It is true that increased performance is normally associated with increased L*; however, L* for a given chamber is usually increased by increasing chamber length, which is the determining factor. L* is only a measure of the gas residence time after vaporization and

combustion is completed; it is the liquid droplet residence time which is important and is determined by chamber length.

(2) Modification of the Mark 125 Injector

(U) Performance and compatibility analyses were performed with the basic Mark 125 injector to determine what changes could be made to improve compatibility. These analyses revealed two significant factors: (1) a net outward fuel momentum is present which results in fuel being impacted on the wall; and (2) approximately 30% of the fuel enters the convergent section of the chamber in an unvaporized state (Figure VI-85). The net outward fuel momentum problem could be corrected by eliminating the radial flow component in the second and third tube rows from the wall. (This was confirmed by hydroflow testing the injector in the laboratory.) The potential incompatibility problem in the convergent section due to the large percentage of unvaporized fuel entering that zone could only be resolved by producing a finer pattern. Without completely redesigning the injector, the only practical method found to achieve the finer pattern was to replace the tubes with a larger number of smaller tubes. Because of the complexity involved, it was decided to attempt this modification on the outer three rows to tubes only and depend upon the uniformly combusted outer periphery to act as a buffer zone and prevent inboard fuel from reaching the wall. The analytical aspects, for each of these modifications, i.e., outer three rows straight and increased tubes on the periphery, are discussed in the following paragraphs.

(a) Mark 125 3 ORST Injector

(C) This injector was designed to improve the compatibility of the Mark 125 injector by (1) placing the outer row of fuel tubes farther away from the chamber wall and (2) directing the fuel tubes in the second and third rows parallel to the chamber axis. To eliminate performance

VI, E, Supporting Studies (cont.)

loss from a poor mass distribution of propellant, the second and third rows of fuel tubes were added to the outer row, which then consists of 96 tubes. Inboard fuel tubes were then repositioned to uniformly fill the space created by moving the second and third rows outboard. The injector pattern is shown in Figure VI-4. The calculated performance of the 3 ORST injector (4.2% ERL) is identical to the basic Mark 125. No improvement of compatibility in the convergent section was expected since nothing was changed to improve the vaporization of fuel.

(b) Candelabra Injector

(C) The candelabra element was designed as a means of producing axial fuel streams and increasing the fuel vaporization rate in the Mark 125 injector. The injector is shown in Figure VI-3 and was made by replacing the outer three rows of fuel tubes on the Mark 125 with elements having a six-tube manifold. The evaluation of the candelabra injector was based on the assumption that the fuel flow through the secondary injector was constant except for an 11% reduction in the candelabra elements (due to the 90 degree turns in the fuel passages). Fuel vaporization rates were calculated for the tubes and the candelabra elements--the vaporization curves appear in Figure VI-86. As shown, the candelabra elements had better vaporization rates than the tubes. The performance analysis indicated that the candelabra injector produced a 3.9% ERL compared to 4.2% ERL for the basic Mark 125 injector.

(3) Analytical Selection of New Injectors

(U) To improve both performance and compatibility, increased vaporization of fuel was required. The largest influence of vaporization is the mass median drop size. High vaporization rate, with all other injection parameters held constant, is inversely proportional to the mass median drop radius to the 1.45 power. Three methods were considered for

VI, E, Supporting Studies (cont.)

decreasing the drop size from that of the Mark 125 injector. The first was to increase the number of injection elements, the second to impinge fuel streams upon one another, and third to employ large differential injection velocities between the parallel oxidizer gas and the injected fuel. The effect of impinging jets on the mass median drop size is shown in Figure VI-87. The points corresponding to the Mark 125 and impinging platelet injectors are noted on the curve for reference. The effect of increased relative velocity was predicted by Ingebo (Reference 1). He demonstrated that the resultant drop size could be descirbed by the following equation:

$$\frac{\text{Jet Diameter}}{\text{Effective Drop Diameter}} = 2.64\ (D_j V_j)^{1/2} + .97\ D_j \Delta V$$

where

D_j = jet diameter, in.
V_j = injection velocity, ft/sec
ΔV = relative velocity, ft/sec

(U) Using the criteria of increased vaporization, together with that of secondary fuel having no radial momentum component, two new injector concepts were designed, designated the WARP injector and the Platelet injector. The analyses performed for each are discussed in the following paragraphs.

(a) WARP Injectors

(U) The WARP injector concept had the significant advantage over the Mark 125 injector in that the oxidizer flow was controlled (using a face plate) with respect to the mixture ratio of each fuel tube,

(1) Ingebo, Robert D., Drop-Size Distributions for Impinging-Jet Breakup in Airstreams Simulating the Velocity Conditions in Rocket Combustors, NACA TN 4222, 1958.

VI, E, Supporting Studies (cont.)

since the tubes were surrounded with a specified amount of gas. Further, the fuel tubes could be shortened within the face plate orifice cones, which increases the differential velocity of the two propellants. The increased velocity difference results in greater shear force on the fuel, which increases its vaporization.

(U) Three versions of the WARP injector were analyzed, designated the WARP I, WARP II, and WARP III injectors. The characteristics of these injectors are shown in Figure VI-88, with the performance predictions in Figure VI-83. In the analyses, shortened tubes were assumed for the WARP II and WARP III injectors, while tubes extending to the plane of the injector face were assumed for the WARP I injector. (In the WARP III injector which was test fired, the tubes also extended to the plane of the injector face.) A schematic showing the element configurations is shown in Figure VI-89. The effect of shortening the fuel tubes is shown in the vaporization curves in Figure VI-85.

(C) The WARP III design was found to be the best of the three with respect to performance and compatibility. The performance analysis of this injector resulted in a predicted performance loss of only 1.2% ERL.

(c) Platelet Injectors

(U) The platelet injector concept has a significant advantage over the other ARES injectors because of the increased number of fuel slots, and the increase in vaporization rate of the fuel. This injector was built in two configurations: one with axially directed fuel streams, called the Showerhead Platelet, and one with impinging fuel streams, called the Impinging Platelet Injector. The axial and impinging vanes are shown in

VI, E, Supporting Studies (cont.)

Figure VI-16. Both vane types are constructed by etching the fuel channels to a depth of 0.015 in. on each of the two plates and brazing the plates together.

(C) The showerhead injector has a total of 2464 fuel slots, distributed over 88 vanes. Each slot is 0.030 in. wide by 0.060 in. long. The slots on the vanes are separated by a distance of 0.020 in. The impinging platelet injector had the same number of fuel injection vanes arranged in the same pattern as the showerhead injector; however, the total number of fuel slots was increased from 2464 to 3696. The slots are smaller, 0.030 in. by 0.020 in., and are arranged in pairs (1848 total pairs) which impinge at a angle of 60°. The velocity of the fuel streams as they emerged from the vanes are 46.7 and 93.5 ft/sec for the showerhead and platelet injectors, respectively. The distance from the outermost fuel slot to the chamber wall is approximately 0.130 in. for both injectors.

(C) The calculated energy release loss for the showerhead platelet injector was 2.8% ERL, an improvement of 1.4% over the Mark 125 injector. As can be seen in Figure VI-85, 92% of the fuel is vaporized before it is expelled through the throat. In addition, 0.6% mixture ratio distribution loss (MRD) was calculated using the stream tube technique and assuming uniform primary oxidizer gas at the plane fuel injection. The majority of this loss results at the outer periphery in the 0.130-in. gap between the wall and the first fuel injection orifice. The mixture ratio distribution loss is the same for both the showerhead and impinging injector configurations.

(C) Using the vaporization model, the impinging platelet injector shows a very low energy release loss of 0.4% ERL. This is the result of (1) the increased number of fuel streams; (2) smaller fuel streams; and (3) increased atomization of fuel streams due to their impingement, which is enhanced by the increased injection velocity. It should be

noted, however, that even though the energy release loss obtained analytically is negligible, a practical limit of about 1% ERL (3 sec I_s) should be expected. This is because conditions which are normally insignificant when the fuel vaporization is incomplete become a source of performance loss when the vaporization approaches 100%. The primary consideration is that as the stoichiometric mixture ratio is approached, the diffusion of the fuel vapor, rather than vaporization, becomes the rate-controlling mechanism. This implies that even though the fuel is vaporized, unless the atmosphere immediately surrounding the fuel vapor contains oxidizer, no combustion will take place. The impinging platelet injector was the only injector evaluated where the above consideration became insignificant.

2. Air Flow Primary Combustor Gas Distribution Study

a. Introduction and Objective

(U) The secondary injector performance and compatibility improvement test program (see Section VI,C,5,b,(3)) denoted a severe incompatibility between the injector and the film-cooled ablative chamber. Following Test 1.2-16-WAM-010, detailed analysis of these few tests indicated this condition was caused by an adverse mass distribution across the secondary combustor gas injector. This lowered the peripheral mixture ratio to a fuel-rich condition which in turn reacted with the oxidizer coolant. An injector air flow test program was therefore initiated with the objective of: (1) evaluating the validity of this hypothesis, (2) determining the cause of the suspected mass distribution, and (3) developing corrective devices which would eliminate or tailor these distributions to give a compatible condition between the injector and the coolant on the chamber wall.

VI, E, Supporting Studies (cont.)

b. Summary

(U) The air flow test program extended over a ten week period in which 350 tests were conducted on 65 hardware combinations. All tests were performed in Aerojet's Aerophysics Laboratory. Before testing began, a model operating point analysis was conducted to determine the pressure and flow requirements necessary to effect hot test similarity.

(U) The actual test program was initiated by first evaluating the existing test firing configuration used on Test 1.2-16-WAM-010. The results of this investigation denoted a skewed flow profile together with a low mass flow about the injector periphery. These results thereby confirmed the hot test analysis which denoted a fuel-rich injector mixture ratio on the outer zones of the injector which in turn would burn with the oxidizer coolant. A summary of the 14 tests conducted toward this objective is shown tabulated in Group 1 of Figure VI-90.

(U) The second effort consisted of defining the individual component flow characteristics so that corrective action could be instituted in the proper location. Eleven tests were performed during this evaluation are also summarized as Group 2 of Figure VI-90.

(U) The third group of tests evaluated various techniques to achieve even gas flow across the injector face. This series encompassed 114 tests and evaluated devices such as: diffuser cones, a conical-shaped flow diverter that resembled a "coolie" hat, a multihole orifice to remove the skewed flow of the unsymmetrical primary combustor turbulator assembly, symmetrical turbulators, and inserts for the diffuser cone to bias the flow to the outer annulus of the flow channel. This group of tests is summarized in Group 3 of Figure VI-91.

VI, E, Supporting Studies (cont.)

(U) The fourth effort evaluated total pressure drop techniques to even the injector mass flow. Such devices as screens of various mesh, cross-grid plates, and notched screens to divert the flow discretely were employed. In all cases, these screens were attached to the leading edge of the injector vanes. This group of 78 tests defined the potential of using total pressure drop devices to achieve an even mass flow distribution. The summary of this testing is given in Figure VI-92 as Group 4 testing. Two hot tests using this technique were conducted defining structural attachment problems of the screen to the injector during engine start and shutdown transients.

(C) With the structural weakness of the screen approach defined, the air flow program next evaluated multihole plates to develop the necessary total pressure drop for mass distribution control. For initial testing, a previously tested WARP III face was evaluated. Discrete enlarging of the existing holes produced a high mass flow about the injector periphery. This calculated mixture ratio distribution (MRD) loss was 9.4 sec. A second modification reduced this flow bias to a 3.6-sec MRD loss but with a slightly low mass flow about the injector periphery. Air flow testing with this distribution system is summarized in Figure VI-93, Group 5.

(C) Structural weakness of the WARP III plate necessitated air flow development of another multihole plate, this time a WARP II injector face plate. Sixteen air flow tests were performed to tailor the injector mass flow. A plate yielding 3.6 sec of MRD loss resulted having a satisfactory mass flow on the chamber periphery. This air flow testing is summarized in Figure VI-94 as Group 6 testing.

(C) To further minimize mixture ratio distribution loss and increase the structural integrity of the flow distribution plates, another air flow series was conducted using a specially drilled plate. This 712-hole

plate yielded a 1.4-sec loss improvement over the previous WARP II plate, again with satisfactory gas flow at the injector wall. This testing, summarized in Figure VI-95 as Group 7 testing, completed the air flow test program.

(U) In summary, the air flow program provided the means for the correction of the skewed gas flow from the primary combustor turbulator assembly, together with the development of a total pressure drop plate to tailor the oxidizer gas distribution to a satisfactory condition. As a result of this effort, three changes were made to the staged-combustion test engine. First, the unsymmetrical primary combustor turbulators were replaced with symmetrical turbulators. Second, the multihole orifice plate installed at the inlet to the adapter-diffuser (which had been used to decrease the effect of the skewed flow resulting from the unsymmetrical turbulators) was removed, since its function was eliminated with the turbulator change. Third, the total pressure drop plate developed in the air flow program was installed at the injector inlet.

(C) The pressure drop plate greatly improved the compatibility of the injector and chamber through tailoring of the oxidizer gas distribution. There is still some flow distribution unbalance at the plane of the injector face, however, giving an estimated mixture ratio distribution loss of 2.2 sec. This is mainly caused by the geometry of the injector vanes and the diameter change from the injector inlet to outlet of 8.5 to 9.5 in. The best way to eliminate the remaining maldistribution is through redesign of the injector. However, if required, further improvement could be made by modifying the pressure drop plate to equalize the radial and circumferential distribution.

VI, E, Supporting Studies (cont.)

c. Test System

(1) Physical Arrangement

(U) The inert gas flow facility of the Aerophysics Laboratory was used for the entire air flow test program. The complex consists of a 600-psi compressor, a large air storage vessel, a flow control valve, a flow nozzle for measurement of flow rate, a plenum chamber, the test article, and an exhaust stack. Five and 6-in. plumbing is used throughout to reduce pressure drops. A layout of this facility is presented in Figure VI-96.

(U) All tests performed in this facility utilized actual test hardware, whenever possible, to expedite testing. Figure VI-97 illustrates the internal geometry of the basic gas flow model passages and the location of the instrumentation probes used to determine mass flow. Four nozzles were included in the end plate which, when choked, yielded a chamber Mach number similar to the actual hot test.

(2) Instrumentation

(U) The major piece of instrumentation used was a total pressure probe capable of both rotation about the chamber centerline and translation along the centerline. Details of this probe are given in Figure VI-98. The probe contains ten total pressure tubes and two static pressure tubes.

(U) Each of the tubes was connected to one side of a manometer containing unity oil. The other side of each manometer was connected to a static pressure tap just upstream of the injector. Reference to this back pressure was required to reduce the height of fluid so that unit oil could be used to measure pressure differential. The upstream pressure tap was also connected to a mercury manometer for static pressure reference.

VI, E, Supporting Studies (cont.)

(U) In addition to the manometers, the pressure and temperature of air upstream of the flow nozzle were recorded to allow calculation of the flow mass rate. Absolute atmospheric pressure was obtained from Aerojet's Plant Test Operation's barometer.

(3) Operation

(U) Operation of the test facility was accomplished in the following manner. First, the main tank valve was opened and the flow control valve positioned by the test operator to obtain the desired value of upstream pressure. A photograph of the control room where the operator controls the test is included in Figure VI-99. Next, a Polaroid photograph (see Figure VI-98) was taken to record the manometer data after the manometers had settled out. The operation of the camera shutter signals a blinking light in the test bay, thus informing test personnel to rotate the probe to the next position and reload the camera. A television camera permitted remote observation of the manometer heights. Once these operations were completed, the process was repeated until available air was exhausted or the series was completed.

(4) Data Acquisition

(U) The manometer data were obtained in the form of photographs using a Polaroid camera which was signaled from the control room. Strip chart recordings of flow nozzle pressure and temperature were made on an oscillograph. The photographs show manometer column height in 0.2-in. increments and can be interpolated into smaller intervals. This sensitivity was considered quite accurate when the manometer fluid was unit oil (specific gravity = 1.00).

VI, E, Supporting Studies (cont.)

(5) Data Reduction

(U) From the photographs, the difference between average static pressure (probes 8 and 11) and total pressure at 10 points on the chamber radius is obtained. This pressure difference is a measure of the velocity head in this annulus. The velocity is then calculated and compared to the desired value at the recorded mass flow rate. In this way, a three-dimensional profile can be built showing the relative mass flow per unit area by rotating the pressure probe through 360 degrees, since the density is constant across the entire cross-section. This three-dimensional profile then shows the flow profile over the entire injector surface.

d. Model Operating Point Analysis

(U) The air flow model operating point was designed to match normally considered similarity conditions with the compromise of using existing hardware whenever possible. The resulting cold flow operating conditions compared to hot test conditions are listed in Figure VI-100. Primary consideration on the operating point was given to matching the similarity numbers of Reynolds, Mach, and Prandtl.

(1) Reynolds Number

(U) Reynolds number similarity is considered to be obtained for this air model test case since both systems are above the critical value of 10^5 where rough wall loss coefficients become nearly constant with increasing values.

VI, E, Supporting Studies (cont.)

(2) Mach Number

(U) The Mach number for the injector was matched by regulating the upstream pressure in conjunction with correct sizing of the downstream chamber four-hole exit area.

(3) Prandtl Number

(U) Prandtl number similarity is considered matched for this type of testing because heat-transfer phenomena have a small effect on the mass distribution through the injector.

(4) Resonance Time

(U) Matching of the chamber resonance time was impossible since existing hot test hardware was used extensively. Shortening of the system to make up for the 50% difference in acoustic velocity was therefore impossible. Because dynamic response is of little value in this type of testing, this similarity condition was not considered important.

(5) Injector Velocity

(U) Injector velocity was allowed to vary in order that the Mach numbers be matched.

(6) Acoustic Velocity

(U) Matching of the acoustic velocity was impossible since facility limitations prevented heating of the air.

VI, E, Supporting Studies (cont.)

(7) Viscosity

(U) As was the case with the acoustic velocity, the viscosity could not be matched because of air temperature heating limitations.

(8) Gas Density

(U) The gas density could not be matched since the system was operating at near maximum pressure.

(9) Ratio of Specific Heats

(U) The specific heat ratio could not be matched because of the entirely different characteristics of air and the high NO_2 content primary combustor gases.

e. Discussion of Results

(1) Original System Evaluation

(U) The original system evaluated was that test fired on hot tests 1.2-16-WAM-007 through 1.2-16-WAM-010. Similar to that depicted in Figure VI-97, this system included the primary combustor barrels, unsymmetrical turbulator assembly, the diffuser-adapter section, the platelet injector, a multihole orifice at entrance to the adapter section, and a 9.625-in.-dia chamber.

(U) The injector was probed at eight points about the circumference, four in the long vane areas and four in the short vane areas. The results showed two distinct flow characteristics; (a) the flow was highly skewed, clinging to the side of the injector opposite the last turbulator vane,

VI, E, Supporting Studies (cont.)

and (b) in the other quadrants, flow was low at the wall and significantly less than desired values. A graphical representation of this flow characteristic is given in Figure VI-101, showing the percent excess flow, negative or positive, which exists at any station. This relationship establishes the variation from the desired flow. Small variations in the velocity in the outermost zones of the injector have a larger effect than in the injector center, since the face area varies as the square of the radius. Primary concern, as far as numerical mass imbalance, is therefore given to the outer inch of the injector radius, where 40% of normal flow exists.

(C) The mixture ratio distribution loss for the original configuration was calculated to be 1.1 sec. This low value, considering the heavily unbalanced and skewed flow, results since the periphery is largely fuel-rich. The fuel in this area burns with the transpiration coolant, eliminating any performance loss. However, the compatibility aspect of this condition is intolerable, since the burned coolant can no longer protect the chamber wall.

(U) A summary of this testing with results, configuration, applicable hot tests and calculated mixture ratio distribution loss appears as Group 1 in Figure VI-90.

(2) Component Flow Characteristics

(U) This test series was conducted to evaluate the particular flow characteristics of each of the basic pieces of test hardware. With this information, the necessary corrective action was initiated knowing the effect of the basic components. This testing is summarized in Figure VI-90 as Group 2.

VI, E, Supporting Studies (cont.)

(U) The first area evaluated was the skewness believed to be produced by the unsymmetrical turbulator assembly in conjunction with the multihole orifice. No injector was used. Tests without the turbulators followed and lastly, tests without the turbulators and multihole orifice plates were conducted.

(U) Evaluation of these data indicated the diffuser-adapter was highly cored in all tests. Skewed flow existed in all tests with a slight improvement when the multihole orifice was used. The high core flow indicated the diffuser flow was separating from the 15-degree (included angle) wall. The nonaxisymmetric flow condition is produced by the unsymmetrical turbulator and attachment of the separated flow in the stalled diffuser.

(U) This testing evidenced the need to install flow correction devices in the diffuser to eliminate the stalled condition. Available diffuser information indicated the 15-degree angle wall was sufficient for nonseparated flow if plenum conditions exist upstream. In the actual test engine, the long primary combustor duct upstream (L/D = 4) requires the use of a smaller diffuser angle.

(3) Even Gas Flow Evaluation

(U) This testing included 21 series of 118 tests to define the flow improvement characteristics of various mass distribution devices. The low cost of air flow testing was uniquely suited to testing of many configurations which would normally be eliminated following a more expensive critical analysis and design review. This Group 3 testing is summarized in Figure VI-91, Pages 1 through 4.

(U) As can be seen in the figure, many configurations of flow correction devices were employed. The first approach used a conical

VI, E, Supporting Studies (cont.)

diversion device which resembled a coolie hat. A schematic representation of various gas distribution devices is shown in Figure VI-102. Configuration 3 represents the coolie hat configuration. This device was quite satisfactory in diverting the flow to the outside but difficult to balance with the flow beneath the hat. Four porosities were employed without satisfactory results.

(U) A second system investigated was to remove diffuser separation by effectively reducing the diffuser angle. For this purpose, a 4-degree diffuser cone insert was installed in the adapter reducing the flow angles to half its former value. Schematically, this system is shown in Figure VI-102, Configuration 2. This technique was also difficult to balance and required several iterations on the capture area for the inner diffuser cone.

(U) During the preceding two series, it was observed that the unsymmetrical turbulators and the flow straightening multihole orifice (MHO) were biasing the flow to one side. Several attempts at resizing the MHO produced undesirable results. To correct this problem, a symmetrical turbulator assembly was designed which would not skew the flow from its normal axisymmetric path. The results of this testing, Configuration 2, Figure VI-102, denoted a definitive improvement in reducing the unsymmetrical flow.

(U) The results of these aerodynamic-type corrective measure tests indicated high system sensitivity, therefore requiring that total pressure drop be used to correct the skewed flow distribution. When the coolie hat had high pressure drop, the flow was symmetrical but heavy on the outside. As the pressure drop was decreased, by opening up the hat area to adjust the core flow, the skewness reappeared.

VI, E, Supporting Studies (cont.)

(4) Injector Screens Evaluation

(U) The first attempts to control gas flow through the use of total pressure drop were done with a screen attached to the leading edge of the injector vanes. The screen porosity was 57% through flow. Eighty-three tests were conducted using four variations of screen porosity. The tests conducted during this phase of the air flow program appear in Figure VI-92 as Group 4. Since high peripheral flow was desired, the first screen was cut with a 1/4-in. gap from the injector wall. Results of this testing indicated the diffuser was still coring because the pressure drop was low.

(U) The second screen extended to the injector wall, thereby increasing the system total pressure drop. Desirable edge flow was obtained with a definite improvement in nonaxisymmetric flow. Flow data from the injector's long and short vane areas indicated that a high flow existed at the short vane intersections. Blockage plugs were then installed to reduce this flow. Too high a flow reduction was obtained. The screen was then notched to obtain the required flow condition. The resulting flow distribution is shown in Figure VI-103. This configuration was hot-tested on Tests 1.2-16-WAM-014 and 015 with satisfactory flow results.

(U) Hot testing of the notched screen gas distribution approach demonstrated the inherent weakness of screens to high temperature and pressure induced structural loads. To increase the strength, a plate having milled intersecting slots of the same porosity as the screen was air tested. This plate, designated a cross-grid plate, did not produce enough total pressure drop to pattern the flow to a desirable characteristic.

(U) To further reduce system sensitivity, a double screen of higher total pressure drop was tested with very favorable results.

VI, E, Supporting Studies (cont.)

With the demonstrated problems of screens on hot test, this flow device was dropped in favor of drilled plates.

(5) WARP III Face Plate Evaluation

(C) To correct the structural problem demonstrated with the screen gas distribution approach, a drilled plate distribution system was evaluated. The first plate to be evaluated was the face plate from the WARP III injector, previously run on Test 1.2-16-WAM-011 (see Figure VI-104). The plate was modified by increasing the hole size from 0.172 to 0.197 in. dia to give a tolerable pressure drop. A high wall flow characteristic was obtained as shown in Series 29-38 in Figure VI-93. This high flow wall condition is shown in the percent excess flow plot of Figure VI-105. The calculated mixture ratio distribution loss for this flow characteristic was 4.2%. This configuration was hot tested in Test 1.2-16-WAM-017.

(C) The hot test showed excellent wall compatibility in the chamber cylindrical section confirming the high peripheral oxidizer mass flow indicated in air testing. The performance, however, was quite low, indicating a high mixture ratio distribution loss as previously calculated by air testing. To increase performance, another modification was made to the plate to increase the center mass flow, thereby lowering the peripheral flow. This was accomplished by chamfering the inlet side of every other hole in the platelet center (102 holes total). This modified case was hot tested prior to air laboratory model testing. Compatibility information from the hot test, 1.2-16-WAM-018B, indicated the excess flow at the wall had been reduced. Also, an oxidizer deficiency had been created just inboard from the wall as a severe incompatibility was evidenced in the convergent section of the chamber. These results were checked in air flow test series 40, runs 1 through 9. The mass flow plot in Figure VI-106 shows a large reduction in oxidizer flow about

VI, E, Supporting Studies (cont.)

0.5 in. in from the outside edge, thereby confirming hot test results. A mixture ratio distribution loss calculation indicated a loss of 3.6 sec based on air flow results.

(U) The last series of tests on the WARP III plate was done for technical information to see whether a multihole plate could be modified to give a very even gas flow. Twelve tests followed with excellent results and indicated complete capability to tailor the gas flow.

(6) WARP II Face Plate Evaluation

(U) Structural weaknesses of the WARP III plate generated on the two test firings and the many hole size changes necessitated the development of a new gas flow distribution plate. For this purpose, the WARP II injector face plate from an unassembled injector kit was used. The primary difference between this plate and the previously tested plate was in the number of holes (753 holes versus 712 of the WARP III). This testing encompassed 16 tests as summarized in Figure VI-94, Group 6 testing.

(C) Initial air lab testing indicated an excessive total pressure drop and high peripheral flow. Successive chamfering of the leading edge of the holes, lowering the entrance loss, resulted in a desirable mass flow distribution. A 3.6 sec MRD loss was calculated for this distribution. This mass distribution is shown in Figure VI-107.

(U) This very acceptable flow condition was used on hot tests, 1.2-16-WAM-019 through -023, and satisfactory results were obtained.

VI, E, Supporting Studies (cont.)

(7) Drilled Plate Evaluations

(U) In an effort to reduce the mixture ratio distribution loss while improving the structural characteristics, a new plate was designed and air flow tested. The drilled plate had an identical hole pattern and size to the WARP II face plate. The only difference was in the elimination of intersecting chamfer on the downstream side of the plate.

(U) Initial testing was directed to possible peripheral flow caused by leakage around the plate in its register. Following these tests, a series of tests were conducted to tailor the flow by chamfering the leading edge of the areas which were deficient in mass flow.

(C) A total of 67 air flow tests were conducted yielding a plate which produced only 2.2 sec of MRD loss at an area ratio of 12:1. At an area ratio of 20:1, this loss increased to 2.3 sec. These tests are summarized in Figure VI-95 as group seven testing. The resulting mass distribution is shown in Figure VI-108. Hot testing on this plate encompassed Tests 1.2-16-WAM-023 through -026 and 1.2-13-WAM-003 through 1.2-13-WAM-051, without modification or replacement.

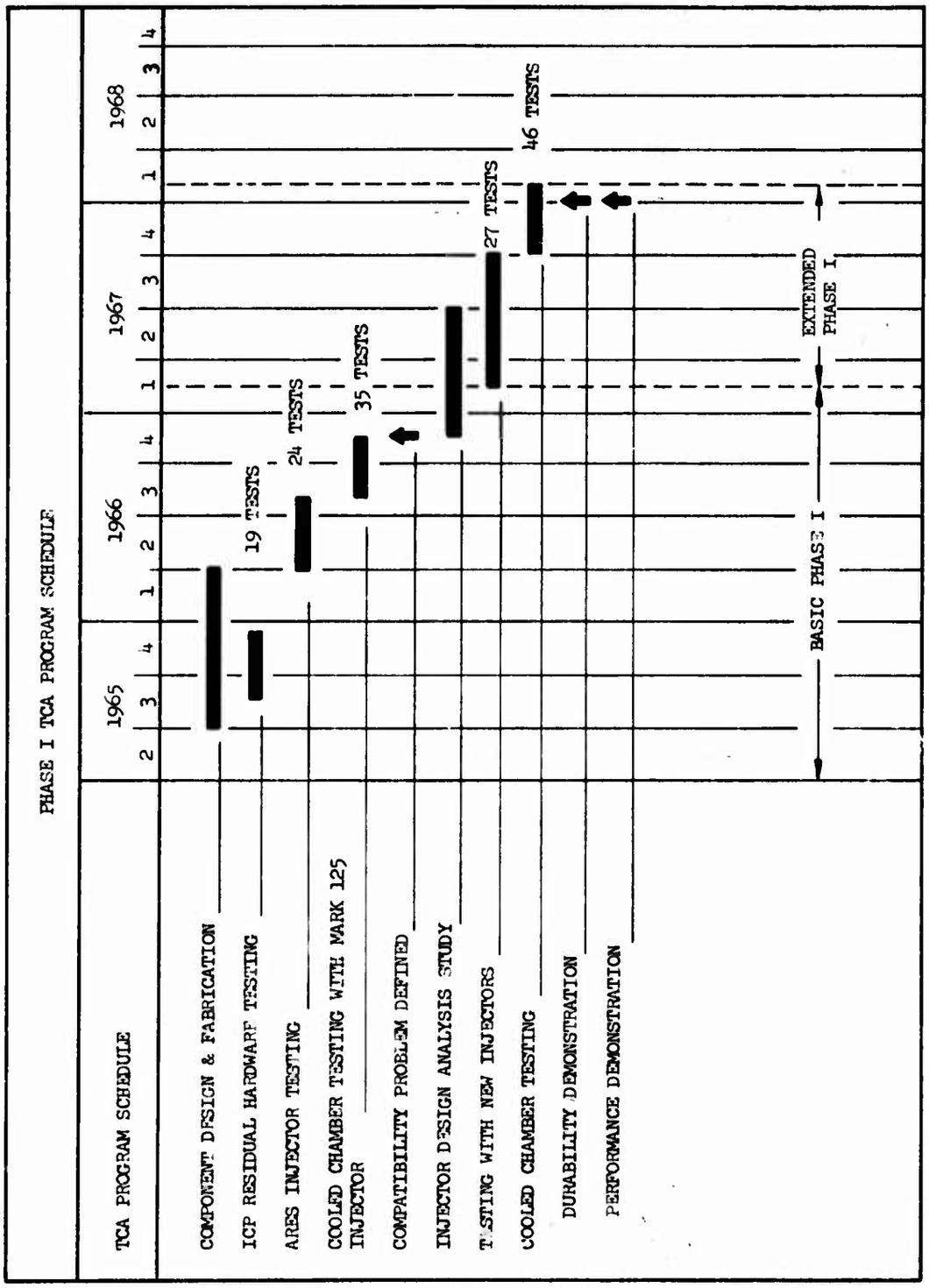

Phase I TCA Program Schedule

Figure VI-1

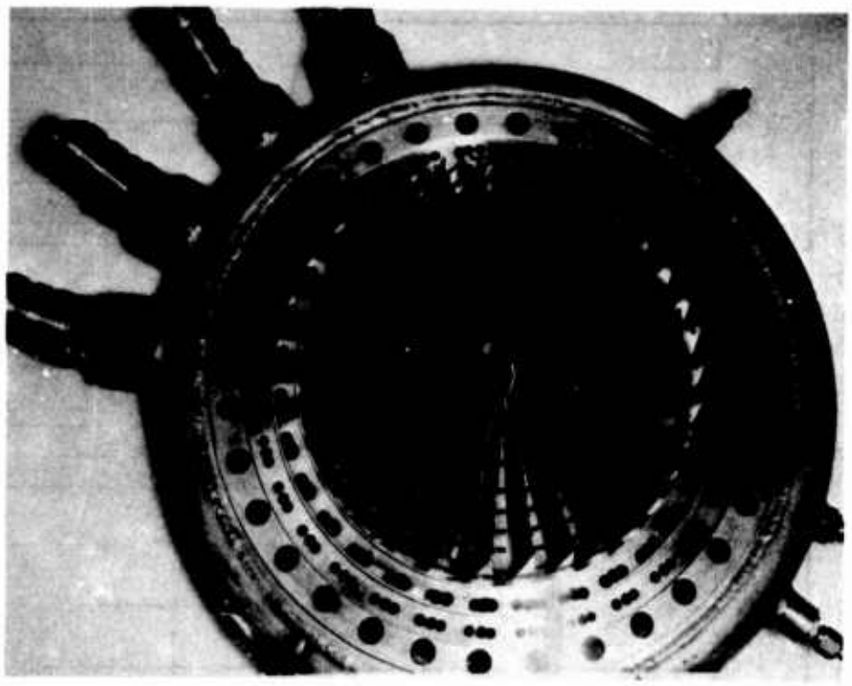

Figure VI-2. Basic Mark 125 Injector (u)

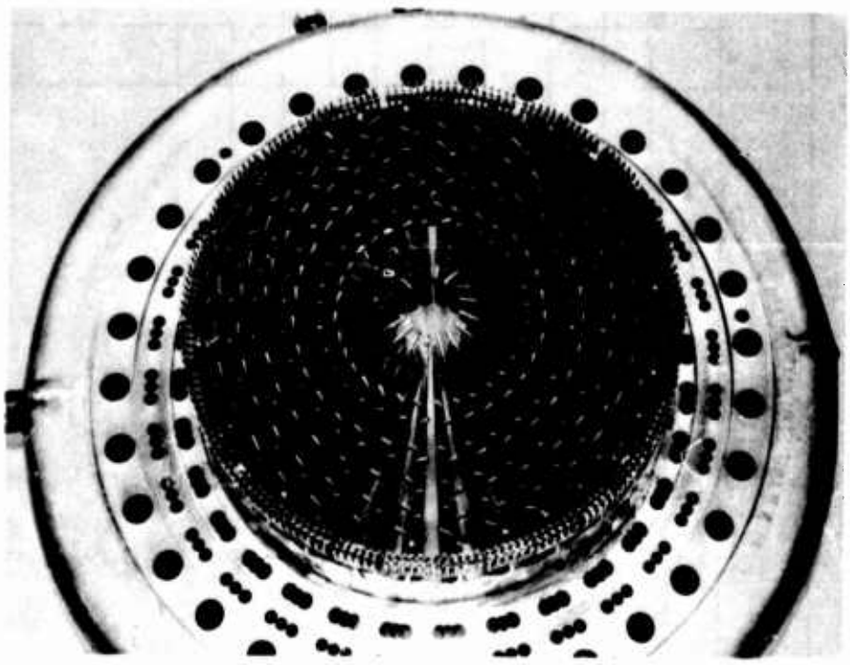

Figure VI-3. Mark 125 Candelabra Injector (u)

Figure VI-2, Figure VI-3

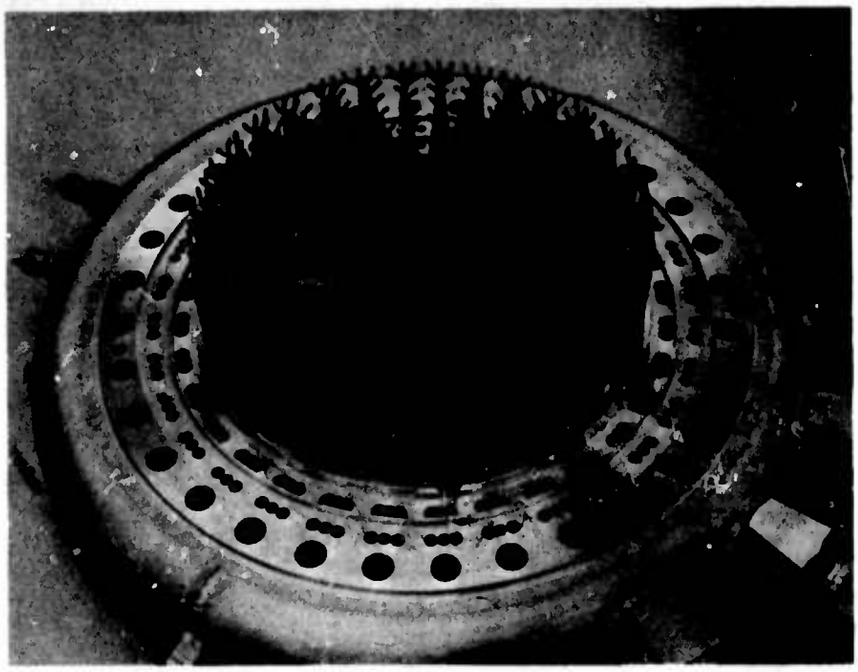

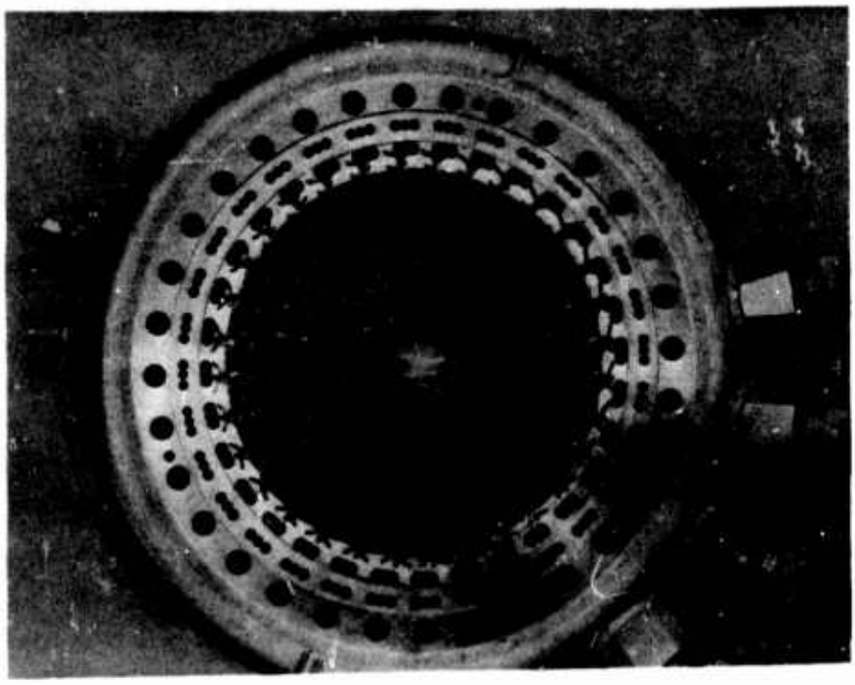

Mark 125 3 ORST Injector (u)

Figure VI-4

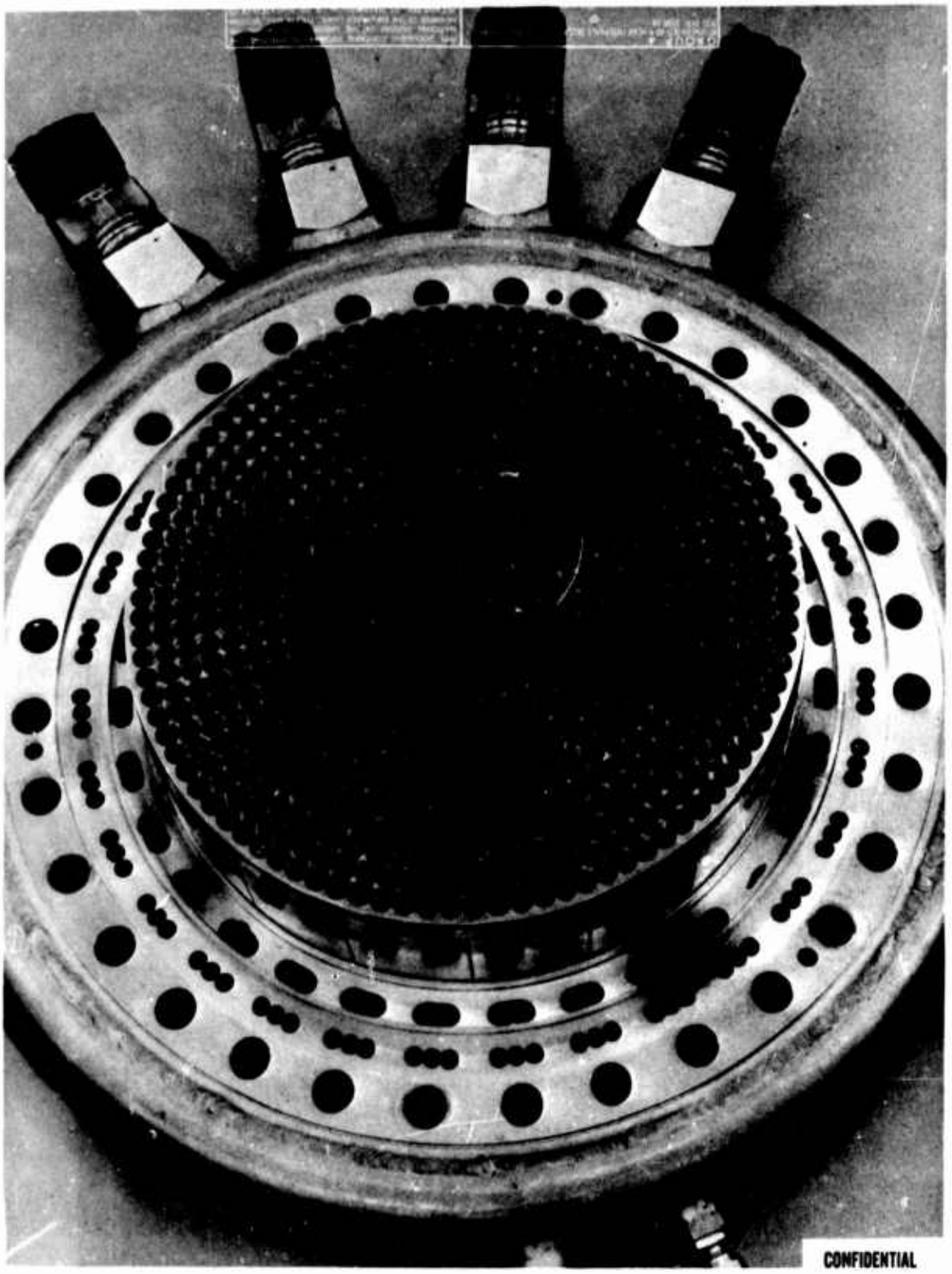

WARP I Injector (U)

Figure VI-5

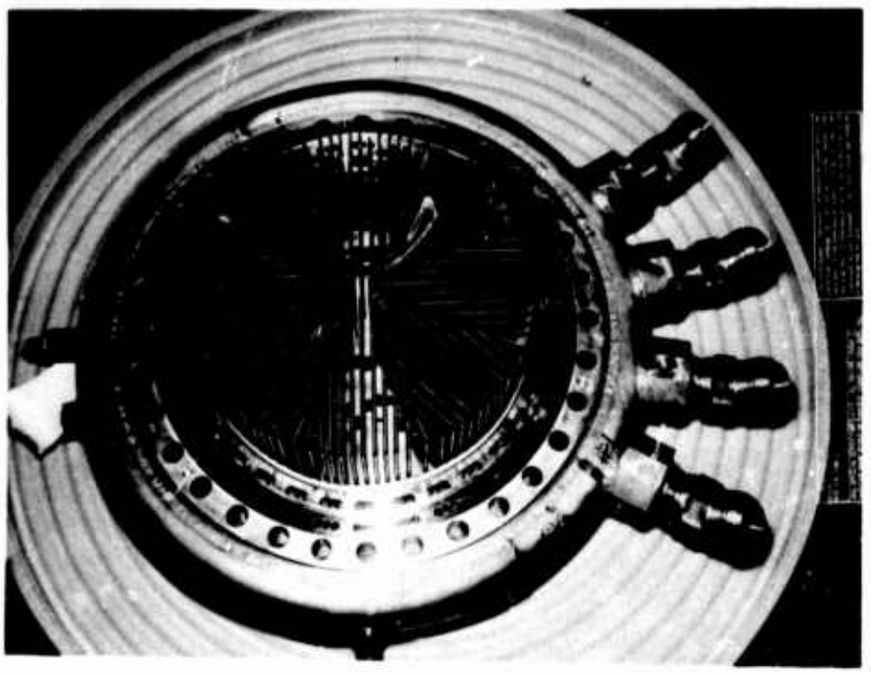

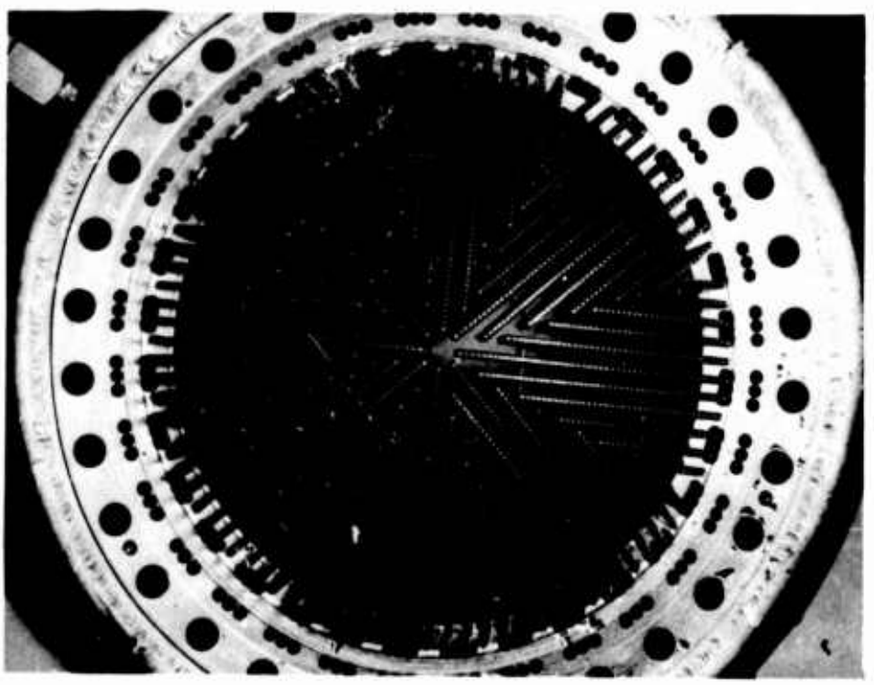

Platelet Injector (u)

Figure VI-6

	GENERAL DATA										MEASURED DATA				
	DATE	DUR.	DATA PERIOD	INJ.	S/N	CHAM.	S/N	A_t	S	L*	PCSC	MR_{inj}	$\dot{W}_{OFC}$	F_{SL}	$\dot{W}$
TEST NUMBER	-	sec.	sec.	-	-	-	-	$in.^2$	-	in.	psia	-	#/sec	lbs	#
1.2-16-WAM-001	03/14/67	1.976	None	WARP I	1	ABL-STL	1	21.6	11.6	32.3	2914	2.18	0	PERFORMANC	
1.2-16-WAM-002	03/20/67	1.964	None	Mk 125	Cand	ABL-STL	1	22.6	11.1	30.8	2731	2.21	0	PERFORMANC	
1.2-16-WAM-003	04/19/67	2.006	1.75-2.10	Mk 125	5	ABL-STL	1	23.5	10.7	29.6	2663	2.16	0	99750	3
1.2-16-WAM-004	04/25/67	2.147	2.05-2.25	Mk 125	5	ABL-STL	2	22.1	11.5	31.5	2847	2.18	0	97301	3
1.2-16-WAM-005	05/01/67	3.489	2.59-3.59	Mk 125	5	ABL-ABL	1	24.9	10.3	27.9	2847	2.22	41.1	108669	4
1.2-16-WAM-006	05/22/67	1.243	None	WARP II	1	ABL-STL	2	22.2	11.5	31.4	SHORT DURATION TEST - NO STEADY				
1.2-16-WAM-007	06/28/67	2.420	1.97-2.47	SH-PL	1	ABL-STL	3	22.2	11.4	31.3	2824	2.12	0	98454	3
1.2-16-WAM-008	07/03/67	2.526	2.08-2.58	SH-PL		ABL-STL	3	23.8	10.6	29.2	2759	2.14	0	102779	3
1.2-16-WAM-009	07/05/67	2.520	2.07-2.57	SH-PL	1	ABL-STL	4	23.3	[illegible]	30.0	2767	1.97	0	100473	3
1.2-16-WAM-010	07/10/67	1.750	None	SH-PL	1	ABL-ABL	2	21.3	11.9	32.5	2780	2.23	36.0	SHORT DURA	
1.2-16-WAM-011	07/20/67	1.159	None	WARP III	1	ABL-STL	5	21.3	12.0	32.7	SHORT DURATION TEST - NO STEADY				
1.2-16-WAM-012	07/28/67	1.820	1.72-1.82	WARP IIIM	1	ABL-STL	5	21.7	11.7	32.1	2758	2.50	0	94380	3
1.2-16-WAM-013	07/31/67	2.512	2.01-2.51	WARP IIIM	1	ABL-STL	5	23.2	11.0	29.8	2630	2.37	0	95152	3
1.2-16-WAM-014	08/08/67	2.508	1.96-2.46	SH-PL	1	ABL-STL	6	22.1	11.5	31.5	2816	2.28	0	98771	3
1.2-16-WAM-015	08/10/67	3.512	2.51-3.51	SH-PL	1	ABL-ABL	2	22.4	11.4	31.1	2811	2.23	35.4	97388	3
1.2-16-WAM-016	08/18/67	3.520	2.52-3.52	IM-PL	3	ABL-ABL	3	21.3	11.9	32.7	2793	2.20	34.7	93586	3
1.2-16-WAM-017	08/31/67	3.523	2.52-3.52	IM-PL	3	ABL-ABL	4	22.3	11.4	31.3	2702	2.19	35.8	94496	3
1.2-16-WAM-018B	09/01/67	3.531	2.06-3.06	IM-PL	3	ABL-STL	6	23.4	10.9	29.9	2732	2.20	36.4	98543	3
1.2-16-WAM-019	09/11/67	2.508	2.00-2.51	IM-PL	3	ABL-STL	5	25.0	10.3	27.9	2711	2.17	0	108128	3
1.2-16-WAM-020	09/18/67	2.528	2.00-2.53	IM-PL	3	TRA-ABL	1	21.5	11.8	53.2	2885	2.28	54.6	99361	3
1.2-16-WAM-021	09/19/67	2.229	2.03-2.53	IM-PL	3	TRA-ABL	1	22.0	11.6	52.1	2821	2.21	53.4	98957	3
1.2-16-WAM-022	09/20/67	3.036	2.00-3.04	IM-PL	3	TRA-ABL	1	22.9	11.1	50.0	2746	2.22	52.0	98426	3
1.2-16-WAM-023	09/21/67	2.516	2.02-2.52	IM-PL	3	TRA-ABL	1	23.7	10.8	48.3	2755	2.12	52.1	101479	3
1.2-16-WAM-024	10/02/67	2.995	2.50-3.00	IM-PL	3	TRA-ABL	1	21.8	11.3	52.4	2714	2.10	54.0	95477	3
1.2-16-WAM-026	10/11/67	2.987	1.99-2.99	Mk 125	3	TRA-ABL	1	22.1	11.4	52.0	2904	2.16	47.1	99356	3
1.2-13-WAM-003	10/25/67	3.010	2.00-3.00	WARP IIIM	1	ABL-ABL	5	21.9	11.5	31.6	2839	2.05	35.7	100109	3
1.2-13-WAM-004	10/28/67	1.512	1.41-1.51	IM-PL	3	ABL-ABL	6	21.1	12.1	35.0	2788	2.23	40.7	97816	3
1.2-13-WAM-015	11/16/67	2.008	1.51-2.01	SH-PL (PID)	2	ABL-ABL	5	22.9	11.1	29.0	2702	2.13	0	99109	3
1.2-13-WAM-016	11/17/67	2.005	1.51-2.01	SH-PL (PID)	1	ABL-ABL	5	24.3	10.5	27.9	2621	2.15	0	99753	3

MEASURED DATA				PERFORMANCE DATA			PERFORMANCE LOSSES					% PERFORMANCE				
MR_{inj}	$\dot{W}_{OFC}$	F_{SL}	$\dot{W}_{eng}$	$I_{S_{SL}}$	$I_{S_{VAC}}$	THEO. $I_{S_{VAC}}$	MRDL	NGL	NFL	FCL	ERL	$\dot{W}_{OFC}$	FCL	ERL	$I_{S_{VAC}}$	$I_{S_{SL}}$
-	#/sec	lbs	#/sec	sec.	sec.	sec.	sec.	sec.	sec.	sec.	sec.	%	%	%	%	%
2.18	0	PERFORMANCE DATA COMPROMISED DUE TO INJECTOR EROSION														
2.21	0	PERFORMANCE DATA COMPROMISED DUE TO INJECTOR EROSION														
2.16	0	99750	351.9	283.5	294.0	316.0	1.1	5.1	4.2	0	11.6	0	0	3.7	93.0	92.3
2.18	0	97301	338.4	287.5	298.5	217.2	1.1	5.2	4.2	0	8.2	0	0	2.6	94.1	93.6
2.22	41.1	108669	401.7	270.5	279.9	314.1	1.1	4.9	4.2	14.1	9.9	10.3	4.5	3.2	89.1	88.9
T DURATION TEST - NO STEADY STATE DATA																
2.12	0	98454	342.4	287.6	298.3	317.5	1.1	5.2	4.2	0	8.7	0	0	2.7	94.0	93.7
2.14	0	102779	359.0	286.3	296.6	316.0	1.1	5.1	4.2	0	9.0	0	0	2.8	93.9	93.3
1.97	0	100473	350.1	287.0	297.6	317.0	1.1	5.2	4.2	0	8.9	0	0	2.8	93.9	93.5
2.23	36.0	SHORT DURATION NO STEADY STATE PERFORMANCE DATA														
T DURATION TEST - NO STEADY STATE DATA																
2.50	0	94380	341.0	276.8	287.6	209.0	1.1	5.0	4.1	0	11.2	0	0	3.6	93.1	90.2
2.37	0	95552	342.4	279.1	289.9	311.4	1.1	5.0	4.1	0	11.3	0	0	3.6	93.1	90.9
2.28	0	98771	343.6	287.5	298.3	315.0	0	5.2	4.2	0	7.3	0	0	2.3	94.7	93.6
2.23	35.4	97388	360.1	270.5	280.8	316 2	0	4.9	4.2	19.0	7.3	9.8	6.0	2.3	88.8	88.1
2.20	34.7	93586	344.8	271.4	282.2	317.9	4.2	4.9	4.2	16.5	5.9	10.0	5.2	1.9	88.8	88 4
2.19	35.8	94496	355.6	265.7	276.1	317.0	9.4	4.8	4.2	16.6	5.9	10.1	5.2	1.9	87.1	86.5
2.20	36.4	98543	364.4	270.4	280.6	316.0	3.6	4.9	4.2	15.8	5.9	10.0	5.0	1.9	88.8	88.1
2.17	0	108128	377.7	286.3	296.2	315.0	3.6	5.1	4.2	0	5.9	0	0	1.9	94.0	93.3
2.28	54.6	99361	376.9	263.6	273.4	315.6	3.6	4.7	4.2	23.8	5.9	14.7	7.54	1.9	86.6	85.9
2.21	53.4	98957	373.1	265.2	275.1	317.0	3.6	4.8	4.2	23.4	5.9	14.3	7.38	1.9	86.8	86.4
2.22	52.3	98426	372.6	264.2	274.1	316.0	3.6	4.8	4.2	23.4	5.9	14.0	7.40	1.9	86.7	86.1
2.12	52.1	101479	379.3	267.5	277.3	316.4	3.6	4.8	4.2	20.6	5.9	13.7	6.51	1.9	87.6	87.1
2.10	54.0	95477	359.0	265.9	276.0	317.5	2.2	4.8	4.2	24.4	5.9	15.0	7.93	1.9	86.9	86.6
2.16	47.1	99356	378.4	262.6	272.2	317.2	5.3	4.7	4.2	20.6	10.2	12.5	6.50	3.5	85.8	85.5
2.05	35.7	100109	355.1	271.5	281.9	318.3	2.2	4.9	4.2	14.9	10.2	11.1	4.68	1.9	88.6	88.0
2.23	40.7	97816	352.3	267.1	277.6	317.4	2.2	4.9	4.2	22.7	5.9	11.6	7.15	1.9	87.5	86.9
2.13	0	99109	341.6	290.1	301.0	316.9	2.2	5.2	4.2	0	4.3	0	0	1.4	95.0	94.5
2.15	0	99753	346.3	288.0	298.9	315.6	2.2	5.2	4.2	0	5.1	0	0	1.6	94.7	93.8

ARES Secondary Injector Test Data and Performance Summary (U)

Figure VI-7

Report 10830-F-1, Phase I, Supplement 1

Symbol	Title
ABL-ABL	Ablative Chamber - Ablative Nozzle
ABL-STL	Ablative Chamber - Steel Nozzle
A_t	Throat Area
Chamb	Chamber Type
Data Period	Time from FS_1 during which data was sampled
Dur	Test Duration
ERL	Energy Release Loss
FCL	Film Cooling Loss
FS_1	Engine Fire Switch
F_{VAC}	Vacuum Thrust
IM-PL	Impinging Platelet Injector
Inj	Injector Type
$I_{S_{SL}}$	Sea Level Specific Impulse
$I_{S_{VAC}}$	Vacuum Specific Impulse
L^*	Characteristic Length
Mk 125	Mark 125 - 3 ORST Injector
MRDL	Mixture Ratio Distribution Loss
MR_{INJ}	Injector Mixture Ratio
NFL	Nozzle Friction Loss
NGL	Nozzle Geometry Loss
PCSC	Secondary Chamber Pressure, total
SH-PL	Showerhead Platelet Injector
SH-PL (PID)	Showerhead Platelet Injector with Performance Improvement Device
S/N	Serial Number
Theo $I_{S_{VAC}}$	Theoretical Vacuum Specific Impulse
TRA-ABL	Transpiration Chamber-Ablative Throat and Nozzle
Trans.	Transpiration Thrust Chamber
WARP I	WARP Injector, Type I
WARP II	WARP Injector, Type II
WARP III	WARP Injector, Type III
WARP IIIM	WARP Injector, Type III without Face Plate
$\dot{W}_{eng}$	Engine Total Weight Flow
$\dot{W}_{OFC}$	Film Coolant Weight Flow
ε	Area Ratio

Nomenclature List, Secondary Injector Program, Performance Analysis

Figure VI-8

(This page is Unclassified)

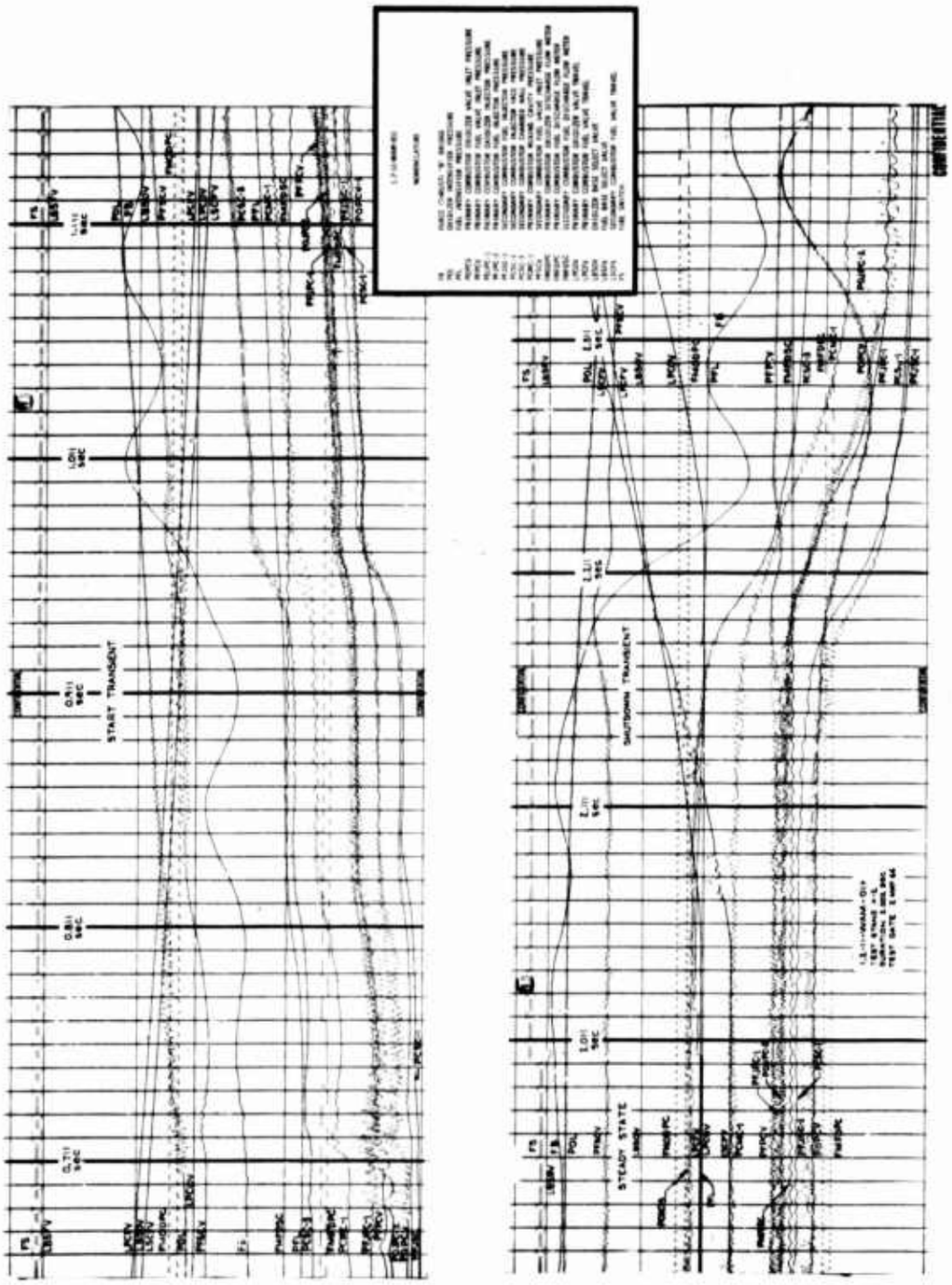

Typical Oscillograph, Secondary Injector Test (u)

Figure VI-9

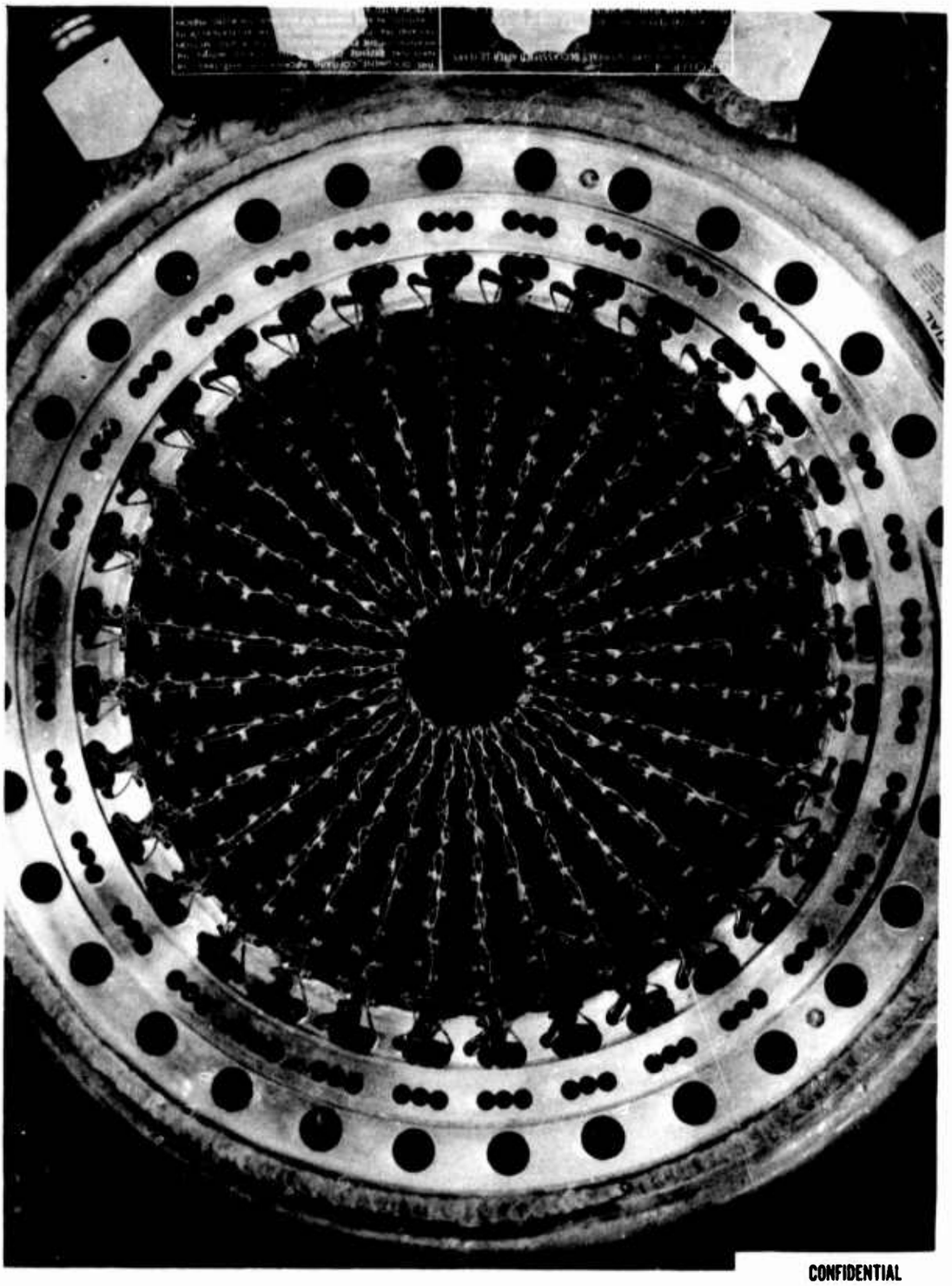

Mark 125 3 ORST Injector--Reinforced (U)

Figure VI-10

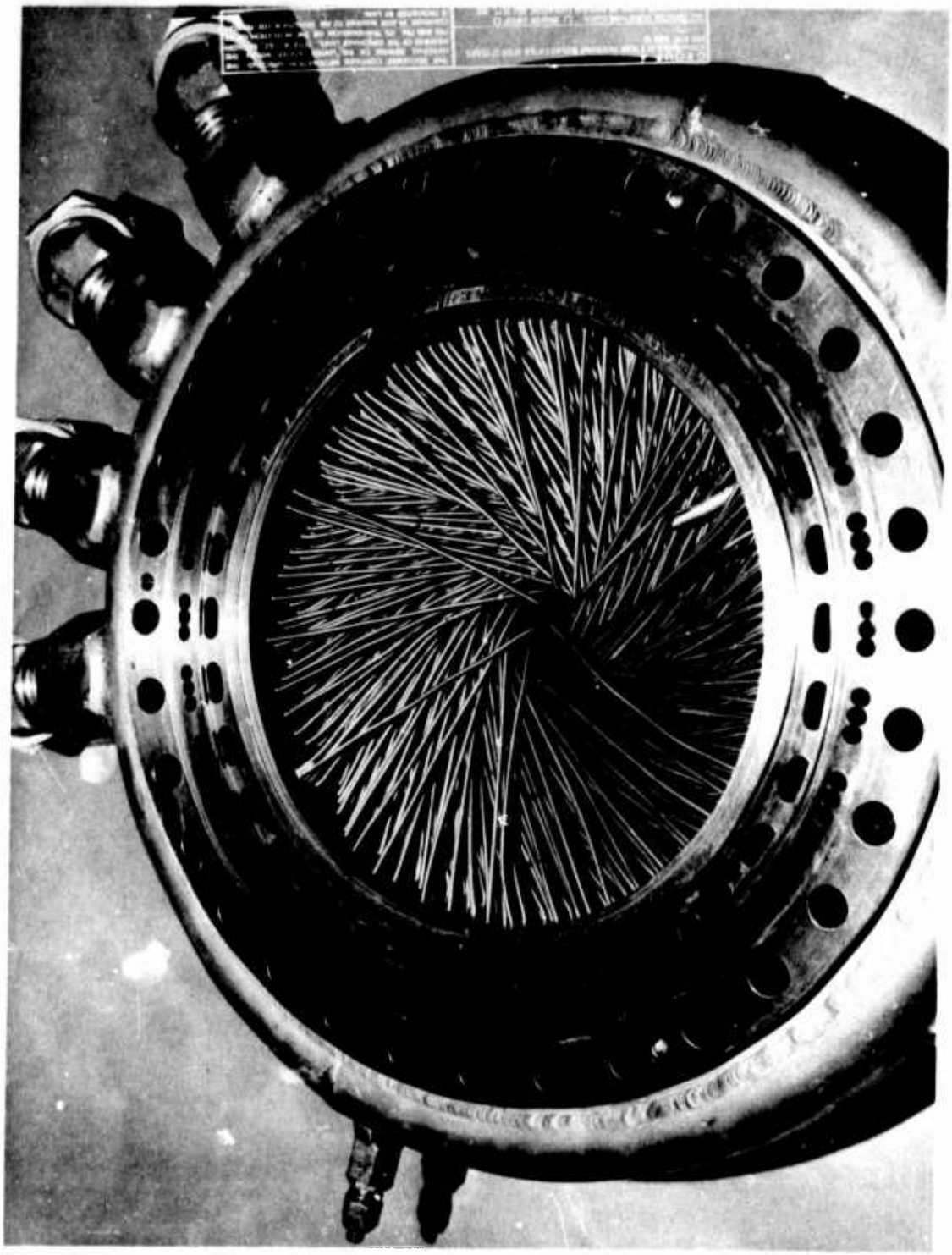

WARP I Injector, Upstream View (u)

Figure VI-11

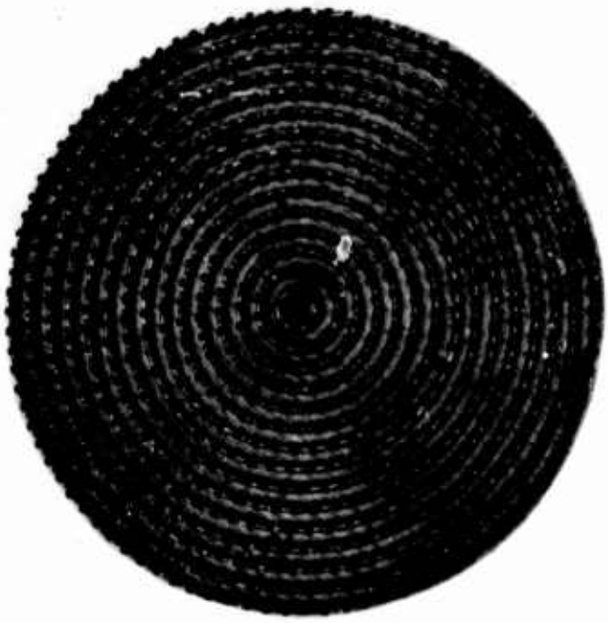

Figure VI-12. WARP II Injector Faceplate - Backside

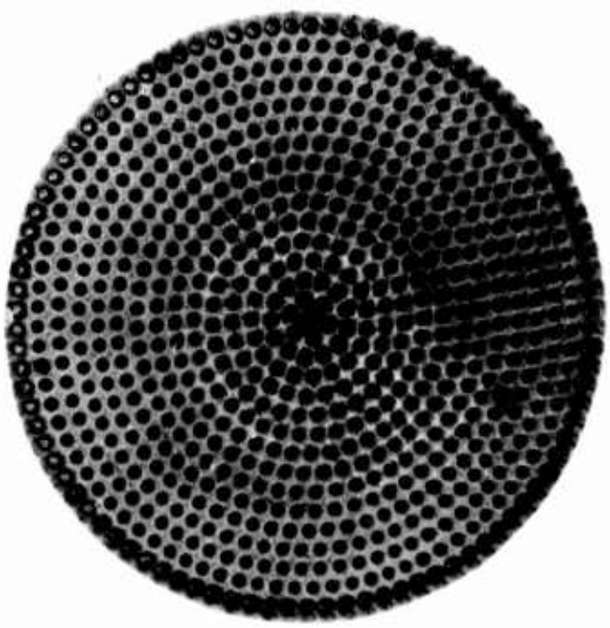

Figure VI-13. WARP II Injector Faceplate - Faceside

Figure VI-12, Figure VI-13

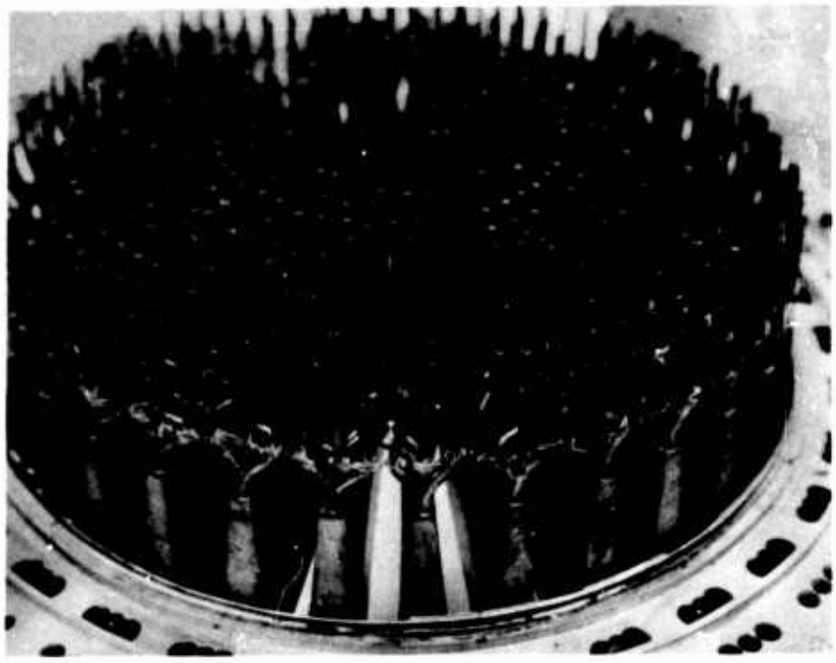

Figure VI-14. WARP III Injector Fuel Manifolding (u)

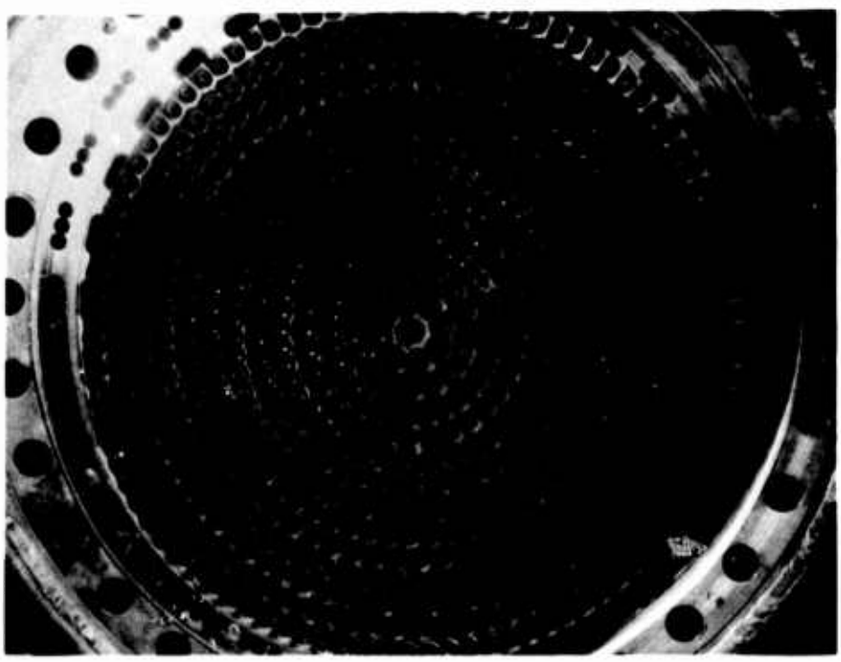

Figure VI-15. WARP III Injector - Face View (u)

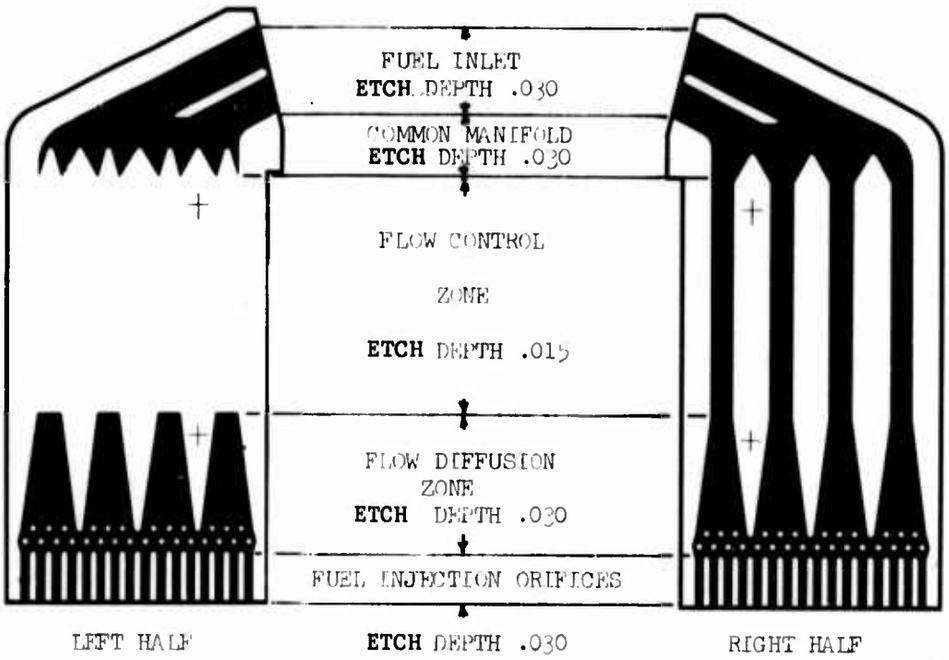

TYPICAL SHOWERHEAD INJECTOR
VANE

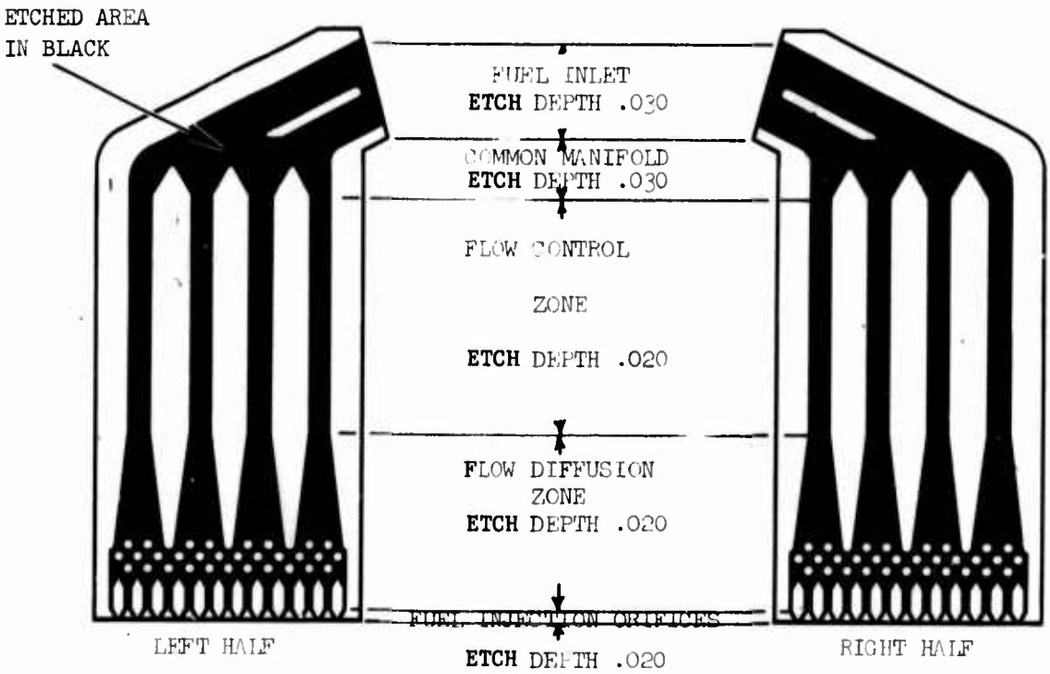

Typical Platelet Injector Vanes

Figure VI-16

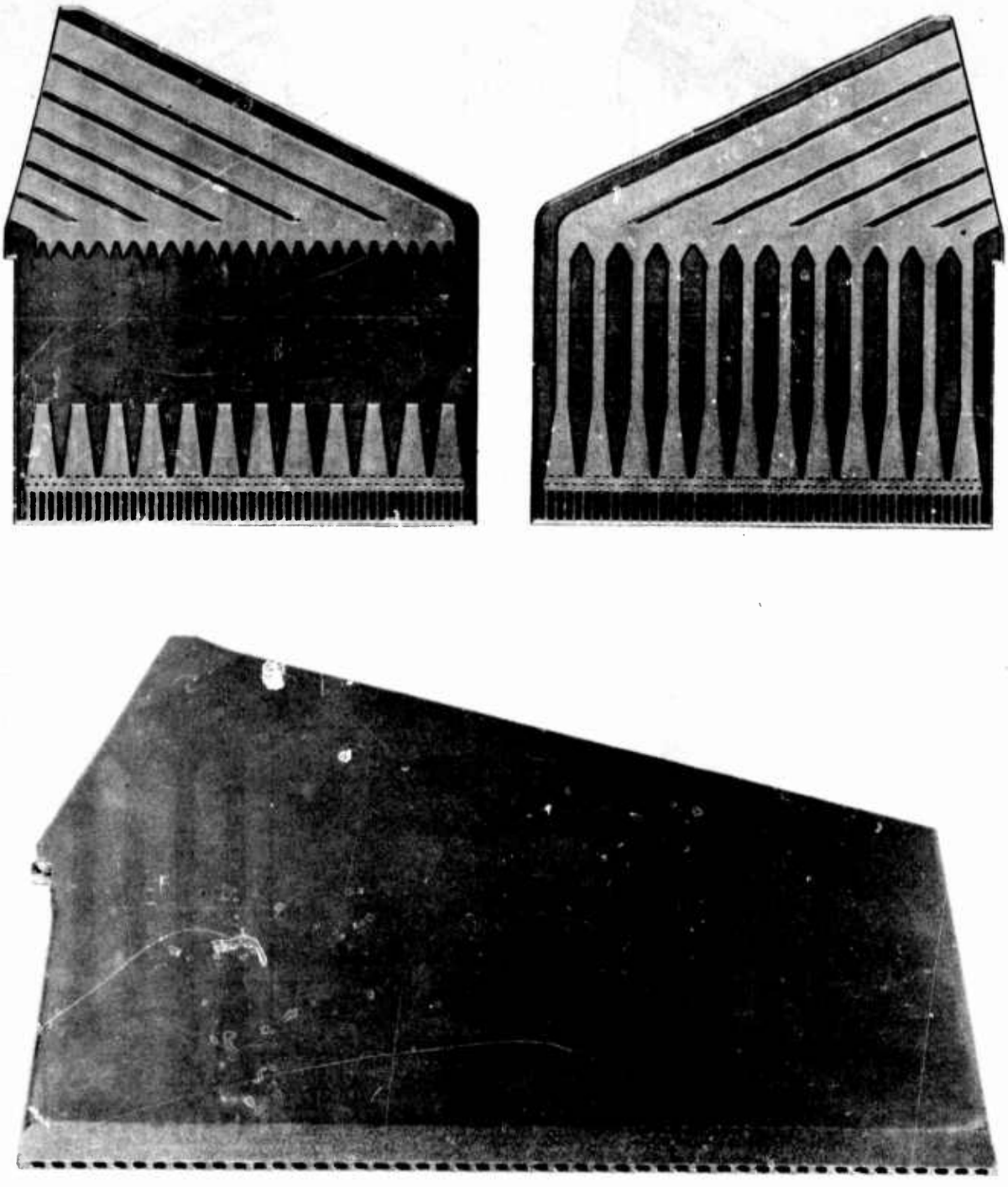

Showerhead Vane Halves and Assembled Vane

Figure VI-17

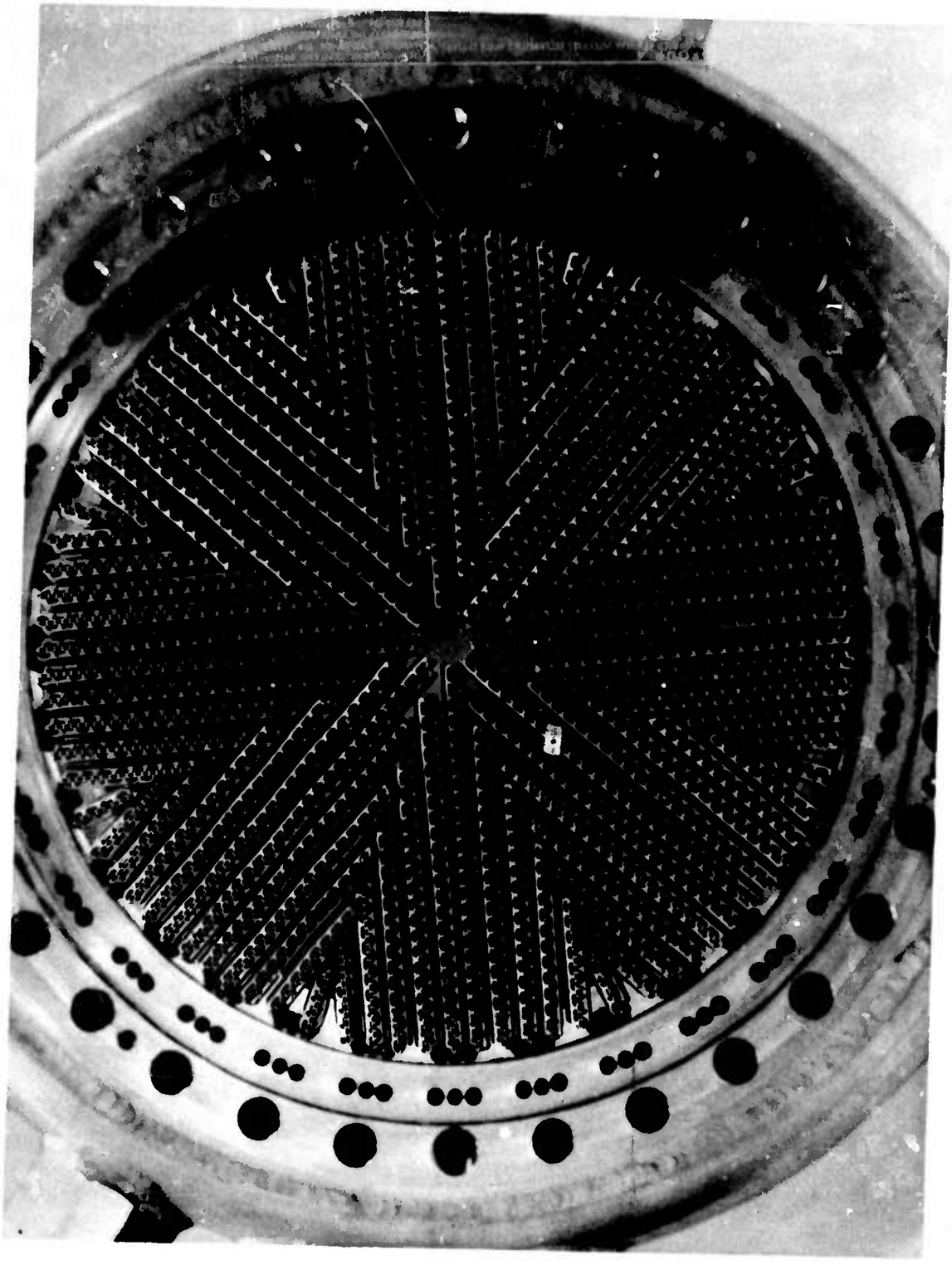

CONFIDENTIAL

Platelet Injector--Strip Modification (U)

Figure VI-18

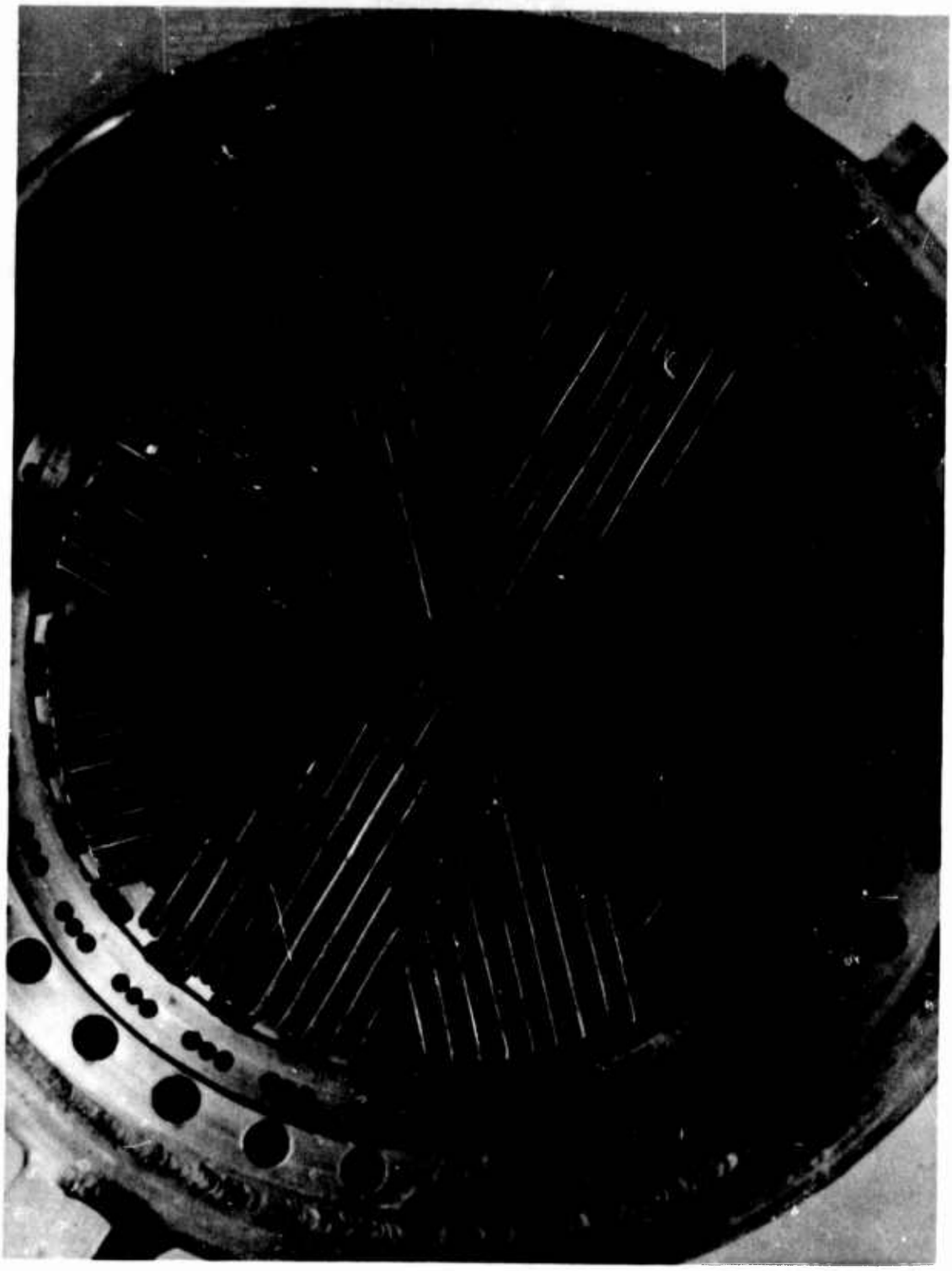

CONFIDENTIAL

Platelet Injector--Rod Modification (U)

Figure VI-19

Figure VI-20. Uncooled Ablative Thrust Chambers, 30 and 40 in. L*

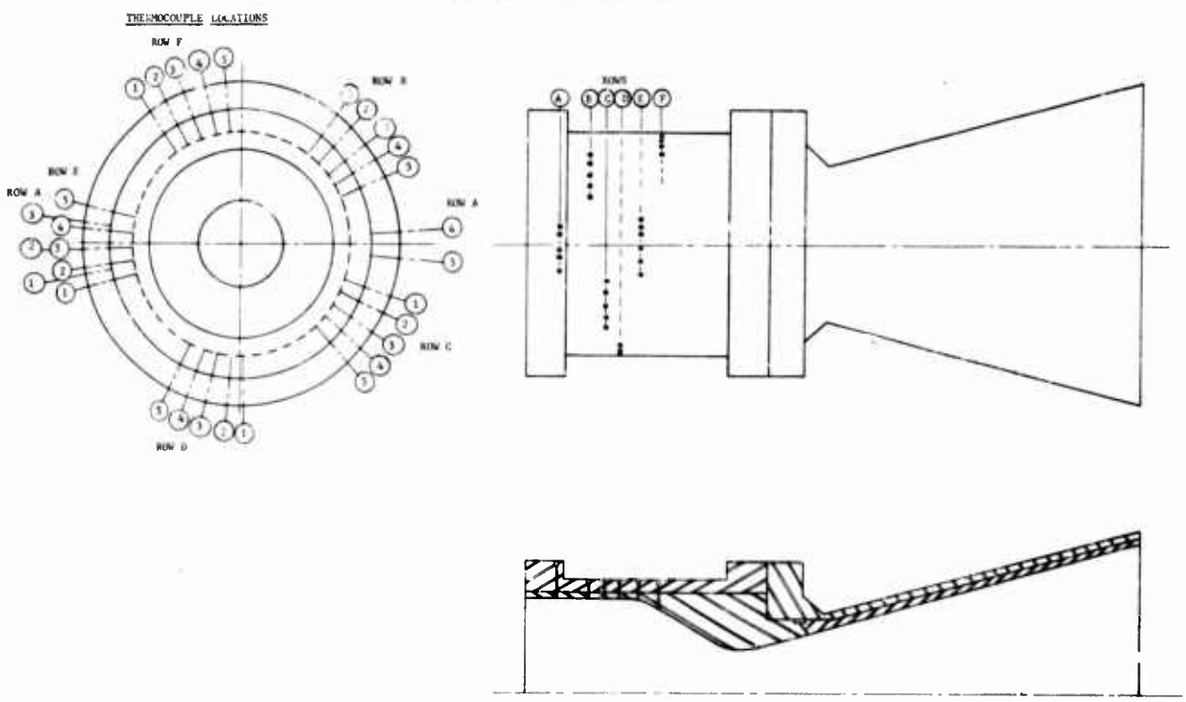

Figure VI-21. Uncooled Instrumented Thrust Chamber Schematic

Figure VI-20, Figure VI-21

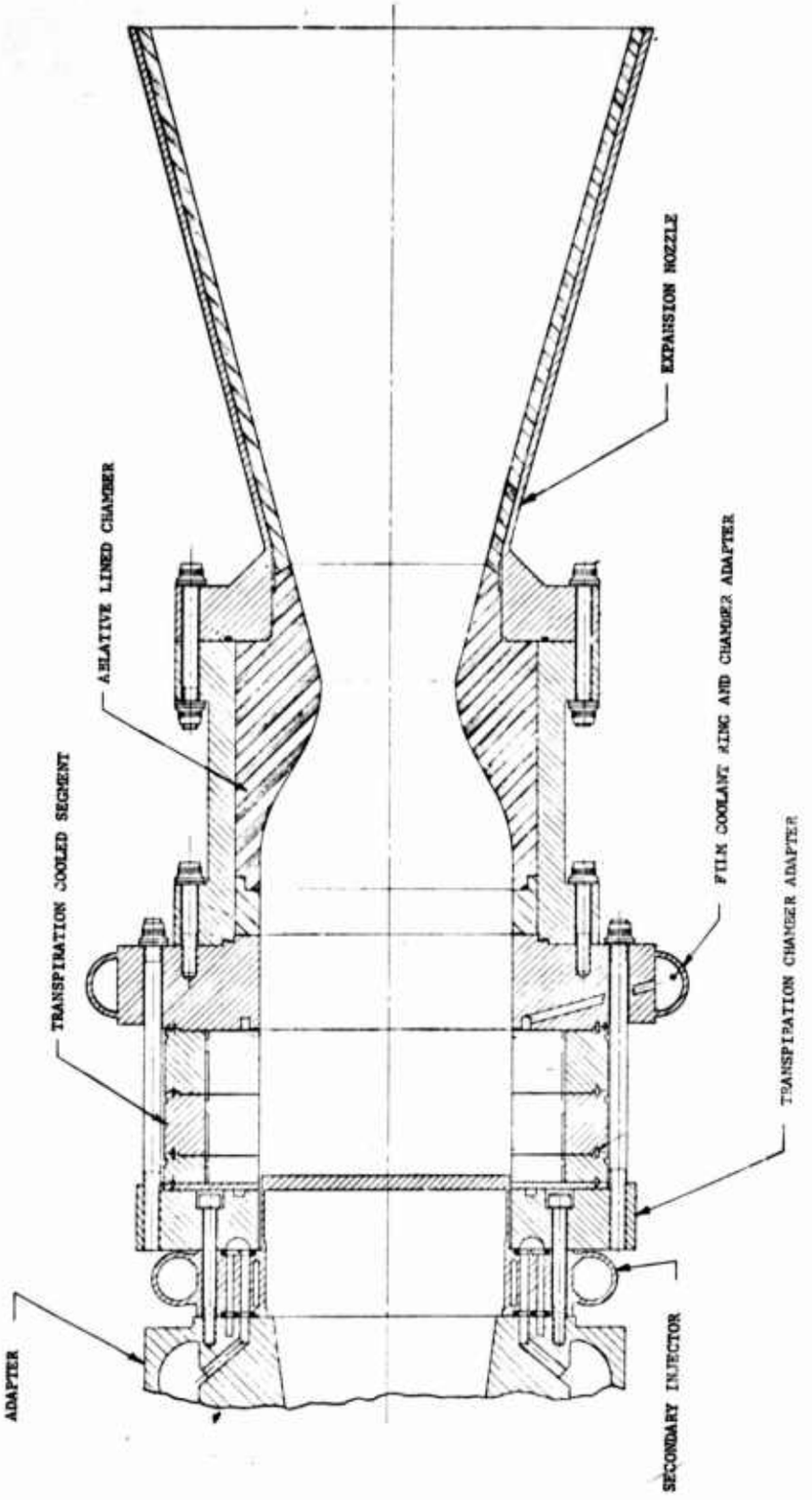

Transpiration-Ablative Thrust Chamber Assembly

Figure VI-22

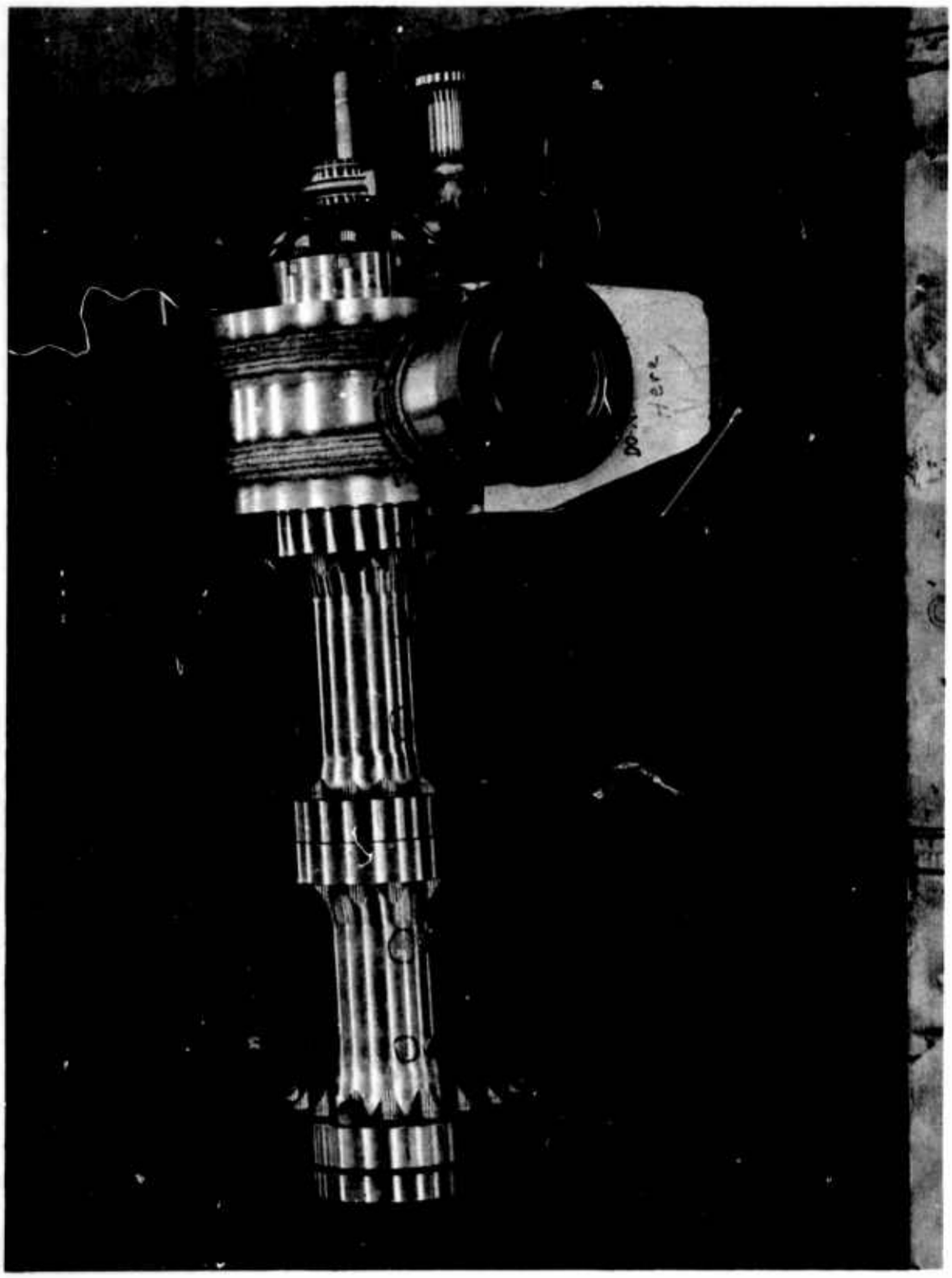

Primary Combustor Assembly

Figure VI-23

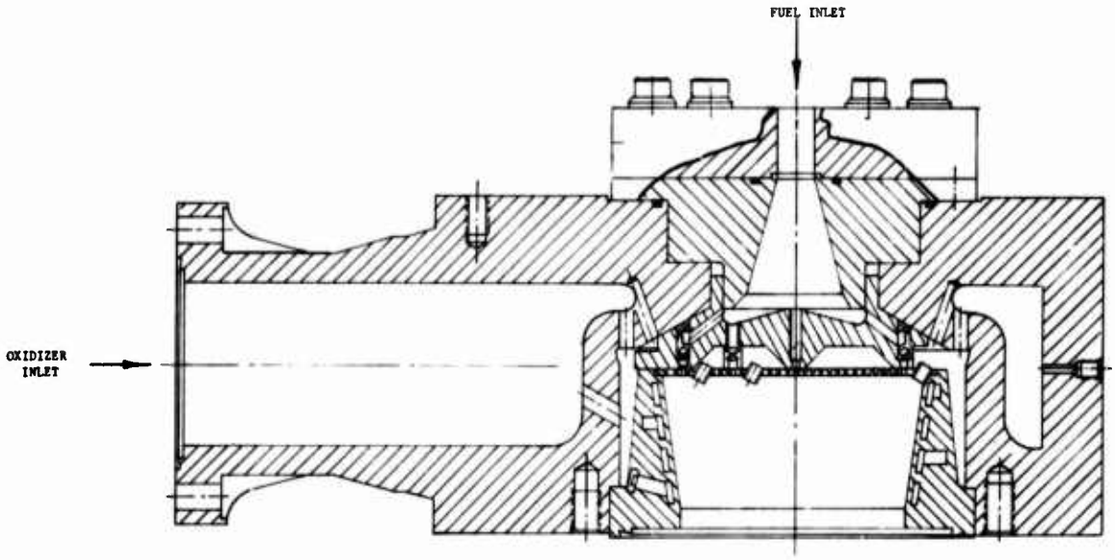

Primary Injector

Figure VI-24

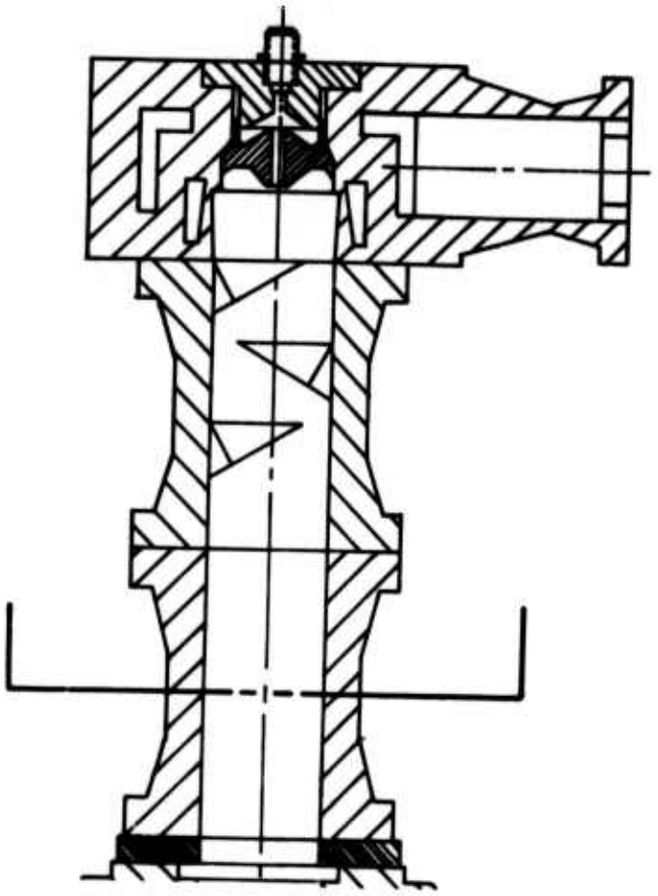

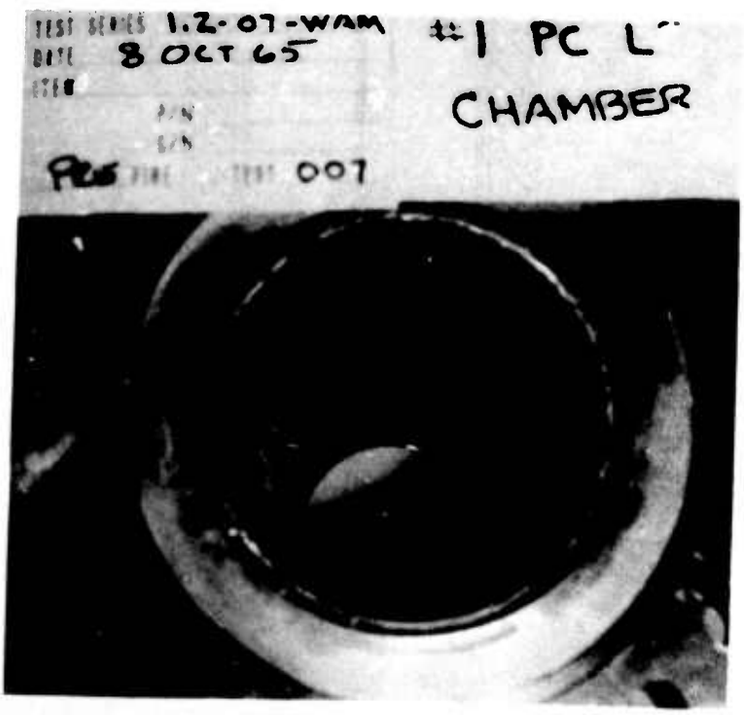

Primary Combustion Chamber with Moon-Shaped Turbulators

Figure VI-25

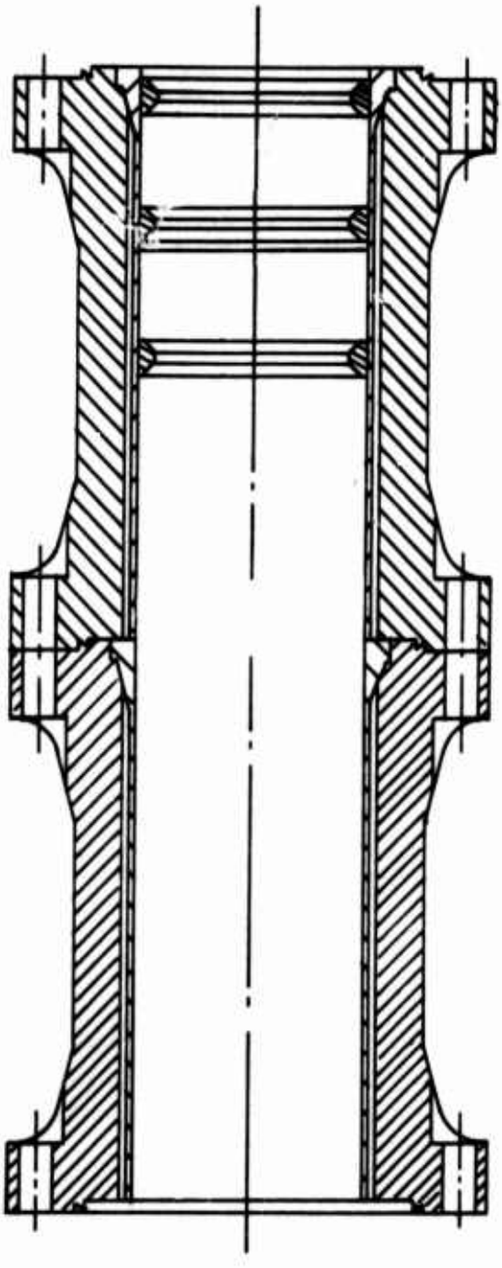

Primary Combustion Chamber with Concentric Turbulators

Figure VI-26

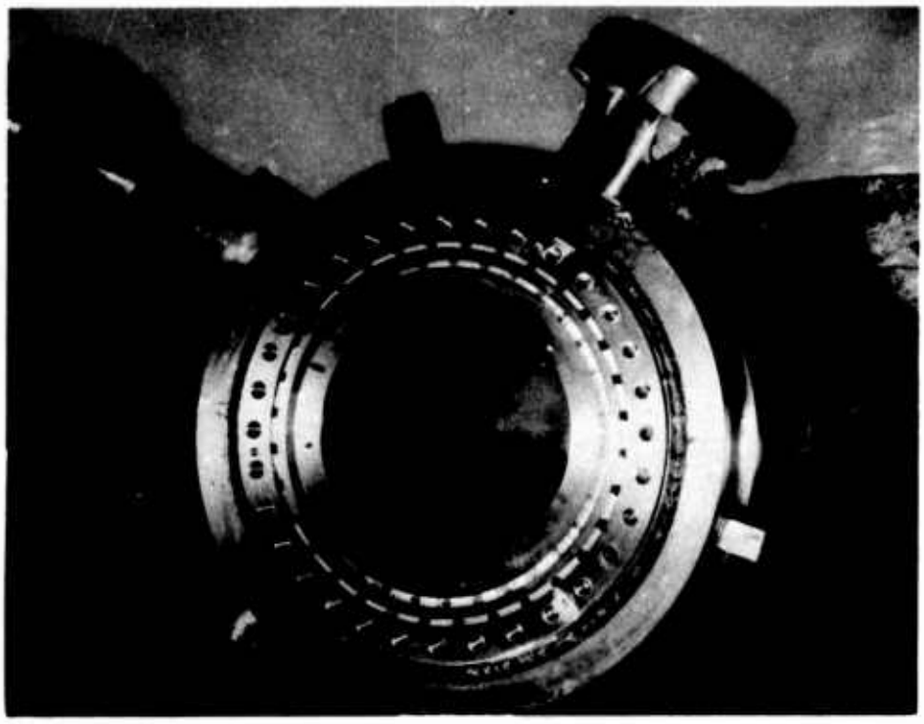

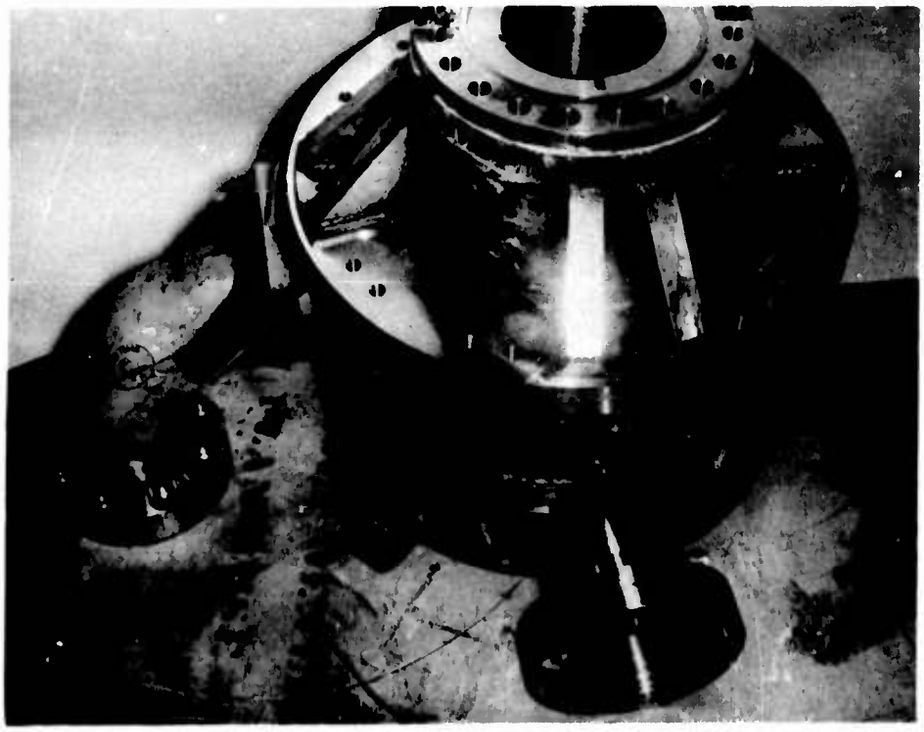

Secondary Combustor Test Stand Adapter

Figure VI-27

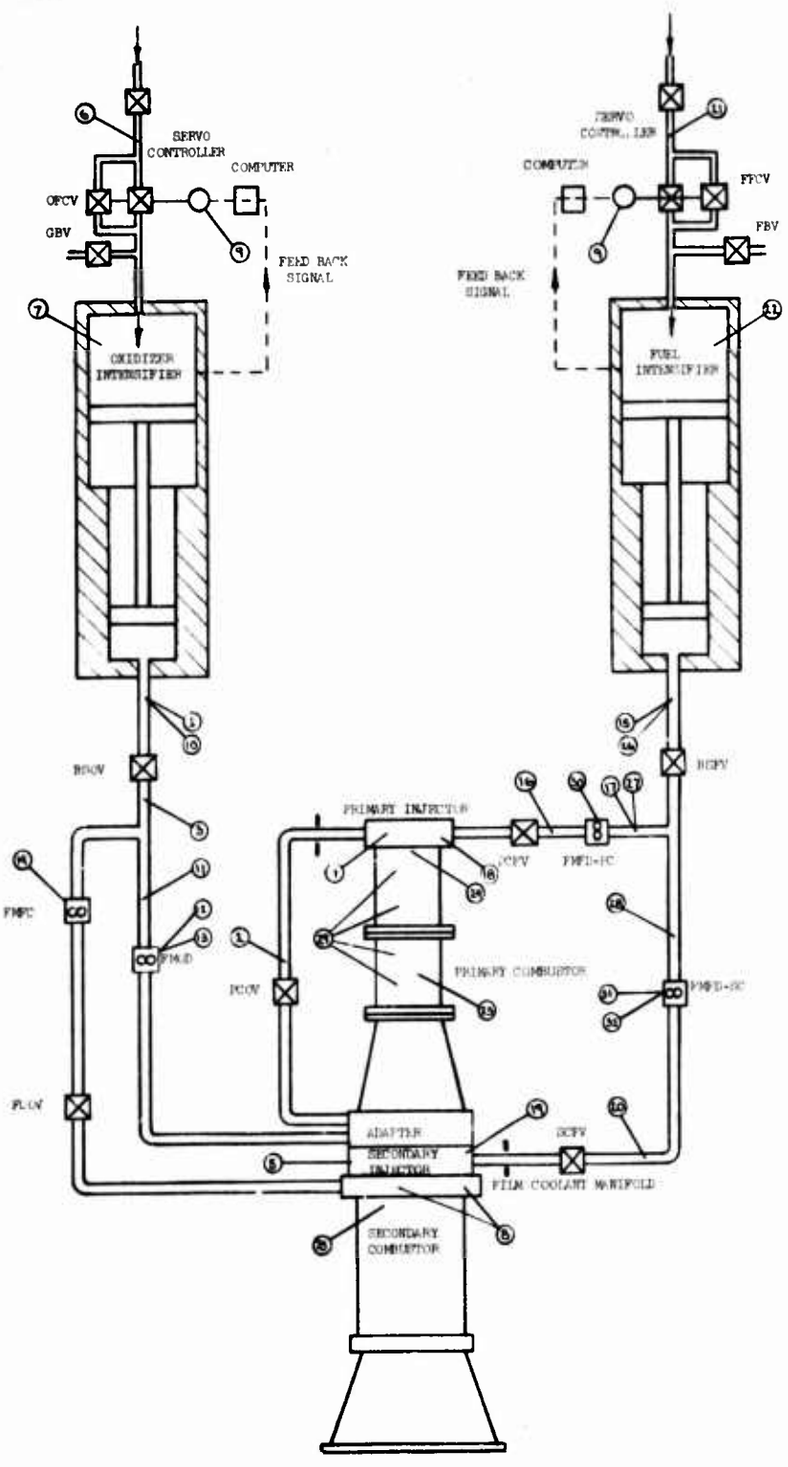

NO.	S
1	P
2	P
3	P
4	P
5	P
6	P
7	P
8	P
9	P
10	T
11	T
12	F
13	F
14	F
15	F
16	F
17	F
18	F
19	F
20	F
21	F
22	F
23	F
24	F
25	F
26	T
27	T
28	T
29	T
30	I
31	I
32	I

NO.	SYMBOL	TITLE
1	PoL	Oxidizer Intensifier Outlet Pressure
2	PoPCV	Oxidizer Primary Combustor Valve Pressure
3	PoD	Oxidizer Discharge Pressure
4	PoJPC	Oxidizer Primary Combustor Injector Pressure
5	PoJSC	Oxidizer Secondary Combustor Injector Pressure
6	PGoFCV	Oxidizer Flow Control Valve Gas Pressure
7	PGoB	Oxidizer Gas Side Booster Pressure
8	PoMC	Oxidizer Coolant Manifold Pressure (1 and 2)
9	PHD	Hydraulic Discharge Pressure
10	ToL	Oxidizer Temperature Intensifier Outlet
11	ToDFM	Oxidizer Temperature Primary Combustor Flow Meter
12	FMoD	Oxidizer Flow Meter Primary Combustor
13	FMVoD	Oxidizer Digital Flow Primary Combustor
14	FMoD-FC	Oxidizer Film Coolant Flow Meter
15	PfL	Fuel Intensifier Outlet Pressure
16	PfPCV	Fuel Primary Combustor Valve Pressure
17	PfD	Fuel Discharge Pressure
18	PfJPC	Fuel Primary Combustor Injector Pressure
19	PfJSC	Fuel Secondary Combustor Injector Pressure
20	PfSCV	Fuel Secondary Combustor Valve Pressure
21	PGfFCV	Fuel Flow Control Valve Gas Pressure
22	PGfB	Fuel Gas Side Booster Pressure
23	PcPC	Chamber Pressure (1 and 2) Primary Combustor
24	PcMC	Chamber Pressure (1 and 2) Mixing Cavity
25	PcSC	Chamber Pressure Secondary Combustor
26	TfL	Fuel Temperature Intensifier Outlet
27	TfDFM-PC	Fuel Temperature Primary Combustor Flow Meter
28	TfDFM-SC	Fuel Temperature Secondary Combustor Flow Meter
29	TcPC	Primary Combustor Chamber Temperatures (5 through 8)
30	FMfD-PC	Fuel Flow Meter Primary Combustor
31	FMfD-SC	Fuel Flow Meter Secondary Combustor
32	FMVfD-SC	Fuel Digital Flow Secondary Combustor

ARES Intensifier-Fed Engine Flow and Instrumentation Schematic

Figure VI-28

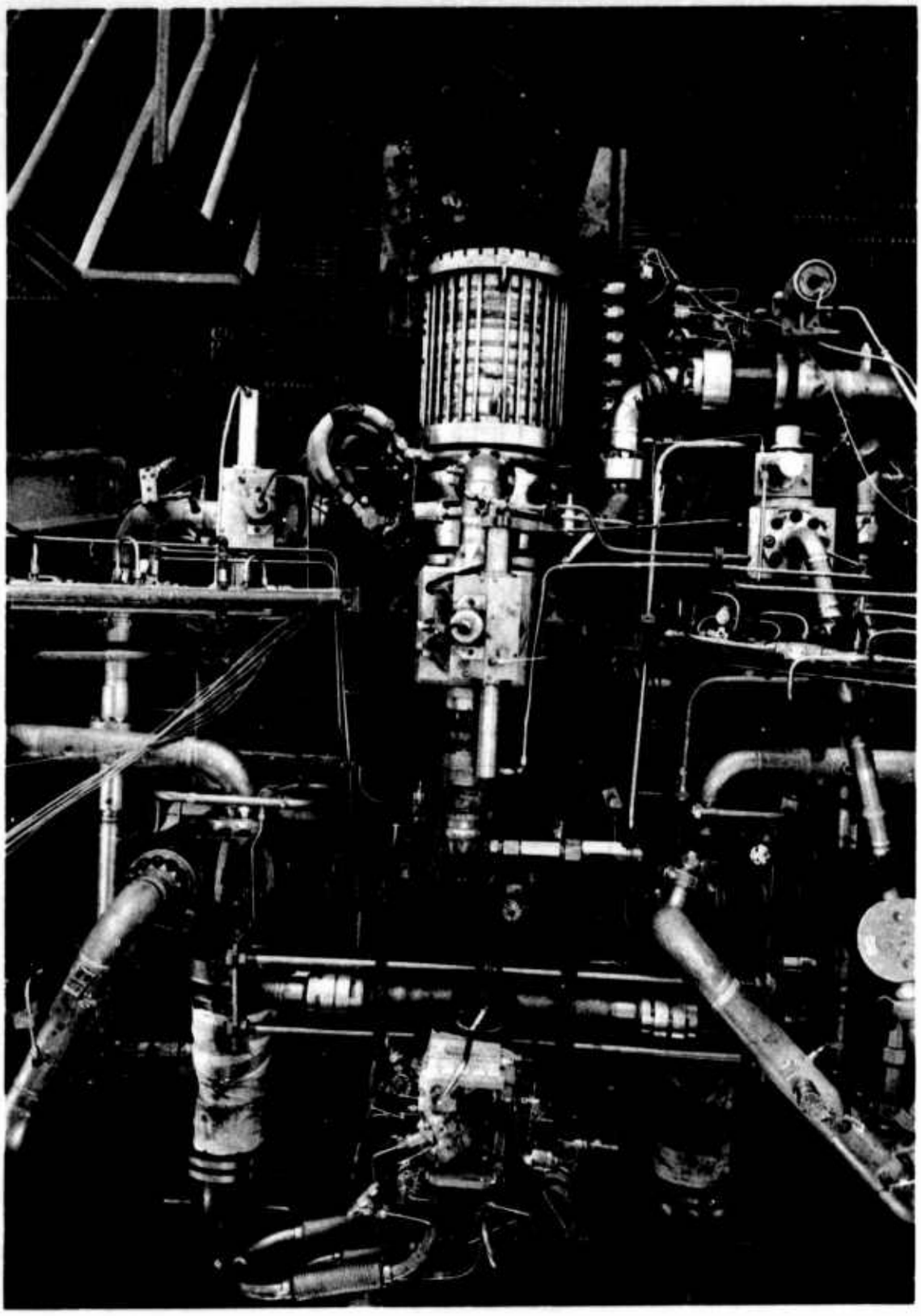

Staged-Combustion Test Engine

Figure VI-29

NO.	SYMBOL	TITLE
1	P_OD-f(MS)	Oxidizer Discharge Pressure Micro System
2	P_OJ_{PC}-lf(MS)	Oxidizer Primary Combustor Injector Pressure (Micro System)
3	P_fD-f(MS)	Fuel Discharge Pressure (Micro System)
4	P_{fDPC}-f(MS)	Fuel Primary Combustor Discharge Pressure (Micro System)
5	P_{fDSC}-f(MS)	Fuel Secondary Combustor Discharge Pressure (Micro System)
6	P_{fJPC}-2f(MS)	Fuel Primary Combustor Injector Pressure (Micro System)
7	P_{fJSC}-f(MS)	Fuel Secondary Combustor Injector Pressure (Micro System)
8	P_{CMC}-lf(K)	Mixing Cavity Chamber Pressure (Kistler)
9	P_{cPC}-lf(P)	Primary Combustor Chamber Pressure (Photocon)

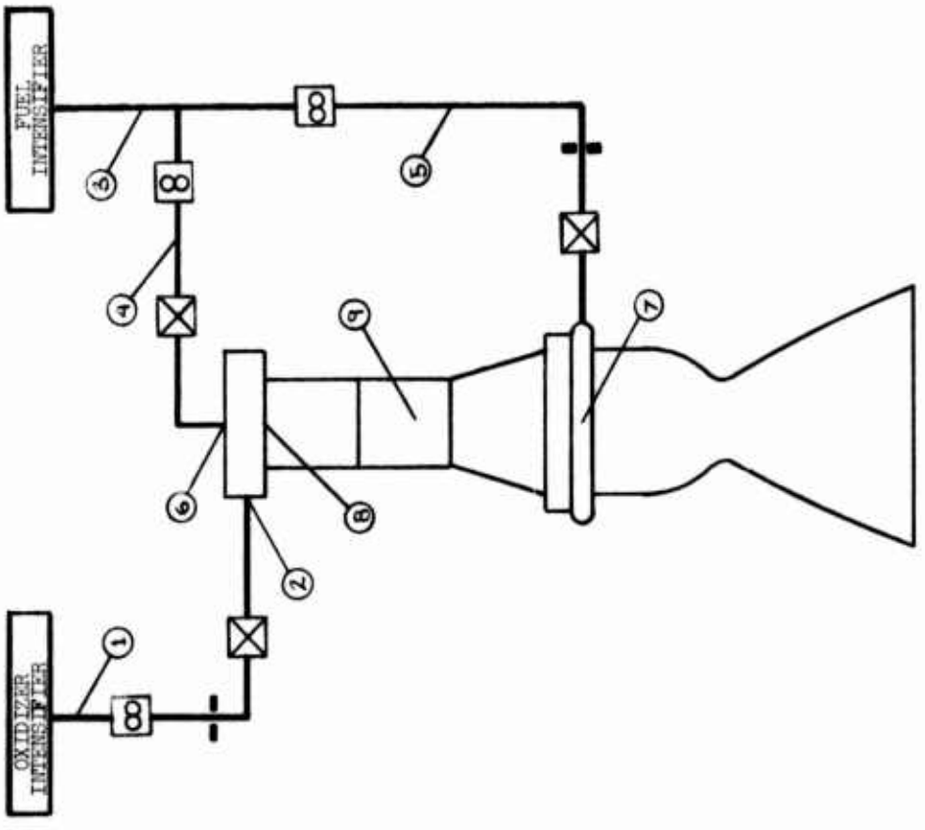

High-Frequency Instrumentation Schematic

Figure VI-30

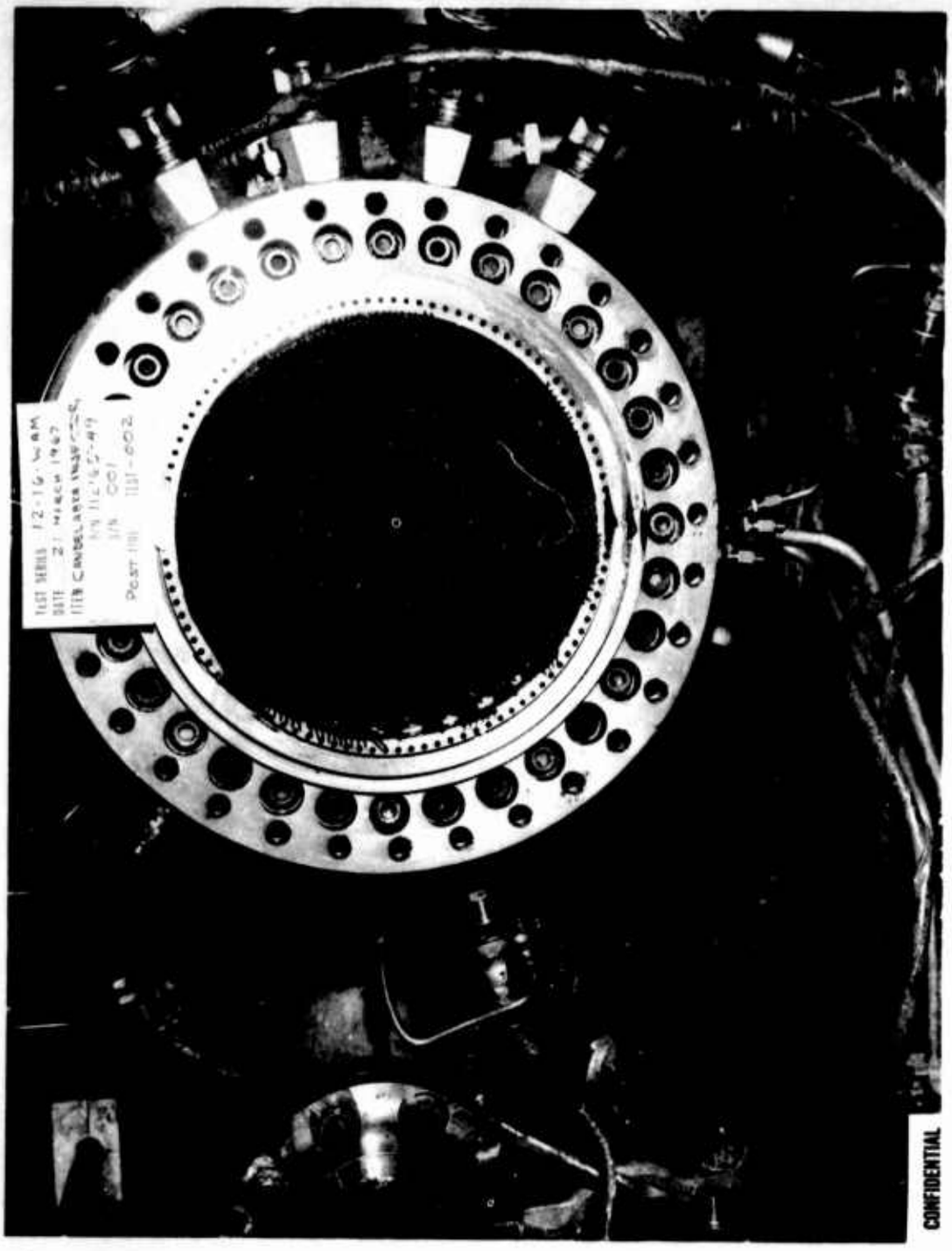

Candelabra Injector--Postfire (U)

Figure VI-31

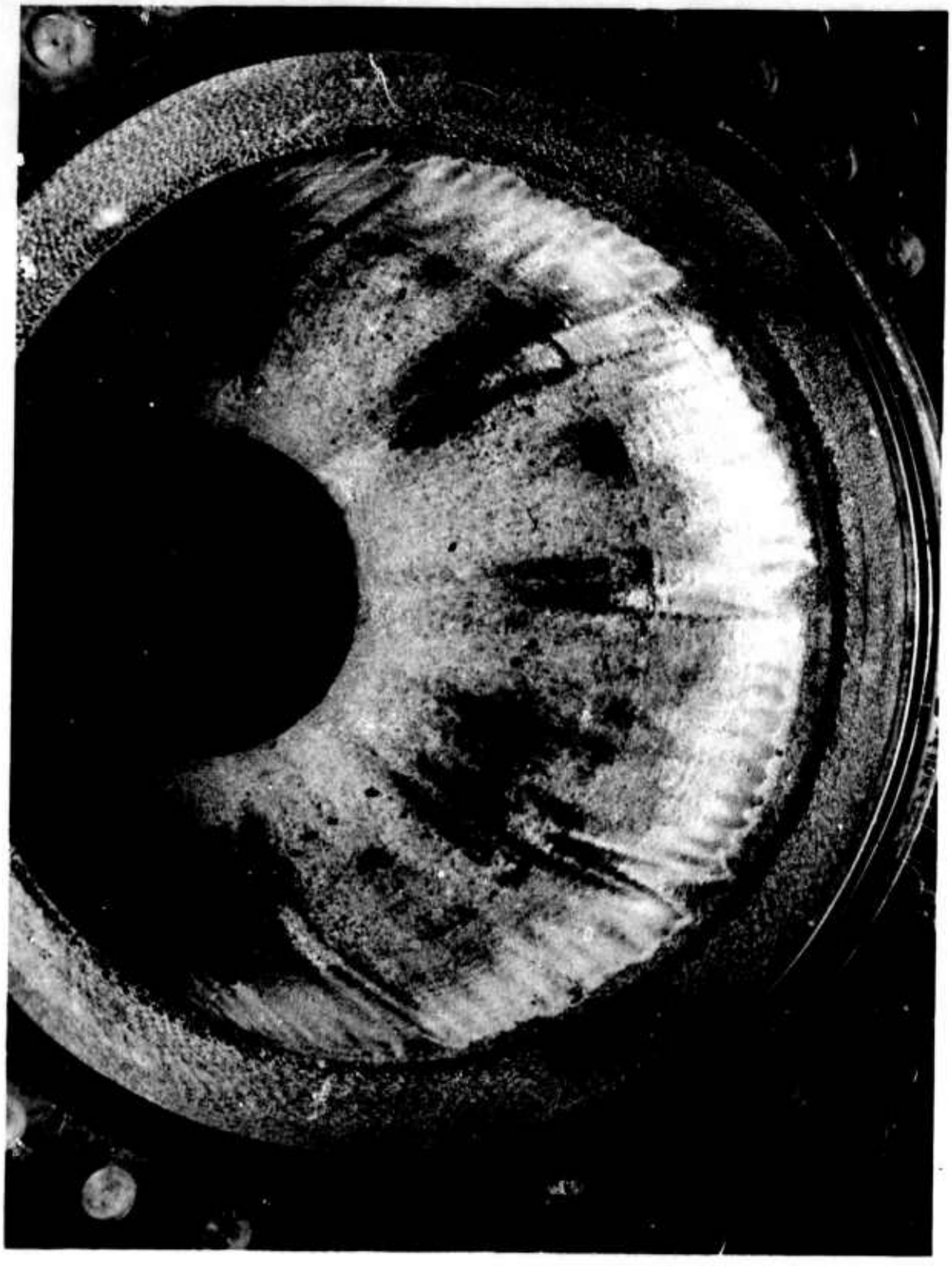

Chamber Streaks Post Test 1.2-16-WAM-007

Figure VI-32

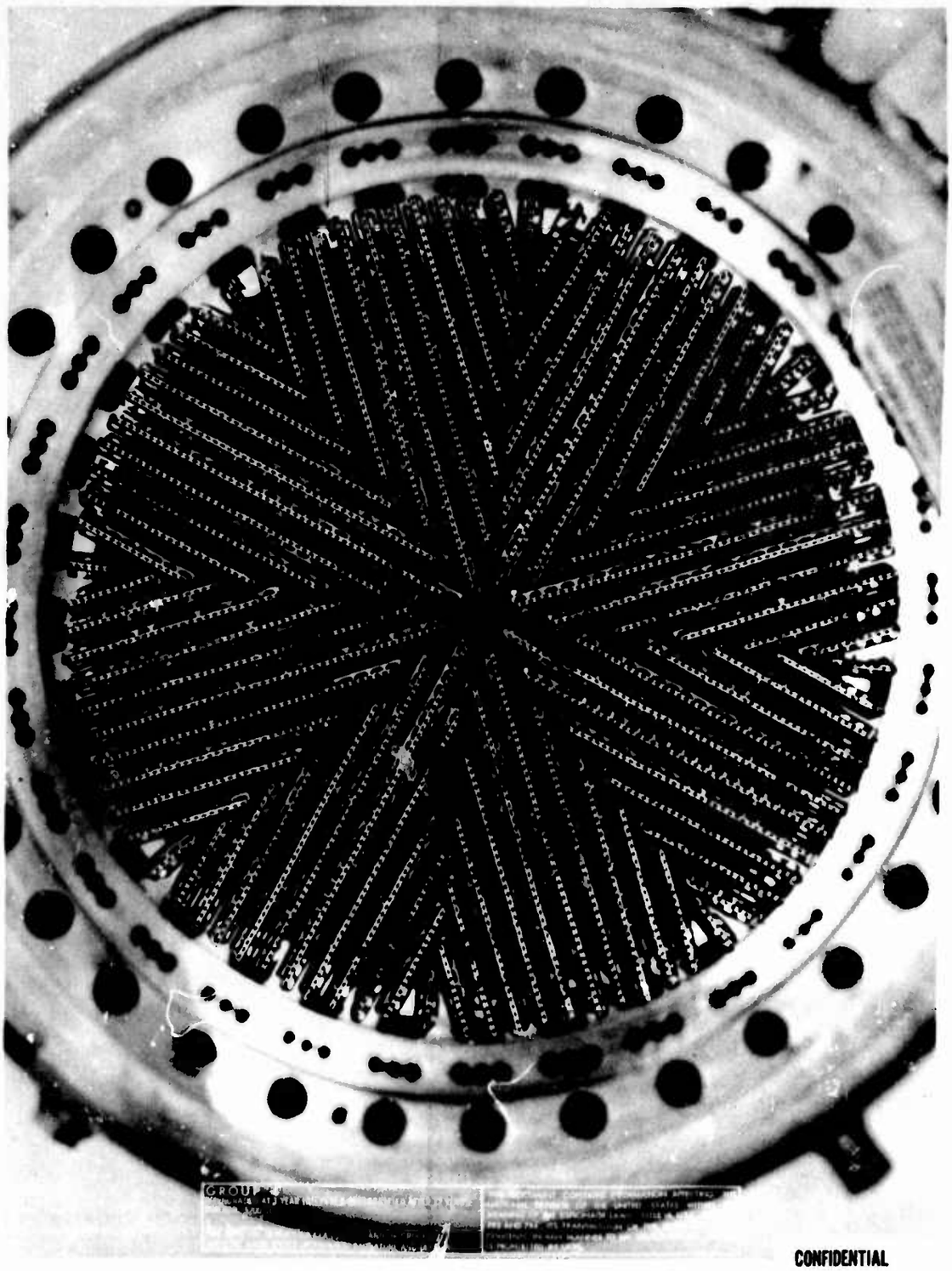

Platelet Injector with Performance Strips--Posttest (U)

Figure VI-33

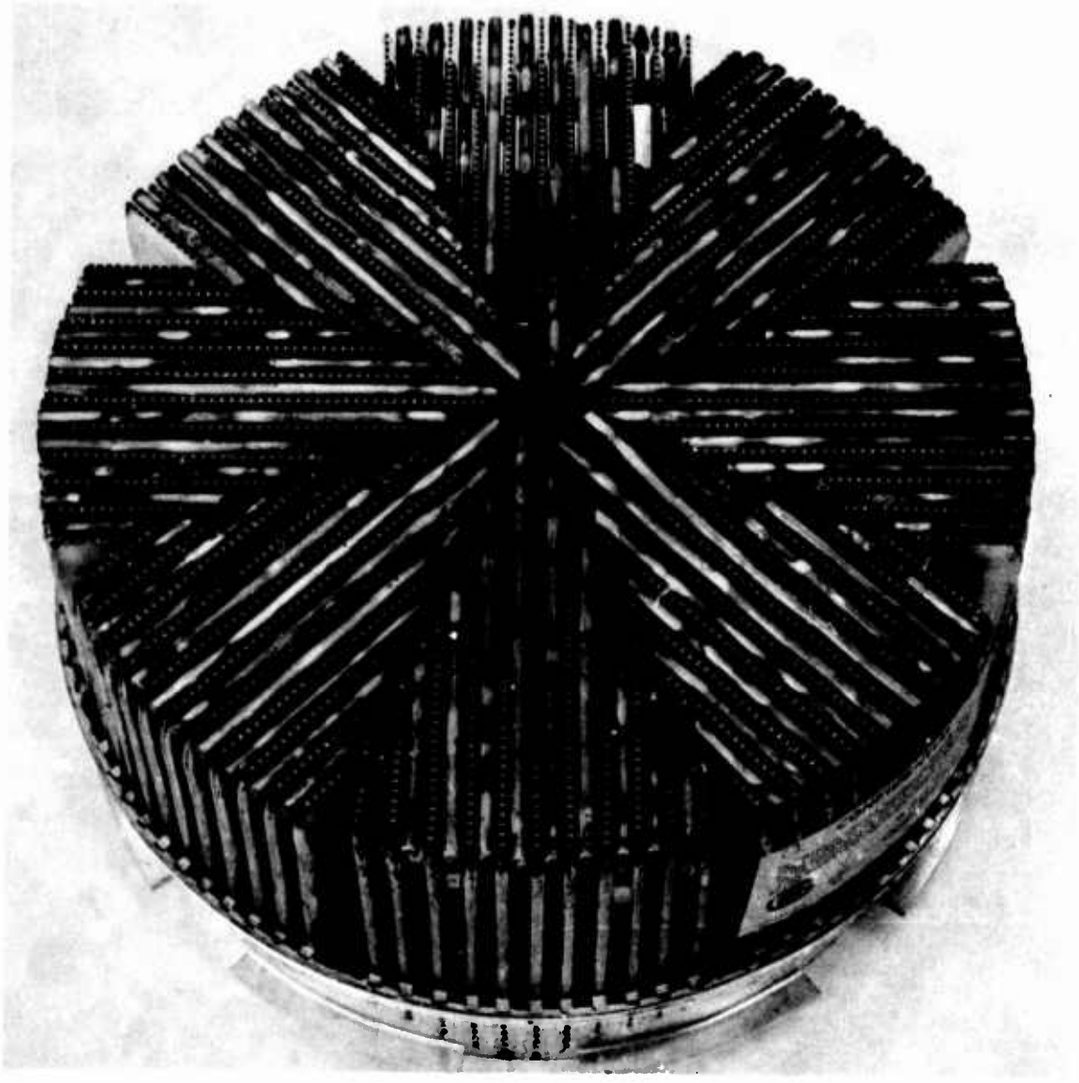

Platelet Injector with Performance Rods--Posttest (U)

Figure VI-34

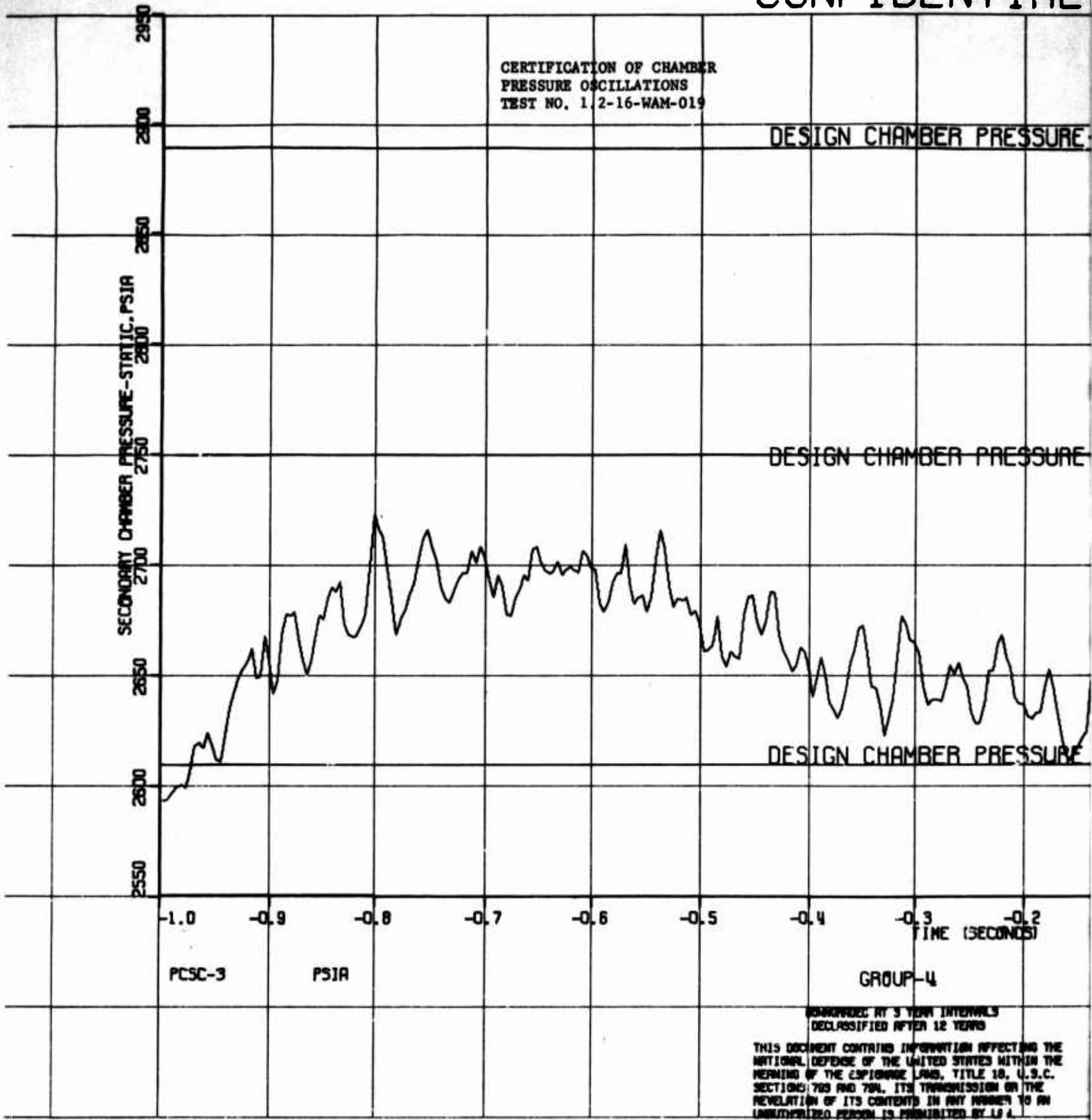

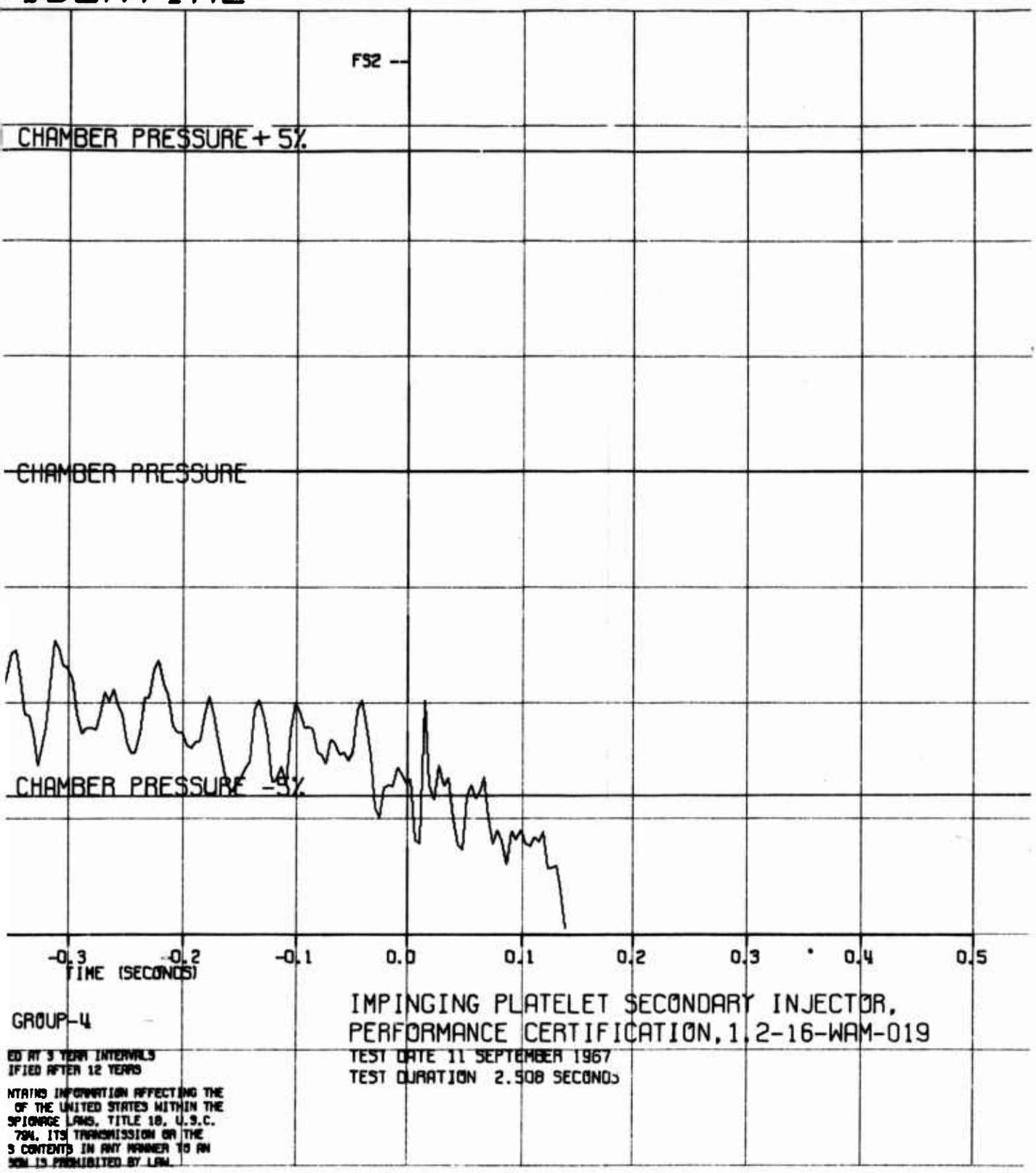

GROUP-4

IMPINGING PLATELET SECONDARY INJECTOR,
PERFORMANCE CERTIFICATION, 1.2-16-WAM-019
TEST DATE 11 SEPTEMBER 1967
TEST DURATION 2.508 SECONDS

Certification of Chamber Pressure Oscillations,
Test 1.2-16-WAM-019 (U)
Figure VI-35

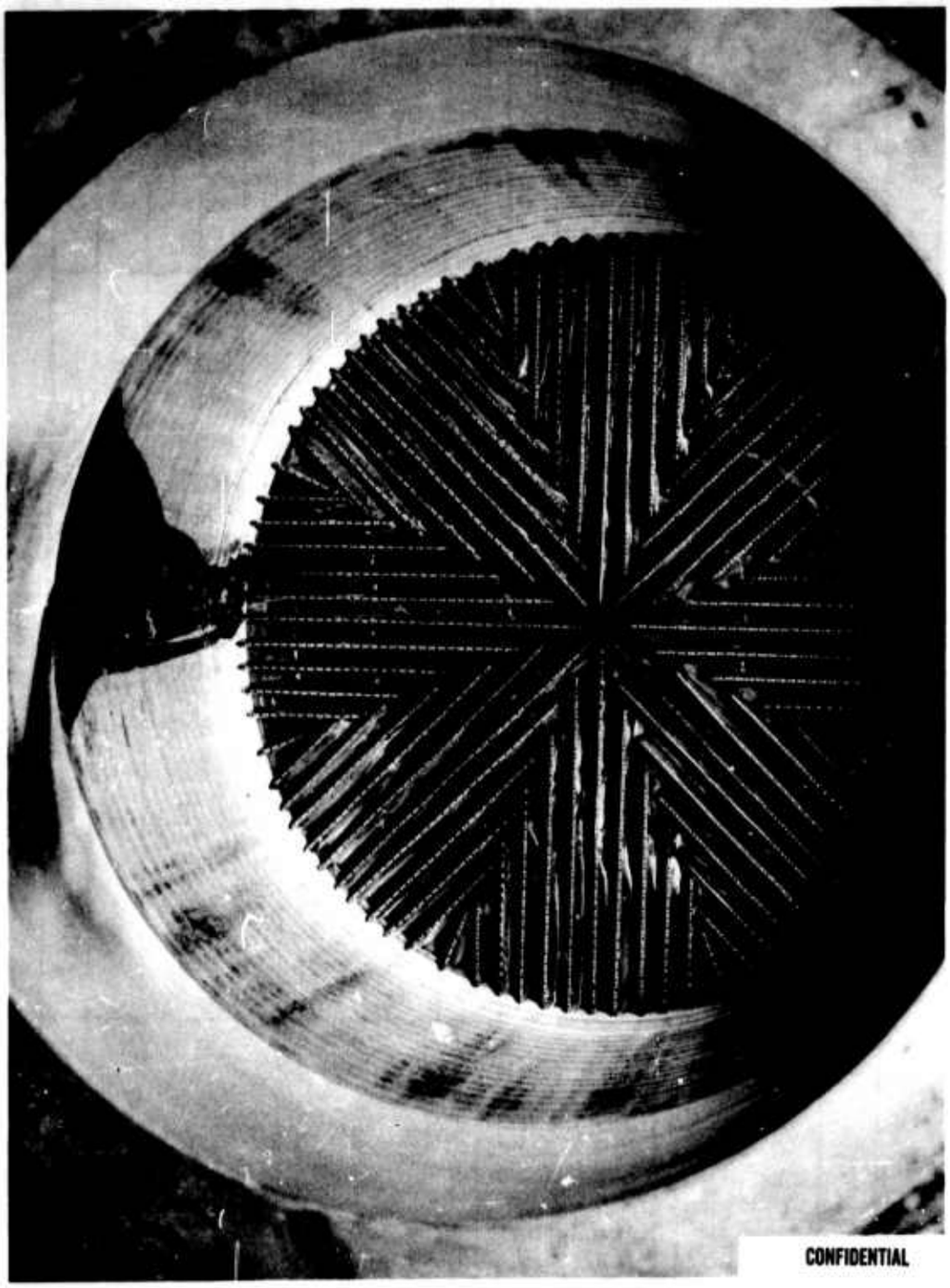

Transpiration-Ablative Combustion Chamber
(Post Test)

Figure VI-36

INJECTOR	GAS DISTRIBUTION DEVICE	TEST	PERFORMANCE LOSS, %		
			MRD	ERL	FCL
Mark 125 - 3 ORST	Original	1.2-16-WAM-003 & 004	0.4	3.14	0
		1.2-16-WAM-005			4.5
	Drilled Plate	1.2-16-WAM-026	1.7		6.5
WARP I	Original	1.2-16-WAM-001	No steady state performance data obtained.		
WARP II	Original	1.2-16-WAM-006			
WARP III	Original	1.2-16-WAM-011			
WARP III w/o Face Plate	Original	1.2-16-WAM-012 & 013	0.4	3.6	0
Showerhead Platelet	Original	1.2-16-WAM-007 thru .010	0.4	2.80	0
	Notched Screen	1.2-16-WAM-014 & 015	0	2.30	0,6.0
SH. Pl. w/Scalloped P.I.D.	Drilled Plate	1.2-13-WAM-015	0.7	1.40	0
SH. Pl. w/Bar P.I.D.	Drilled Plate	1.2-13-WAM-016		1.60	
Impinging Platelet	Diffuser Cone	1.2-16-WAM-016	1.3	1.9	5.2
	WARP III Plate	1.2-16-WAM-017	3.0		5.0
		1.2-16-WAM-018B	1.1		
	WARP III Plate, Mod.	1.2-16-WAM-019 thru -023	1.1		0-7.5
	Drilled Plate	1.2-16-WAM-024 & 025	0.6		7.9

CONFIDENTIAL

Secondary Injector Program, Performance Loss Summary

Figure VI-37

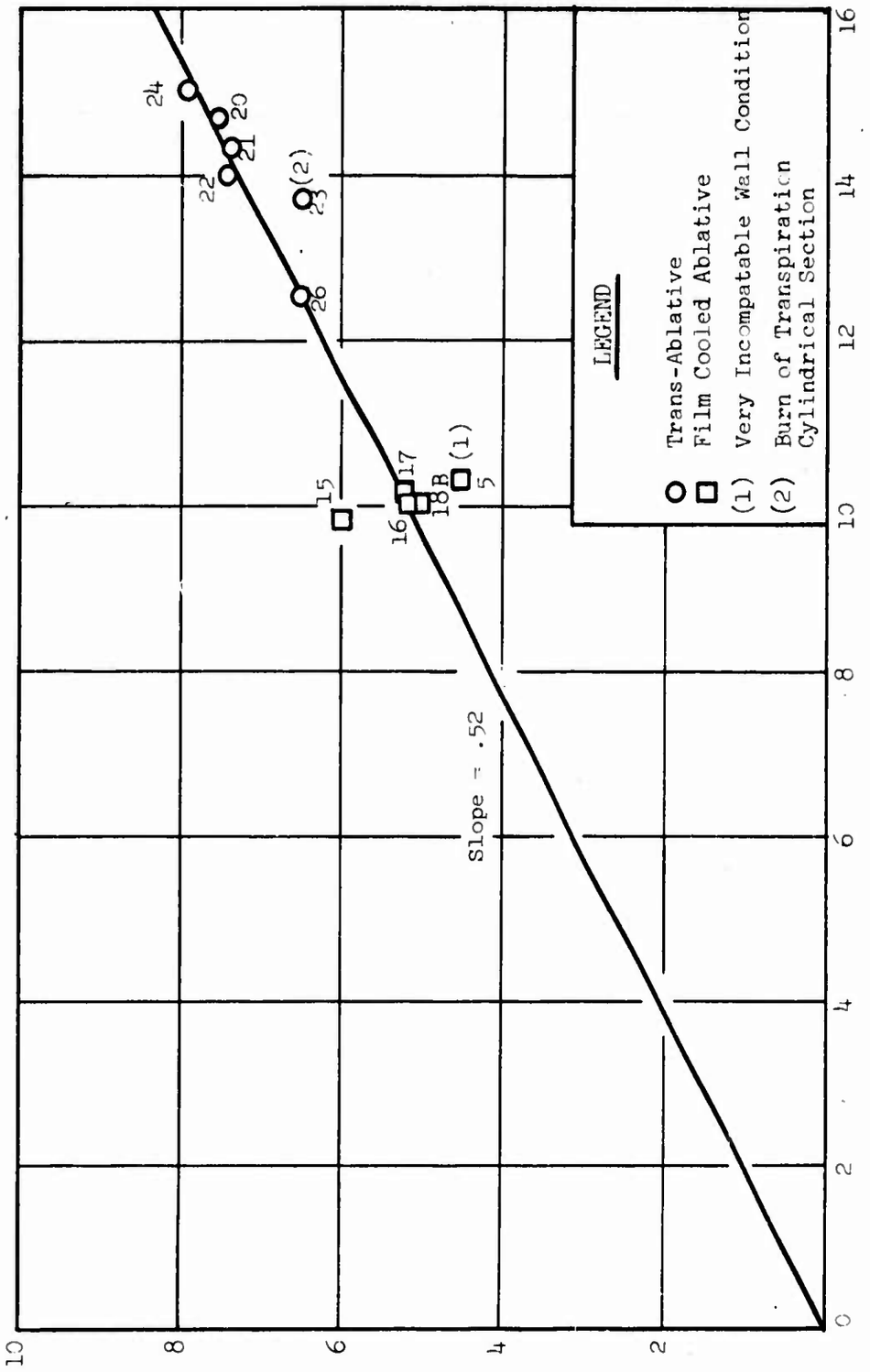

CONFIDENTIAL

ARES Film Coolant Performance Loss

Figure VI-33

1.2-16-WAM

Test No.		-005	-010	-015	-016	-017	Theo. Temp.	
$\dot{W}_{FC}$, lb/sec		41.8	36.0	36.1	34.8	36.6	35	40
Duration sec		3.49	1.76	3.51	3.52	3.52		
Injector Type		Mk 125 3 ORST	Sh Pl	Sh Pl w/screen	Im Pl w/cone	Im Pl w/plate		
Thermocouple Numbers	Distance from Injector Face, in.	RECORDED TEMPERATURE, °F						
A1	0.50	420	350	340	400	350	230	200
A2		395	BO	INV.	520	INV.		
A3		INV.	350	380	400	400		
A4		420	670	400	740	500		
A5		390	BO	2300	BO	-		
B1	2.16	480	1120	1600	BO	440	440	360
B2		700	600	600	600	BO		
B3		720	700	960	BO	850		
B4		550	Ques.	650	450	BO		
B5		700	500	INV.	720	-		
C1	2.93	870	480	500	1400	BO	590	480
C2		700	1330	1300	BO	BO		
C3		790	970	1800	BO	750		
C4		1180	580	900	BO	880		
C5		970	800	500	730	-		
D1	3.73	1020	1180	1360	BO	920	790	660
D2		1050	580	1700	BO	600		
D3		560	700	1010	BO	1020		
D4		1280	950	1800	BO	740		
D5		980	700	980	1600	-		
E1	4.62	1000	BO	BO	130	1450	970	800
E2		1100	BO	770	1010	BO		
E3		1500	BO	550	930	1280		
E4		830	BO	520	BO	900		
E5		Ques.	BO	1180	800	-		
F1	5.66	2100	1350	1400	900	BO	1150	950
F2		1810	1170	1500	BO	1100		
F3		BO	860	1320	OS	1150		
F4		BO	BO	1700	BO	-		
F5		1070	1180	1230	BO	-		
G1	8.06		BO	INV.		1600	1510	
G2						580		
G3						1300		
G4						BO		
G5						1680		

NOTES: INV. - Invalid
BO - Burnout
OS - Overscale
Ques. - Questionable Data

Thermal Data Summary - Instrumented Ablative Test Series

Figure VI-39

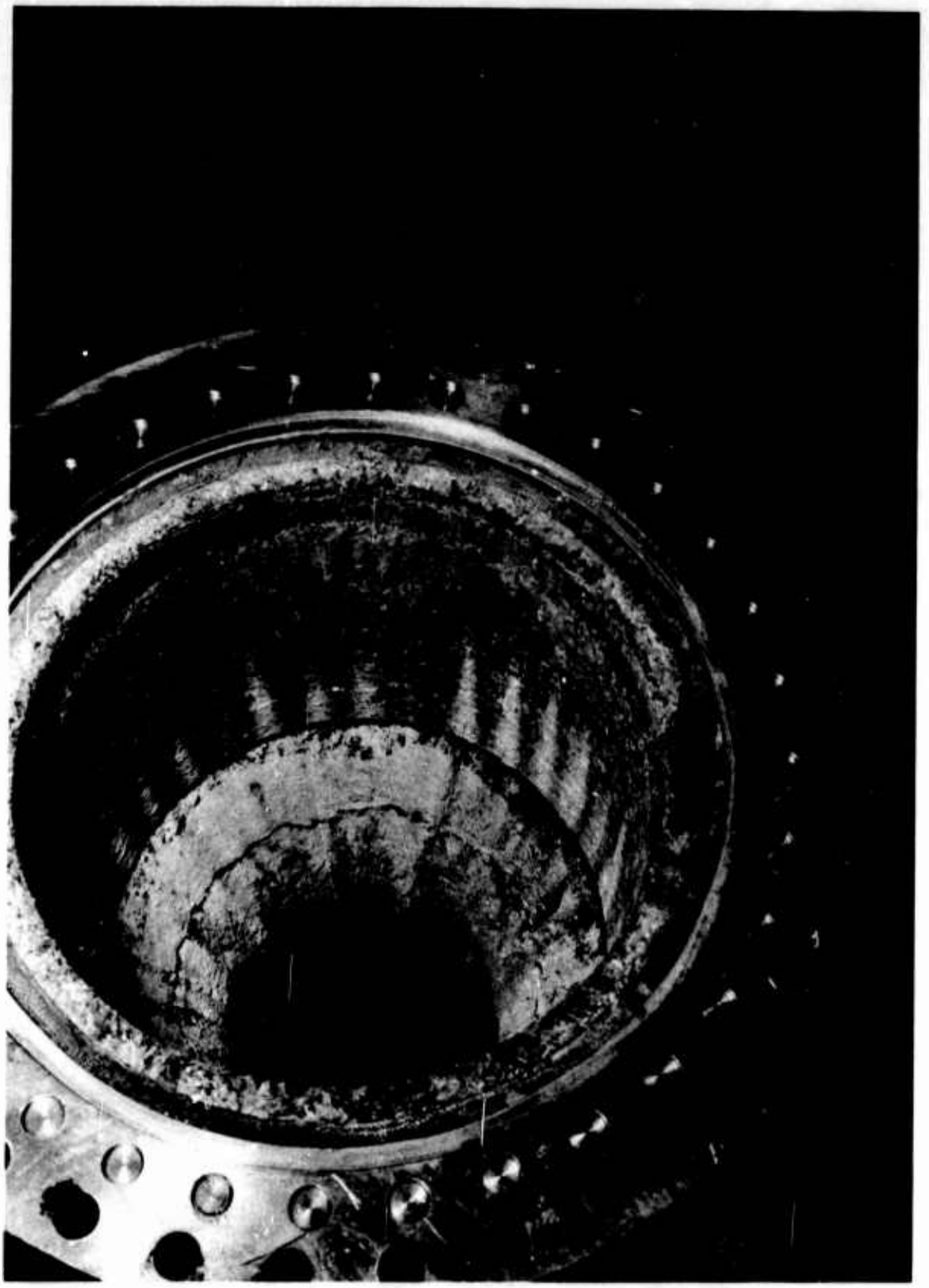

Ablative Chamber, Post Test Showing Streaks

Figure VI-40

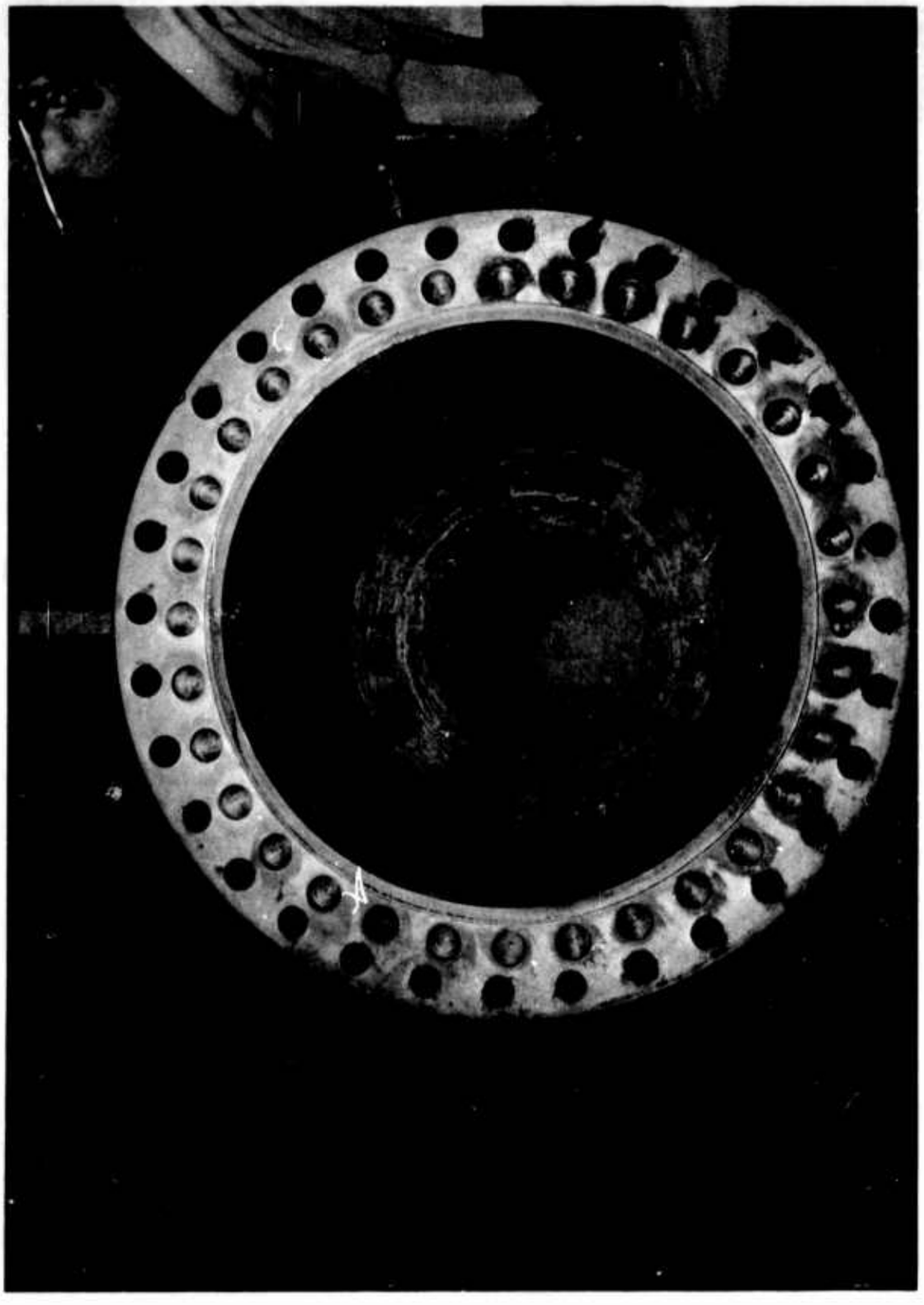

Ablative Chamber Post Test Showing Erosion Pattern

Figure VI-41

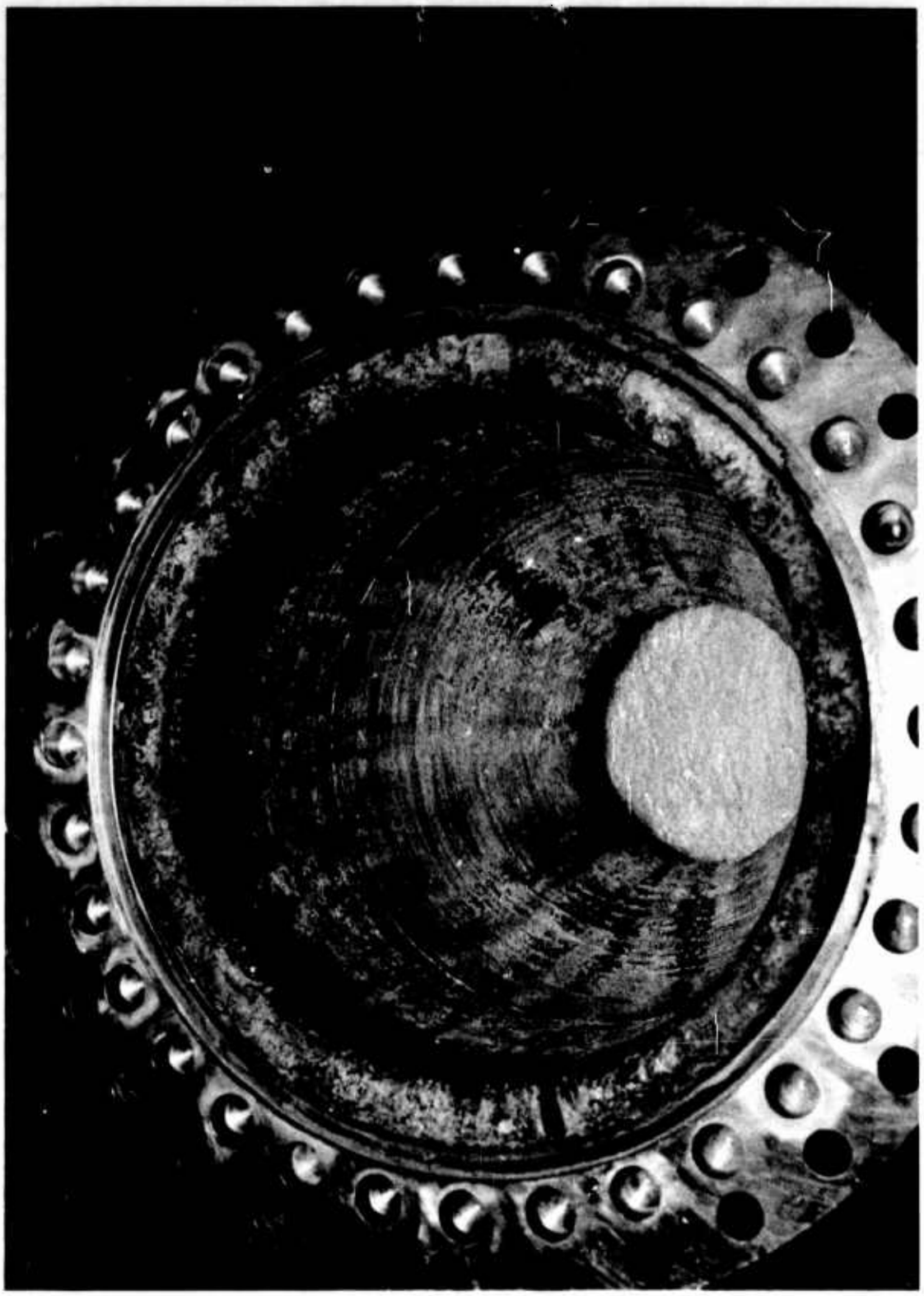

Ablative Chamber Post Test Showing Minimum of Streaking

Figure VI-42

Compartment Number	Thermocouple Number	Depth, in.	Test No. 1.2-16-WAM-			
			-020 °F	-021 °F	-022 °F	-023 °F
1	15	.005	500	230	231	219
	18	.004	430	238	277	243
2	9	.002	720	815	923	1352
	10	.005	565	675	726	822
	11	.0035	500	500	617	875
	12	.006	840	745	1021	1283
3	1	.002	485	510	551	652
	2	.0035	460	470	445	528
	3	.003	395	450	464	494
	4	.004	315	-	-	363
	5	.003	520	550	549	605
	6	.006	570	545	599	674

Measured Temperature Data, Trans-Ablative Chamber, Test Series 12.-16-WAM

Figure VI-43

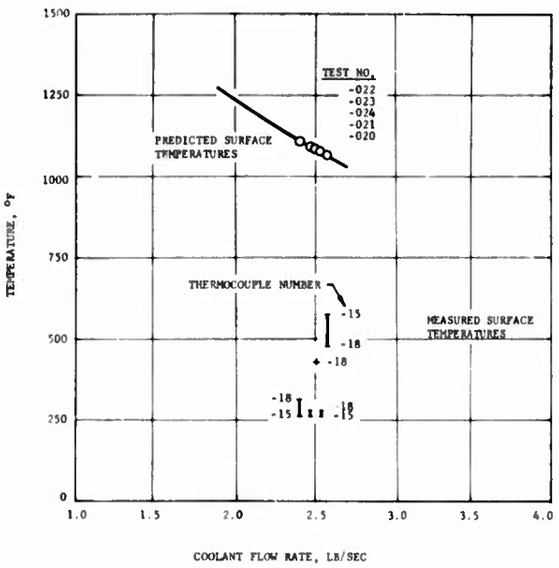

Figure VI-44. Compartment No. 1 Temperature Summary, Trans-Ablative Chamber

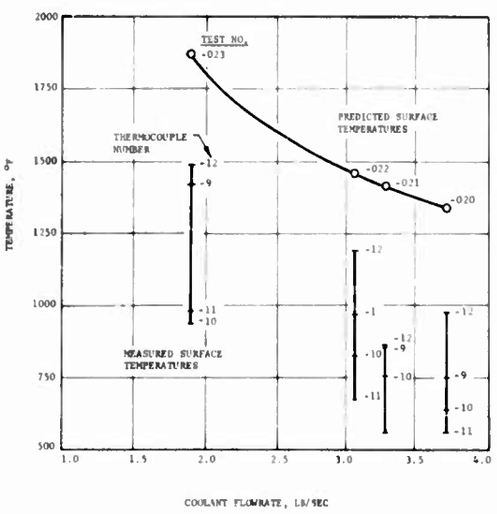

Figure VI-45. Compartment No. 2 Temperature Summary, Trans-Ablative Chamber

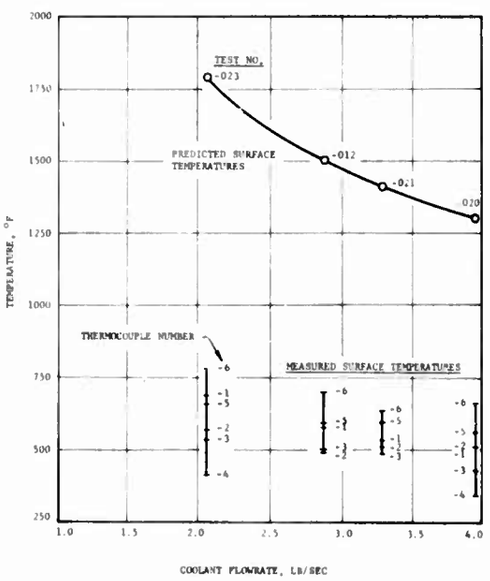

Figure VI-46. Compartment No. 3 Temperature Summary, Trans-Ablative Chamber

Figure VI-44
Figure VI-45, Figure VI-46

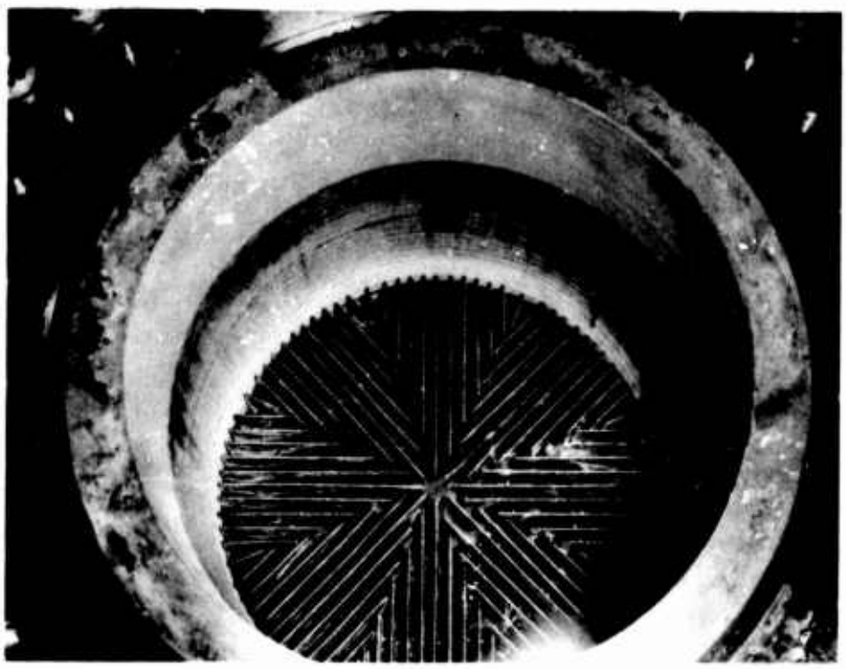

Figure VI-47. Transpiration-Ablative L* Section (u)

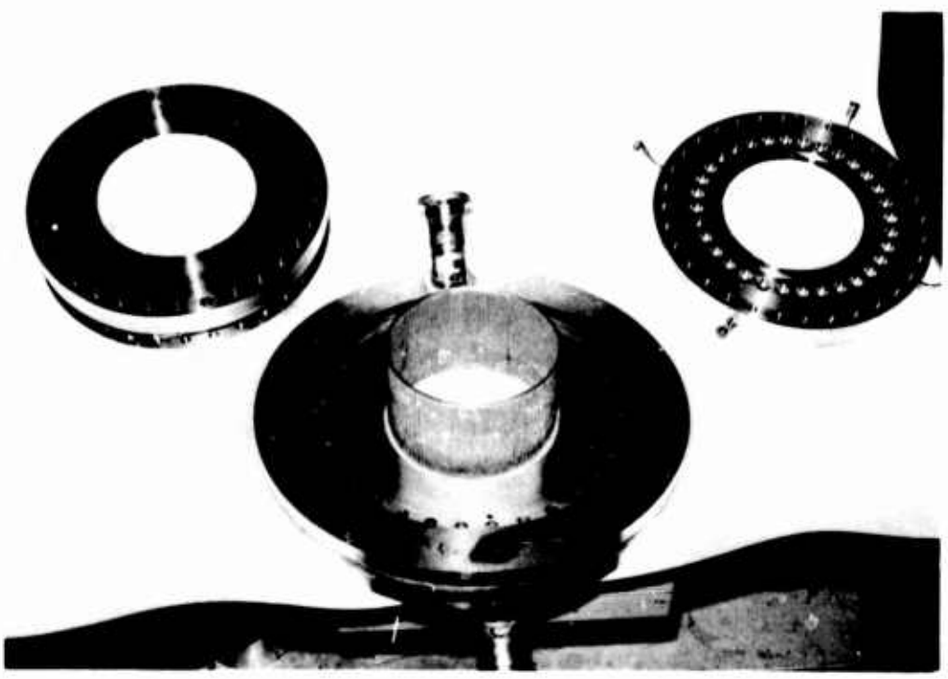

Figure VI-48. Composite Combustion Chamber (u)

Figure VI-47, Figure VI-48

SERIES	TEST	CHAMBER SERIAL NO.	INJECTOR SERIAL NO.	DUR. SEC.	WOFC LBS/SEC N_2O_4	NOZZLE INSTALLED	OBJECTIVE
I	025	3	3	1.157	40 B (2)	No	Compatability Check-out
	005	3	3	1.108	50 B (2)	No	Compatability Check-out
	006	3	3	3.990	48.5	Yes	Performance Evaluation
	007	3	3	17.251	52.0	No	Duration Evaluation
	008	3	3	1.483	43.4	No	1st Cutback Evaluation
	009	3	3	3.028	41.2	Yes	1st Cutback Performance Evalu
	010	3	3	20.057	40.9	No	1st Cutback Duration Evaluati
	011	3	3	1.521	36.2	Yes	2nd Cutback Evaluation
	012	3	3	3.084	35.9	Yes	2nd Cutback Performance Evalu
	013	3	3	3.674	36.7	No	2nd Cutback Duration Evaluati
	014	3	3	1.542	31.3	Yes	3rd Cutback Evaluation
II	017	4	4	1.524	51.1	Yes	Chamber Hydraulic Balance Eva
	018	4	4	1.524	38.8	Yes	1st Cutback Eval. to Prev. Ex
	019	4	4	3.023	36.3	Yes	1st Cutback Performance Evalu
	020	4	4	1.523	31.4	No	2nd Cutback Eval. to SN-3 Fai
	021	4	4	3.019	30.9	Yes	2nd Cutback Performance Evalu
	022	4	4	1.515	32.9	Yes	3rd Cutback Evaluation
	023	4	4	3.009	30.8	Yes	3rd Cutback Performance Evalu
	024	4	4	20.486	28.1	No	Duration Demo. @ 89.5% Perform
	025	4	4	1.464	30.5	Yes	4th Cutback Evaluation
	026	4	4	1.504	31.5	Yes	4th Cutback Repeat Evaluation
	027	4	4	5.021	30.3	Yes	5th Cutback Evaluation (Durin
III	028	5	5	1.513	49.4	No	Hydraulic Balance Evaluation
	029	5	5	.934	35 B (2)	Yes	1st Cutback Evaluation to 35
	030	5	3	1.521	34.9	Yes	1st Cutback Repeal Evaluation
	031	5	3	3.049	34.1	Yes	1st Cutback Performance Demo.
	032	5	3	1.505	31.5	Yes	2nd Cutback Evaluation
	033	5	3	3.021	30.9	Yes	2nd Cutback Performance Demo.
	034	5	3	2.003	30.4	Yes	3rd Cutback Performance Demo.
	035	5	3	2.002	29.7	Yes	4th Cutback Performance Demo.
	036	5	3	3.027	29.5	Yes	Repeat Performance Demo. @ 89
	037	5	3	3.019	29.8	Yes	Repeat Performance Demo. @ 89
	038	5	3	20.922	28.4	Nc	Duration Demo. @ 89%
	039	5	3	20.708	28.5	No	Duration Demo. @ 89%
	040	5	3	20.791	29.0	No	Duration Demo. @ 89%
	041	5	3	2.268	27.8	Yes	5th Cutback Performance Demo.
	042	5	3	2.261	26.4	Yes	6th Cutback Performance Demo.
	043	5	3	2.264	25.3	Yes	7th Cutback Performance Demo
	044	5	3	2.261	25.3	Yes	Repeat Performance Demo @ 90%
	045	5	3	2.261	25.2	Yes	Repeat Performance Demo @ 90%
	046	5	3	11.380	25.3	No	Duration Demonstration @ 90%
IV	047	4R	3	2.257	33.5	Yes	Performance Checkout @ 35 lbs
	048	4R	3	2.259	31.6	Yes	1st Cutback Evaluation
	049	4R	3	2.256	29.3	Yes	2nd Cutback Evaluation
	050	3R	4R	2.258	33.5	Yes	Performance Checkout @ 35 lbs
	051	3R	4R	2.253	31.5	No	1st Cutback Evaluation

(1) Specific Impulse Determined From IS_{SL} Versus Coolant Flow Relationship Developed From Te

(2) Balance Value

OBJECTIVE	RESULTS	PERF. $\%I_{SSL}$
ility Check-out	Excessive Discoloration Between Compartments 5 & 6	-
ility Check-out	Eliminated Discoloration Between Compartments 5 & 6	-
nce Evaluation	No Abnormalaties, Minor Streaks	86.1
Evaluation	No Abnormalaties, Minor Streaks	86.0(1)
ack Evaluation	Brown to Bluish in Throat Section	87.1(1)
ack Performance Evaluation	Compartments 2 & 3, Dark Brown. Spots in Compts 5 & 6	87.4
ack Duration Evaluation	No Abnormalaties, Nozzle Evidenced Blue Streaks	87.5(1)
ack Evaluation	No Additional Discoloration	88.2
ack Performance Evaluation	No Change	87.8
ack Duration Evaluation	Premature Shutdown by Malfunction Sensing Device	88.0(1)
ack Evaluation	Chamber Erosion Initiated in Compartment #6	88.6
Hydraulic Balance Eval.	No Discoloration, Minor Streaks	86.2
ack Eval. to Prev. Exper.	No Discoloration, Minor Streaks	87.7
ack Performance Evaluation	Slight Discoloration, Minor Streaks	88.3
ack Eval. to SN-3 Fail Flow	Slight Discoloration, More Noticeable Streaking	89.2
ack Performance Evaluation	Slight Discoloration, Nozzle Exhibits Blue Streaks	89.5
ack Evaluation	Slight Discoloration, Nozzle Exhibits Blue Streaks	88.3
ack Performance Evaluation	Slight Discoloration, Black Nozzle Streaks	89.5
Demo. @ 89.5% Performance	Satisfactory Duration Demonstration	90.5(1)
ack Evaluation	Minor Erosion During Start Between Compts 5 & 6	89.7
ack Repeat Evaluation	Satisfactory Wall Condition	88.9
ack Evaluation (During S.S.)	Nozzle Burnout in Compartments 9, 10, 11 and 12	89.6
: Balance Evaluation	No Discolorations	86.5(1)
ack Evaluation to 35 #/Sec	Malfunction, Injector Seal Failure Initiated Inj. Damage	86.9
ack Repeal Evaluation	Slight Discoloration, Noticeable Streaks	88.1
ack Performance Demo.	Slight Discoloration, Noticeable Streaks	87.5
ack Evaluation	Slight Discoloration, Noticeable Streaks	88.5
ack Performance Demo.	Slight Discoloration, Noticeable Streaks	88.6
ack Performance Demo.	Slight Discoloration, Noticeable Nozzle Streaks	89.0
ack Performance Demo.	Slight Discoloration, Noticeable Nozzle Streaks	89.1
rformance Demo. @ 89%	No Adverse Wall Conditions	88.4
rformance Demo. @ 89%	No Adverse Wall Conditions	89.4
Demo. @ 89%	No Increase in Wall Discoloration With Dur.	89.3(1)
Demo. @ 89%	No Change	89.1(1)
Demo. @ 89%	No Change	89.1(1)
ck Performance Demo.	Dark Chamber, Heavy Nozzle Streaks	88.8
ck Performance Demo.	No Change	89.5
ck Performance Demo.	Demonstrated Contractually Required Performance	90.3
rformance Demo @ 90%	Demonstrated Contractually Required Performance	90.3
rformance Demo @ 90%	Demonstrated Contractually Required Performance	90.2
Demonstration @ 90%	Nozzle Burnout in Compartments 8, 9, 10, 11 and 12	90.3
ce Checkout @ 35 lbs/sec	No Adverse Wall Conditions	88.1
ck Evaluation	No Adverse Wall Conditions	88.7
ck Evaluation	Burn-out in Compartment #6 Adjacent to Repaired Area	88.7
ce Checkout @ 35 lbs/sec	No Adverse Wall Conditions	89.2
ck Evaluation	Vane Leak Initiated Chamber Deterioration	89.4(1)

ip Developed From Tests Where Nozzle Extension Was Used.

Summary, Transpiration Cooled Chamber Test Program (U)

Figure VI-49

ARES COOLED CHAM

TEST DATA AND PERFORMANCE

	GENERAL DATA										ME	
	DATE	DUR.	DATA PERIOD	INJ.	S/N	CHAM.	S/N	A_t	ϵ	L*	PCSC	MR_{inj}
TEST NUMBER		sec	sec					$in.^2$		in.	psia	
1.2-16-WAM-025	10/05/67	1.157	None	IM-PL	3	TRANS	3	21.3	5.6	34.8	SHORT DURATION	
1.2-13-WAM-005	10/31/67	1.018	None	IM-PL	3	TRANS	3A	21.5	5.7	34.5	SHORT DURATION	
1.2-13-WAM-006	11/1/67	3.990	2.94-3.94	IM-PL	3	TRANS	3A	21.4	19.9	34.6	2860	2.18
1.2-13-WAM-007	11/3/67	17.251	16.20-17.20	IM-PL	3	TRANS	3A	21.4	5.6	34.6	2939	2.216
1.2-13-WAM-008	11/7/67	1.488	1.39-1.49	IM-PL	3	TRANS	3A	21.4	5.6	34.6	2863	2.235
1.2-13-WAM-009	11/7/67	3.028	2.0-3.0	IM-PL	3	TRANS	3A	21.4	19.9	34.6	2855	2.202
1.2-13-WAM-010	11/8/67	20.057	2.0-20.01	IM-PL	3	TRANS	3A	21.4	5.6	34.6	2744	2.200
1.2-13-WAM-011	11/9/67	1.521	1.42-1.52	IM-PL	3	TRANS	3A	21.5	19.8	34.6	2810	2.230
1.2-13-WAM-012	11/9/67	3.084	2.0-3.0	IM-PL	3	TRANS	3A	21.5	19.9	34.6	2777	2.160
1.2-13-WAM-013	11/9/67	3.674	2.62-3.62	IM-PL	3	TRANS	3A	21.5	5.6	34.6	2748	2.175
1.2-13-WAM-014	11/14/67	1.542	1.39-1.51	IM-PL	3	TRANS	3A	21.9	19.6	34.1	2747	2.178
1.2-13-WAM-017	11/27/67	1.524	1.32-1.52	IM-PL	4	TRANS	4	21.3	20.0	34.7	2867	2.236
1.2-13-WAM-018	11/28/67	1.524	1.38-1.49	IM-PL	4	TRANS	4	21.3	20.0	34.7	2753	2.241
1.2-13-WAM-019	11/28/67	3.023	2.0-3.0	IM-PL	4	TRANS	4	21.3	19.9	34.7	2768	2.230
1.2-13-WAM-020	12/01/67	1.523	1.36-1.52	IM-PL	4	TRANS	4	21.3	19.9	34.7	2788	2.198
1.2-13-WAM-021	12/4/67	3.019	2.0-3.0	IM-PL	4	TRANS	4	21.3	19.9	34.7	2806	2.22
1.2-13-WAM-022	12/5/67	1.515	1.37-1.48	IM-PL	4	TRANS	4	21.3	19.9	34.7	2797	2.25
1.2-13-WAM-023	12/5/67	3.009	2.46-2.96	IM-PL	4	TRANS	4	21.3	19.9	34.7	2823	2.20
1.2-13-WAM-024	12/6/67	20.486	19.99-20.49	IM-PL	4	TRANS	4	21.4	5.7	34.7	2866	2.25
1.2-13-WAM-025	12/8/67	1.464	1.36-1.46	IM-PL	4	TRANS	4	21.4	19.9	34.6	2817	2.26
1.2-13-WAM-026	12/12/67	1.504	1.36-1.46	IM-PL	4	TRANS	4	21.4	19.9	34.6	2860	2.25
1.2-13-WAM-027	12/13/67	5.021	4.00-4.50	IM-PL	4	TRANS	4	21.4	19.9	34.6	2852	2.20
1.2-13-WAM-028	12/15/67	1.513	1.36-1.46	IM-PL	5	TRANS	5	21.2	5.4	34.8	2803	2.22

(1) Specific Impulse determined from $I_{S_{SL}}$ versus coolant flow relationship developed from tests where extension nozzle was

ES COOLED CHAMBER

AND PERFORMANCE SUMMARY

MEASURED DATA					PERFORMANCE DATA			PERFORMANCES LOSSES					% PERFORMANCE			
PCSC	MR_{inj}	$\dot{W}_{OFC}$	F_{SL}	$\dot{W}_{eng}$	$I_{S_{SL}}$	$I_{S_{VAC}}$	THEO. $I_{S_{VAC}}$	MRDL	NGL	NFL	FCL	ERL	$\dot{W}_{OFC}$	FCL	$I_{S_{VAC}}$	$I_{S_{SL}}$
psia		#/sec	lbs	#/sec	sec	sec	sec	sec	sec	sec	sec	sec	%	%	%	%
SHORT DURATION TEST - NO PERFORMANCE DATA																
SHORT DURATION TEST - NO PERFORMANCE DATA																
2860	2.18	48.5	99071	369.8	267.9	284.8	329.5	5.6	2.7	3.1	27.3	6.3	13.11	8.20	86.4	86.1
2939	2.216	52.0	91677	381.2	240.5	245.1	296.8	NO PERFORMANCE ANALYSIS-EXTENSION NOZZLE REMOVED								86.0(1)
2863	2.235	43.4	88819	366.3	242.5	247.3	296.4	NO PERFORMANCE ANALYSIS-EXTENSION NOZZLE REMOVED								87.1(1)
2855	2.202	41.2	98607	362.6	271.9	289.1	329.3	5.6	2.8	3.1	22.4	6.3	11.36	6.80	87.8	87.4
2744	2.200	40.9	85231	350.2	243.4	248.4	297.3						11.67		83.6	87.5(1)
2810	2.230	36.2	97447	355.1	274.4	292.0	328.5	5.6	2.8	3.1	18.7	6.3	10.18	5.68	88.9	88.2
2777	2.160	35.9	95665	350.2	273.2	291.0	329.5	5.6	2.8	3.1	21.7	6.3	10.26	6.28	88.3	87.8
2748	2.175	36.7	85494	347.9	245.7	250.8	297.6	NO PERFORMANCE ANALYSIS-EXTENSION NOZZLE REMOVED								88.0(1)
2747	2.178	31.3	95482	346.3	275.7	293.7	329.1	5.6	2.8	3.1	17.6	6.3	9.03	5.34	89.3	88.6
2867	2.236	51.1	98200	366.3	268.1	285.0	328.4	2.3	2.7	3.1	29.0	6.3	13.94	8.80	86.8	86.2
2753	2.241	38.8	95245	349.3	272.7	290.5	328.3	2.3	2.8	3.1	23.3	6.3	11.10	7.07	88.5	87.7
2768	2.230	36.3	97225	354.0	274.6	292.2	328.6	2.3	2.8	3.1	21.9	6.3	10.25	6.65	88.9	88.3
2788	2.198	31.4	96511	347.7	277.6	295.5	329.4	2.3	2.8	3.1	19.4	6.3	9.04	5.89	89.7	89.2
2806	2.22	30.9	96933	348.1	278.4	296.2	328.9	2.3	2.8	3.1	18.2	6.3	8.88	5.52	90.1	89.5
2797	2.25	32.9	96073	349.8	274.7	292.5	327.9	2.3	2.8	3.1	20.9	6.3	9.41	6.34	89.2	88.3
2823	2.20	30.8	97514	350.2	278.5	296.3	329.4	2.3	2.8	3.1	18.6	6.3	8.79	5.64	89.9	89.5
2866	2.25	28.1	89356	354.2	252.3	257.3	296.1	NO PERFORMANCE ANALYSIS-EXTENSION NOZZLE REMOVED								90.5(1)
2817	2.26	30.5	97331	348.8	279.0	296.9	327.6	2.3	2.8	3.1	16.2	6.3	8.74	4.92	90.6	89.7
2860	2.25	31.5	97776	353.5	276.6	294.1	327.9	2.3	2.8	3.1	19.3	6.3	8.91	5.86	89.7	88.9
2852	2.20	30.3	98586	353.9	278.6	296.2	329.3	2.3	2.8	3.1	18.6	6.3	8.55	5.64	89.9	89.6
2803	2.22	49.4	86014	362.0	237.6	242.2	295.9	NO PERFORMANCE ANALYSIS-EXTENSION NOZZLE REMOVED								86.5(1)

CONFIDENTIAL

n nozzle wasused.

ARES Cooled Chamber Test Data and Performance Summary (U)

Figure VI-50
Sheet 1 of 2

ARES COOLED CHAMBER

TEST DATA AND PERFORMANCE SUMMARY

	GENERAL DATA										MEASURE		
	DATE	DUR.	DATA PERIOD	INJ.	S/N	CHAM.	S/N	A_t	ϵ	L*	PCSC	MR_{inj}	$\dot{W}_{OF}$
TEST NUMBER		sec	sec					$in.^2$		in.	psia		#/s
1.2-13-WAM-029	12/18/67	.934	None	IM-PL	5	TRANS	5	21.2	19.9	34.8	MALFUNCTION -		
1.2-13-WAM-030	12/20/67	1.521	1.42-1.52	IM-PL	3	TRANS	5	21.3	19.9	34.7	2722	2.19	34.9
1.2-13-WAM-031	12/20/67	3.049	2.55-3.05	IM-PL	3	TRANS	5	21.3	19.9	34.7	2884	2.19	34.1
1.2-13-WAM-032	12/21/67	1.505	1.41-1.51	IM-PL	3	TRANS	5	21.3	20.1	34.7	2807	2.22	31.5
1.2-13-WAM-033	12/21/67	3.021	2.52-3.02	IM-PL	3	TRANS	5	21.2	20.2	34.7	2857	2.21	30.9
1.2-13-WAM-034	12/26/67	2.003	1.50-2.00	IM-PL	3	TRANS	5	21.2	20.2	34.7	2841	2.19	30.4
1.2-13-WAM-035	12/27/67	2.002	1.45-1.95	IM-PL	3	TRANS	5	21.3	20.0	34.7	2806	2.22	29.7
1.2-13-WAM-036	12/27/67	3.027	2.40-2.90	IM-PL	3	TRANS	5	21.3	20.0	34.7	2856	2.19	29.5
1.2-13-WAM-037	12/27/67	3.019	2.39-2.89	IM-PL	3	TRANS	5	21.4	19.9	34.7	2756	2.20	29.8
1.2-13-WAM-038	12/28/67	20.922	20.37-20.87	IM-PL	3	TRANS	5	21.3	5.5	34.7	2858	2.20	28.4
1.2-13-WAM-039	12/29/67	20.708	20.16-20.66	IM-PL	3	TRANS	5	21.3	5.5	34.7	2854	2.20	28.5
1.2-13-WAM-040	12/29/67	20.791	20.24-20.74	IM-PL	3	TRANS	5	21.3	5.5	34.7	2798	2.23	29.0
1.2-13-WAM-041	1/2/68	2.268	1.77-2.27	IM-PL	3	TRANS	5	21.4	21.4	34.6	2576	2.20	27.8
1.2-13-WAM-042	1/2/68	2.261	1.76-2.26	IM-PL	3	TRANS	5	21.4	20.0	34.6	2786	2.20	26.4
1.2-13-WAM-043	1/3/68	2.264	1.76-2.26	IM-PL	3	TRANS	5	21.3	20.1	34.7	2815	2.20	25.3
1.2-13-WAM-044	1/3/68	2.261	1.76-2.26	IM-PL	3	TRANS	5	21.4	20.7	34.6	2820	2.18	25.3
1.2-13-WAM-045	1/3/68	2.261	1.76-2.26	IM-PL	3	TRANS	5	21.4	20.0	34.6	2830	2.19	25.2
1.2-13-WAM-046	1/4/68	11.380	2.0-3.0	IM-PL	3	TRANS	5	21.4	5.5	34.6	2871	2.19	25.3
1.2-13-WAM-047	1/16/68	2.257	1.76-2.26	IM-PL	3	TRANS	4.6	21.4	19.8	34.6	2823	2.19	33.5
1.2-13-WAM-048	1/17/68	2.259	1.76-2.26	IM-PL	3	TRANS	4.6	21.4	20.9	34.6	2834	2.21	31.6
1.2-13-WAM-049	1/17/68	2.256	1.76-2.26	IM-PL	3	TRANS	4.6	21.4	20.1	34.6	2755	2.20	29.3
1.2-13-WAM-050	1/22/68	2.258	1.76-2.26	IM-PL	4.5	TRANS	3B	22.5	18.9	32.8	2700	2.20	33.5
1.2-13-WAM-051	1/22/68	2.253	1.75-2.25	IM-PL	4.5	TRANS	3B	22.6	5.4	32.8	2775	2.17	31.5

(1) Specific Impulse determined from I_{SSL} versus coolant flow relationship developed from tests where extension nozzle was used

LED CHAMBER

ERFORMANCE SUMMARY

MEASURED DATA					PERFORMANCE DATA			PERFORMANCES LOSSES					% PERFORMANCE			
PCSC	MR_{inj}	$\dot{W}_{OFC}$	F_{SL}	$\dot{W}_{eng}$	$I_{S_{SL}}$	$I_{S_{VAC}}$	THEO. $I_{S_{VAC}}$	MRDL	NGL	NFL	FCL	ERL	$\dot{W}_{OFC}$	FCL	$I_{S_{VAC}}$	$I_{S_{SL}}$
psia		#/sec	lbs	#/sec	sec	sec	sec	sec	sec	sec	sec	sec	%	%	%	%
MALFUNCTION - OXIDIZER VALVE FAILED TO OPEN															CONFIDENTIAL	
2722	2.19	34.9	93491	345.8	270.3	288.3	329.5	5.6	2.8	3.1	23.4	6.3	10.08	7.1	87.5	86.9
2884	2.19	34.1	98958	361.1	274.1	291.3	329.5	5.6	2.8	3.1	20.4	6.3	9.45	6.19	88.4	88.1
2807	2.22	31.5	95877	351.7	272.3	290.3	329.0	5.6	2.8	3.1	20.9	6.3	8.96	6.34	88.3	87.5
2857	2.21	30.9	98140	356.6	275.2	293.0	329.3	5.6	2.8	3.1	[illegible]	6.3	8.68	5.62	89.0	88.5
2841	2.19	30.4	97270	353.1	275.5	293.2	329.7	5.6	2.8	3.1	18.7	6.3	8.62	5.68	88.9	88.6
2806	2.22	29.7	96824	349.6	277.0	294.8	328.9	5.6	2.8	3.1	16.3	6.3	8.51	4.95	89.7	89.0
2856	2.19	29.5	98394	354.9	277.3	294.9	329.5	5.6	2.8	3.1	16.8	6.3	8.31	5.10	89.5	89.1
2756	2.20	29.8	94751	344.5	275.1	293.2	329.3	5.6	2.8	3.1	18.3	6.3	8.66	5.56	89.0	88.4
2858	2.20	28.4	88632	354.3	250.2	255.1	296.9	NO PERFORMANCE ANALYSIS-EXTENSION NOZZLE REMOVED								89.4(1)
2854	2.20	28.5	88572	354.5	249.8	254.7	296.9	NO PERFORMANCE ANALYSIS-EXTENSION NOZZLE REMOVED								89.3(1)
2798	2.23	29.0	86760	349.1	248.5	253.4	296.1	NO PERFORMANCE ANALYSIS-EXTENSION NOZZLE REMOVED								89.1(1)
2676	2.20	27.8	92069	333.4	276.1	294.8	329.4	5.6	2.8	3.1	16.8	6.3	8.34	5.10	89.5	88.8
2786	2.20	26.4	96146	345.4	278.4	296.5	329.5	5.6	2.8	3.1	16.6	6.3	7.64	5.05	90.0	89.5
2815	2.20	25.3	97195	345.9	281.0	299.3	329.6	5.6	2.9	3.1	13.7	6.3	7.28	4.16	90.4	90.3
2820	2.18	25.3	97471	347.1	280.8	299.0	329.6	5.6	2.9	3.1	14.0	6.3	7.26	4.25	90.4	90.3
2830	2.19	25.2	97636	347.9	280.6	298.8	329.6	5.6	2.8	3.1	14.2	6.3	7.21	4.26	90.3	90.2
2871	2.19	25.3	89219	354.1	252.0	256.9	296.9	NO PERFORMANCE ANALYSIS-EXTENSION NOZZLE REMOVED								90.3
2823	2.19	33.5	97292	355.0	274.0	291.5	329.4	5.6	2.8	3.1	20.3	6.3	9.43	6.07	88.5	88.1
2834	2.21	31.6	97906	354.6	276.1	293.9	329.3	5.6	2.8	3.1	17.6	6.3	8.90	5.34	89.2	88.7
2755	2.20	29.3	96581	348.0	277.5	295.7	329.5	5.6	2.8	3.1	17.0	6.3	8.43	4.86	89.7	88.7
2700	2.20	33.5	97247	351.8	276.4	294.2	328.1	2.3	2.8	3.1	19.4	6.3	9.52	4.92	89.7	89.2
2775	2.17	31.5	90311	359.3	251.4	256.4	296.9	NO PERFORMANCE ANALYSIS-EXTENSION NOZZLE REMOVED								89.4(1)

ısion nozzle was used.

ARES Cooled Chamber Test Data and Performance Summary (U)

Figure VI-50
Sheet 2 of 2

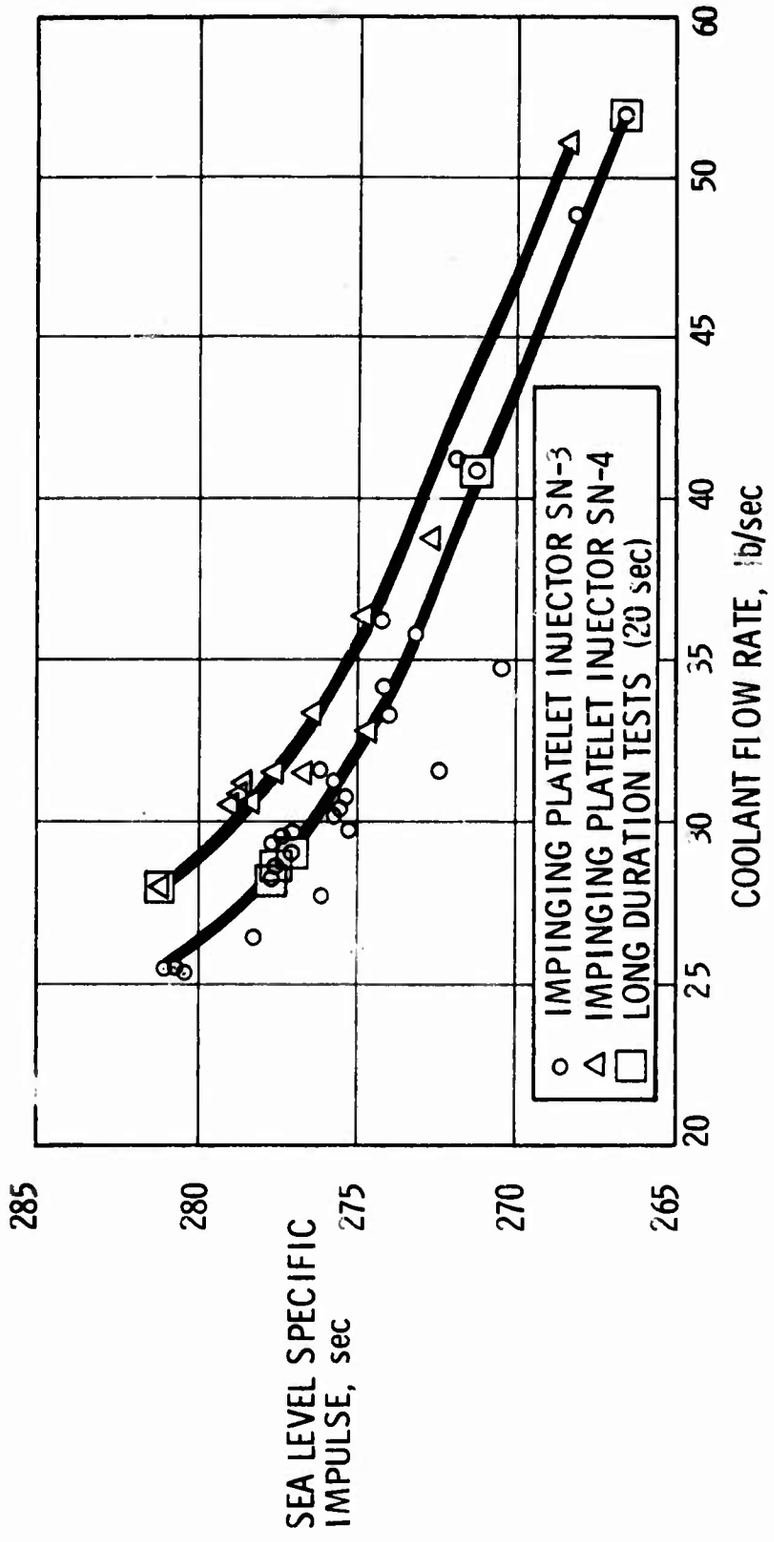

Transpiration-Cooled Chamber Performance Summary (U)

Figure VI-51

PARAMETER	UNITS	REQUIREMENT	TEST DATA		
			1.2-13-WAM-043	1.2-13-WAM-044	1.2-13-WAM-045
THRUST	LBS_f	100,000 ± 5000	97195	97471	97636
CHAMBER PRESSURE	PSIA	2,800 ± 140	2815	2820	2830
OSCILLATIONS	PERCENT	± 5% Pc	± 1.25	± 1.13	± 1.22
DURATION, STEADY STATE	SEC.	1.0	1.12	1.12	1.17

CONFIDENTIAL

Figure VI-52

Cooled Chamber Program Performance Demonstration Conditions (U)

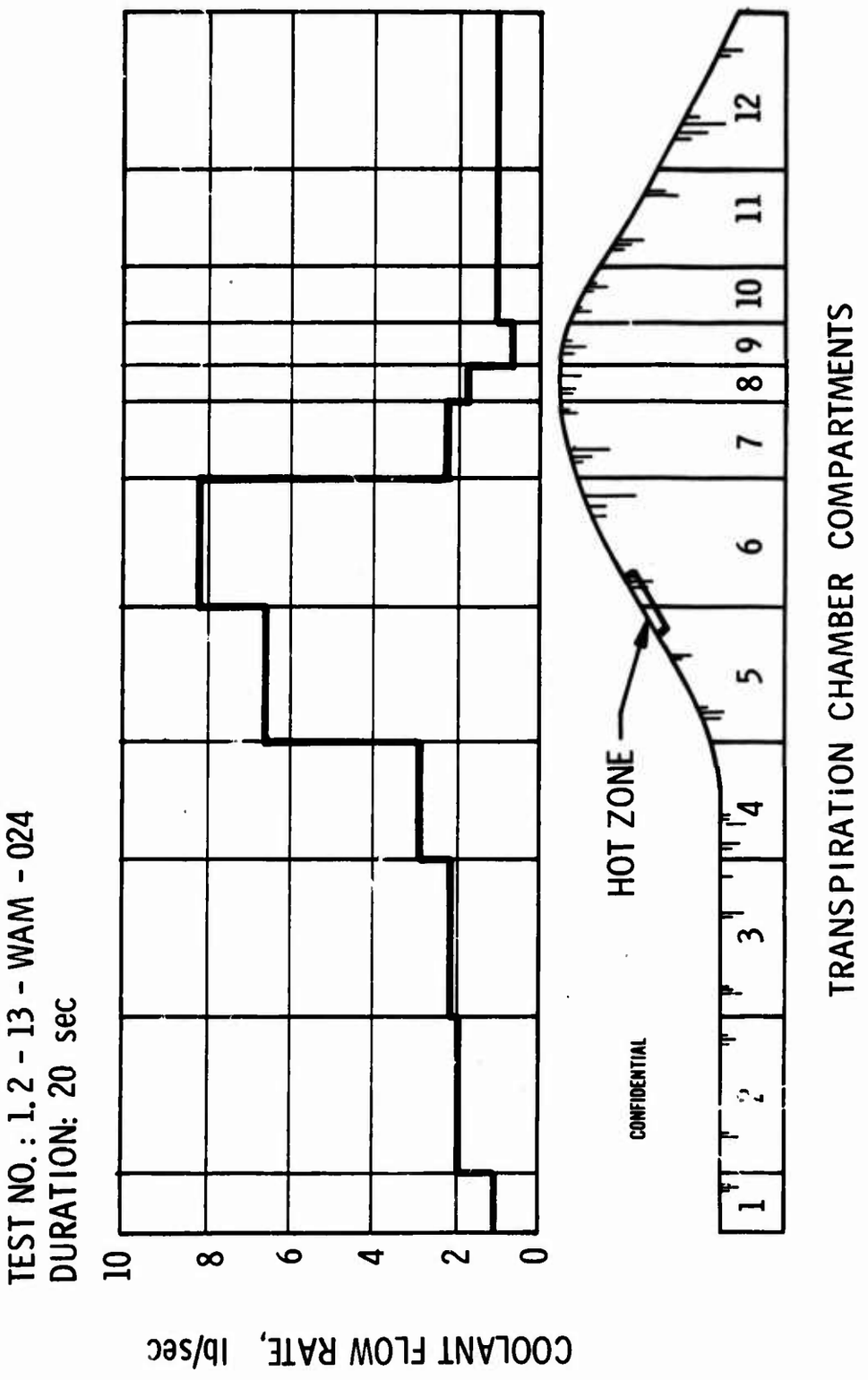

Transpiration Chamber Flow Distribution (U)

Figure VI-53

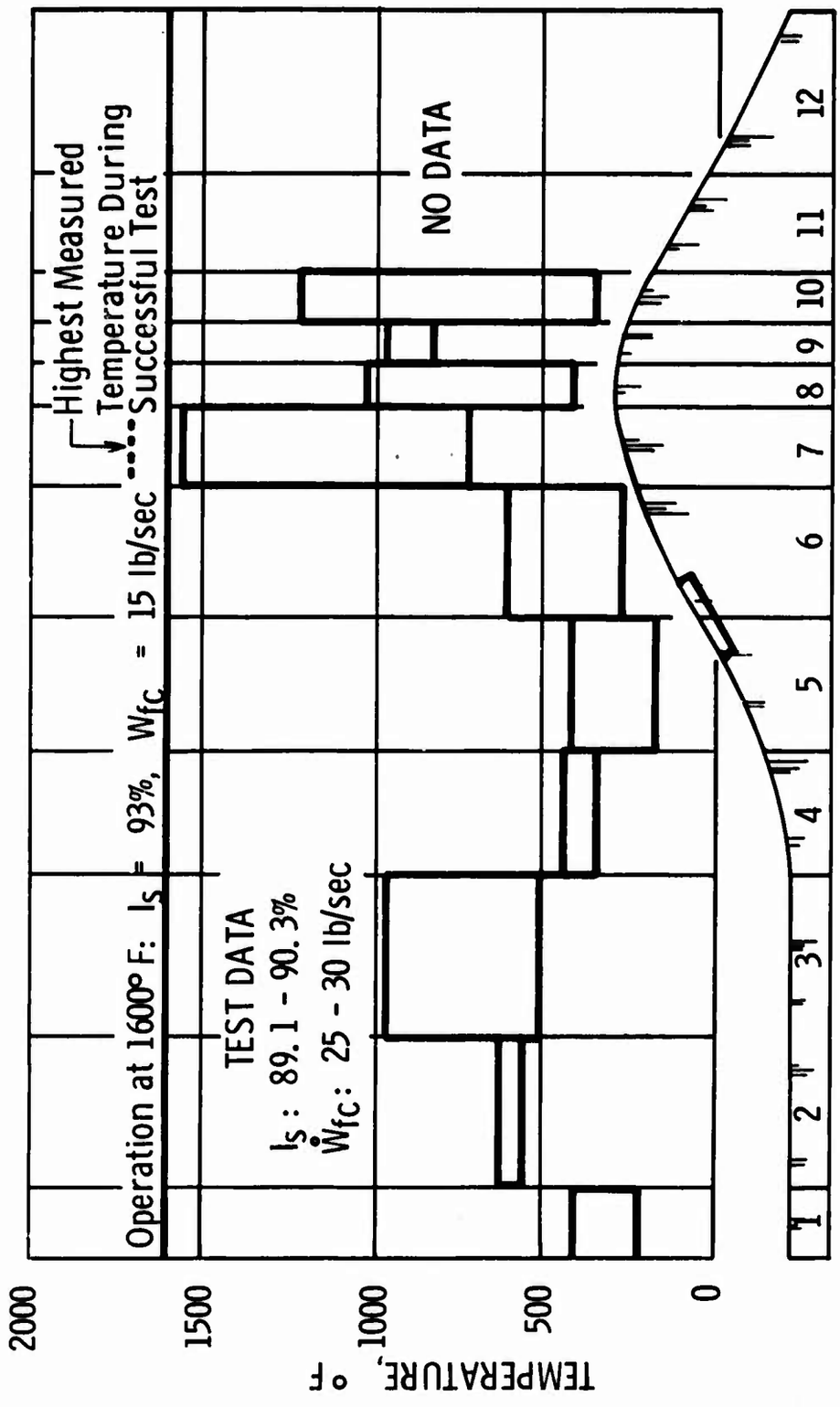

Transpiration Chamber Temperature Summary (U)

Figure VI-54

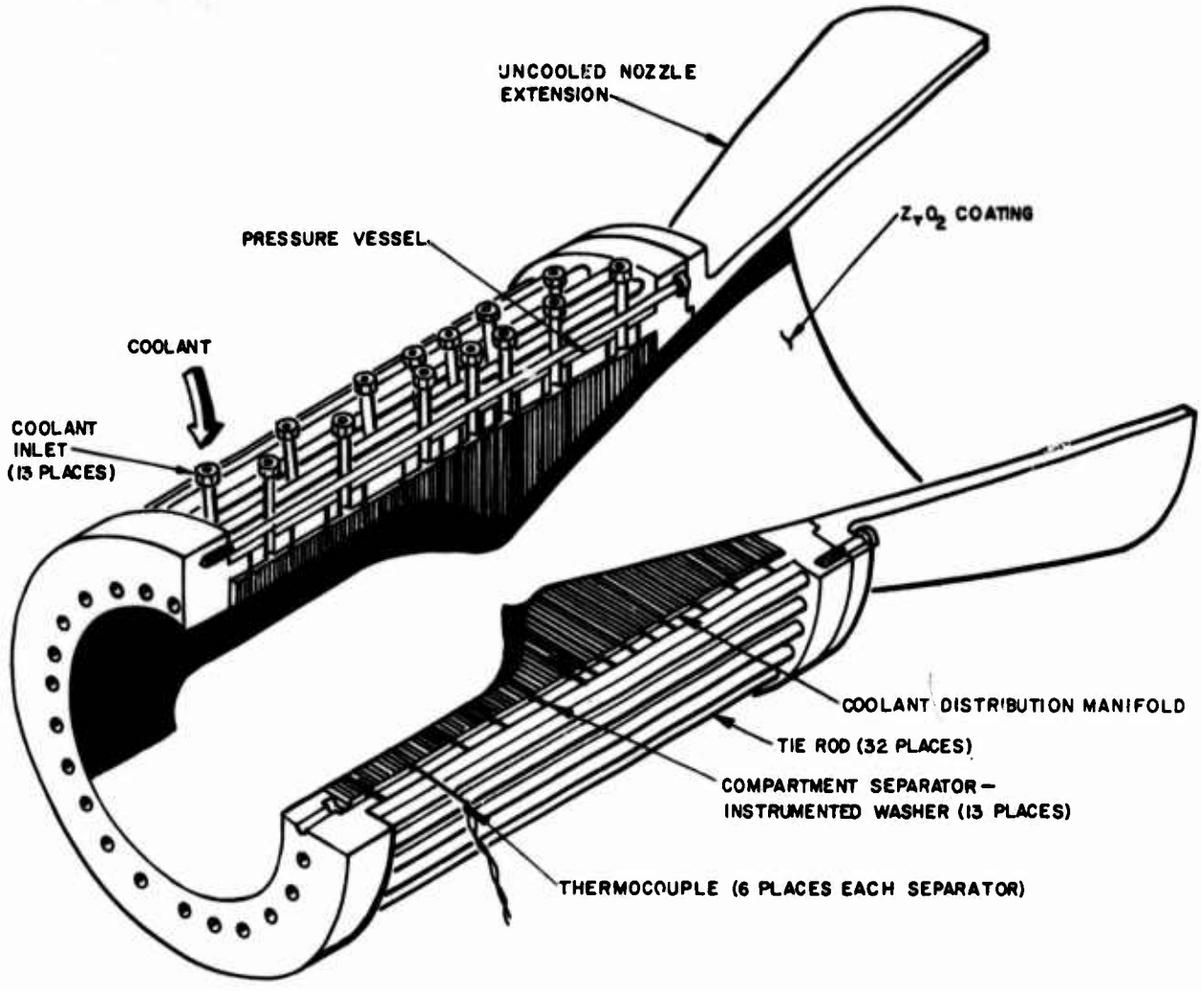

Transpiration-Cooled Combustion Chamber

Figure VI-55

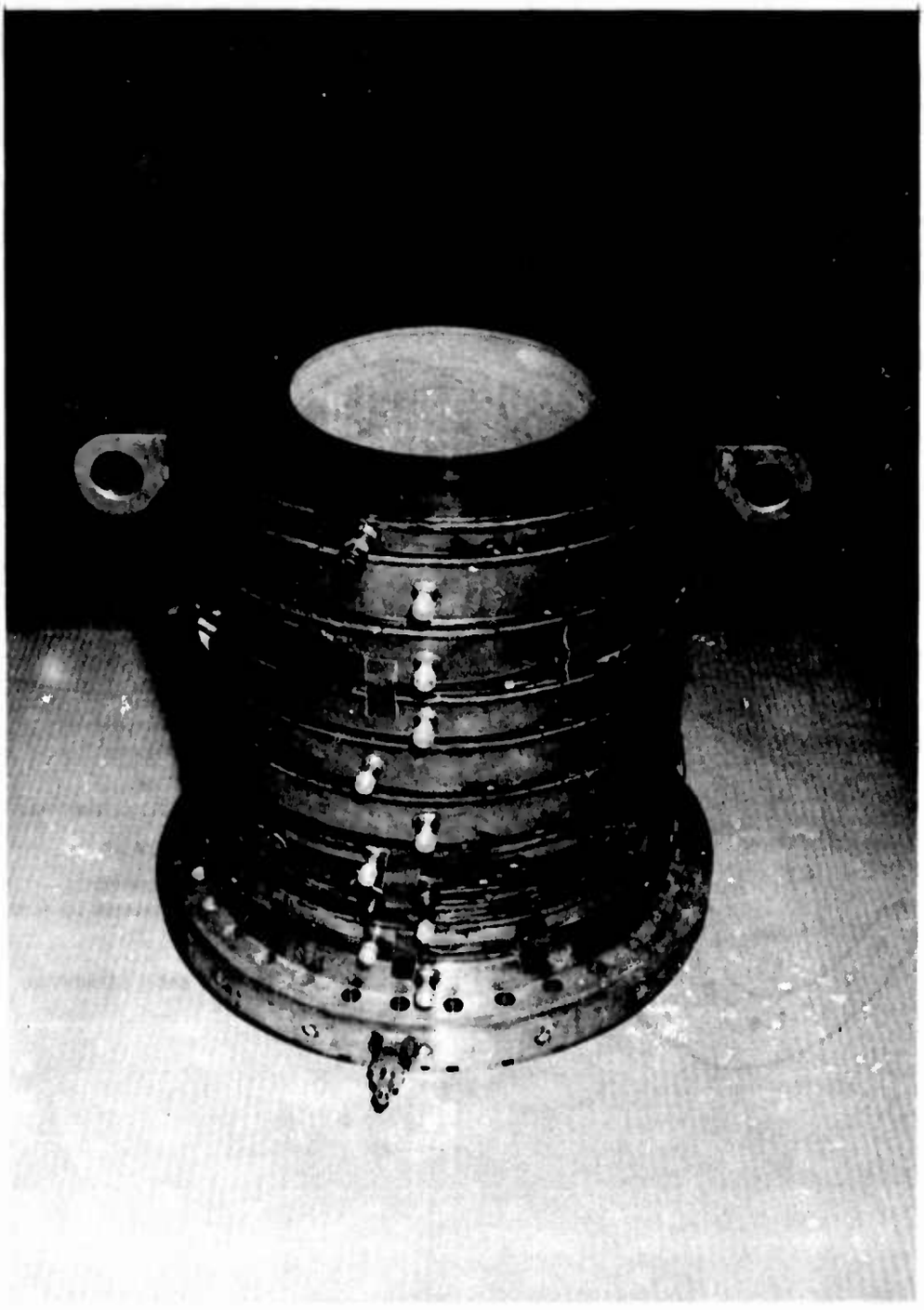

Transpiration-Cooled Combustion Chamber

Figure VI-56

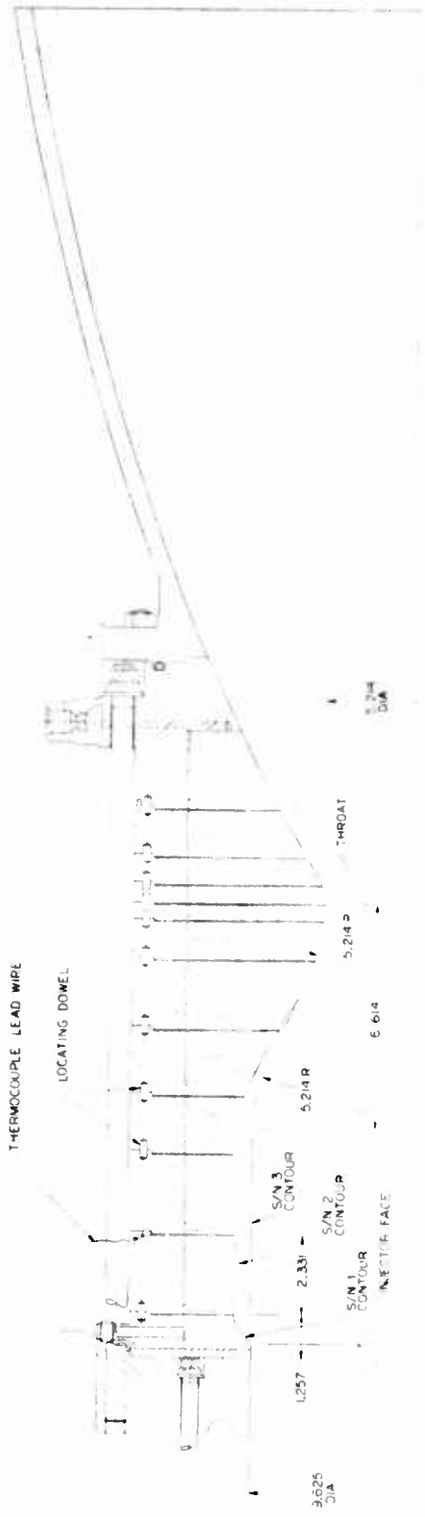

Layout of Transpiration-Cooled Chamber

Figure VI-57

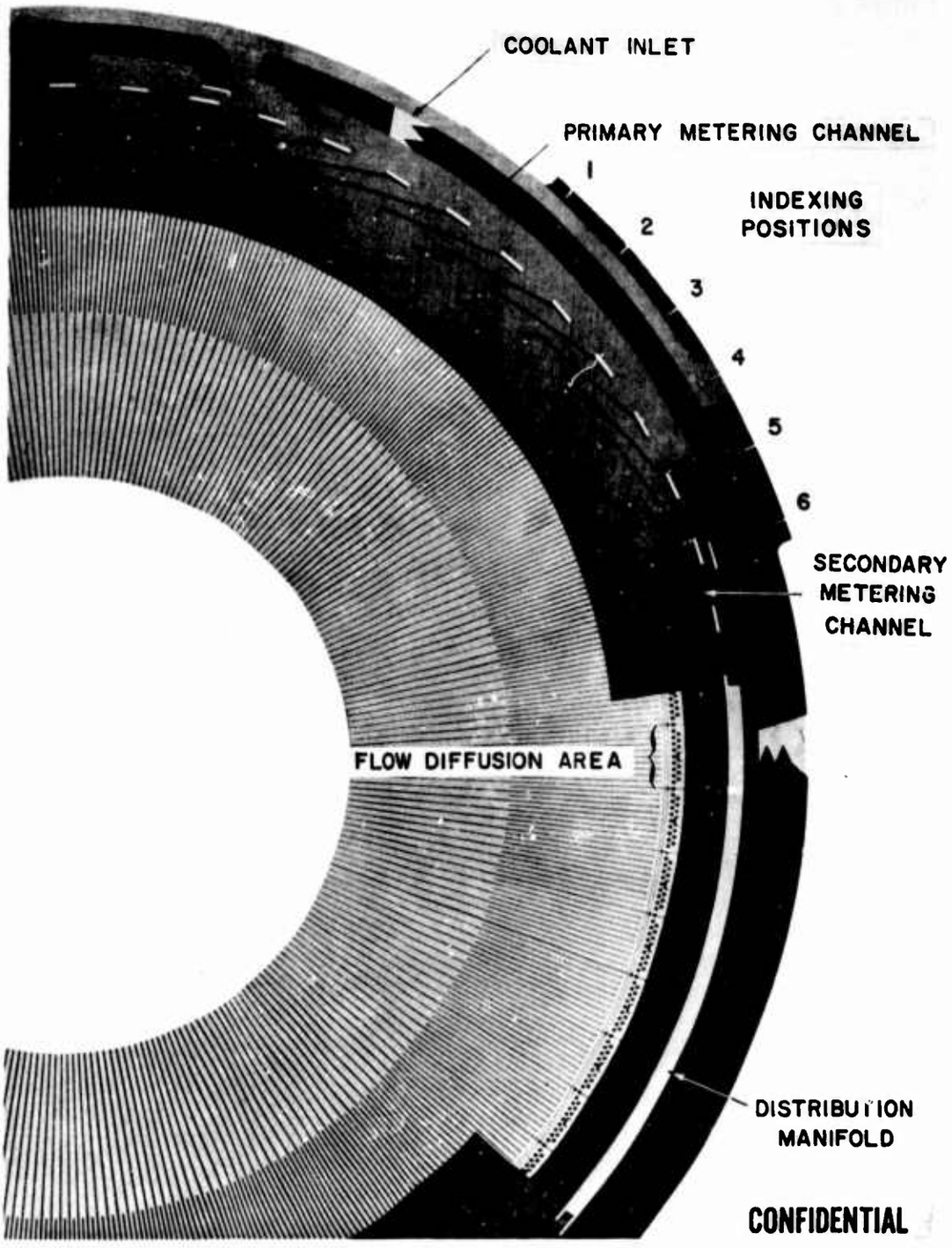

Sectional Washer Pairs for Transpiration Chambers (u)

Figure VI-58

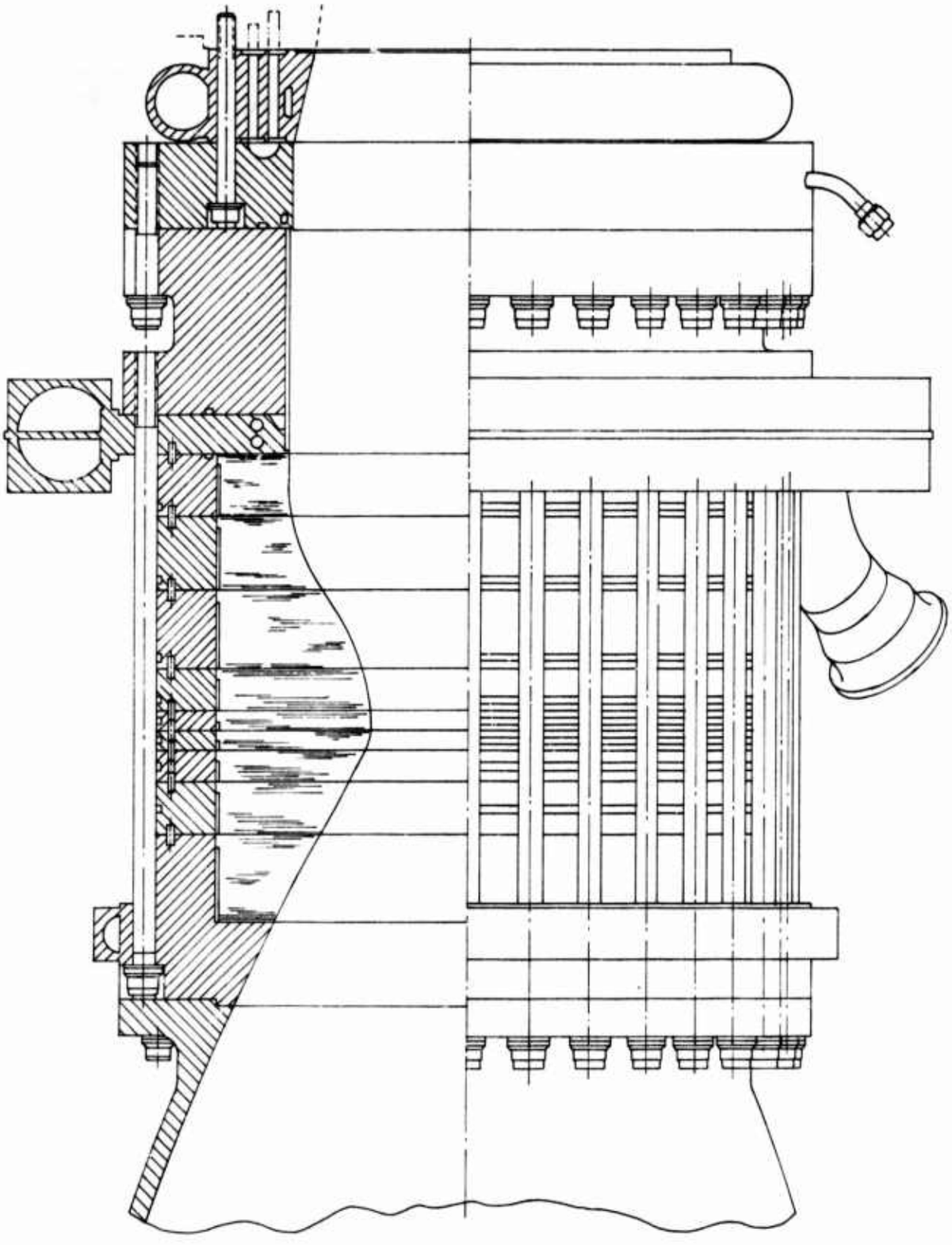

Composite Combustion Chamber

Figure VI-59

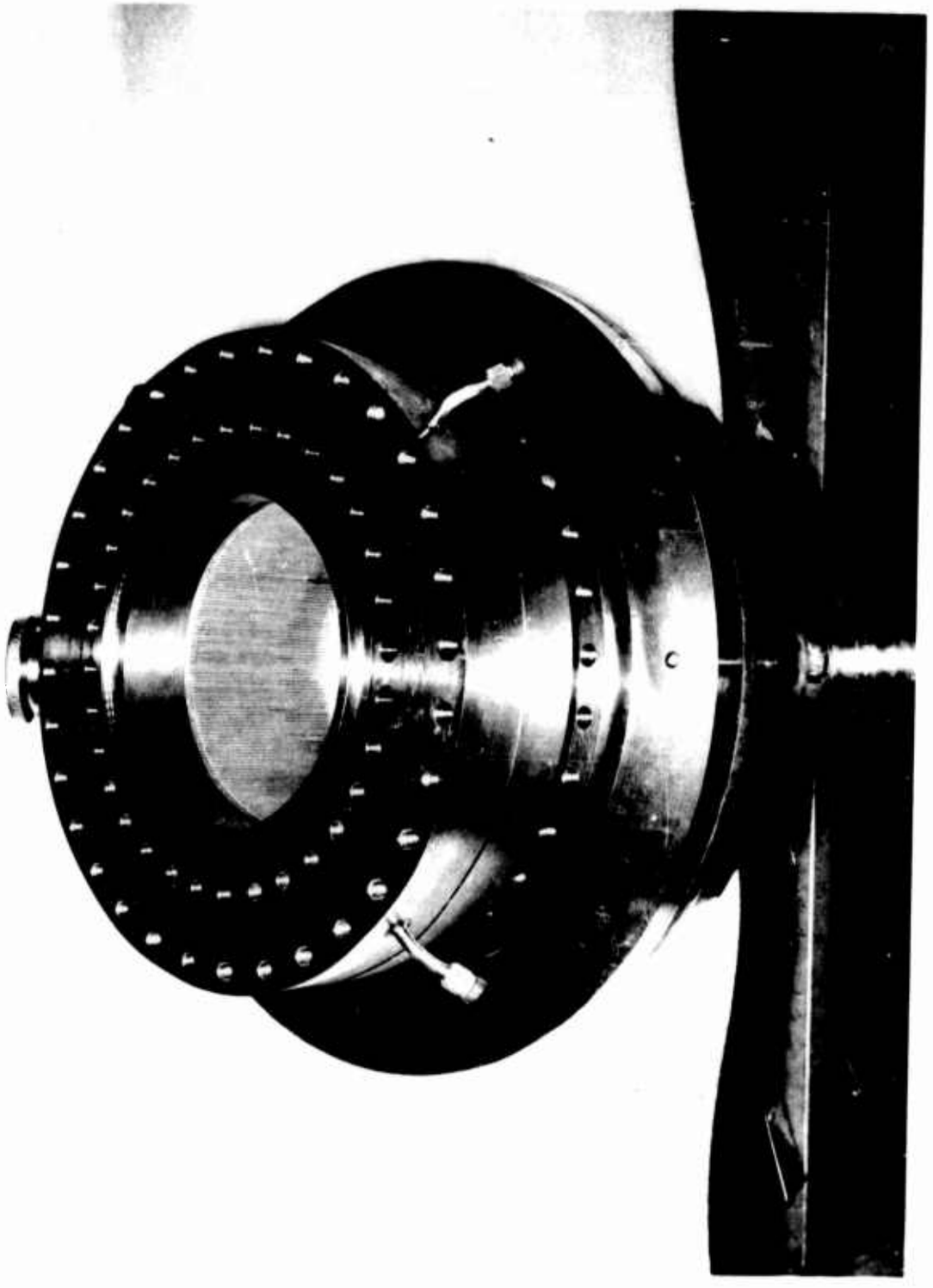

Regeneratively-Cooled Chamber Segment-Composite Chamber

Figure VI-60

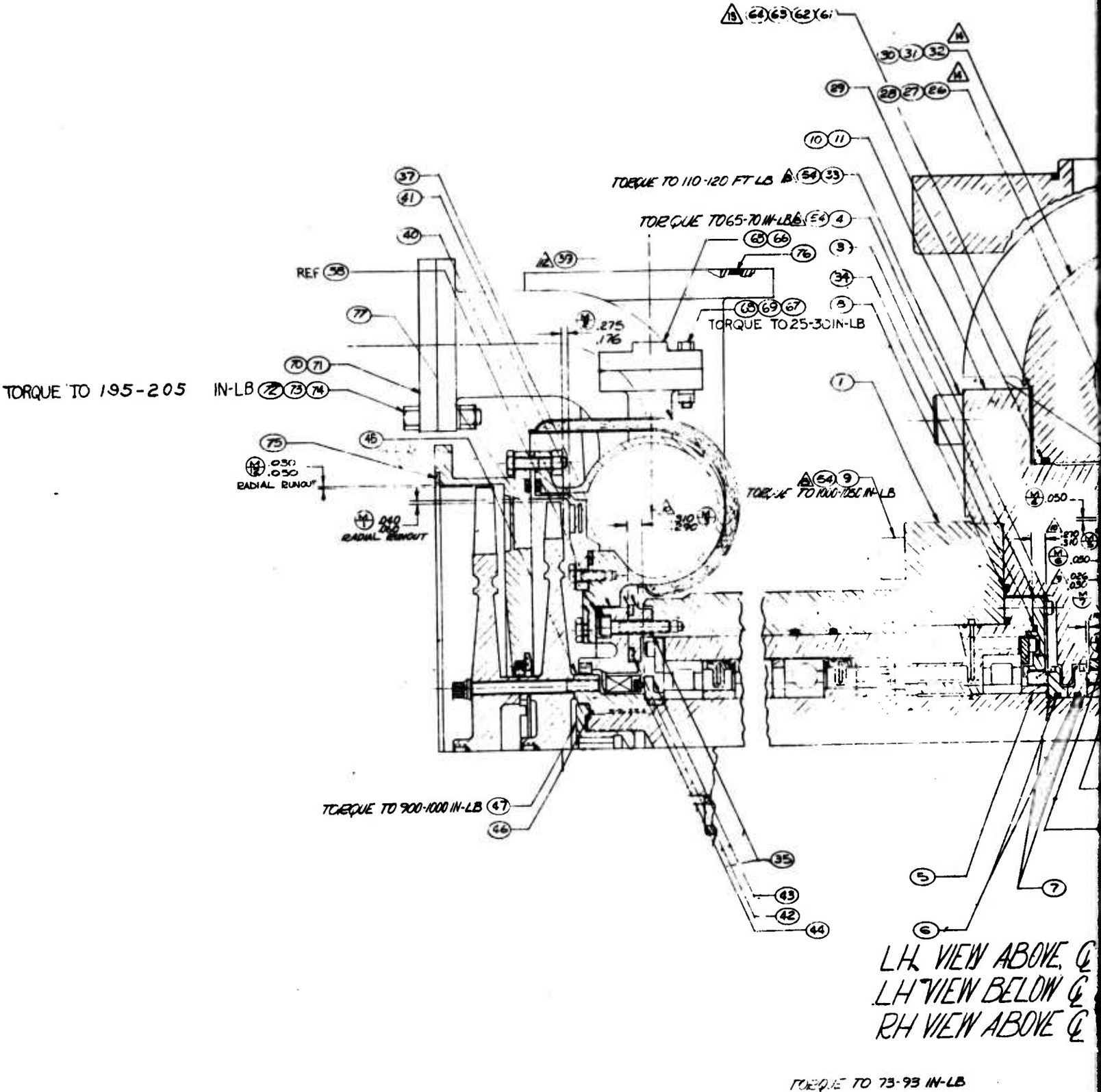
TORQUE TO 195-205 IN-LB
REF
TORQUE TO 110-120 FT LB
TORQUE TO 65-70 IN-LB
TORQUE TO 25-30 IN-LB
TORQUE TO 900-1000 IN-LB
TORQUE TO 100-150 IN-LB
RADIAL RUNOUT
RADIAL RUNOUT
LH VIEW ABOVE ℄
LH VIEW BELOW ℄
RH VIEW ABOVE ℄
TORQUE TO 73-93 IN-LB

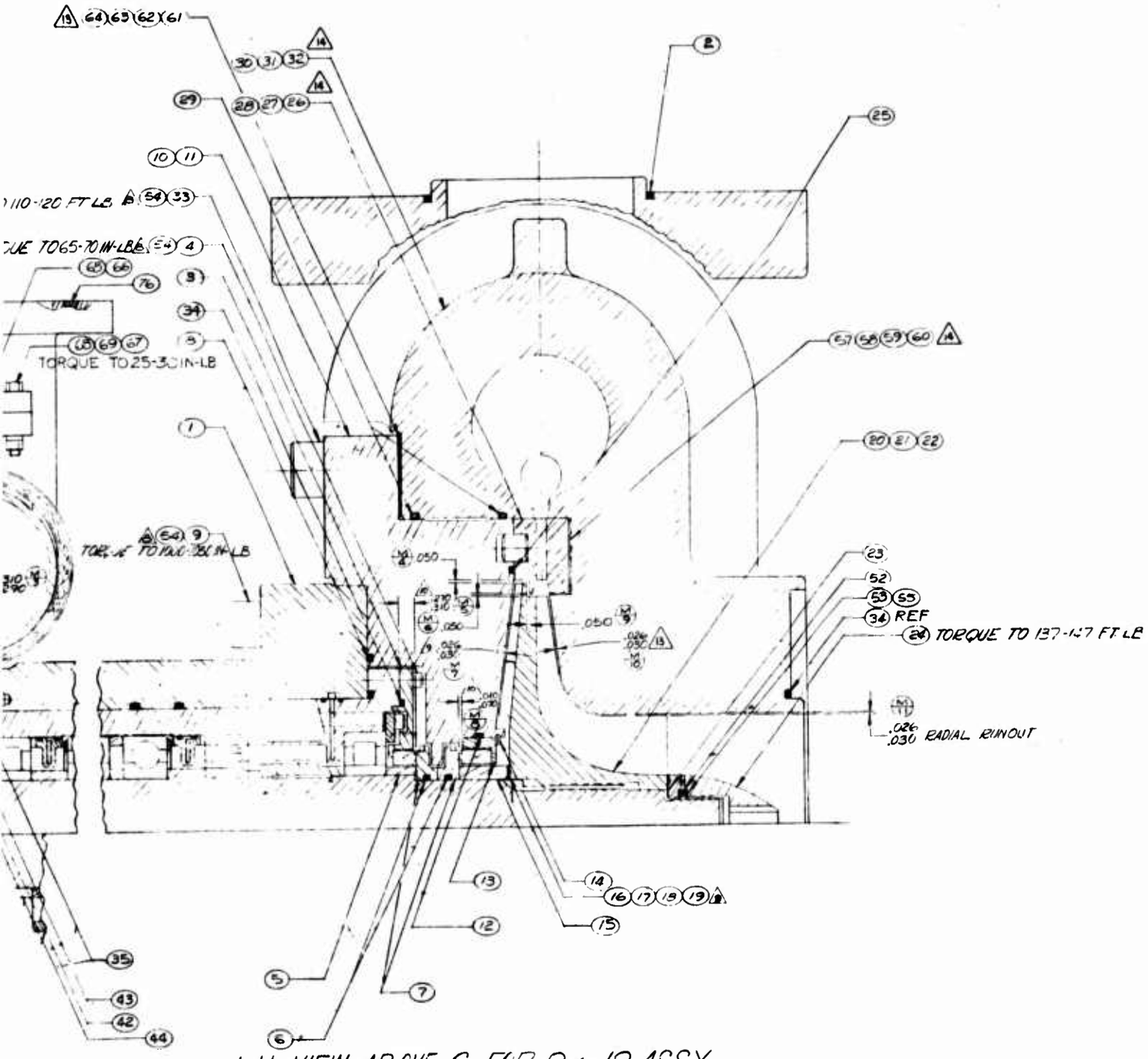

ARES Test Engine Turbopump

Figure VI-61

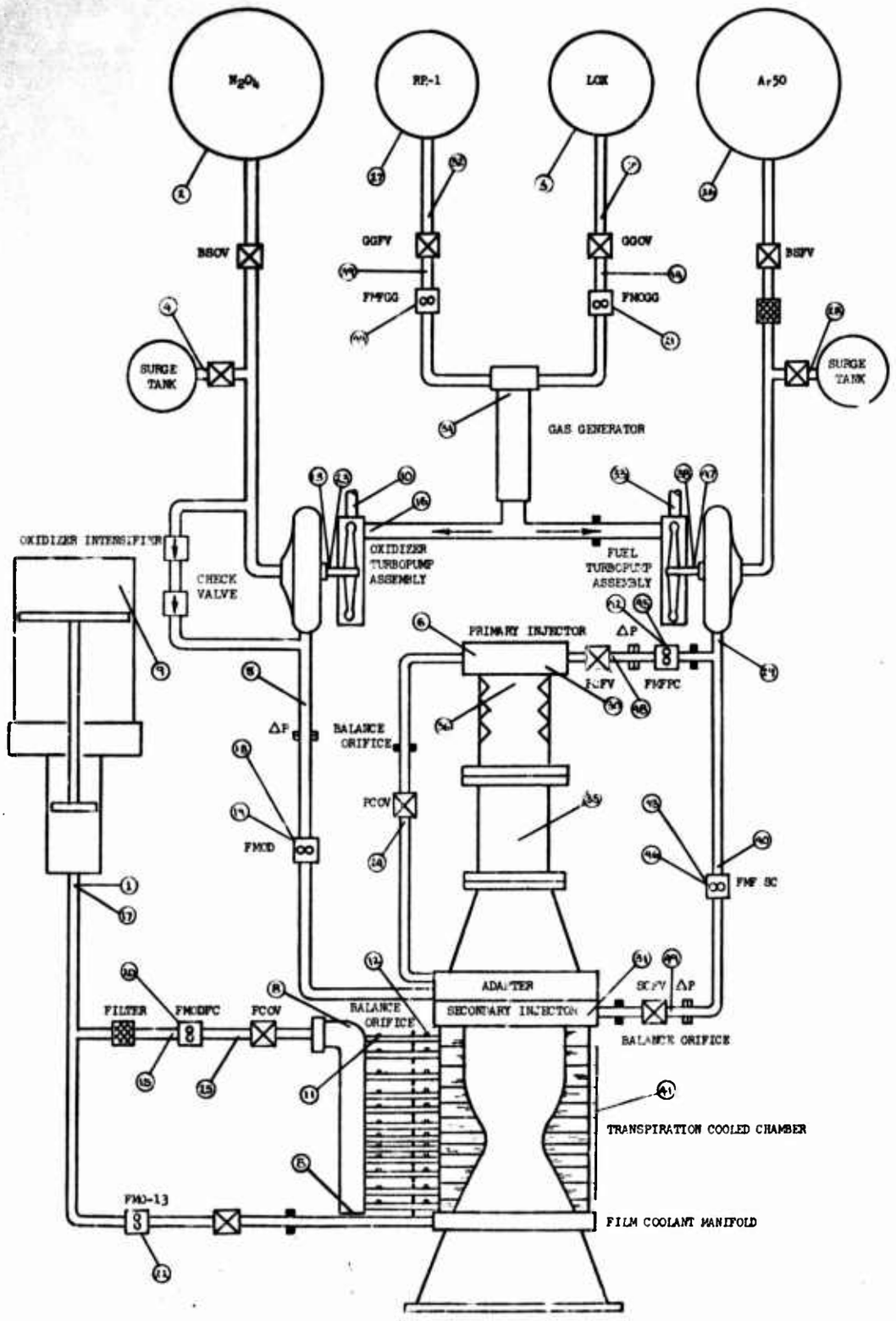
N_2O_4
RP-1
LOX
Ar50
BSOV
GGFV
GGOV
BSFV
FMFGG
FMOGG
SURGE TANK
SURGE TANK
GAS GENERATOR
OXIDIZER INTENSIFIER
CHECK VALVE
OXIDIZER TURBOPUMP ASSEMBLY
FUEL TURBOPUMP ASSEMBLY
PRIMARY INJECTOR
ΔP
FMFPC
ΔP
BALANCE ORIFICE
FCOV
FMOD
FMF SC
ADAPTER
SECONDARY INJECTOR
SCFV
ΔP
BALANCE ORIFICE
FILTER
FMODPC
FCOV
BALANCE ORIFICE
TRANSPIRATION COOLED CHAMBER
FMO-13
FILM COOLANT MANIFOLD

NO.	SYMBOL	TITLE
1	PoL	Oxidizer Intensifier Outlet Pressure
2	PoT	Oxidizer Tank Pressure
3	PoTGG	Oxidizer Gas Generator Tank Pressure
4	PoSB	Oxidizer Surge Bottle Pressure
5	PoD	Oxidizer Discharge Pressure
6	PoJPC	Oxidizer Primary Combustor Injector Pressure
7	PoLGG	Oxidizer Gas Generator Line Pressure
8	PoMC	Oxidizer Coolant Manifold Pressure 1 and 2
9	PGoB	Oxidizer Gas Side Booster Pressure
10	PTi-o	Oxidizer Turbine Inlet Pressure
11	PCI	Oxidizer Coolant Orifice Inlet Pressure (1 through 12)
12	PCO	Oxidizer Coolant Orifice Outlet Pressure (1 through 12)
13	ToB	Oxidizer Bearing Temperature
14	ToFMGG	Oxidizer Temperature Gas Generator Flow Meter
15	ToDFM	Oxidizer Temperature Primary Combustor Flow Meter
16	TTi-o	Oxidizer Temperature Turbine Inlet
17	ToL	Oxidizer Temperature Intensifier Outlet
18	FMoD	Oxidizer Flow Meter Primary Combustor
19	FMVoD	Oxidizer Digital Flow Primary Combustor
20	FMoDFC	Oxidizer Flow Meter Film Coolant
21	FMoGG	Oxidizer Flow Gas Generator
22	FMo-13	Oxidizer Flow Meter Nozzle Film Coolant
23	NT-o	Turbine Speed Oxidizer Pump
24	PCoV	Oxidizer Valve Primary Combustor
25	PCoV	Oxidizer Valve Secondary Combustor
26	PfT	Fuel Tank Pressure
27	PfTGG	Fuel Gas Generator Tank Pressure
28	PfSB	Fuel Surge Bottle Pressure
29	PfD	Fuel Discharge Pressure
30	PfJPC	Fuel Primary Combustor Injector Pressure
31	PfJSC	Fuel Secondary Combustor Injector Pressure
32	PfLGG	Fuel Gas Generator Line Pressure
33	PTi-f	Fuel Turbine Inlet Pressure
34	PcGG	Chamber Pressure Gas Generator
35	PcPC	Chamber Pressure Primary Combustor
36	PcMC	Chamber Pressure Mixing Cavity
37	PcSC	Chamber Pressure Secondary Combustor
38	TfB	Fuel Bearing Temperature
39	TfFMGG	Fuel Temperature Gas Generator Flow Meter
40	TfDFM-SC	Fuel Temperature Secondary Combustor Flow Meter
41	TcSC	Secondary Combustor Temperatures (1 through 66)
42	FMfDSC	Fuel Flow Meter Primary Combustor
43	FMfDSC	Fuel Flow Meter Secondary Combustor
44	FMfGG	Fuel Flow Meter Gas Generator
45	FMVfDPC	Fuel Digital Flow Primary Combustor
46	FMVfDSC	Fuel Digital Flow Secondary Combustor
47	NT-f	Turbine Speed Fuel Pump
48	PCfV	Fuel Valve Primary Combustor
49	SCfV	Fuel Valve Secondary Combustor

ARES Pump-Fed Engine Flow and Instrumentation Schematic

Figure VI-62

Report 10830-F-1, Phase I, Supplement 1

BASIC PARTS LIST

DRAWING NO.

SHEET OF

LET.	DATE	REVISION	BY	CK'D

TITLE ENGINE CONFIGURATION H-2 PUMP FED

AEROJET-GENERAL CORPORATION

DRAWN DATE

CHECKED

APPROVED

SIZE	DWG. NO.	REV.	1	2	3	4	5	6	PART NAME	NO. REQ'D.		
E	1129668		X						ENGINE CONFIGURATION, H-2 PUMP FED	1		
E	285004-9			X					TURBOPUMP ASSEMBLY - OXIDIZER	1		
E	285004-19			X					TURBOPUMP ASSEMBLY - FUEL	1		
E	703545-9			X					EXHAUST PIPE - TURBINE	2		
E	708277-9			X					GAS GENERATOR ASSEMBLY	1		
E	1122831-179			X					MODULAR SECONDARY COMBUSTOR ENGINE	1		
									CONFIGURATION			
E	1123250-19				X				TRANSPIRATION COOLED CHAMBER	1		
E	1123184-19				X				SKIRT	1		
E	1132900-19				X				INJECTOR ASSEMBLY, PLATELET	1		
E	1154703-1				X				ORIFICE PLATE	1		
E	1122025-9				X				ADAPTER, SECONDARY INJECTION	1		
E	1129432-9				X				PRIMARY COMBUSTOR CHAMBER	1		
E	1129432-49				X				PRIMARY COMBUSTOR CHAMBER	1		
E	710397-39				X				PRIMARY COMBUSTOR INJECTOR	1		
E	246954				X				VALVE, BALL 2.50	2		
E	246954				X				VALVE, BALL 2.00	2		
E	113W64A				X				VALVE, BALL 1.00	1		
									CONSOLIDATED CONTROLS CORP.			
E	1132750								VALVE, BALL 2.50 - REWORKED 246954			

Basic Parts List

Figure VI-63

CHAMBER S/N	(1)		3												
TEST NUMBER	025	005	006	007	008	009	010	011	012	013	014	017	018	019	
DURATION	1.157	1.016	3.998	17.25	1.488	3.028	20.06	1.521	3.084	3.674	1.542	1.524	1.524	3.023	1
COMPARTMENT COOLANT FLOW, LB/SEC N_2O_4 ①			2.41	3.23	4.13	3.85	3.81	2.47	2.36	2.43	* 1.99	3.70	* 1.0	.99	
②			4.72	5.58	* 2.04	2.04	2.07	2.05	2.06	2.08	2.10	5.24	* 2.64	2.61	
③	SHORT DURATION, NO STEADY STATE FLOW DATA	SHORT DURATION, NO STEADY STATE FLOW DATA	5.06	5.11	* 3.04	2.31	2.35	2.32	2.34	2.35	2.38	4.95	* 2.86	2.81	
④			4.60	5.49	○ 6.1	6.22	5.49	* 4.46	4.28	4.46	* 3.96	4.53	6.18	5.11	
⑤			7.22	7.40	7.92	7.69	7.50	* 5.82	5.84	5.85	* 4.53	6.25	7.24	6.75	
⑥			◇ 7.50	◇ 7.50	○ 8.1	○ 7.27	○ 7.81	8.65	○ 8.62	○ 8.88	* 7.70	8.34	8.60	8.46	
⑦			3.67	3.96	4.21	4.03	3.97	* 3.66	3.61	3.76	* 3.13	4.54	* 3.69	3.54	
⑧			2.49	2.43	2.62	2.59	2.74	* 2.42	2.40	2.41	* 2.19	1.80	1.90	1.76	
⑨			1.71	2.08	2.26	2.08	2.07	* 1.33	◇ 1.24	◇ 1.29	* 1.00	2.37	* 1.31	1.25	
⑩			2.35	2.35	* 1.28	1.28	1.28	* 1.18	1.19	1.19	* 1.08	2.25	* 1.16	1.38	
⑪			3.99	4.02	* .675	1.02	.711	.682	1.02	1.02	1.02	4.40	* 1.03	1.03	
⑫			3.27	3.29	* 1.16	1.17	1.17	1.16	1.17	1.17	1.17	2.75	* 1.28	1.29	
⑬			None	8.59	No	No	8.70	No	No	8.80	No	None	None	No	
$\dot{W}_{OFCT}$	ORIFICE	N/A	N/A	49.09	52.44	43.53	41.55	40.97	36.46	36.13	36.89	32.25	51.12	38.91	36.99	3
	POTTER	N/A	N/A	48.49	52.03	43.41	41.18	40.88	36.16	35.92	36.68	31.27	51.08	38.75	36.29	3

LEGEND:

(1) TEST SERIES 1.2-16-WAM-XXX, ALL OTHER TESTS CONDUCTED ON TEST SERIES 1.2-13-WAM-XXX

◇ CALCULATED FLOW

○ ESTIMATED FLOW

□ FLOW QUESTIONABLE

△ FLOW INCREASE

* FLOW REDUCTION

018	019	020	021	022	023	024	025	026	027
1.524	3.023	1.523	3.019	1.515	3.009	20486	1.464	1.504	5.021
* 1.0	.99	1.01	.99	* .83	.81	.81	* .72	△ .83	.80
* 2.64	2.61	* 2.05	2.03	* 2.00	1.95	1.94	* 1.70	△ 2.00	1.94
* 2.86	2.81	* 2.36	2.33	* 2.13	2.07	2.08	* 1.98	△ 2.13	2.07
6.18	5.11	* 3.84	3.56	* 2.99	2.81	2.72	* 2.14	△ 3.03	2.86
7.24	6.75	7.13	6.78	7.78	7.06	6.39	8.75	7.83	* 7.18
8.60	8.46	8.40	8.35	8.71	7.96	8.14	9.01	8.85	8.50
* 3.69	3.54	* 2.34	2.30	2.31	2.26	2.24	2.29	2.33	2.27
1.90	1.76	* 1.86	1.82	1.93	1.82	1.75	2.12	2.12	2.03
* 1.31	1.25	* .91	.89	* .75	.74	.74	.75	.76	.75
* 1.16	1.38	* .98	1.08	* .85	.84	.85	* .75	△ .84	.84
* 1.03	1.03	* .84	.84	.84	.82	.83	.84	.84	.83
* 1.28	1.29	* 1.03	1.02	1.02	1.01	1.02	1.06	◇ 1.02	1.02
None	None	None	None	None	None	8.55	None	None	8.79
38.91	36.99	32.76	31.99	32.13	30.19	29.51	32.09	32.58	31.09
38.75	36.29	31.44	30.86	32.87	30.77	28.10	30.48	31.48	30.29

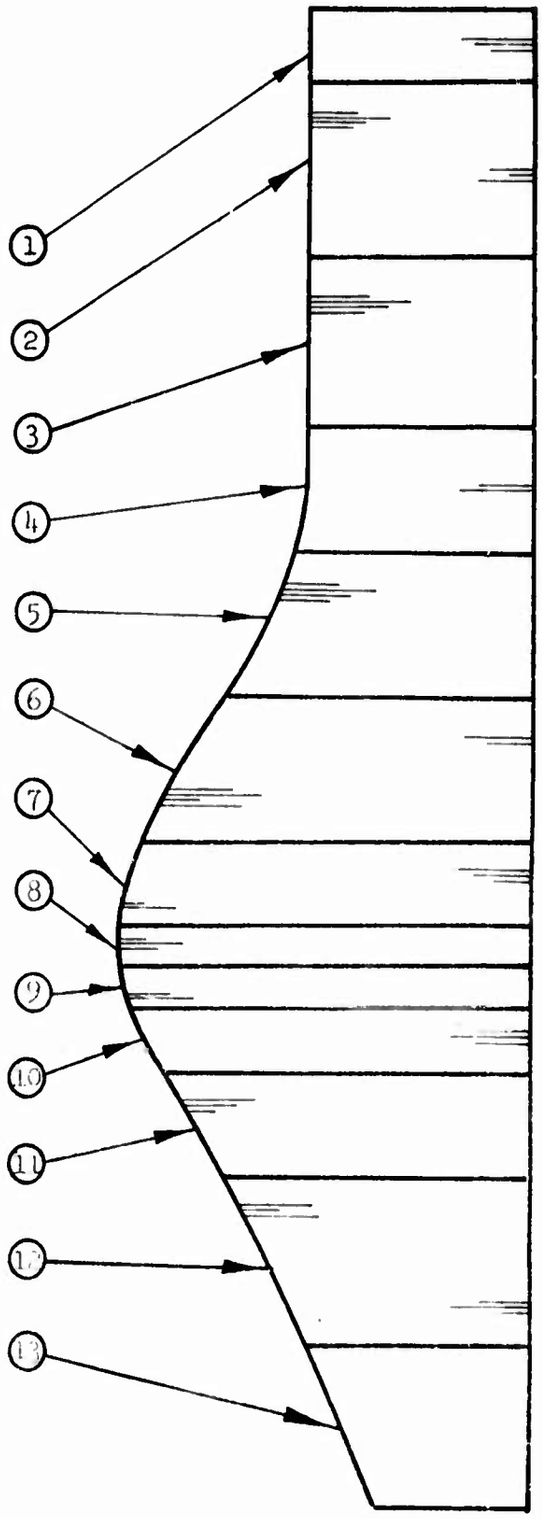

CHAMBER S/N		5															
TEST NUMBER		028	029	030	031	032	033	034	035	036	037	038	039	040	041	042	043	044
DURATION		1.513	0.934	1.521	3.049	1.505	3.021	2.003	2.002	3.027	3.019	20.922	20.708	20.791	2.268	2.261	2.264	2.26
COMPARTMENT COOLANT FLOW LB/SEC N_2O_4	①	3.86		*1.03	.99	*.84	.84	.82	△1.00	.99	1.00	.99	.99	1.00	1.02	.96	.92	.9
	②	5.94		*2.78	2.68	*2.05	2.04	1.99	2.00	1.98	2.01	1.98	1.96	2.00	2.02	1.91	1.83	1.8
	③	5.67		*2.97	2.86	*2.16	2.15	2.10	*1.88	1.85	1.88	1.86	1.86	1.88	1.92	1.82	1.72	1.7
	④	4.86		*3.97	3.85	*3.13	3.10	3.07	*2.69	2.66	2.71	2.64	2.63	2.67	*2.51	2.37	2.26	2.2
	⑤	5.72	TEST STAND MALFUNCTION	6.58	6.62	7.76	7.64	7.60	*7.42	7.19	7.26	6.37	6.32	6.55	*5.95	5.65	5.47	5.4
	⑥	8.48		8.11	8.03	8.56	8.43	8.31	*8.23	8.06	8.20	8.05	8.02	8.13	*7.75	7.42	7.08	7.0
	⑦	5.11		3.67	3.54	*2.30	2.29	2.25	2.25	2.23	2.26	2.23	2.22	2.25	2.24	2.13	2.07	2.0
	⑧	1.50		□1.50	□1.11	□.95	□1.29	□1.23	□1.45	□1.55	□1.59	□1.05	□1.33	□1.73	*2.14	2.03	1.90	1.9
	⑨	1.22		*.82	.79	*.59	.58	.58	.58	.58	.57	.56	.56	.56	.55	.54	.52	.5
	⑩	Inv.		*.85	.80	.82	.82	.83	.83	.82	◇.82	.82	.80	.81	.80	.78	.75	.7
	⑪	Inv.		*.98	.97	*.81	.81	.80	.81	.80	.80	.80	.80	.81	.80	.79	.77	.7
	⑫	◇2.58		*1.28	1.28	*1.01	1.02	1.00	1.01	1.00	1.01	1.01	1.01	1.01	1.00	.98	.96	.9
	⑬	None		None	None	None	None	None	None	None	None	Inv.	8.41	8.42	None	None	None	Non
W_{OPCP}	ORIFICE	N/A	N/A	34.53	33.52	30.98	30.98	30.58	30.16	29.71	30.11	28.35	28.51	29.40	28.70	27.35	26.25	26.2
	METER	49.42	N/A	34.86	34.12	31.52	30.43	30.43	29.74	29.50	29.63	28.38	28.50	28.98	27.80	26.42	25.27	25.3

LEGEND

(1) TEST SERIES 1.2-16-WAM-XX, ALL OTHER TESTS CONDUCTED ON TEST SERIES 1.2-13-WAM-XXX.

◇ CALCULATED FLOW

○ ESTIMATED FLOW

□ FLOW QUESTIONABLE

△ FLOW INCREASE

* FLOW REDUCTION

								4R			3R	
039	040	043	042	043	044	045	046	047	048	049	050	051
20.706	20.791	2.208	2.201	2.204	2.201	2.201	1.350	2.257	2.259	2.256	2.258	2.253
.99	1.00	1.02	.96	.92	.92	.92	.92	1.03	1.01	1.06	1.04	1.06
1.96	2.00	2.02	1.91	1.83	1.84	1.83	1.82	2.06	2.05	2.10	2.09	2.10
1.86	1.88	1.92	1.82	1.72	1.72	1.71	1.70	2.17	*2.00	2.04	2.20	*1.95
2.63	2.67	*2.51	2.37	2.26	2.27	2.26	2.24	2.17	2.14	2.20	3.02	*2.69
6.32	6.55	*5.95	5.65	5.47	5.46	5.44	5.21	8.09	*8.11	*8.41	7.88	*7.59
5.02	5.13	*7.75	7.42	7.08	7.09	7.08	7.06	9.01	*8.60	*8.07	8.66	*8.85
2.22	2.25	2.24	2.13	2.07	2.08	2.07	2.06	2.42	2.37	2.43	2.36	2.38
1.33	1.73	*2.14	2.03	1.90	1.90	1.90	1.88	3.16	*2.70	2.73	2.21	2.29
.56	.56	.56	.54	.52	.52	.52	.52	1.25	*.99	1.06	1.22	*.87
.80	.81	.80	.76	.75	.74	.73	.75	1.11	.85	.85	1.20	*.82
.80	.81	.80	.79	.77	.78	.76	.77	1.05	*.89	.89	1.02	*.84
1.01	1.01	1.00	.98	.96	.96	.96	.96	1.15	1.17	1.17	1.16	1.17
.41	6.42	None	None	None	None	None	5.22	None	None	None	None	None
.51	29.40	28.70	27.35	26.25	26.28	26.20	25.09	34.70	32.93	30.92	34.03	32.80
.50	28.98	27.60	26.42	25.27	25.33	25.22	24.27	33.51	31.56	29.34	33.50	31.47

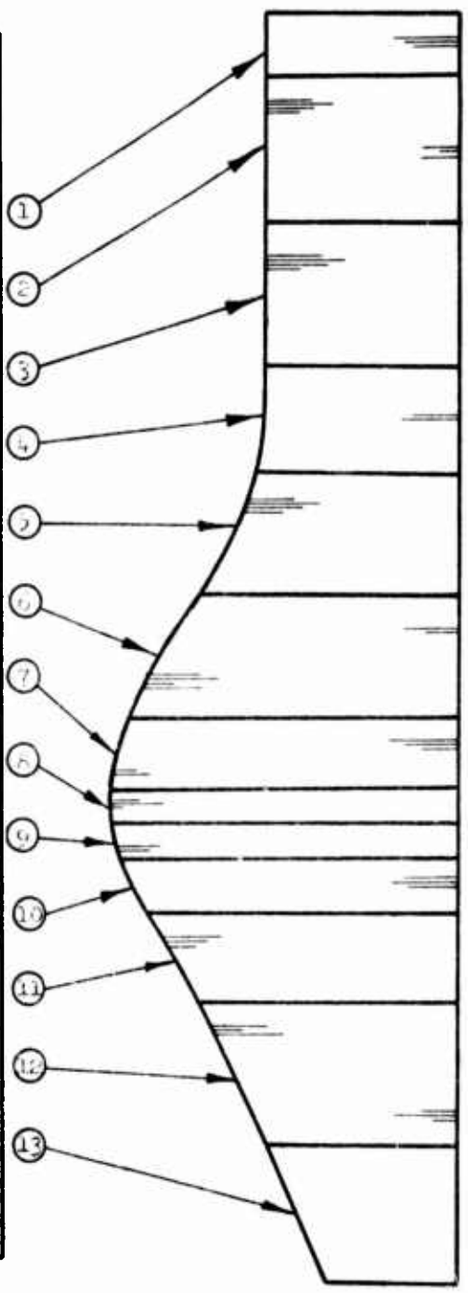

-XXX.

Transpiration Cooled Chamber Flow Summary

Figure VI-64 Page 2 of 2

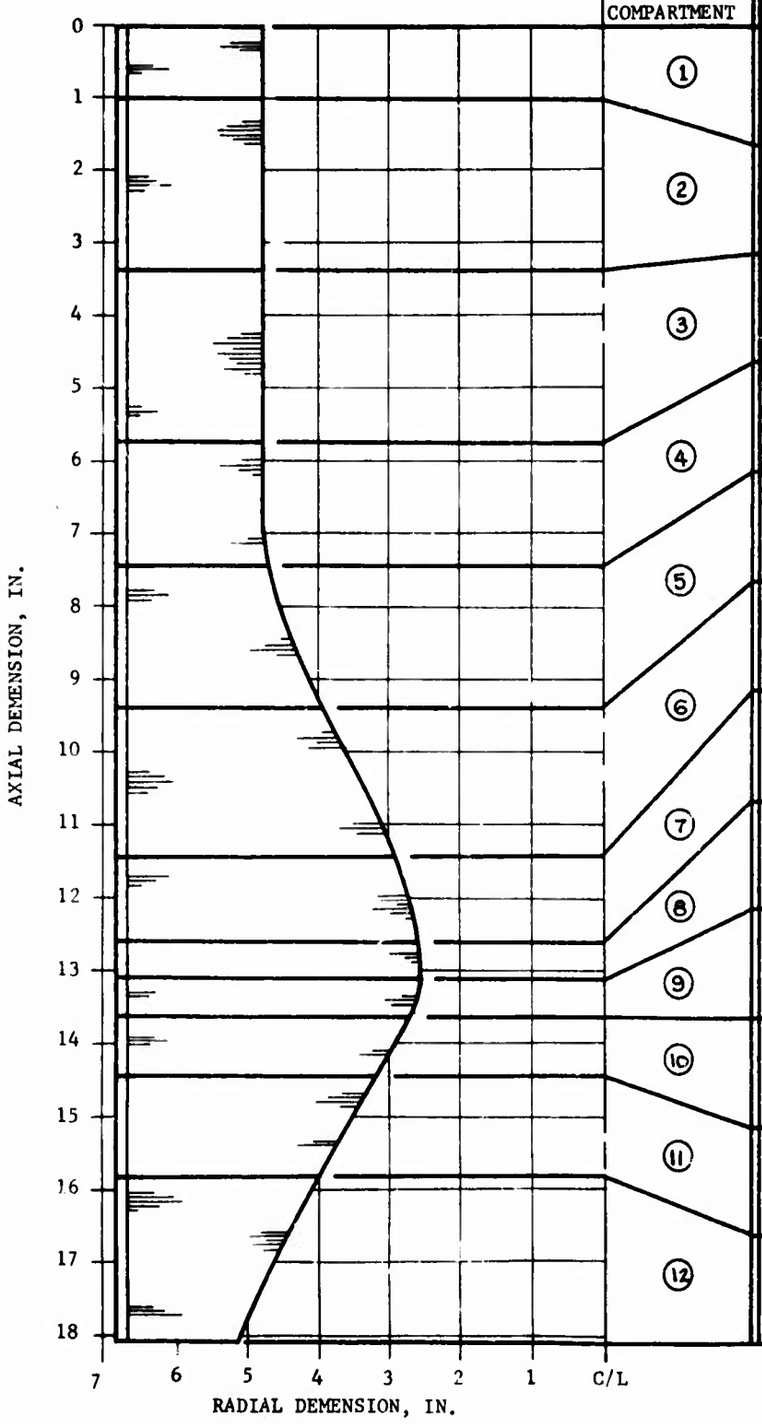

COMPARTMENT	PLATELET CHARACTERISTICS					FLOW RANGE	
	N_P	t_{FP}	t_{MP}	N_{IP}	P_G	MIN.	MA
①	47	.020	.001	1	0	.80	4.
②	111	.020	.001	1	0	1.82	5.
③	111	.020	.001	1	0	1.70	5.
④	60	.020	.001	1	10	2.14	5.4
⑤	92	.020	.001	4	75	4.53	8.0
⑥	185	.010	.001	2	360	7.06	9.0
⑦	103	.010	.001	3	470	2.06	5.1
⑧	44	.010	.001	2	340	1.76	2.7
⑨	48	.010	.001	3	460	.52	2.2
⑩	71	.010	.001	6	460	.73	2.35
⑪	125	.010	.001	6	295	.76	4.02
⑫	109	.020	.001	6	135	.96	3.29

PARTMENT	PLATELET CHARACTERISTICS					FLOW RANGE	
	N_P	t_{FP}	t_{MP}	N_{IP}	P_G	MIN.	MAX.
①	47	.020	.001	1	0	.80	4.13
②	111	.020	.001	1	0	1.82	5.94
③	111	.020	.001	1	0	1.70	5.67
④	80	.020	.001	1	10	2.14	5.49
⑤	92	.020	.001	4	75	4.53	8.09
⑥	185	.010	.001	2	360	7.06	9.01
⑦	103	.010	.001	3	470	2.06	5.11
⑧	44	.010	.001	2	340	1.76	2.73
⑨	48	.010	.001	3	460	.52	2.26
⑩	71	.010	.001	6	460	.73	2.35
⑪	125	.010	.001	6	295	.76	4.02
⑫	109	.020	.001	6	135	.96	3.29

CONFIDENTIAL

LEGEND

N_P = NUMBER OF PLATELETS
t_{FP} = THICKNESS OF FLOW PLATELET
t_{MP} = THICKNESS OF METERING PLATELET
N_{IP} = NUMBER OF INDEXING POSITIONS
P_G = DIFFERENTIAL PRESSURE FROM LEADING EDGE TO TRAILING EDGE OF COMPARTMENT
FLOW RANGE IN LB/SEC N_2O_4

Physical Description of Compartments, Transpiration Cooled Chamber (U)

Figure VI-65

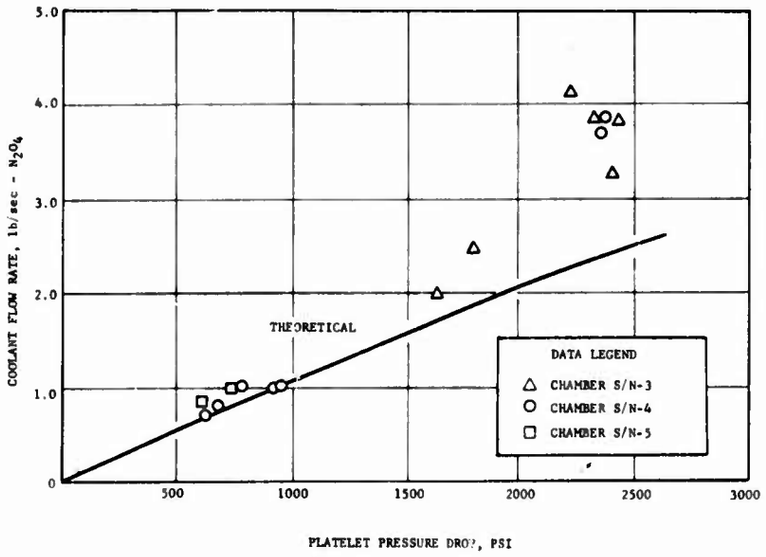

Compartment No. 1

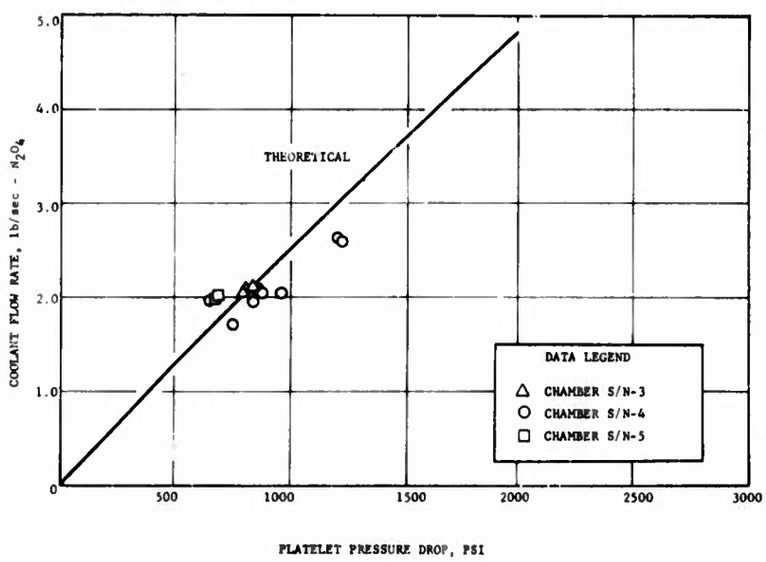

Compartment No. 2

Transpiration Compartment Flow Characteristics

Figure VI-66, Sheet 1 of 6

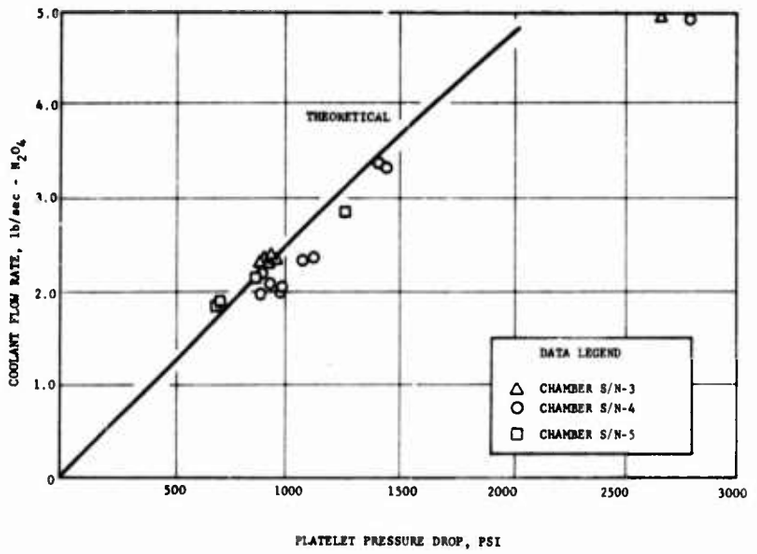

Compartment No. 3

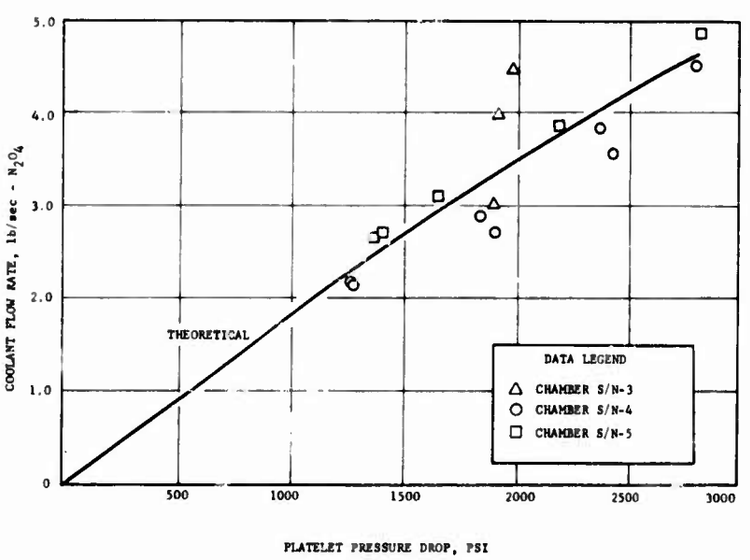

Compartment No. 4

Transpiration Compartment Flow Characteristics

Figure VI-66, Sheet 2 of 6

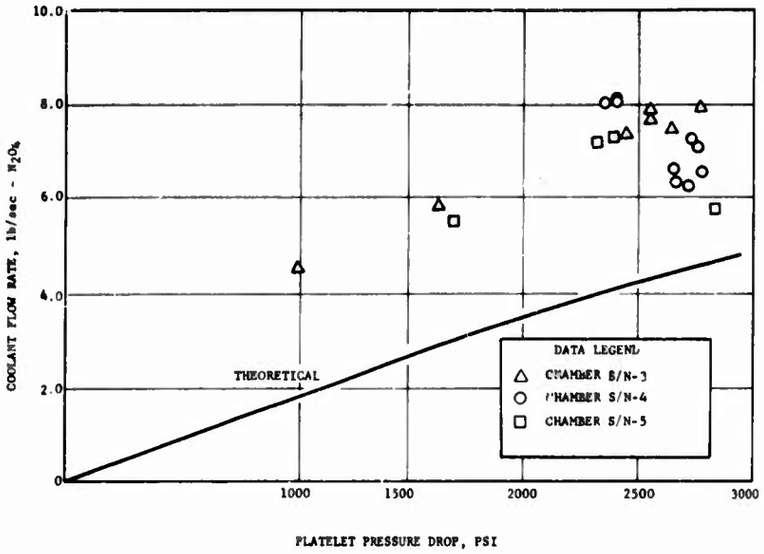

Compartment No. 5

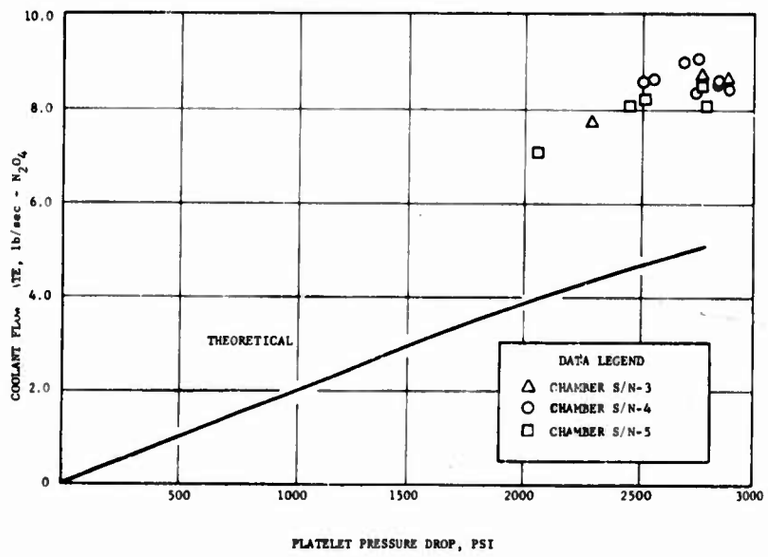

Compartment No. 6

Transpiration Compartment Flow Characteristics

Figure VI-66, Sheet 3 of 6

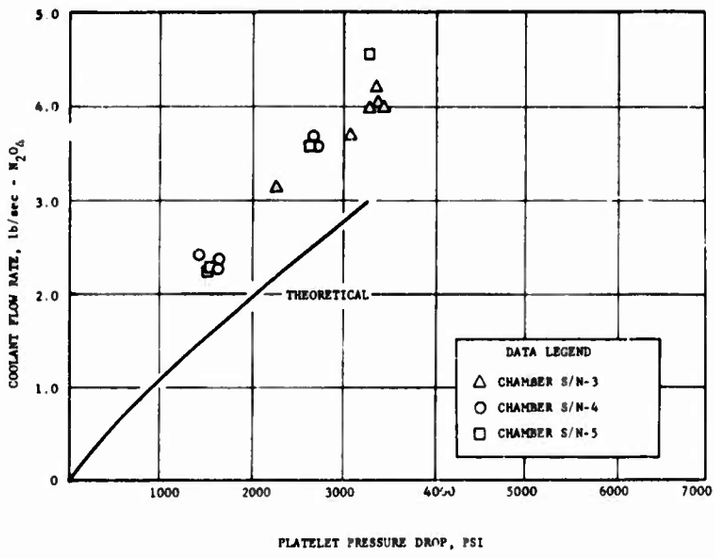

Compartment No. 7

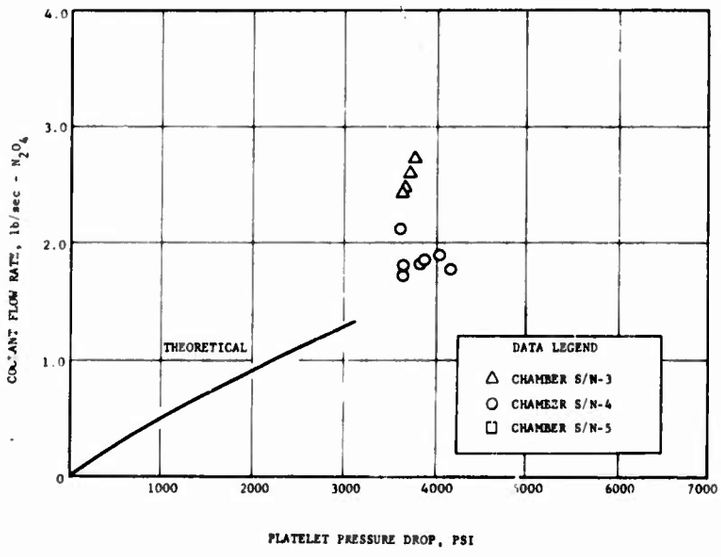

Compartment No. 8

Transpiration Compartment Flow Characteristics

Figure VI-66, Sheet 4 of 6

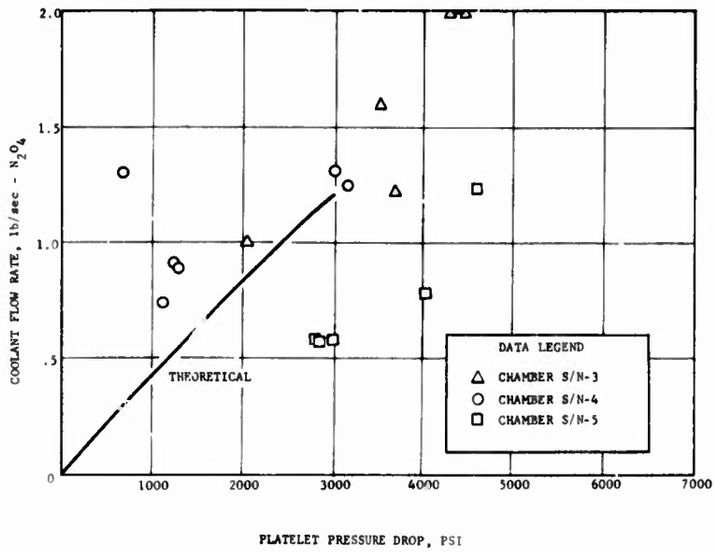

Compartment No. 9

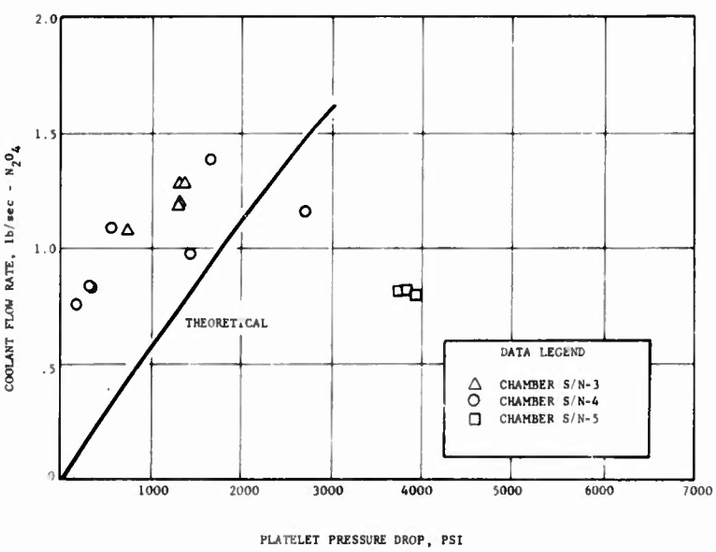

Compartment No. 10

Transpiration Compartment Flow Characteristics

Figure VI-66, Sheet 5 of 6

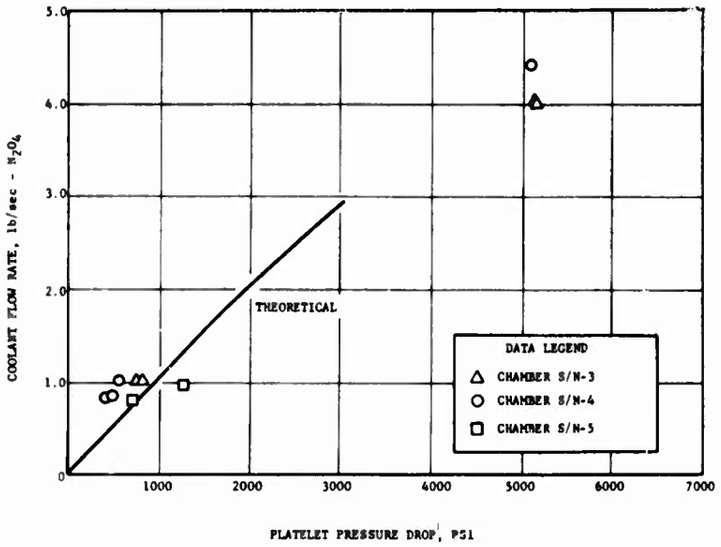

Compartment No. 11

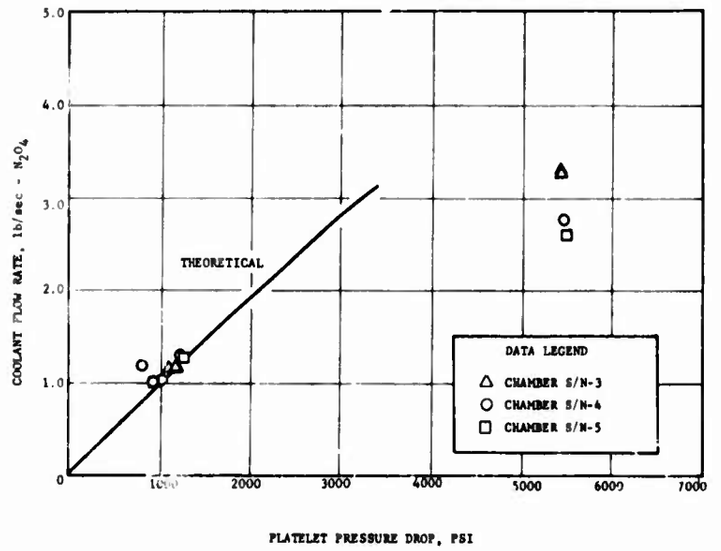

Compartment No. 12

Transpiration Compartment Flow Characteristics

Figure VI-66, Sheet 6 of 6

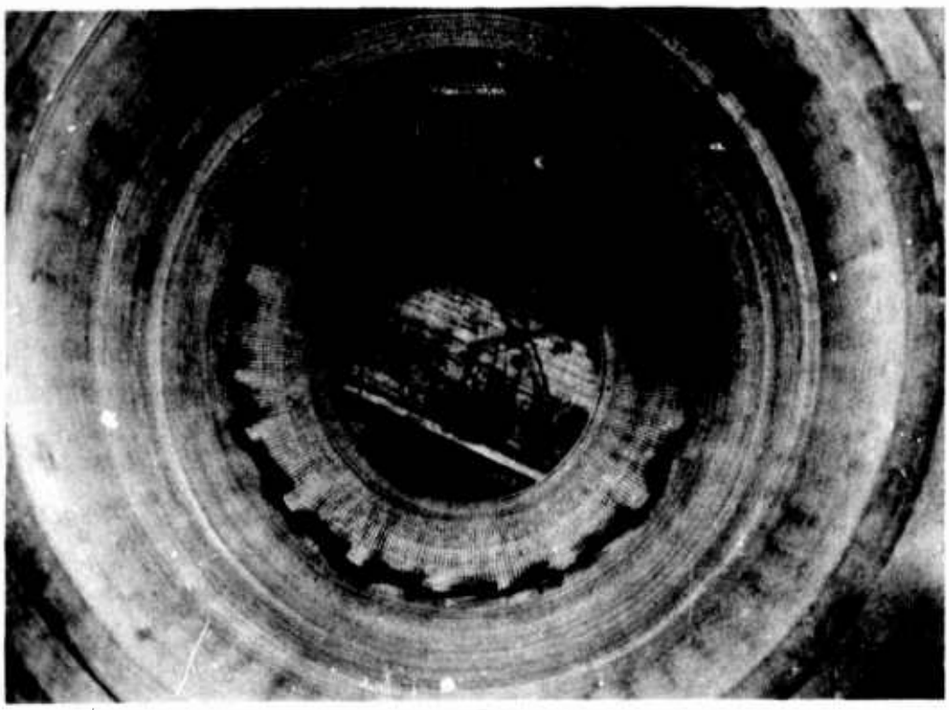

Figure VI-67. Postfire Convergent Section, Transpiration Chamber SN 003, Test 1.2-16-WAM-025

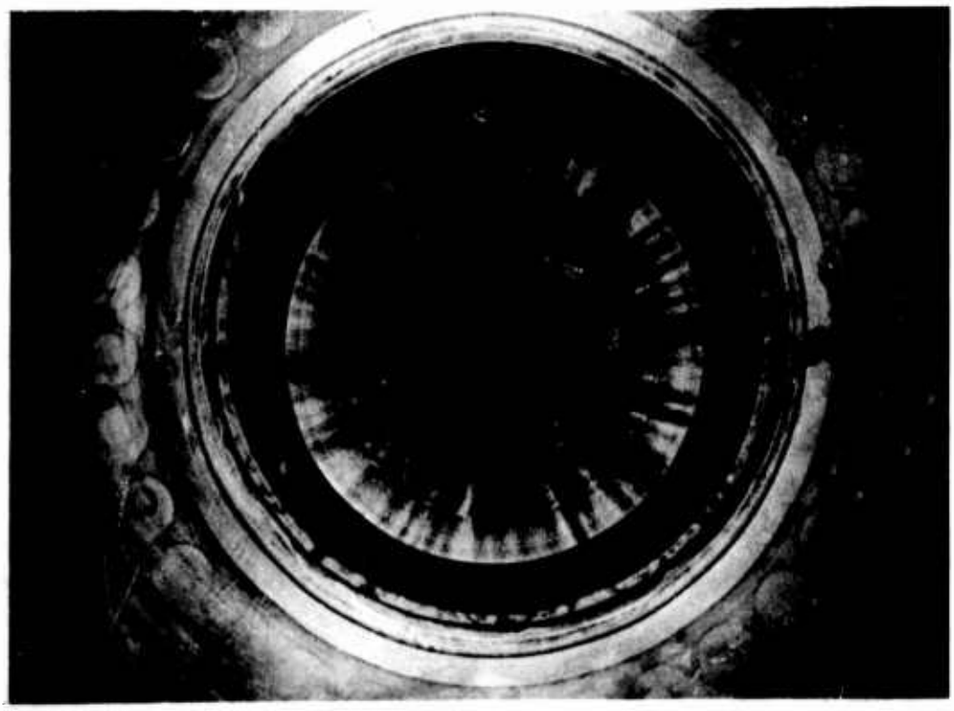

Figure VI-68. Postfire Convergent Section, Transpiration Chamber SN 003, Test 1.2-13-WAM-014

Figure VI-67, Figure VI-68

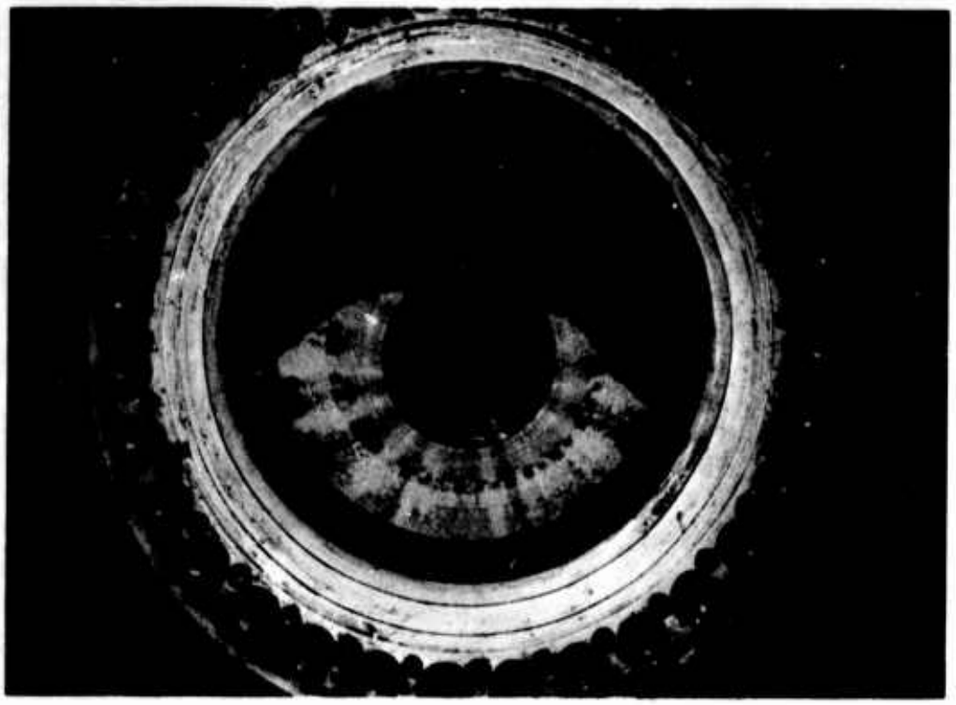

Figure VI-69. Postfire Nozzle Section, Transpiration Chamber SN 003, Test 1.2-13-WAM-014

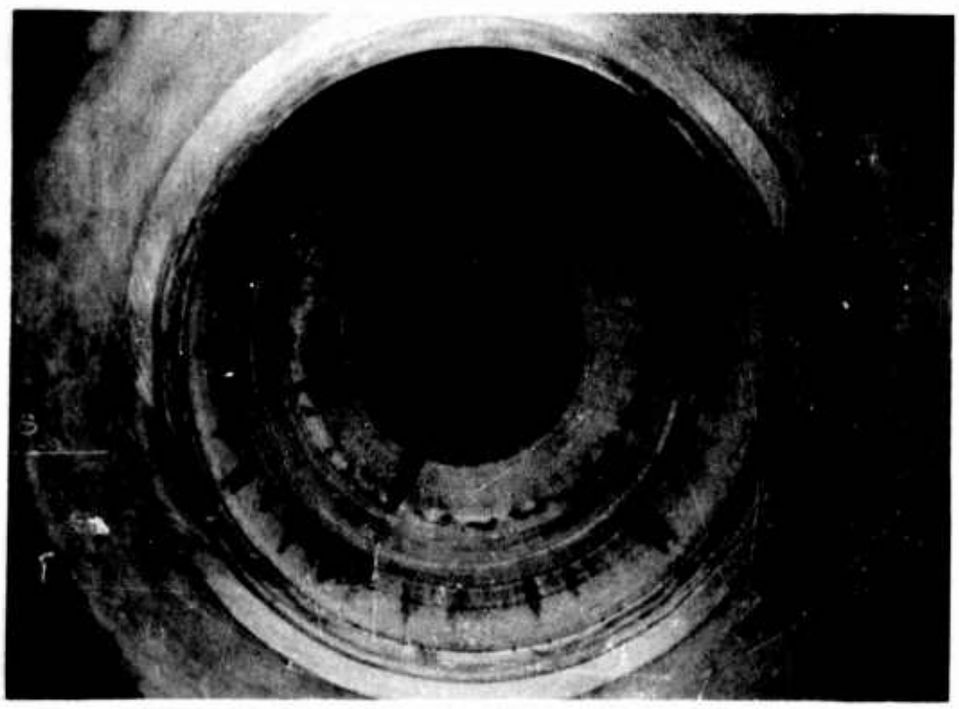

Figure VI-70. Postfire Convergent Section, Transpiration Chamber SN 004, Test 1.2-13-WAM-025

Figure VI-69, Figure VI-70

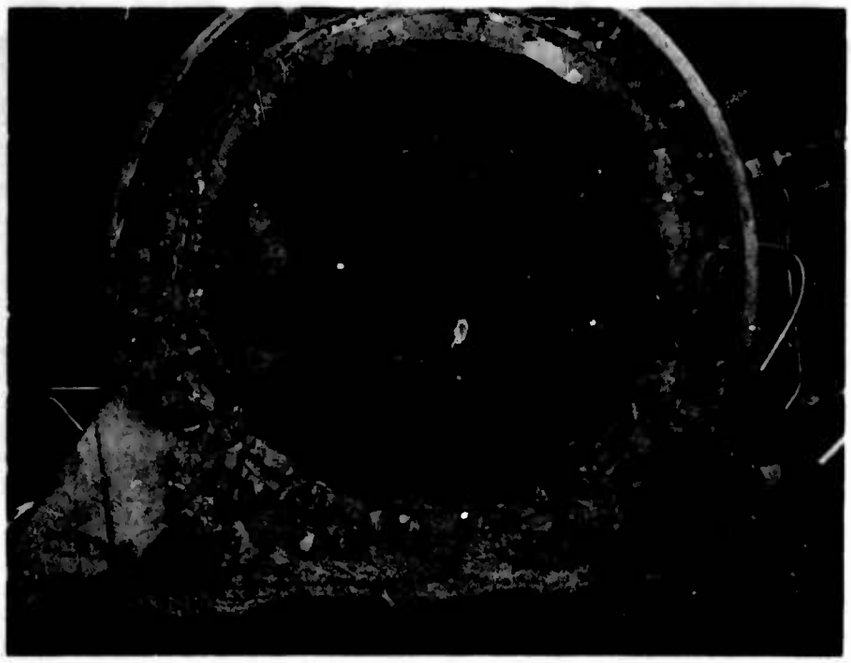

Figure VI-71. Postfire Nozzle Erosion, Transpiration Chamber SN 005, Test 1.2-13-WAM-046 (u)

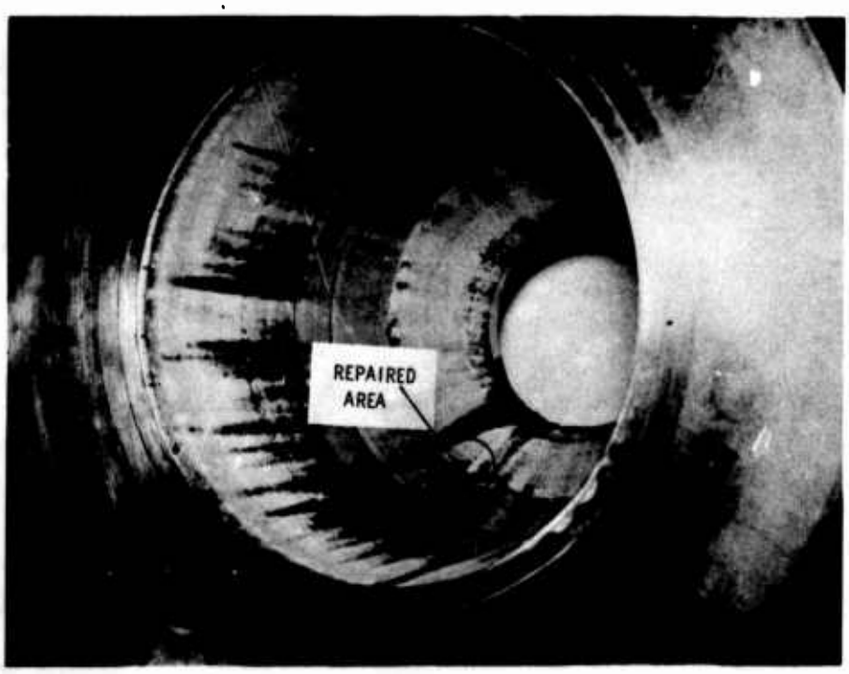

Figure VI-72. Postfire Chamber Erosion, SN 004.6 Transpiration Chamber, Test 1.2-13-WAM-049 (u)

Figure VI-71, Figure VI-72

Figure VI-73. Postfire Chamber Erosion, Transpiration Chamber SN 003, Test 1.2-13-WAM-051 (u)

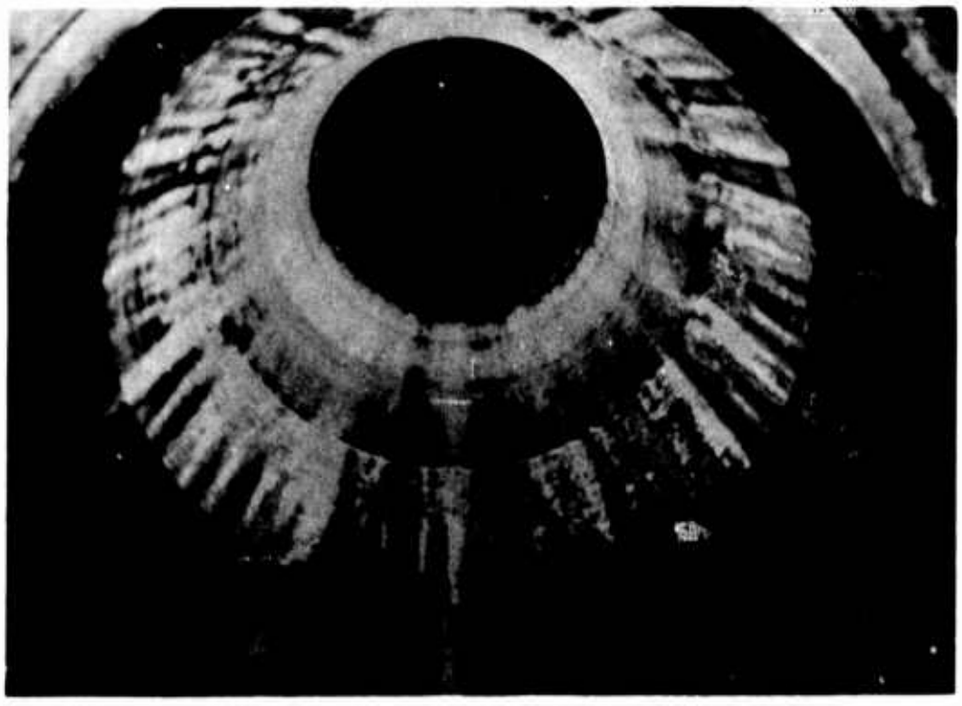

Figure VI-74. Postfire Nozzle Streaks, Transpiration Chamber SN 004, Test 1.2-13-WAM-024 (u)

Figure VI-73, Figure VI-74

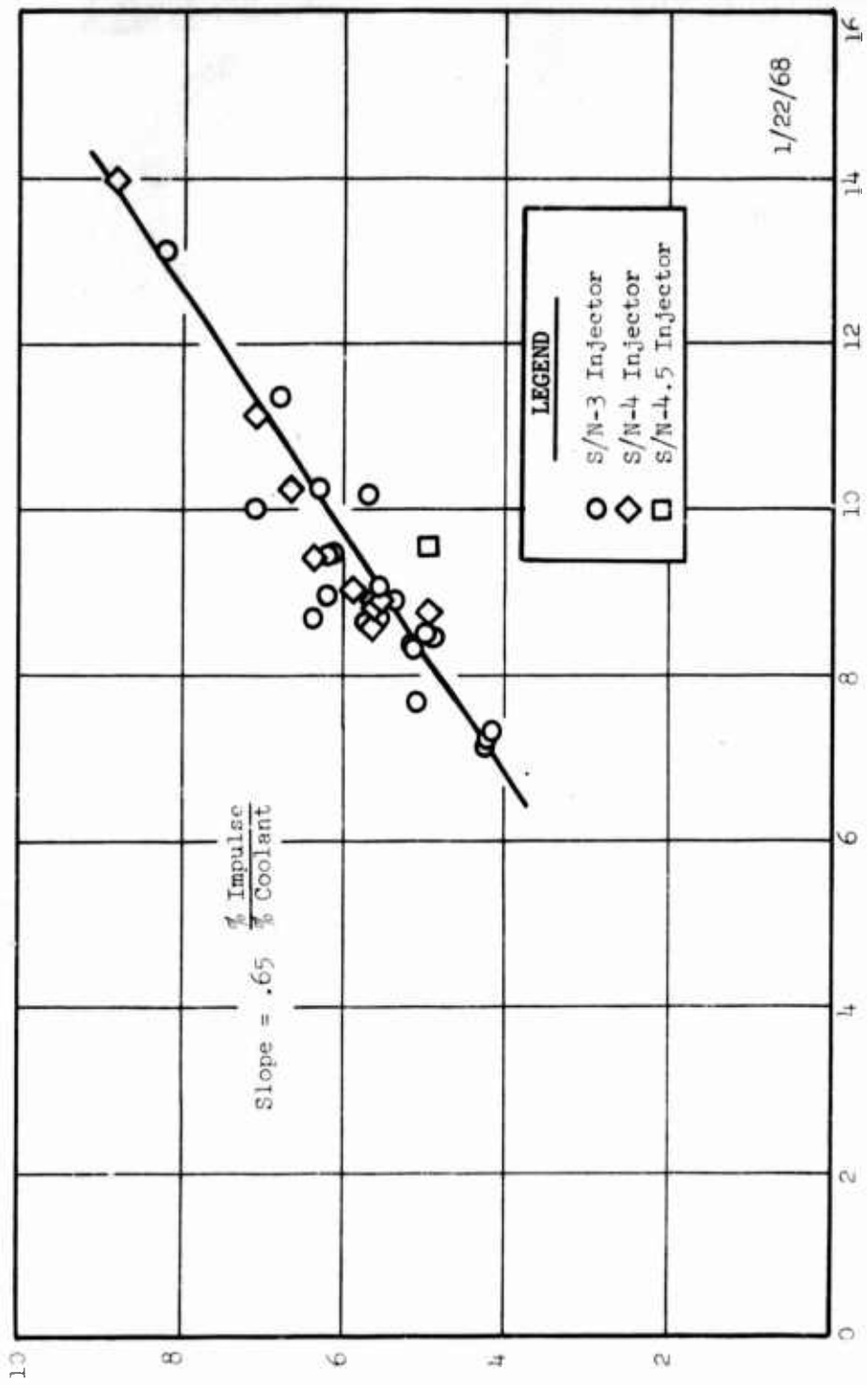

Transpiration Chamber Coolant Performance Loss,
Test Series 1.2-13-WAM (U)

Figure VI-75

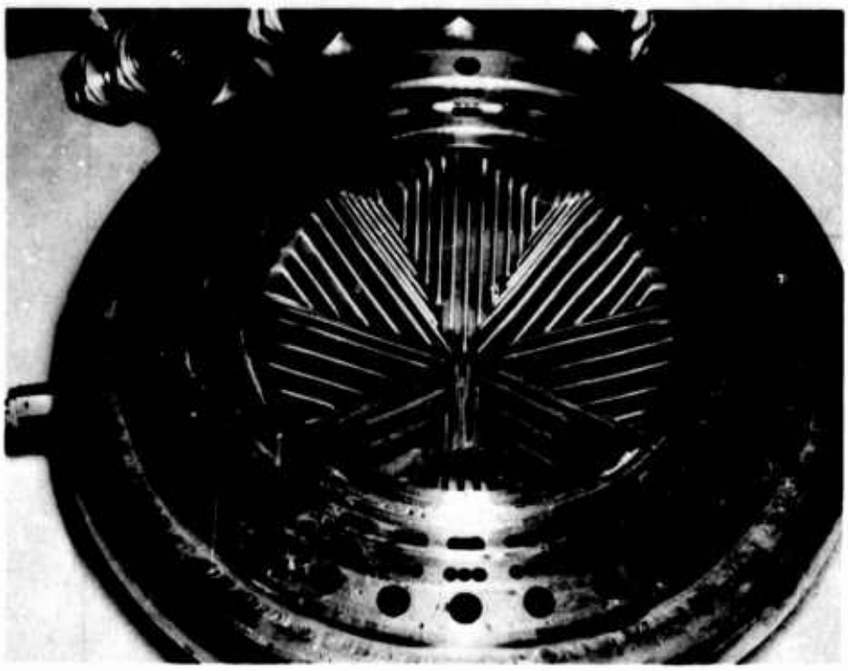

Figure VI-76. Platelet Injector, Upstream Side (u)

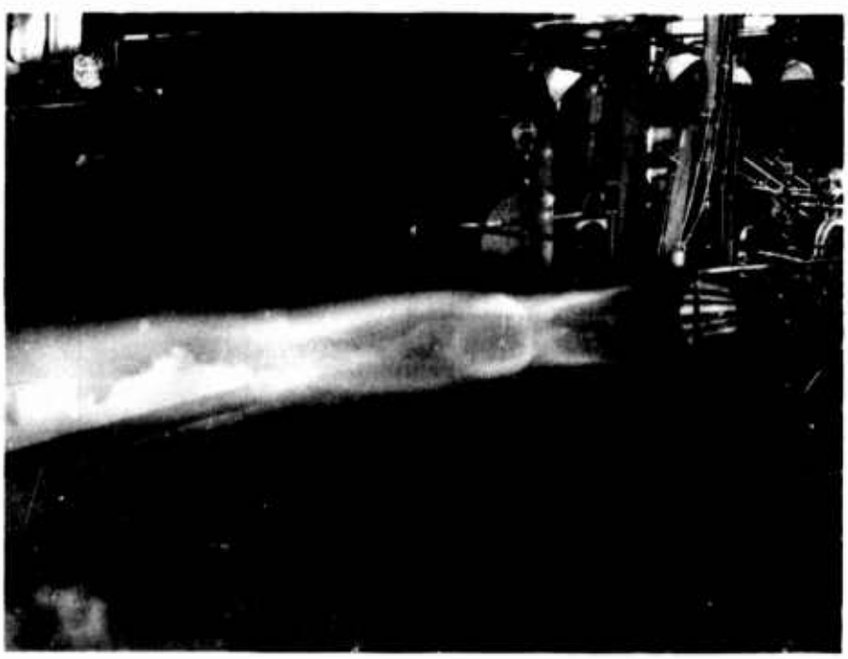

Figure VI-77. ARES Cooled Thrust Chamber Test (u)

Figure VI-76, Figure VI-77

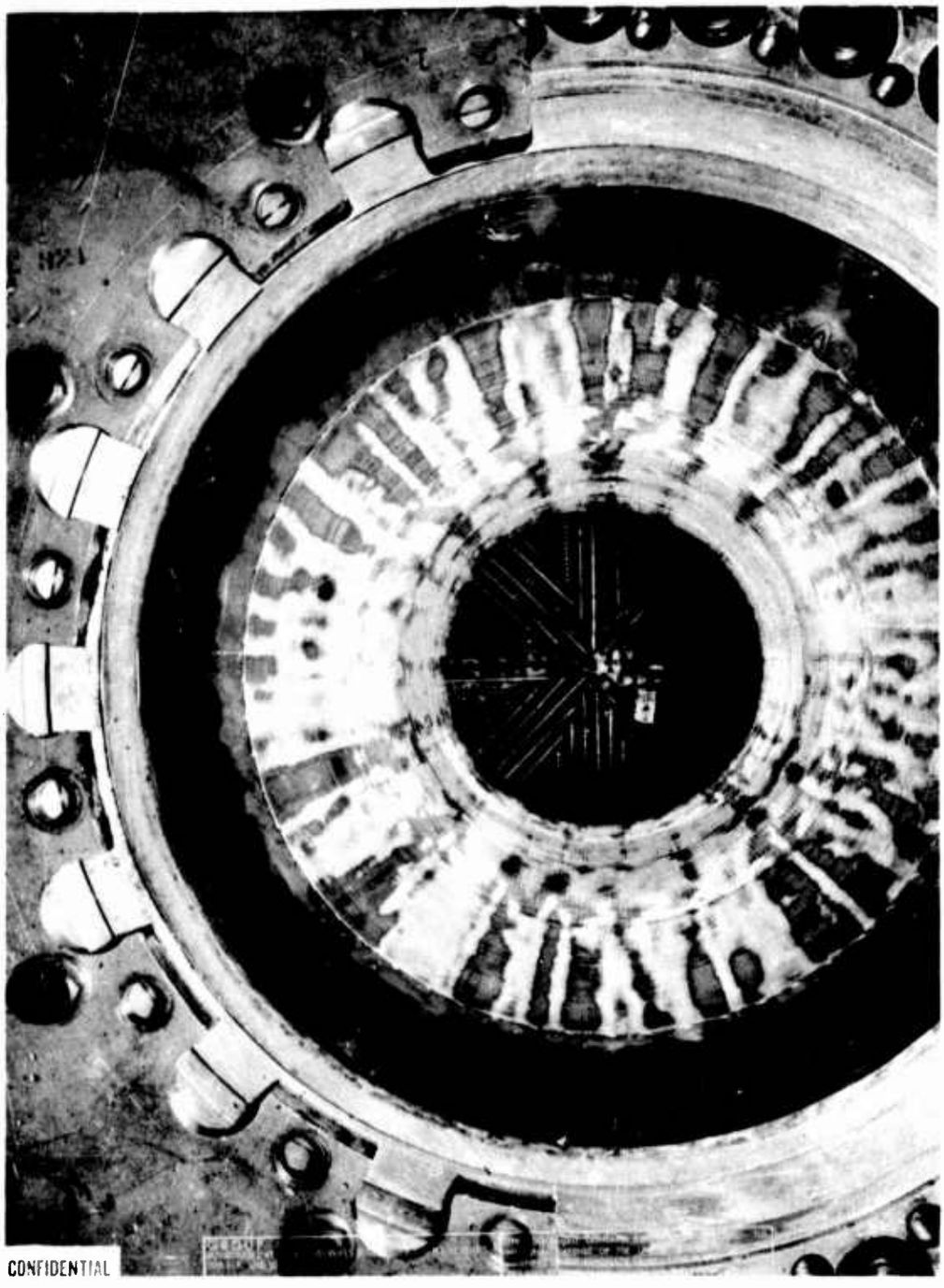

Postfire Trans Chamber Expansion Section,
Test 1.2-13-WAM-038 (U)

Figure VI-78

TEMPERATURES, °F

COMPARTMENT NUMBER	THERMOCOUPLE NUMBER	JUNCTION DEPTH, IN.	TEST NUMBER								
			-028	-030	-031	-032	-033	-034	-035	-036	-037
1	1	.0070		301	332	414					
	2	.0100		314	349	368	415	391	310	343	329
	3	.0060		313	350	399	450	403	225	240	235
2	7	.0020									
	12	.0020	265	433	511	514	642				
3	13	.0050	272	417	532	543	659	617	636	768	711
	14	.0065		784	884						
	15	.0090									
	16	.0060									
	17	.0050									
4	19	.0100							303	349	
	20	.0025									
	24	.0090	332	484	851	426	527	567	556	553	561
5	25	.0020	345	222	222	610	598				
	26	.0050	234	403	434	416	425	417	365	378	374
	27	.0030		139	118	224	329	271	314	180	163
	29	.0015						391	370		
6	31	.0010	425	693	962	276	303	304	309	373	315
	32	.0030		431	475	625	782	642	834	653	653
	33	.0020		466	494	404	387	275	313	308	282
	34	.0080		787							
	35	.0050		543	710	161	196	189	184	218	212
	36	.0020		475	786	258	309	355	370	383	367
7	37	.0020	441	710	1167	935	1409	1265	1264	1414	1370
	38	.0060		478	1327	1500	1681	1372	1003	1268	
	39	.0050		574		705	632	648	734		
	40	.0015									
	42	.0060		680	1292	1132	1493	1551	1505	1540	
8	43	.0050	480	775	665	512	645	651	708	793	727
	44	.0020		534	411	527		607	351	430	246
	46	.0025		763	953				555		
	47	.0050		415	564	234	699				
	48	.0020		320	724	349	1411	1340	1409	1572	
9	50	.0050	395	317	355	503	716	607	718	817	838
10	55	.0050	474	520	422	342	443	851	694	723	743

TEMPERATURES, °F

TEST NUMBER, 1.2-13-WAM-											
34	-035	-036	-037	-038	-039	-040	-041	-042	-043	-044	-045	-046
91	310	343	329		420	409	333	348	298	373	373	475
03	225	240	235	321	331	329	243	255	224	247	264	433
							583	594	611	623	618	629
17	636	768	711	881	835	795	584	607	562	673	693	896
							1372	1438	1218	1412	1470	1359
					1355	1226						
							739	683	617	723	955	944
	303	349		379	384	386	368	397	341	396	420	427
							351	407	380	614	393	460
57	556	553	561	664								
7	365	378	374	279	291	306	376	377	370	383	399	277
1	314	180	163	172	186	172	272	181	158	190	178	219
1	370											
4	309	373	315	380	378	356	293	343	353	350	353	398
2	834	653	653	387	407							
5	313	308	282	262	257	273	274	230	231	261	239	312
9	184	218	212		253		233	350	350	399	425	423
5	370	383	367	492	508	475	474	577	494	577	596	801
5	1264	1414	1370	1468	1463	1432	1337	1444	1337	1481	1532	1427
2	1003	1268										
8	734											
					648	700	595		738	724		
1	1505	1540						1681				
1	708	793	727									
7	351	430	246	860	518	405						
	555											
0	1409	1572										
7	718	817	838	841	1004	855	817		816	892	929	
1	694	723	743	1156		1129	953	1138	1114	1269	1298	

Steady State Temperature Summary Transpiration
Cooled Chamber, SN 005

Figure VI-79

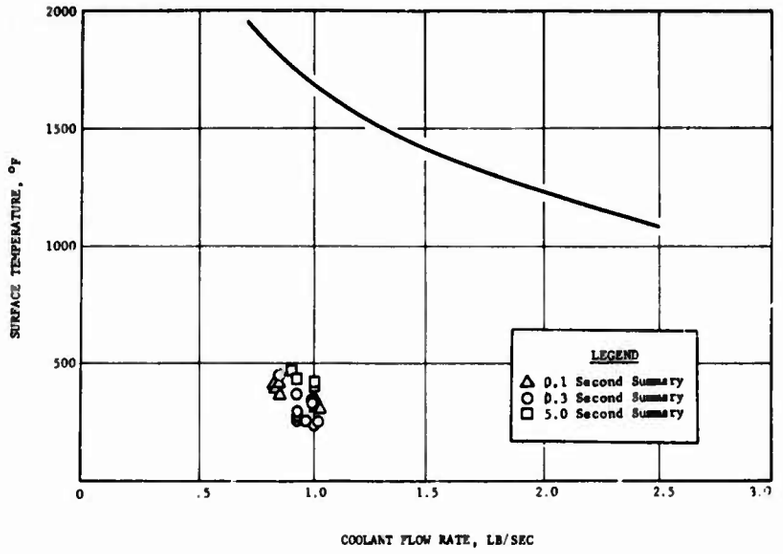

Compartment No. 1

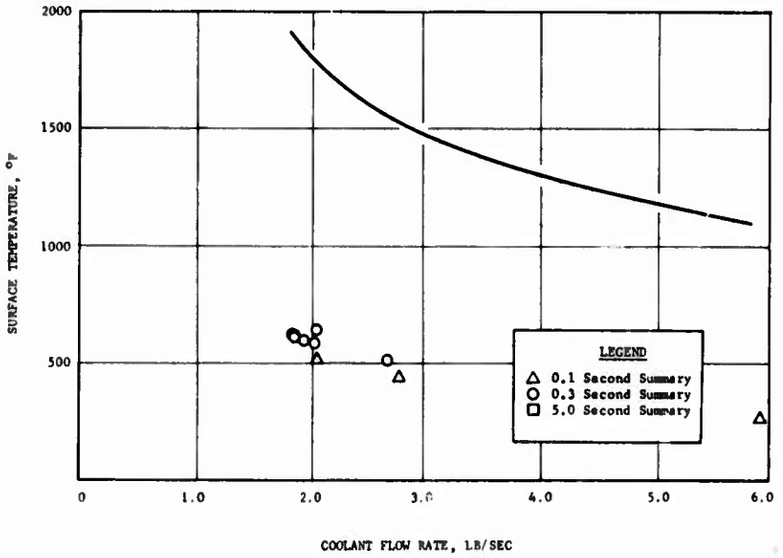

Compartment No. 2

Compartment Temperature Summary, Transpiration-Cooled Chamber SN 005

Figure VI-80, Sheet 1 of 6

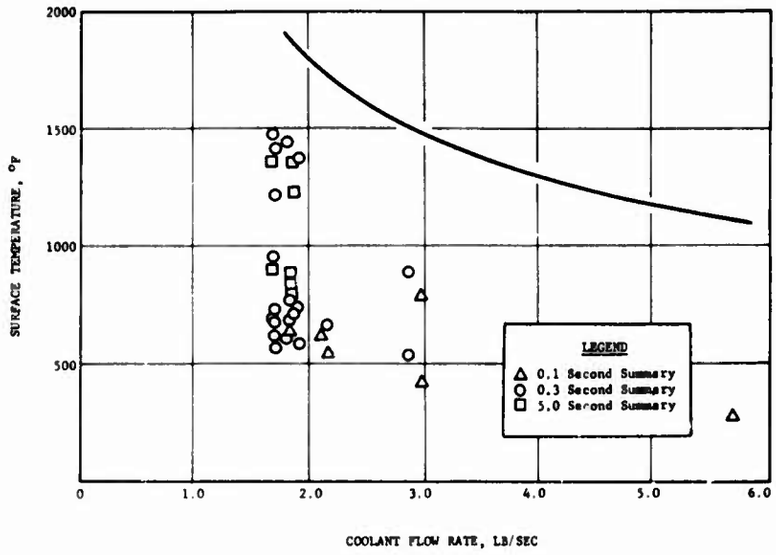

Compartment No. 3

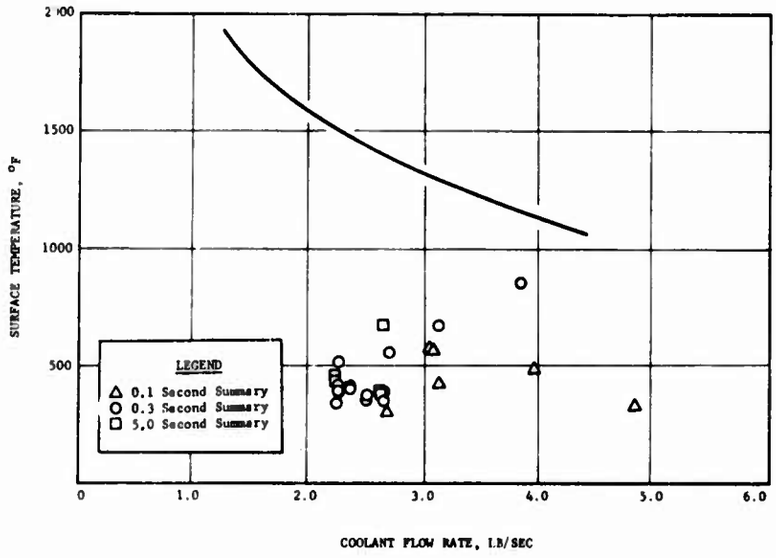

Compartment No. 4

Compartment Temperature Summary, Transpiration-Cooled
Chamber SN 005

Figure VI-80, Sheet 2 of 6

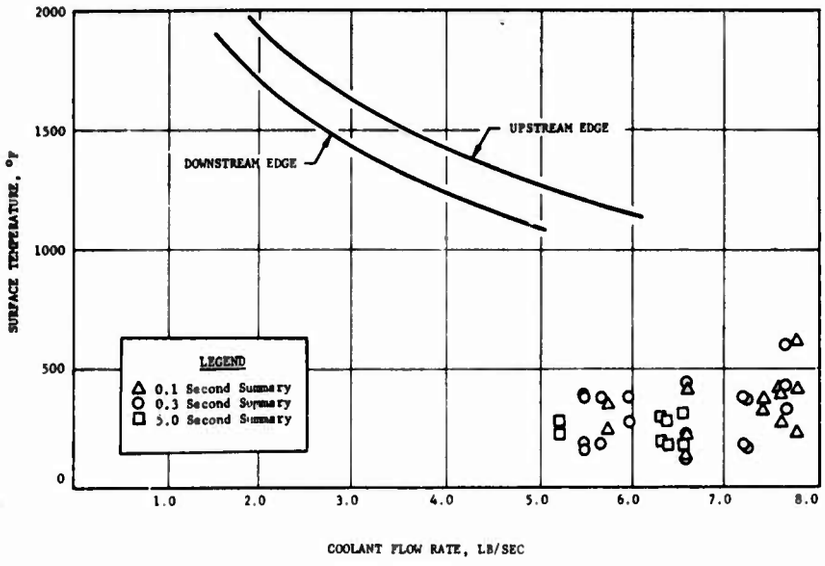

Compartment No. 5

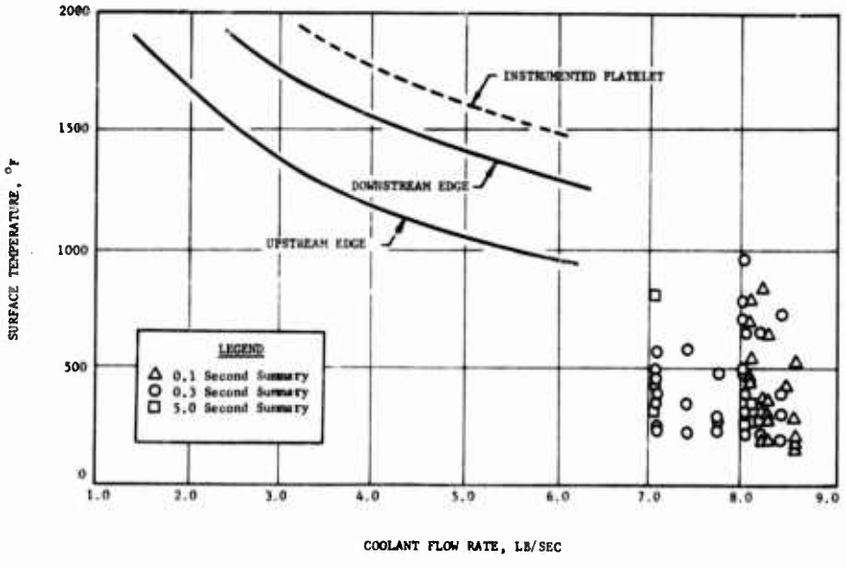

Compartment No. 6

Compartment Temperature Summary, Transpiration-Cooled Chamber SN 005

Figure VI-80, Sheet 3 of 6

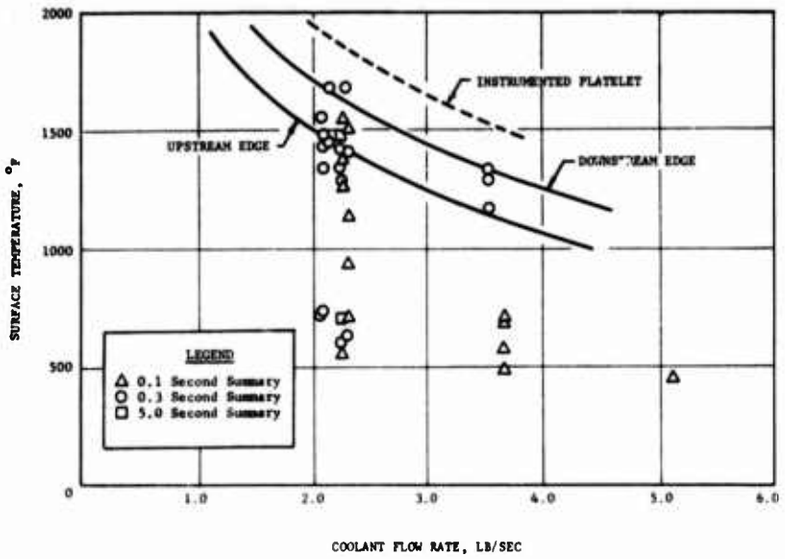

Compartment No. 7

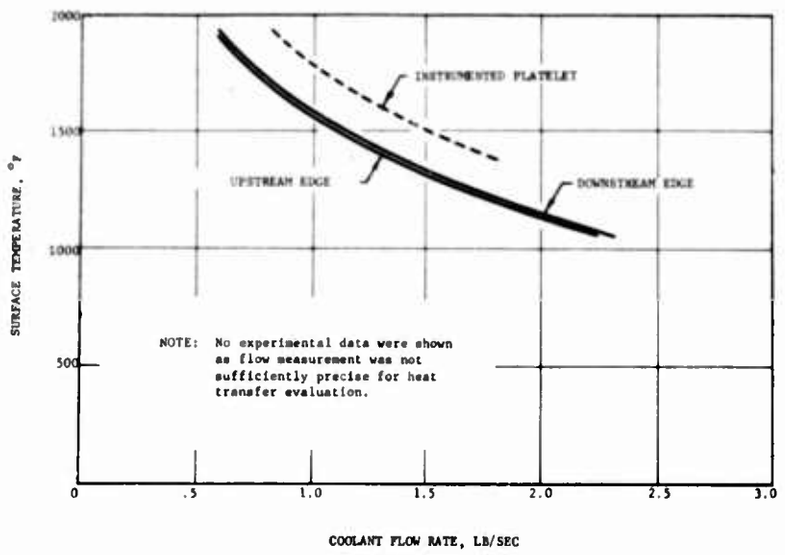

Compartment No. 8

Compartment Temperature Summary, Transpiration-Cooled Chamber SN 005

Figure VI-80, Sheet 4 of 6

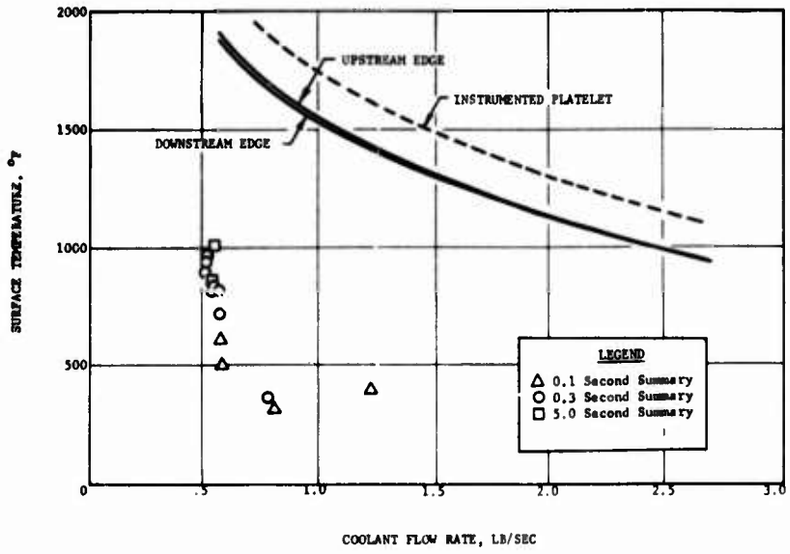

Compartment No. 9

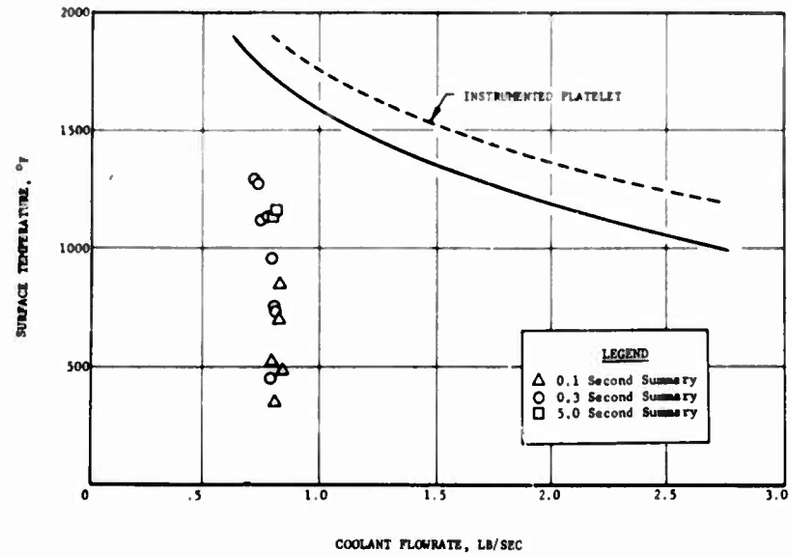

Compartment No. 10

Compartment Temperature Summary, Transpiration-Cooled Chamber SN 005

Figure VI-80, Sheet 5 of 6

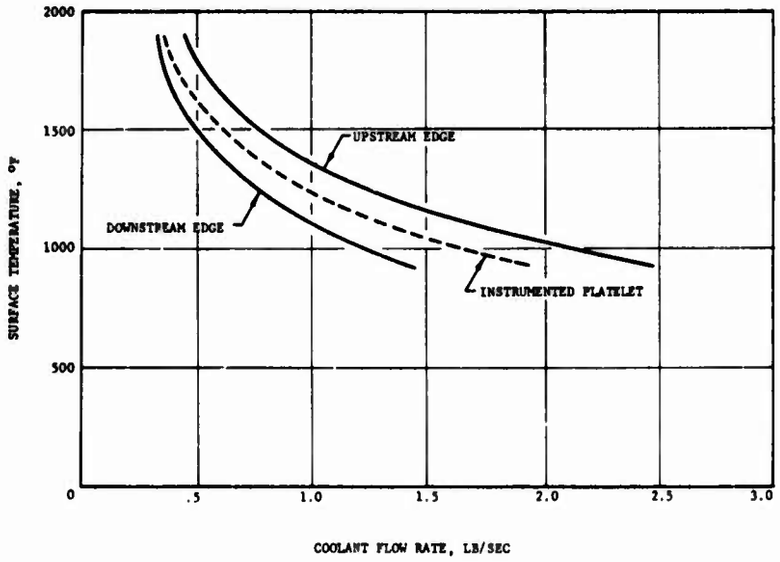

Compartment No. 11

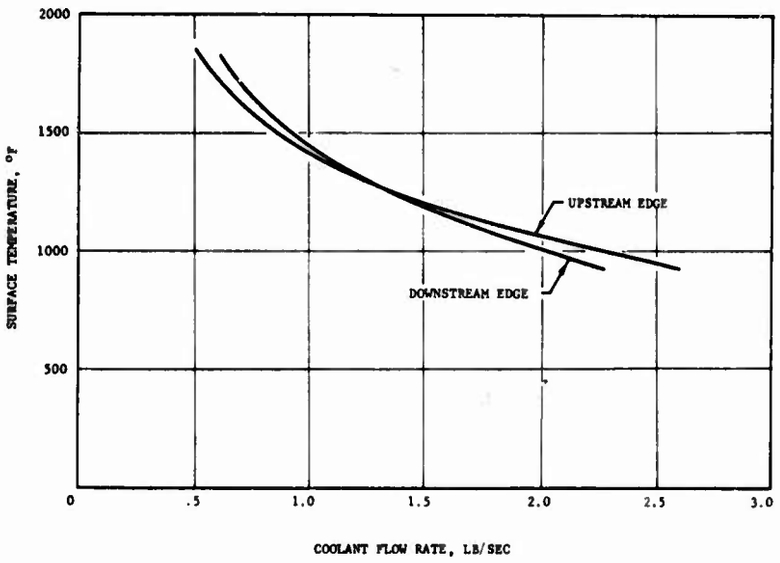

Compartment No. 12

Compartment Temperature Summary, Transpiration-Cooled
Chamber SN 005

Figure VI-80, Sheet 6 of 6

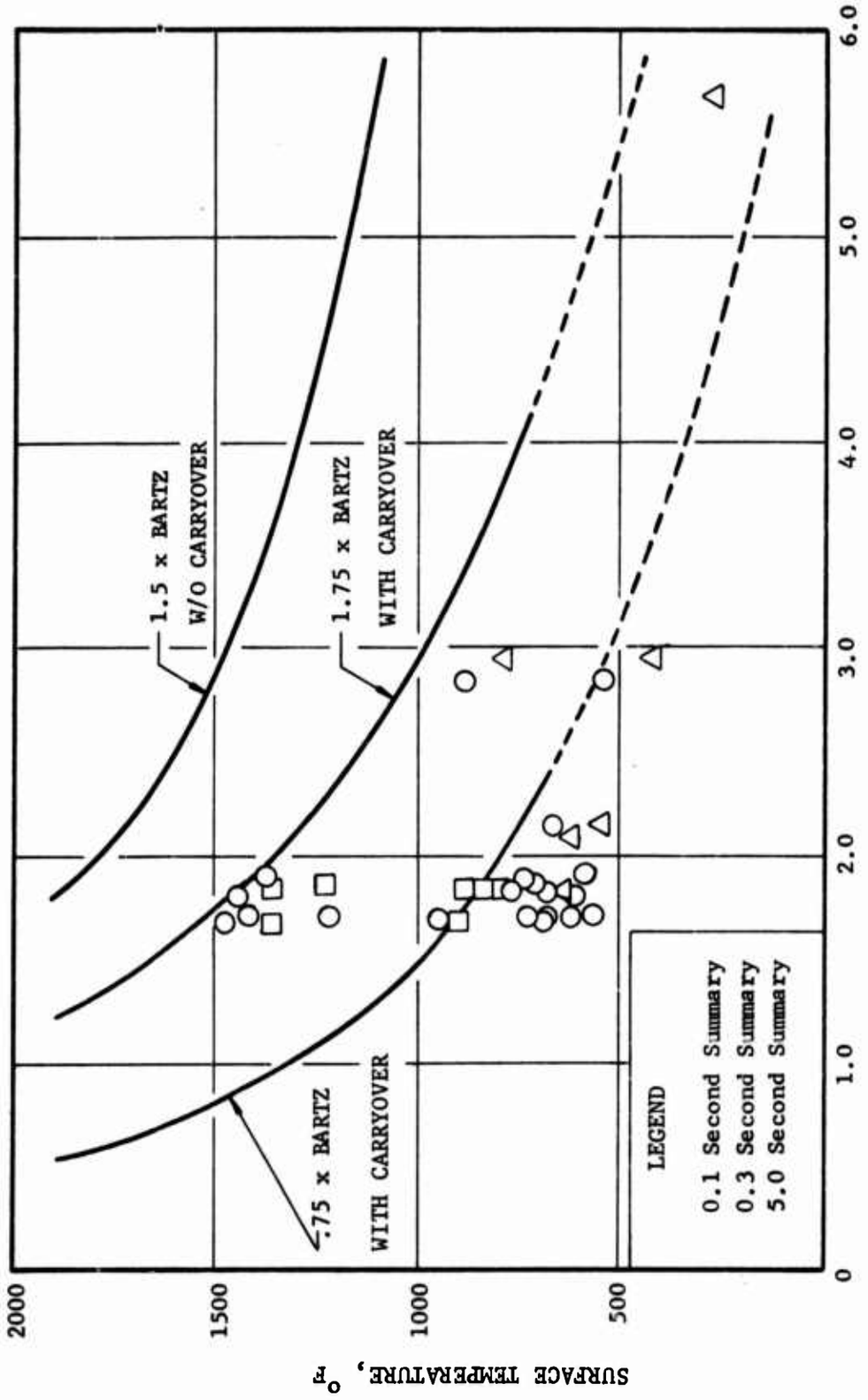

Compartment No. 3 Data Correlation, SN 005 Transpiration-Cooled Chamber

Figure VI-81

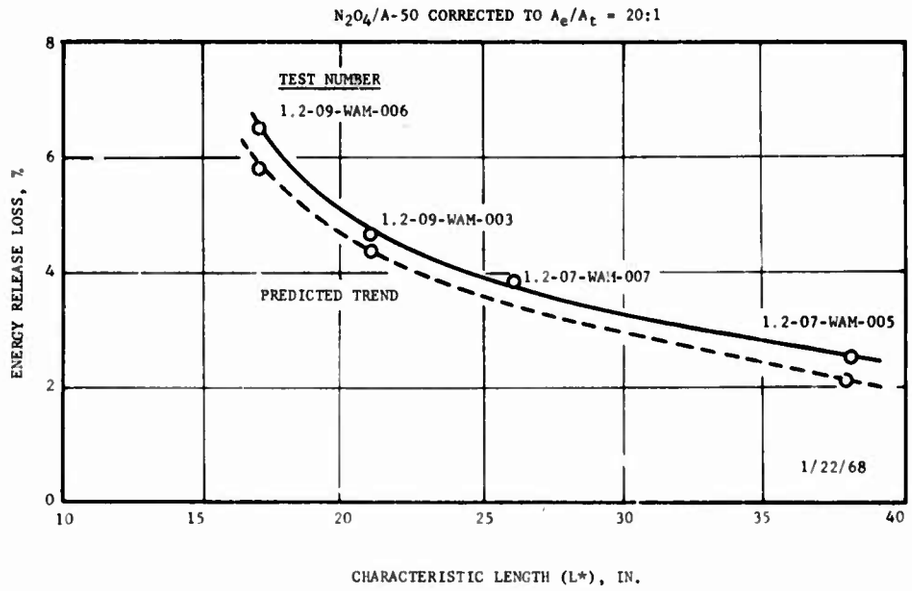

Figure VI-82. Effect of Characteristic Length (L*) on Energy Release Loss Mark 125 (u)

INJECTOR	PREDICTED ERL	NUMBER OF ELEMENTS	DROP ATOMIZATION	RELATIVE VELOCITY	FUEL IMPINGEMENT ON WALL	NET RADIAL FORCES	FUEL DISTRIBUTION	OXIDIZER DISTRIBUTION
MARK 125	4.2%	F	G	F	P	P	G	G
MARK 125 CANDELABRA	3.9%	G	G	F	E	G	G	F
MARK 125 - 3 ORST	4.2%	F	G	F	E	G	G	G
WARP I	3.6%	G	G	F	E	E	E	E
WARP II	1.5%	G	G	E	E	E	E	E
WARP III	1.2%	G	G	E	E	E	E	E
PLATELET, SHOWERHEAD	2.8%	E	G	G	E	E	E	G
PLATELET, IMPINGING	0.4%	E	E	F	E	E	E	G

LEGEND
E = EXCELLENT F = FAIR
G = GOOD P = POOR

Figure VI-83. Performance and Compatibility Characteristics of ARES Injector Configurations (u)

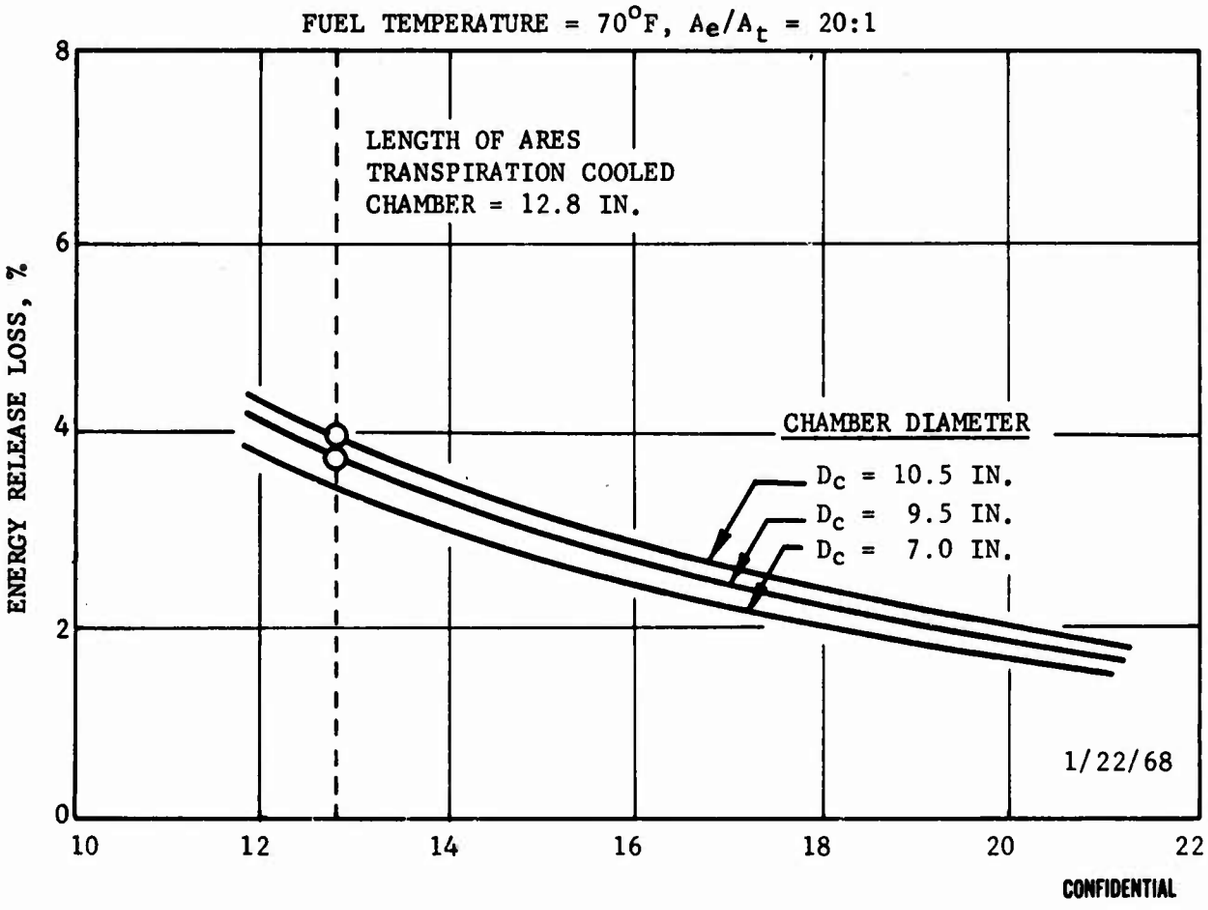

Effect of Chamber Geometry upon Energy Release Loss,
WARP I Injector (U)

Figure VI-84

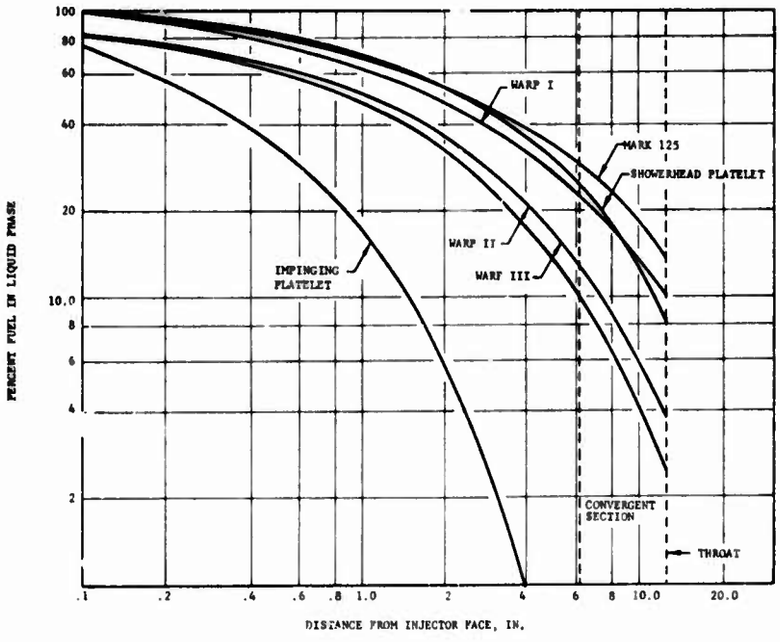

Figure VI-85. Fuel Vaporization Characteristics of ARES Injectors

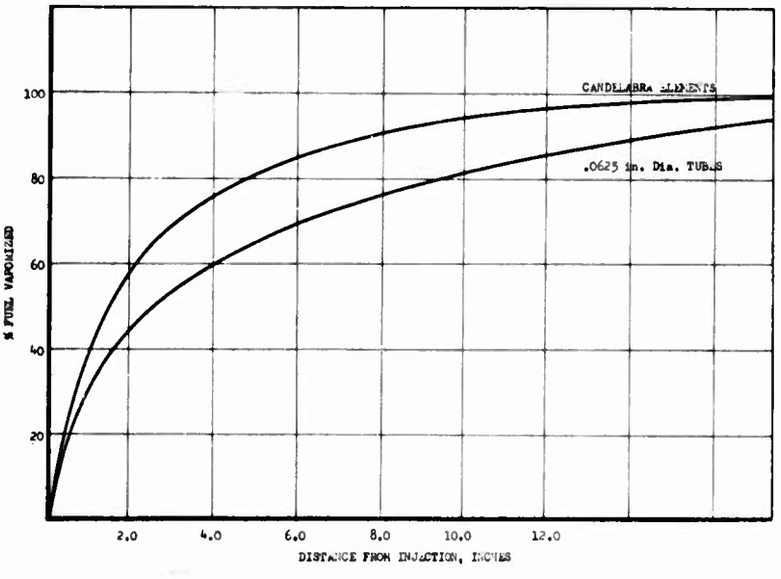

Figure VI-86. Candelabra Injector Fuel Vaporization Rates

Figure VI-85, Figure VI-86

REF. NASA TR-R 67, 1960

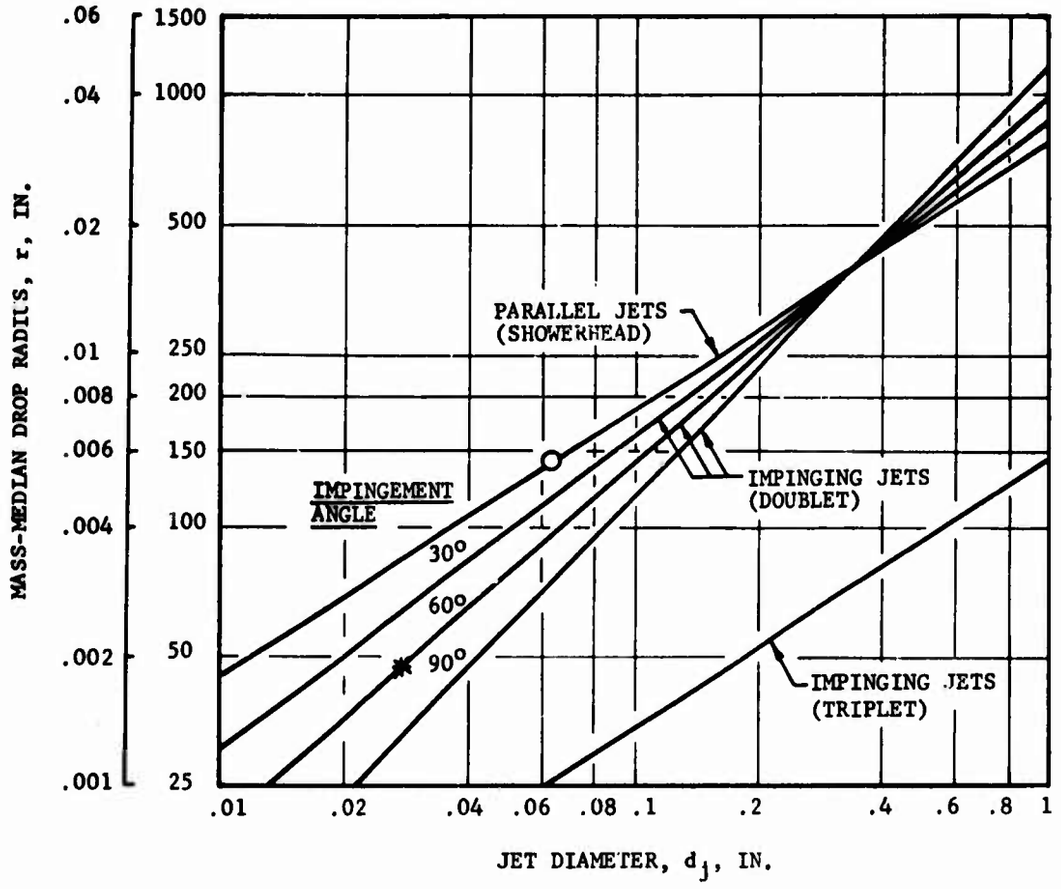

0 MARK 125 INJECTOR
* IMPINGING PLATELET INJECTOR

Drop Size Determined From Experimental Engine Performance

Figure VI-87

INJECTOR	WARP I	WARP II	WARP III
Chamber Dia	9.5 in.	9.5 in.	9.5 in.
No. of Tubes	753	753	712
Ox. Injection Velocity(1)	90 ft/sec	400 ft/sec	400 ft/sec
Fuel Injection Velocity	130 ft/sec	130 ft/sec	100 ft/sec
No. Orifice Circles	16	16	14
Vaporization (2)	77%	86%	89%
Location (3)	0.236 in.	0.236 in.	0.192 in.
Divergence (4)	60°	45°	45°
Fuel Tube Dia.	0.053 in.	0.053 in.	0.0625 in.
Oxidizer Orifice Dia.	0.128 in.	0.128 in.	0.128 in.
DESCRIPTION	Coaxial injection elements. Fuel tube is directed axially and attached to one side of oxidizer annulus. The tube extends to the end of the element.	Coaxial injection elements. The fuel tube is directed axially and extends only to the beginning of the divergent section.	Coaxial injection elements. The fuel tube is directed axially and extends only to the beginning of the divergent section.

(1) At plane of fuel injection.

(2) Fuel Vaporization at entrance to conical section of throat (6.2 in.)

(3) Distance from center of outer element row to chamber wall.

(4) Element divergent section included angle.

WARP I, II and III Injector Characteristics (U)

Figure VI-88

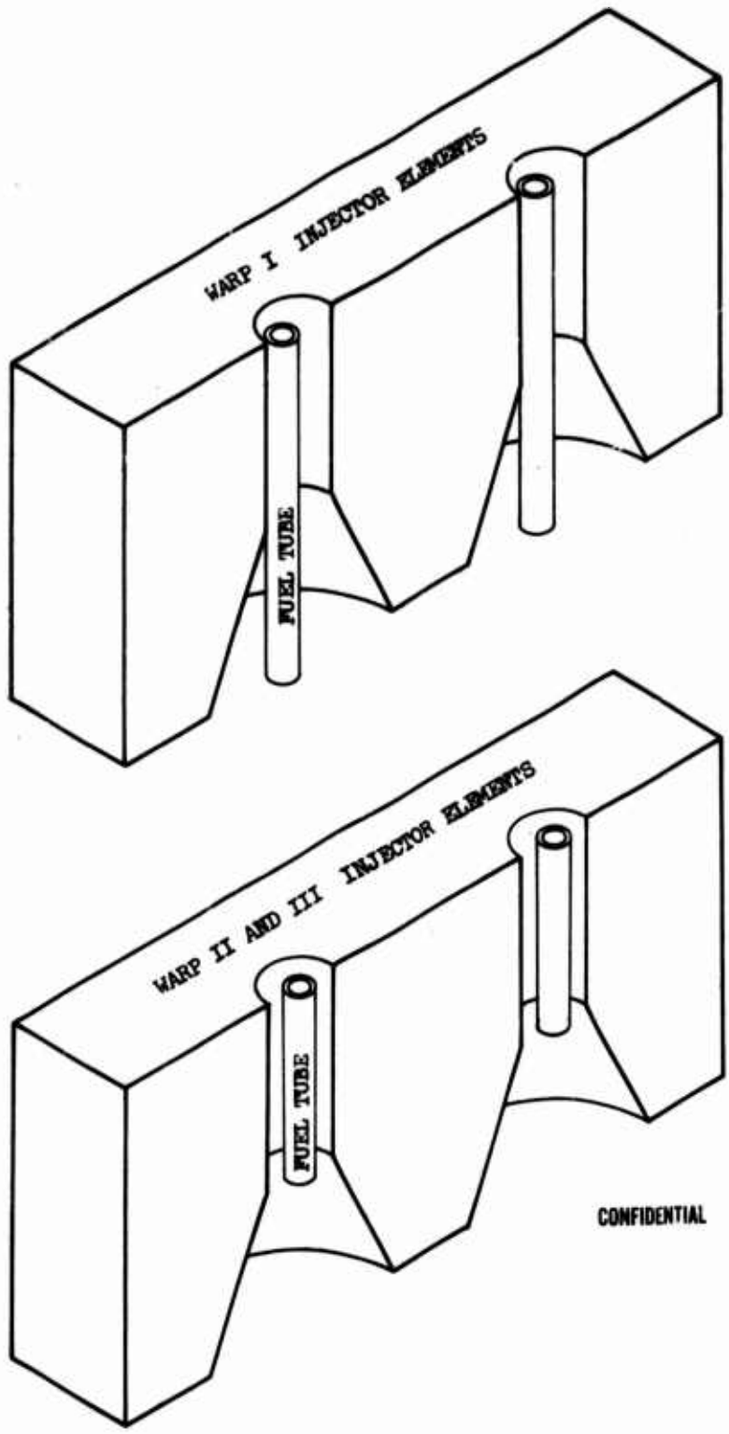

WARP Secondary Injector Element Configurations (U)

Figure VI-89

GROUP 1		ORIGINAL SYSTEM EVALUATION		14 Tests Total	
SERIES	TEST NO.	CONFIGURATION	RESULTS	APPLICABLE TEST	$MRD_{LOSS,SEC}$
#1	1-14	1. Platelet Injector SN-001. 2. Unsymmetrical turbulators. 3. Biased multi-hole orifice plate. 4. Adapter-Diffuser (15° wall).	1. Skewed flow. 2. Low peripheral flow. 3. Flows not uniform radially or circumferentially, and not axi-symmetric. Low peripheral flow.	1.2-16-WAM-007 thru 1.2-16-WAM-010	1.1

GROUP 2		COMPONENT FLOW CHARACTERISTICS		11 Tests Total	
SERIES	TEST NO.	CONFIGURATION	RESULTS	APPLICABLE TEST	$MRD_{LOSS,SEC}$
#2	15-18	1. No injector. 2. Unsymmetrical turbulators. 3. Biased multi-hole orifice plate. 4. Adapter-Diffuser (15° wall).	1. Slightly skewed flow. 2. Low peripheral flow. 3. High core flow.	None	Not calculated.
#3	19-21	1. No injector. 2. No turbulators. 3. Unbiased multi-hole orifice plate. 4. Adapter-Diffuser (15° wall).	1. Flow attachment to diffuser wall. 2. Low peripheral flow. 3. Very high core flow.	None	Not calculated.
#4	22-24	1. No injector. 2. No turbulators. 3. Adapter Diffuser (15° wall)	1. Flow attachment to diffuser wall. 2. Low peripheral flow. 3. Very highly cored.	None	Not calculated.

Air Flow Test Program-Original System Evaluation and Component Flow Characteristics

Figure VI-90

(This page is Unclassified)

GROUP 3		EVEN GAS FLOW EVALUATION		114 Tests Total	
SERIES	TEST NO.	CONFIGURATION	RESULTS	APPLICABLE TEST	$MRD_{LOSS,SEC}$
#5	25-28	1. Platelet SN-001 injector. 2. Unsymmetrical turbulators. 3. Biased multi-hole orifice plate 4. Coolie Hat #1 (119-$\frac{1}{4}$" holes). 5. Adapter-Diffuser (15° wall).	1. Symmetrical flow 2. Very high peripheral flow.	None	Not calculated.
#6	29-33	1. Platelet SN-001 injector. 2. Unsymmetrical turbulators. 3. Biased multi-hole orifice plate #2. 4. Coolie Hat #2 (119-.375" holes). 5. Adapter-Diffuser (15° wall).	1. Symmetrical flow. 2. High peripheral flow. 3. Increased flow in the center.	None	Not calculated.
#7	34-38	1. No injector. 2. No turbulators. 3. No multi-hole orifice plate. 4. Diffuser cone. 5. Adapter-Diffuser (15° wall).	1. Skewed flow. 2. Low peripheral flow. 3. Highly cored flow in center.	None	Not calculated.
#8	39-42	1. No injector. 2. No turbulators. 3. No multi-hole orifice plate. 4. Diffuser cone with screen. 5. Adapter-Diffuers (15° wall).	1. Skewed flow. 2. Low peripheral flow. 3. Flow not uniform radially or circumferentially with high flow in the center.	None	Not calculated.
#9	44-51	1. Platelet injector SN-001 with vane extenders. 2. Symmetrical turbulators. 3. Center body. 4. Adapter-Diffuser (15° wall).	1. Skewed flow. 2. Low peripheral flow. 3. Flows not uniform radially or circumferentially with low peripheral flow.	None	Not calculated.

Air Flow Test Program- Even Gas Flow Evaluation

Figure VI-91
Page 1 of 5

GROUP 3	EVEN GAS FLOW EVALUATION				
SERIES	TEST NO.	CONFIGURATION	RESULTS	APPLICABLE TEST	$MRD_{LOSS,SEC}$
#10	52-57	1. Platelet injector SN-001 with vane extenders. 2. Unsymmetrical turbulators. 3. Biased multi-hole orifice plate #3. 4. Coolie Hat #3 (119-.375" holes, 105-.316" holes) 5. Adapter-Diffuser (15° wall).	1. Symmetrical flow. 2. High peripheral flow.	None	Not calculated.
#11	58-61	1. Platelet injector SN-001 with vane extenders. 2. Unsymmetrical turbulators. 3. Biased multi-hole orifice plate #3. 4. Coolie Hat #4 with lower ½" removed. 5. Adapter-Diffuser (15° wall).	1. Symmetrical flow. 2. Lower peripheral flow than series #10.	None	Not calculated.
#12	62-66	1. Platelet injector SN-001 with vane extenders. 2. Unsymmetrical turbulators. 3. Biased multi-hole orifice plate #3. 4. Screen coolie hat. 5. Adapter-Diffuser (15° wall).	1. Skewed flow. 2. Slightly low peripheral flow.	None	Not calculated.

Figure VI-91
Page 2 of 5

Air Flow Test Program-Even Gas Flow Evaluation

GROUP 3		EVEN GAS FLOW EVALUATION			
SERIES	TEST NO.	CONFIGURATION	RESULTS	APPLICABLE TEST	MRD_{LOSS}, SEC
#13	67-70	1. Platelet injector SN-001 with vane extenders. 2. Unsymmetrical turbulators. 3. Biased multi-hole orifice plate #3. 4. Screen coolie hat. 5. Adapter-Diffuser (15° wall).	1. Skewed flow. 2. High peripheral flow.	None	Not calculated.
#14	71-78	1. Platelet injector SN-001 with vane extenders. 2. Symmetrical turbulators. 3. Screen coolie hat. 4. 4° diffuser cone. 5. Adapter-Diffuser (15° wall).	1. Skewed flow. 2. Low peripheral flow.	None	Not calculated.
#15	79-84	1. Platelet injector SN-001 with vane extenders. 2. Symmetrical turbulators. 3. Screen coolie hat. 4. Adapter-Diffuser (15° wall).	1. Skewed flow. 2. Low peripheral flow.	None	Not calculated.
#16	85-87	1. Platelet injector SN 001 with vane extenders. 2. Symmetrical turbulators. 3. Unbiased multi-hole orifice plate. 4. Screen coolie hat. 5. Adapter-Diffuser (15° wall).	1. Skewed flow. 2. Low peripheral flow. 3. Flows not uniform radially or circumferentially, and not axi-symmetric.	None	Not calculated.

Air Flow Test Program-Even Gas Flow Evaluation

GROUP 3		EVEN GAS FLOW EVALUATION			
SERIES	TEST NO.	CONFIGURATION	RESULTS	APPLICABLE TEST	$MRD_{LOSS,SEC}$
#17	88-96	1. Platelet injector SN-001 with vane extenders. 2. Symmetrical turbulators. 3. Screen coolie hat. 4. 4° diffuser cone with 57% screen. 5. Adapter-Diffuser (15° wall).	1. Skewed flow. 2. Low peripheral flow. 3. Flows not uniform radially or circumferentially with high peripheral flows.	None	Not calculated.
#20	110-115	1. Platelet injector SN 002. 2. Symmetrical turbulators. 3. 4° diffuser cone with screen. 4. Adapter-Diffuser (15° wall).	1. Skewed flow. 2. Low peripheral flow. 3. Low flow in center, high unsymmetrical flow at periphery.	None	Not calculated.
#21	116	1. Platelet injector SN-002. 2. Symmetrical turbulators. 3. 4° diffuser cone. 4. Adapter-Diffuser (15° wall).	1. Highly cored flow in center, no peripheral flow.	None	Not calculated.
#24	17-27	1. Platelet injector SN-002. 2. Symmetrical turbulators. 3. 4° diffuser cone with screen. 4. Adapter-Diffuser (15° wall).	1. Skewed flow. 2. Flow not uniform radially or circumferentially with high peripheral flows.	None	Not calculated.
#25	28	1. Platelet injector SN-002. 2. Symmetrical turbulators. 3. 4° diffuser cone with dash 3 insert. 4. Adapter-Diffuser (15° wall).	1. High peripheral flow. 2. Highly cored flow in center.	None	Not calculated.

Figure VI-91
Page 4 of 5

Air Flow Test Program-Even Gas Flow Evaluation

GROUP 3		EVEN GAS FLOW EVALUATION			
SERIES	TEST NO.	CONFIGURATION	RESULTS	APPLICABLE TEST	$MRD_{LOSS, SEC}$
#26	29-36	1. Platelet injector SN-002. 2. Symmetrical turbulators. 3. 4° diffuser cone with dash 1 insert. 4. Adapter-Diffuser (15° wall).	1. Flow not uniform radially or circumferentially. 2. Low peripheral flow.	None	Not calculated.
#27	1-8	1. Platelet injector SN-003 with vane extenders. 2. Symmetrical turbulators. 3. Screened 4° diffuser. 4. Adapter-Diffuser (15° wall).	1. Skewed flow. 2. Low peripheral flow. 3. Flow not uniform radially or circumferentially.	None	Not calculated.

Figure VI-91
Page 5 of 5

Air Flow Test Program-Even Gas Flow Evaluation

GROUP 4		INJECTOR SCREEN EVALUATION			78 Tests Total
SERIES	TEST NO.	CONFIGURATION	RESULTS	APPLICABLE TEST	$MRD_{LOSS,SEC}$
#18	97-104	1. Platelet injector SN-001 with vane extenders and 8" flat screen disc. 2. Symmetrical turbulators. 3. 4° diffuser cone with screen. 4. Adapter-Diffuser (15° wall).	1. Skewed flow. 2. Low peripheral flow. 3. Flow relatively more uniform radially but not circumferentially.	None	Not calculated.
#19	105-109	1. Platelet injector SN-001 with vane extenders and 8½" flat screen disc. 2. Symmetrical turbulators. 3. 4° diffuser cone with screen. 4. Adapter-Diffuser (15° wall).	1. Slightly skewed flow. 2. Desirable peripheral flow.	None	Not calculated.
#22	1-9	1. Platelet injector SN-001 with vane extenders and notched 8½" screen. 2. Symmetrical turbulators. 3. 4° diffuser with screen. 4. Adapter-Diffuser (15° wall).	1. Slightly skewed flow. 2. Low peripheral flow. 3. Normal short vane area flow.	1.2-16-WAM-014 1.2-16-WAM-015	None
#23	10-16	1. Platelet injector SN-001 with vane extenders and 8½" notched screen. 2. Symmetrical turbulators. 3. 4° diffuser with dash 1 insert. 4. Adapter-Diffuser (15° wall).	1. Flow not uniform circumferentially nor radially.	None	Not calculated.
#31	4-9	1. Platelet injector SN-002 with cross grid screen. 2. Symmetrical turbulators. 3. 4° diffuser cone. 4. Adapter-Diffuser (15° wall).	1. Skewed flow. 2. Low peripheral flow.	None	Not calculated.

Air Flow Test Program- Injector Screen Evaluation

Figure VI-92
Sheet 1 of 3

GROUP 4		INJECTOR SCREEN EVALUATION			
SERIES	TEST NO.	CONFIGURATION	RESULTS	APPLICABLE TEST	$MRD_{LOSS,SEC}$
#33	1-8	1. Platelet injector SN-0 3 without vane extenders. 2. Symmetrical turbulators. 3. 4° diffuser cone with screen. 4. Adapter-Diffuser (15° wall)	1. Flow fairly uniform radially and circumferentially without large deviations from average.	1.2-16-WAM-016	4.2
#34	9-16	1. Cross grid plate. 2. 4° diffuser cone with dash 7A insert (1.75" sharp edge). 3. Symmetrical turbulators. 4. Adapter-Diffuser (15° wall).	1. Relatively more uniform radial flow but not uniform circumferentially flow.	None	Not calculated.
#37	6-13	1. Cross grid plate. 2. Symmetrical turbulators. 3. 4° diffuser cone with dash 6 insert (1.6" sharp edge). 4. Adapter-Diffuser (15° wall).	1. Skewed flow. 2. Low peripheral flow.	None	Not calculated.
#39	1-8	1. Platelet injector SN-002. 2. Symmetrical turbulators. 3. 4° diffuser cone with dash 6 insert (1.6" sharp edge). 4. Adapter-Diffuser (15° wall).	1. Skewed flow. 2. Low peripheral flow. 3. Short P to long vane variation. 4. Low total pressure drop.	None	Not calculated.
#51	1-4	1. Cross grid plate. 2. 4° diffuser cone with 1.5 insert. 3. Symmetrical turbulators. 4. Adapter-Diffuser (15° wall)	1. Low total pressure drop. 2. Non-uniform radial flow.	None	Not calculated.

Figure VI-92
Sheet 2 of 3

Air Flow Test Program-Injector Screen Evaluation

GROUP 4		INJECTOR SCREEN EVALUATION			
SERIES	TEST NO.	CONFIGURATION	RESULTS	APPLICABLE TEST	$MRD_{LOSS,SEC}$
#52	5-8	1. Cross grid plate. 2. 4° diffuser cone with 1.6 insert. 3. Symmetrical turbulators. 4. Adapter-Diffuser (15° wall).	1. No change from #51	None	Not calculated.
#53	9-12	1. Mark 125 injector. 2. Cross grid plate. 3. 4° diffuser cone with 1.6 insert. 4. Symmetrical turbulators. 5. Adapter-Diffuser (15° wall).	1. Uniform flow circumferentially. 2. Very uneven flow radially. 3. Low total pressure drop.	None	Not calculated.
#54	13-20	1. Platelet injector. 2. Cross grid plate. 3. 4° diffuser cone with 1.6 insert. 4. Symmetrical turbulators. 5. Adapter Diffuser (15° wall).	1. Uniform circumferential flow. 2. Relatively uniform radial flow but low flow at periphery. 3. Low total pressure drop.	None	Not calculated.

Figure VI-92
Sheet 3 of 3

Air Flow Test Program--Injector Screen Evaluation

GROUP 5		WARP III FACE PLATE EVALUATIONS			50 Tests Total
SERIES	TEST NO.	CONFIGURATION	RESULTS	APPLICABLE TEST	$MRD_{LOSS,SEC}$
#29	1-3	1. Platelet injector SN-002. 2. WARP III face plate. 3. Symmetrical turbulators. 4. 4° diffuser cone with dash 5 insert (1.5" cone.) 5. Adapter-Diffuser (15° wall).	1. High peripheral flow. 2. Flow uniform circumferentially but not radially with high flow at periphery. 3. High total pressure drop.	None	Not calculated.
#30	1-3	1. Platelet injector SN-002. 2. Symmetrical turbulators. 3. 4° diffuser cone. 4. WARP III face plate. 5. Adapter-Diffuser (15° wall).	1. Very high peripheral flow and virtually zero flow in center. 2. High total pressure drop.	None	Not calculated.
#32	11-20	1. Platelet injector SN-002. 2. Symmetrical turbulators. 3. 4° diffuser cone. 4. WARP III face plate. 5. Adapter-Diffuser (15° wall).	1. Flow uniform circumferentially but not radially - high flow at periphery. 2. High total pressure drop.	None	Not calculated.
#35	1 & 2	1. SN-002 platelet - no extenders. 2. WARP III face plate, Mod #1. 3. Symmetrical turbulators. 4. All holes chamfered & .197 dia. 5. Adapter-Diffuser (15° wall).	1. High peripheral flow.	None	Not calculated.
#36	1-5	1. Platelet injector SN-002. 2. Symmetrical turbulators. 3. 4° diffuser cone. 4. WARP III face plate drilled to .197" holes. No chamfers. 5. Adapter-Diffuser (15° wall).	1. Flow uniform circumferential but not radially with higher flow at center and periphery. 2. No effect after adding 1.6" dia. diffuser insert.	None	Not calculated.

Figure VI-93

Sheet 1 of 3

Air Flow Test Program-Warp III Face Plate Evaluation

GROUP 5		WARP III FACE PLATE EVALUATIONS			
SERIES	TEST NO.	CONFIGURATION	RESULTS	APPLICABLE TEST	$MRD_{LOSS, SEC}$
#38	14-19	1. WARP III face plate with sharp edge entrances. 2. Symmetrical turbulators. 3. Platelet Injector SN-002. 4. Adapter-Diffuser (15° wall)	1. Symmetrical flow. 2. High peripheral flow. 3. Short to long vane variation. Generally increasing flow from center to periphery. 4. Uniform circumferential flow. 5. High pressure drop.	1.2-16-WAM-017	9.4
#40	1-9	1. Platelet injector SN-003. 2. Symmetrical turbulators. 3. 4° diffuser cone and aerodynamic center body. 4 197 hole WARP III face plate with 102 center holes chamfered every other hole. 5. Adapter-Diffuser (15° wall).	1. Slightly high wall flow. 2. Low flow ½" from OD. 3. High total pressure drop. 4. Generally uniform flow circumferentially but not radially. 5. Air flow followed hot test.	1.2-16-WAM-018B	3.6
#41	1-6	1. Platelet injector SN-003. 2. Symmetrical turbulators. 3. 4° diffuser cone. 4. 197 hole WARP III face plate with 102 holes chamfered. 5. Adapter-diffuser (15° wall).	1. No change from previous case with centerbody.	None	Not calculated.
#42	7 & 8	1. WARP III face plate with the 4th row chamfered. 2. Symmetrical turbulators. 3. Platelet injector SN-003. 4. No 4° diffuser cone. 5. Adapter-diffuser (15° wall).	1. High total pressure drop. 2. High flow center and periphery.	None	Not calculated.

Figure VI-93
Sheet 2 of 3

Air Flow Test Program-Warp III Face Plate Evaluation

GROUP 5		WARP III FACE PLATE EVALUATIONS			
SERIES	TEST NO.	CONFIGURATION	RESULTS	APPLICABLE TEST	MRD_{LOSS}, SEC
#43	9 & 10	1. WARP III face plate with the 4th and 5th row chamfered. 2. Symmetrical turbulators. 3. Platelet injector SN-003. 4. Adapter-Diffuser (15° wall).	1. Same as 42. 2. Moved more flow toward periphery.	None	Not calculated.
#44	11 & 12	1. WARP III face plate with the 4th, 5th and 9th rows chamfered. 2. Symmetrical turbulators. 3. Platelet injector SN-003. 4. Adapter-Diffuser (15° wall).	1. Same as 43. 2. Moved more flow toward center.	None	Not calculated.

Figure VI-93
Sheet 3 of 3

Air Flow Test Program-Warp III Face Plate Evaluation

GROUP 6		WARP II FACE PLATE EVALUATIONS		16 Tests Total	
SERIES	TEST NO.	CONFIGURATION	RESULTS	APPLICABLE TEST	$MRD_{LOSS,SEC}$
#45	14 & 15	1. Platelet injector SN-002. 2. Symmetrical turbulators. 3. WARP II face plate (753 holes). 4. Adapter-Diffuser (15° wall).	1. High total pressure drop. 2. Very high peripheral flow.	None	Not calculated.
#46	16 & 17	1. WARP II face plate (753 holes). 2. Symmetrical turbulators. 3. Without injector. 4. Adapter-Diffuser (15° wall).	1. Very high total peripheral flow. 2. High total pressure drop. 3. High peripheral flow.	None	Not calculated.
#47	18 & 19	1. WARP II face plate (753 holes) with the 11th, 13th and 15th row chamfered. 2. Symmetrical turbulators. 3. Platelet injector SN-002. 4. Adapter-Diffuser (15° wall).	1. High total pressure drop. 2. Relatively high peripheral flow. 3. Flow not uniform circumferentially.	None	Not calculated.
#48	20 & 21	1. WARP II face plate (753 holes) with the 6th row chamfered. 2. Symmetrical turbulators. 3. Platelet injector SN-002. 4. Adapter-Diffuser (15° wall).	1. No change from Test 47.	None	Not calculated.
#49	22 & 23	1. WARP II face plate (753 holes) with the 8th row chamfered. 2. Symmetrical turbulators. 3. Platelet injector SN-002. 4. Adapter-Diffuser (15° wall).	1. More uniform flow radially, high total pressure drop better than 48.	None	Not calculated.

Air Flow Test Program-Warp II Face Plate Evaluation

Figure VI-94
Sheet 1 of 2

GROUP 6		WARP II FACE PLATE EVALUATIONS			
SERIES	TEST NO.	CONFIGURATION	RESULTS	APPLICABLE TEST	MRD_{LOSS}, SEC
#50	24-29	1. WARP II face plate (753 holes) with the 2nd row chamfered at 8 teepee locations. 2. Symmetrical turbulators. 3. Platelet injector SN-002. 4. Adapter-Diffuser (15° wall).	1. Slightly skewed flow. 2. Slightly high peripheral flow. 3. Allowable total pressure drop.	1.2-16-WAM-019 thru 1.2-16-WAM-023	3.6

Air Flow Test Program-Warp II Face Plate Evaluation

Figure VI-94
Sheet 2 of 2

GROUP 7		DRILLED PLATE EVALUATIONS		67 Test Total	
SERIES	TEST NO.	CONFIGURATION	RESULTS	APPLICABLE TEST	MRD_{LOSS}, SEC
#55	22-24	1. Drilled face plate. 2. Symmetrical turbulators. 3. No injector. 4. Adapter-Diffuser (15° wall).	1. Uniform flow circumferentially but low radially. High P. 2. High pressure drop.	None	Not calculated.
#56	25-28	1. Drilled face plate with seal. 2. Symmetrical turbulators. 3. No injector. 4. Adapter-Diffuser (15° wall).	1. Uniform flow circumferentially but not radially. 2. High pressure drop.	None	Not calculated.
#57	33-36	1. Drilled face plate without the seal. 2. Symmetrical turbulators. 3. No injector. 4. Adapter-Diffuser (15° wall).	1. Uniform flow circumferentially but not radially. 2. High pressure drop.	None	Not calculated.
#58	41-44	1. Drilled face plate with seal. 2. Symmetrical turbulators. 3. No injector. 4. No diffuser cone.	1. Rleatively uniform flow circumferentially but not radially. 2. Very high pressure drop, zero flow periphery.	None	Not calculated.
#59	36-40	1. Platelet injector SN-002. 2. Concentric turbulators. 3. Drilled face plate. 4. Adapter-Diffuser (15° wall).	1. Uniform flow circumferentially but not radially. 2. Very high pressure drop, zero flow periphery.	None	Not calculated.
#60	45-48	1. Platelet injector SN-002. 2. Symmetrical turbulators. 3. Drilled face plate with every other hole chamfered in the 1st row. 4. Adapter-Diffuser (15° wall).	1. Zero flow at periphery. 2. High flow in center, unfirom circumferentially.	None	Not calculated.

Air Flow Test Program--Drilled Plate Evaluation

Figure VI-95
Sheet 1 of 3

GROUP 7		DRILLED PLATE EVALUATION			
SERIES	TEST NO.	CONFIGURATION	RESULTS	APPLICABLE TEST	MRD_{LOSS}, SEC
#61	1-8	1. Platelet injector SN-002. 2. Symmetrical turbulators. 3. Drilled face plate with every hole chamfered in the 1st row and every other chamfered in the 2nd row. 4. Adapter-Diffuser (15° wall).	1. Very low flow at periphery. 2. High flow in center, uniform circumferentially.	None	Not calculated.
#62	9-16	1. Platelet injector SN-002. 2. Symmetrical turbulators. 3. Drilled face plate with every hole chamfered in rows 1 and 2, and every other hole chamfered in Row 3. 4. Adapter-Diffuser (15° wall).	1. Very low flow at periphery. 2. High flow in center, uniform circumferentially. 3. High total pressure drop.	None	Not calculated.
#63	17-24	1. Platelet injector SN-002. 2. Symmetrical turbulators. 3. Drilled face plate with every hole chamfered in Rows 1, 2 and 3, and every other hole chamfered in Row 4. 4. Adapter-Diffuser (15° wall).	1. Flow uniform circumferentially and almost uniform radially. 2. Still high flow in center and low flow @ 6"-7" dia. 3. Low flow at periphery.	None	Not calculated.
#64	25-32	1. Platelet injector SN-002. 2. Symmetrical turbulators. 3. Drilled face plate with every hole chamfered in Rows 1, 2, 3, and 4, and additional chamfering of Row 1. 4. Adapter-Diffuser (15° wall).	1. Flow uniform circumferentially and almost uniform radially. 2. Still high flow in center and low flow @ 6"-7" dia.	None	Not calculated.

Figure VI-95
Sheet 2 of 3

Air Flow Test Program--Drilled Plate Evaluation

GROUP 7		DRILLED PLATE EVALUATION			
SERIES	TEST NO.	CONFIGURATION	RESULTS	APPLICABLE TEST	MRD_{LOSS}, SEC
#65	1-8	1. Platelet injector SN-002. 2. Symmetrical turbulators. 3. Drilled face plate with Rows 1, 2, 3 and 4 full chamfer, Row #1 drilled to .1905". 4. Adapter-Diffuser (15° wall).	1. Flow uniform circumferentially and almost uniform radially. 2. Still high flow in center and low flow @ 6"-7" dia. 3. Higher flow at periphery.	1.2-16-WAM-024 thru 1.2-16-WAM-026 1.2-13-WAM-003 thru 1.2-13-WAM	2.2 2.4

Air Flow Test Program--Drilled Plate Evaluation

Figure VI-95
Sheet 3 of 3

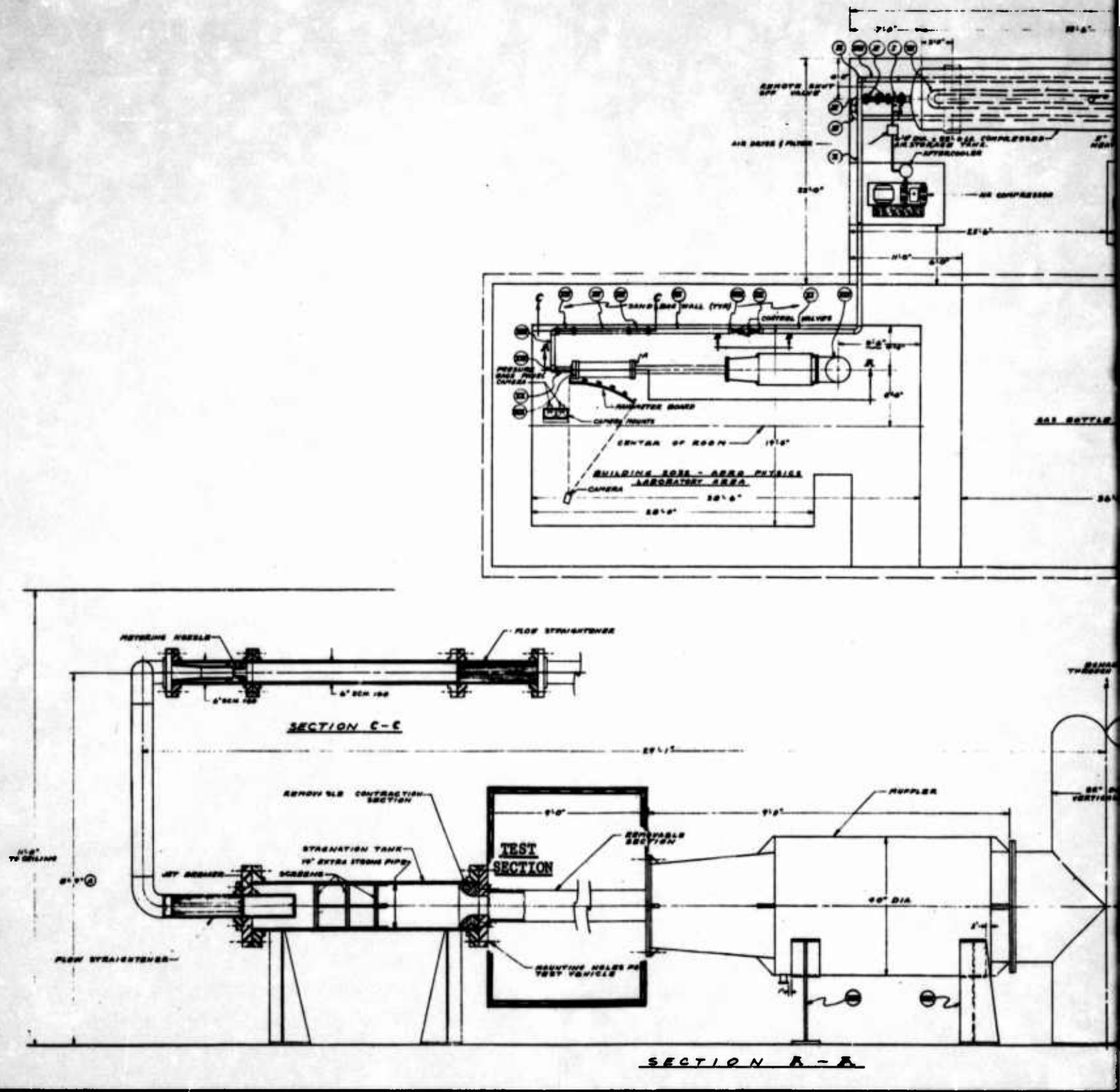
AIR COMPRESSOR
AFTERCOOLER
CONTROL VALVES
CENTER OF ROOM
BUILDING 2022 - AERO PHYSICS LABORATORY AREA
CAMERA
SECTION C-C
SECTION A-A
TEST SECTION
STAGNATION TANK
SCREENS
CONTRACTION SECTION
REMOVABLE SECTION
DIFFUSER
40" DIA
FLOW STRAIGHTENER

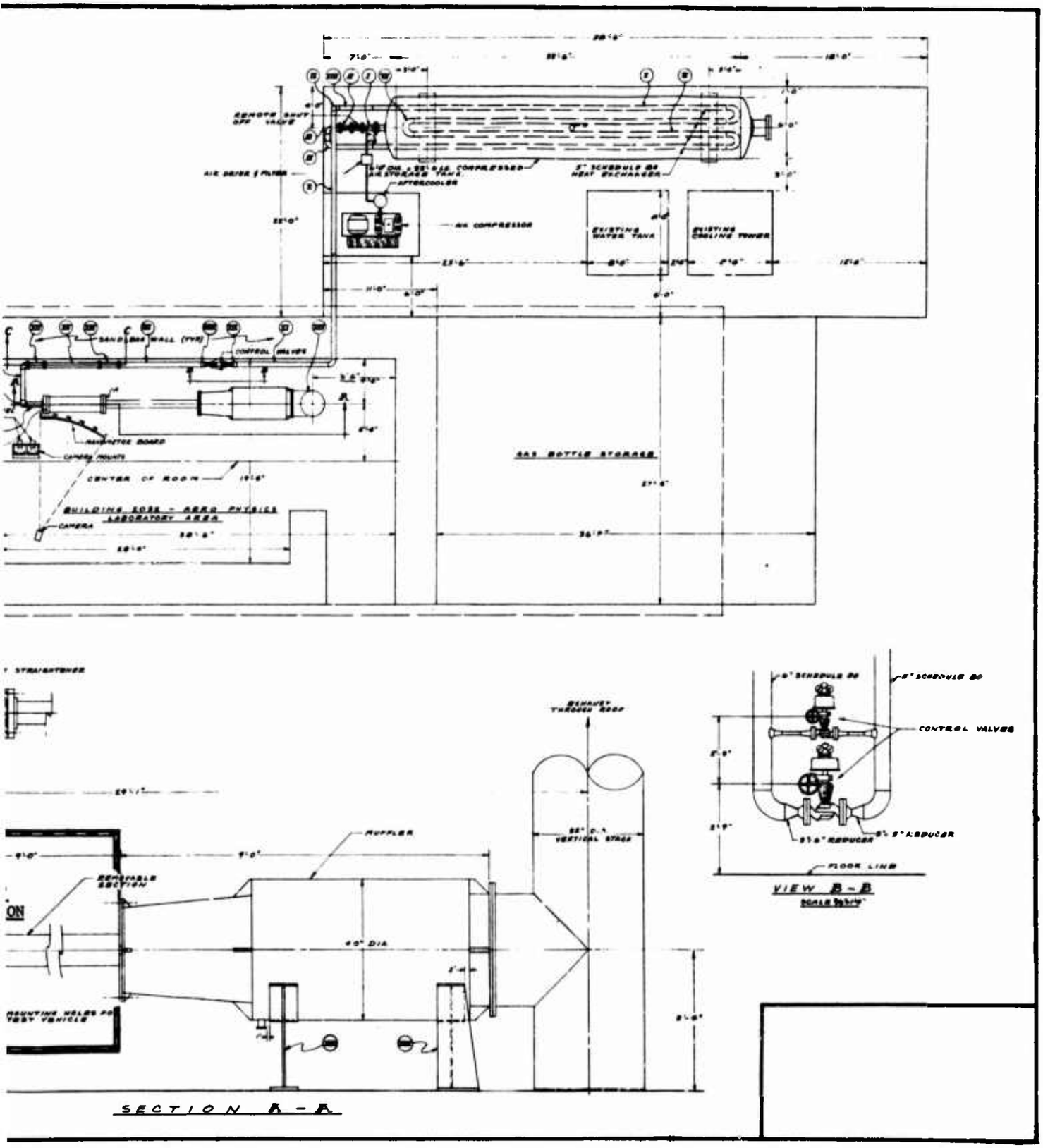

Air Flow Facility Layout

Figure VI-96

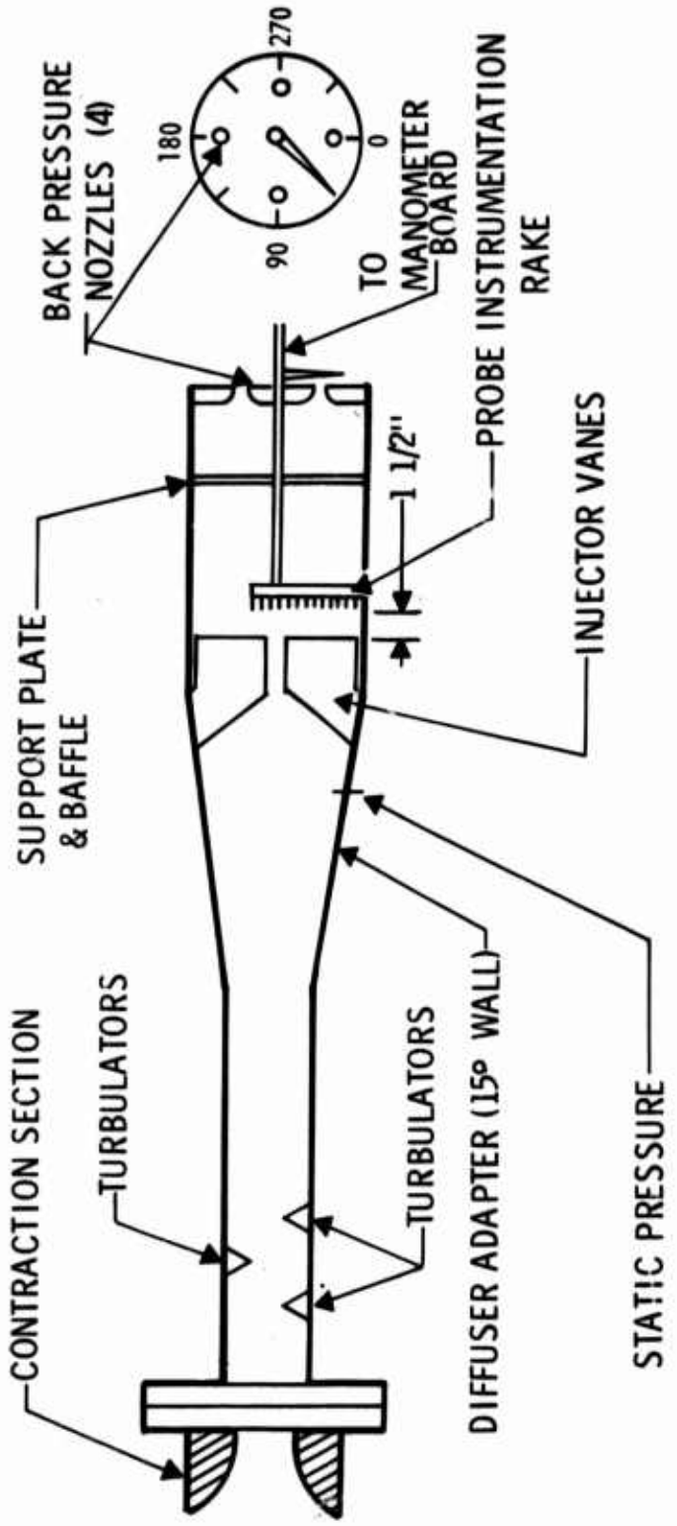

Primary Gas Flow Test Installation

Figure VI-97

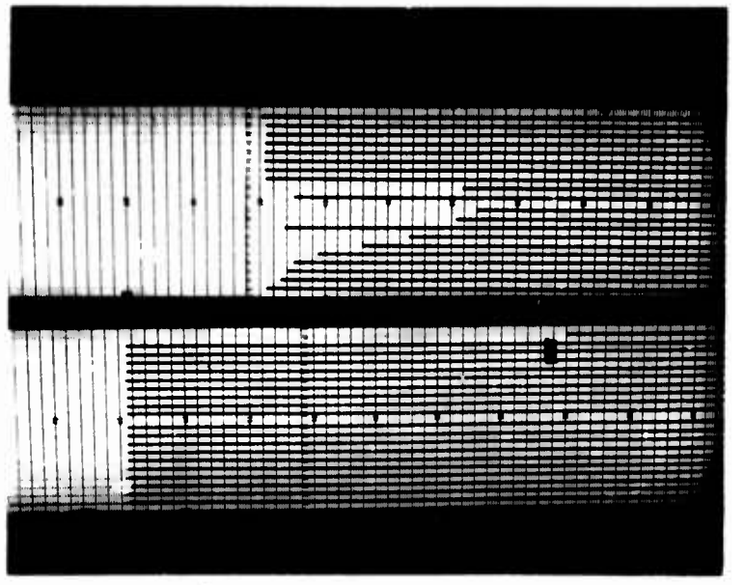

MANOMETER PHOTO

No.	Type	P, in.
1	Total	4.6
2	Total	4.3
3	Total	3.9
4	Total	3.5
5	Total	3.0
6	Total	2.4
7	Total	1.7
8	Static	1.3
9	Total	0.9
10	Total	0
11	Static	-0.5
12	Total	-1.0

Transverse Probe Geometry

Figure VI-98

Air Flow Facility Control Room

Figure VI-99

Condition	Symbol	Air Model	Hot Test	Units
Reynolds Number	R_e	3.19×10^5	1.69×10^7	---
Mach Number	N_m	.05	.0473	---
Prandtl Number	P_R	.713	.624	---
Resonance Time	t_R	3.59×10^{-3}	2.3×10^{-3}	sec.
Injector Velocity	V_g	55.2	82.3	ft/sec
Acousitc Velocity	a_o	1115	1740	ft/sec
Viscosity	μ_g	1.2×10^{-5}	2.424×10^{-5}	lbs/ft-sec
Gas Density	ρ_g	.165	6.3	lbs/ft^3
Ratio of Specific Heats		1.4	1.242	---

Air Flow-Hot Flow Operating Condition Comparison

Figure VI-100

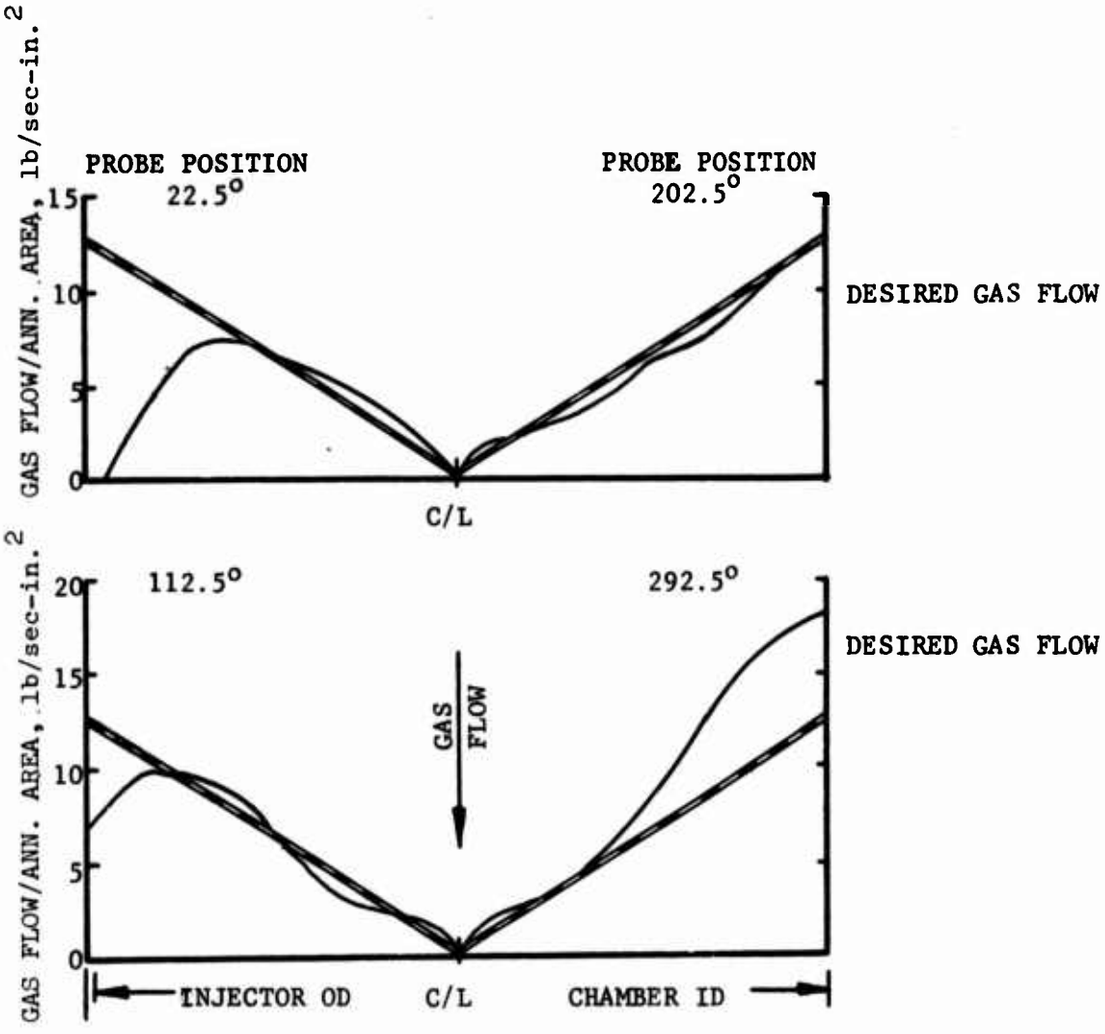

NOTE: "Annular Area" is defined as that area contained in a 1-in.-wide circular annulus having a mean diameter corresponding to any particular diameter across the injector face.

Oxidizer Gas Flow Distribution

Figure VI-101

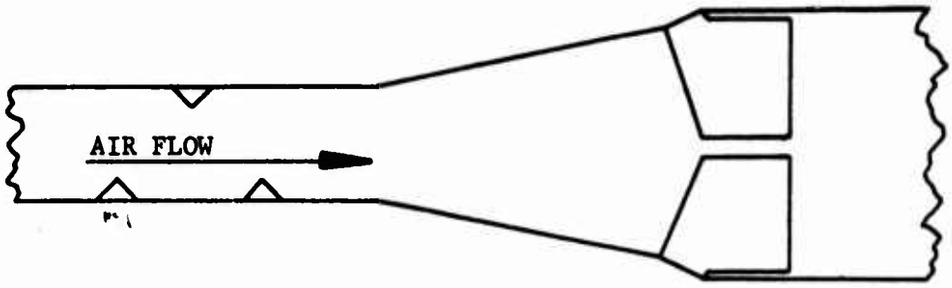

CONF. 1, UNSYMMETRICAL TURBULATORS - PLATELET INJECTOR.

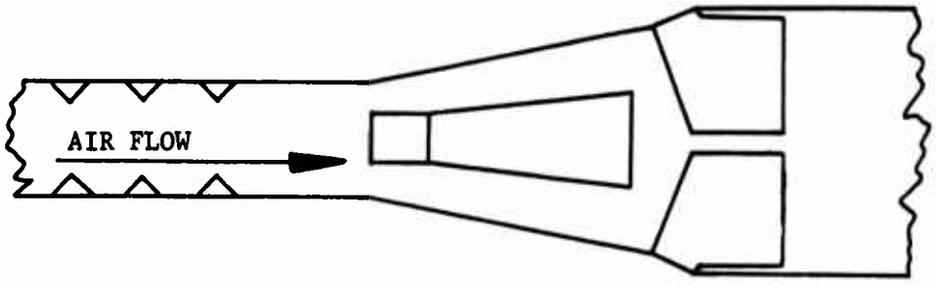

CONF. 2, SYMMETRICAL TURBULATORS - PLATELET INJECTOR - DIFFUSER CONE.

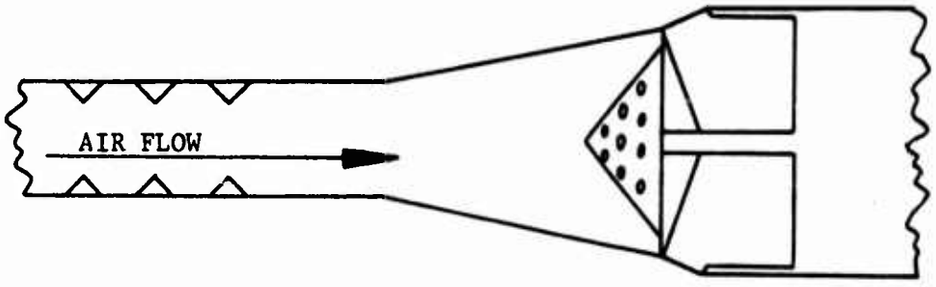

CONF. 3, SYMMETRICAL TURBULATORS - PLATELET INJECTOR (WITH VANE EXTENDERS) - COOLIE HAT.

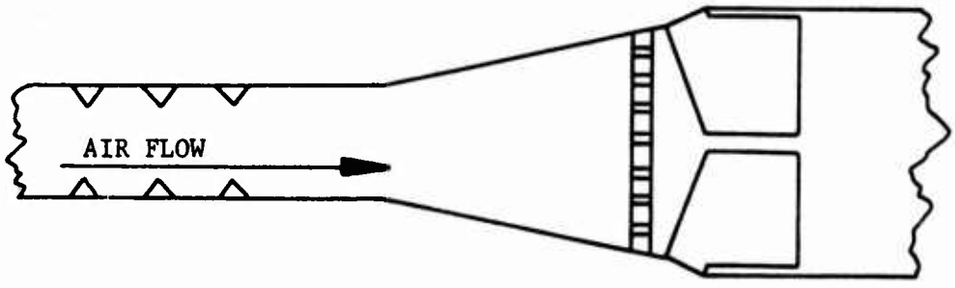

CONF. 4, SYMMETRICAL TURBULATORS - PLATELET INJECTOR, DISTRIBUTION PLATE.

Schematic Representation of Various Air Flow Configurations

Figure VI-102

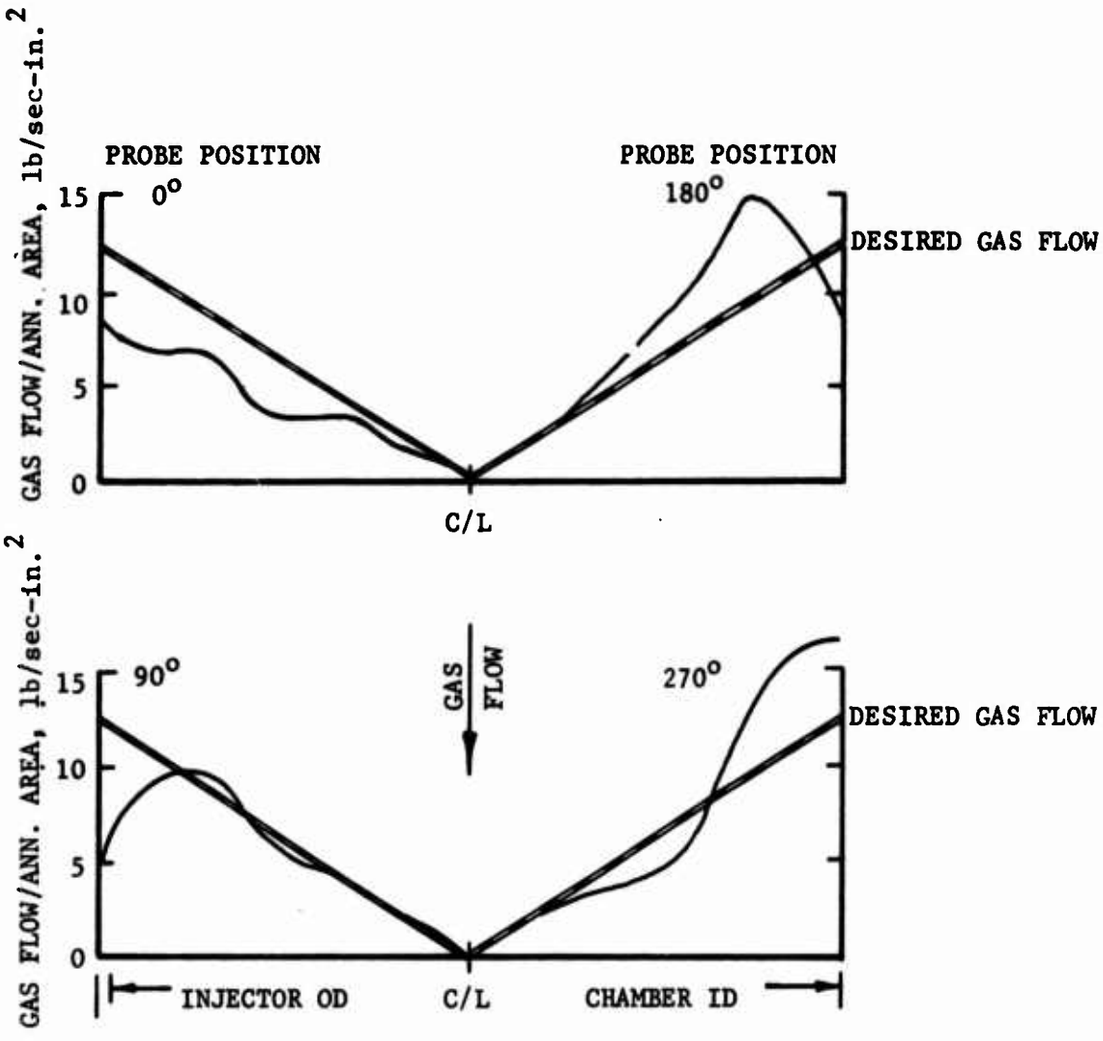

NOTE: "Annular Area" is defined as that area contained in a 1-in.-wide circular annulus having a mean diameter corresponding to any particular diameter across the injector face.

Oxidizer Gas Flow Distribution, Notched Screen, Test 1.2-16-WAM-014 and -015

Figure VI-103

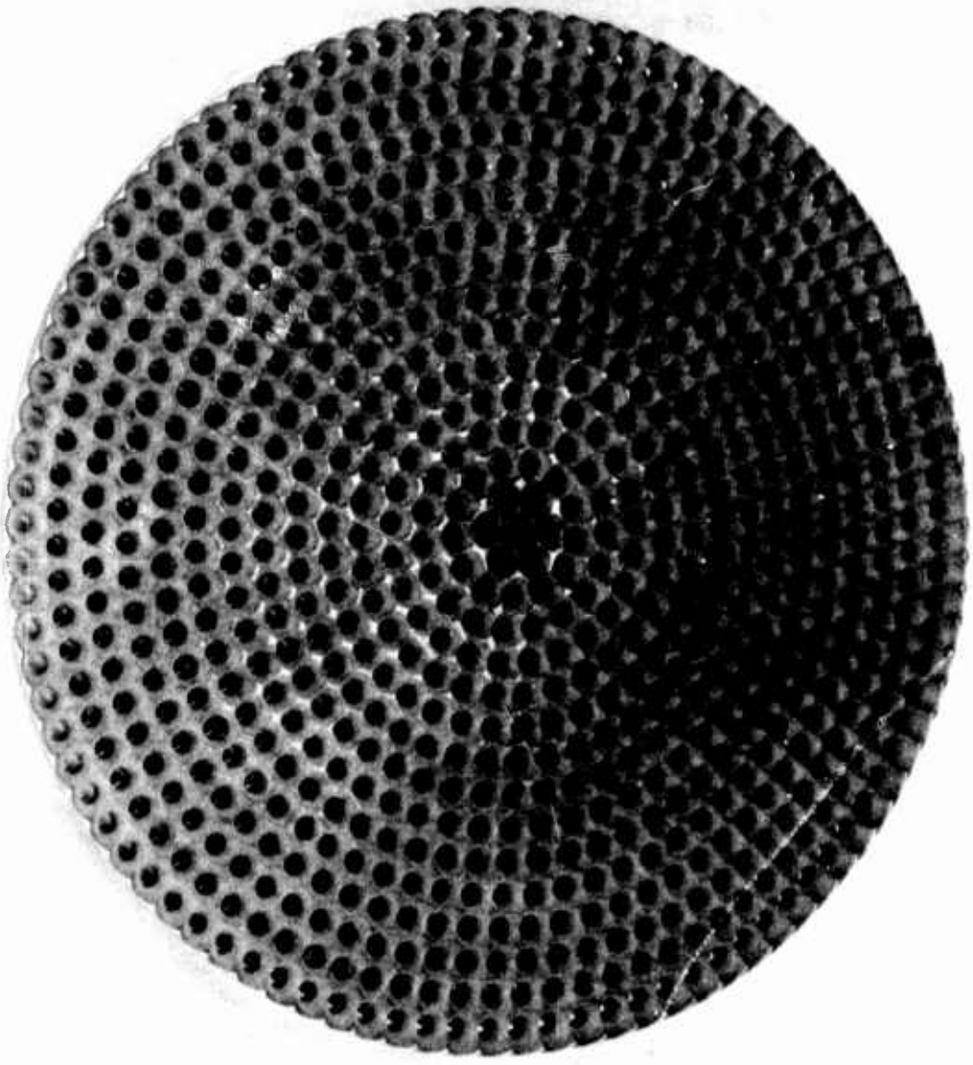

Warp Faceplate-Gas Distribution Plate

Figure VI-104

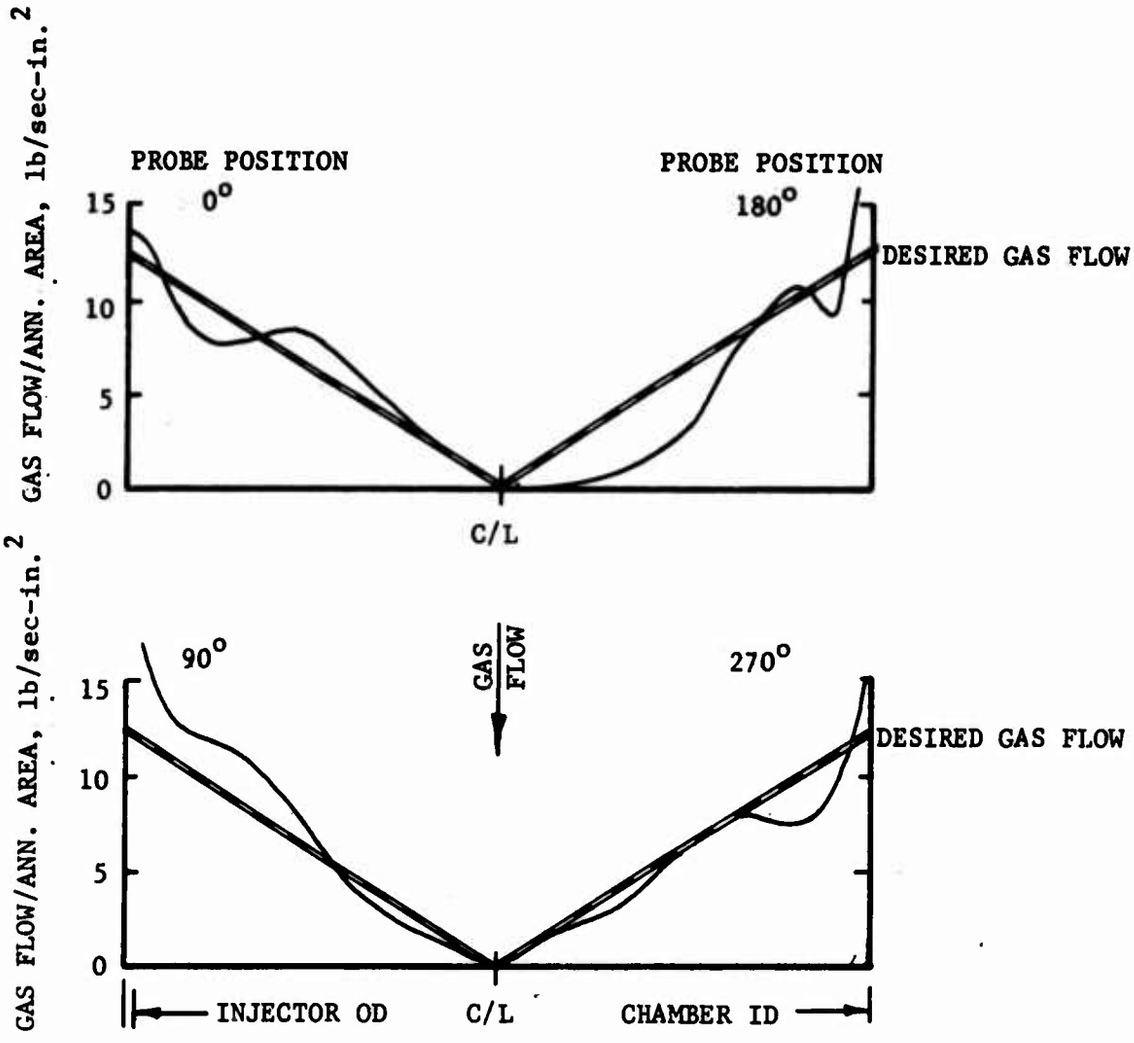

NOTE: "Annular Area" is defined as that area contained in a 1-in.-wide circular annulus having a mean diameter corresponding to any particular diameter across the injector face.

Oxidizer Gas Flow Distribution Warp III Face Plate, Test 1.2-16-WAM-017

Figure VI-105

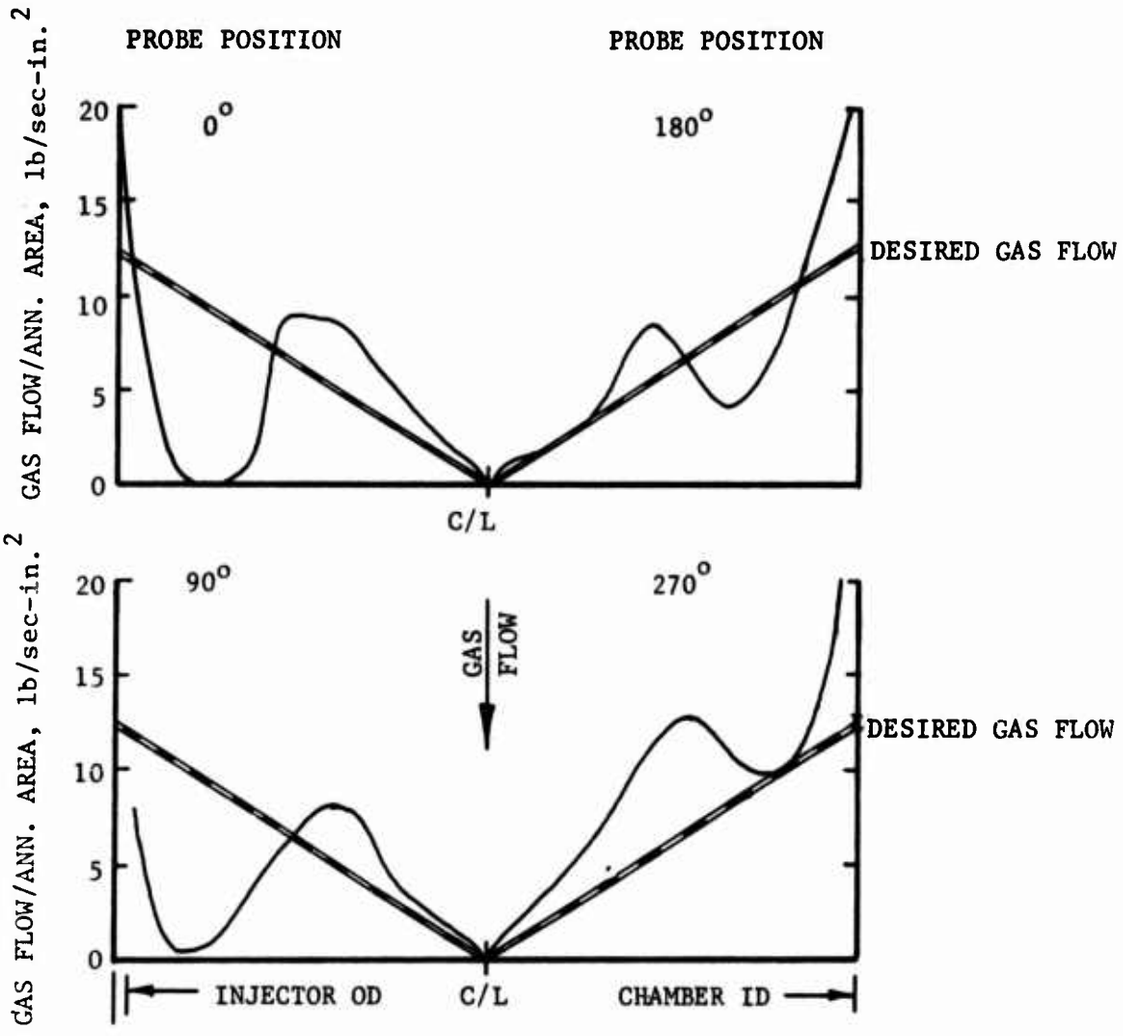

NOTE: "Annular Area" is defined as that area contained in a 1-in.-wide circular annulus having a mean diameter corresponding to any particular diameter across the injector face.

Oxidizer Gas Flow Distribution Warp III Face Plate (Mod I), Test 1.2-16-WAM-018B

Figure VI-106

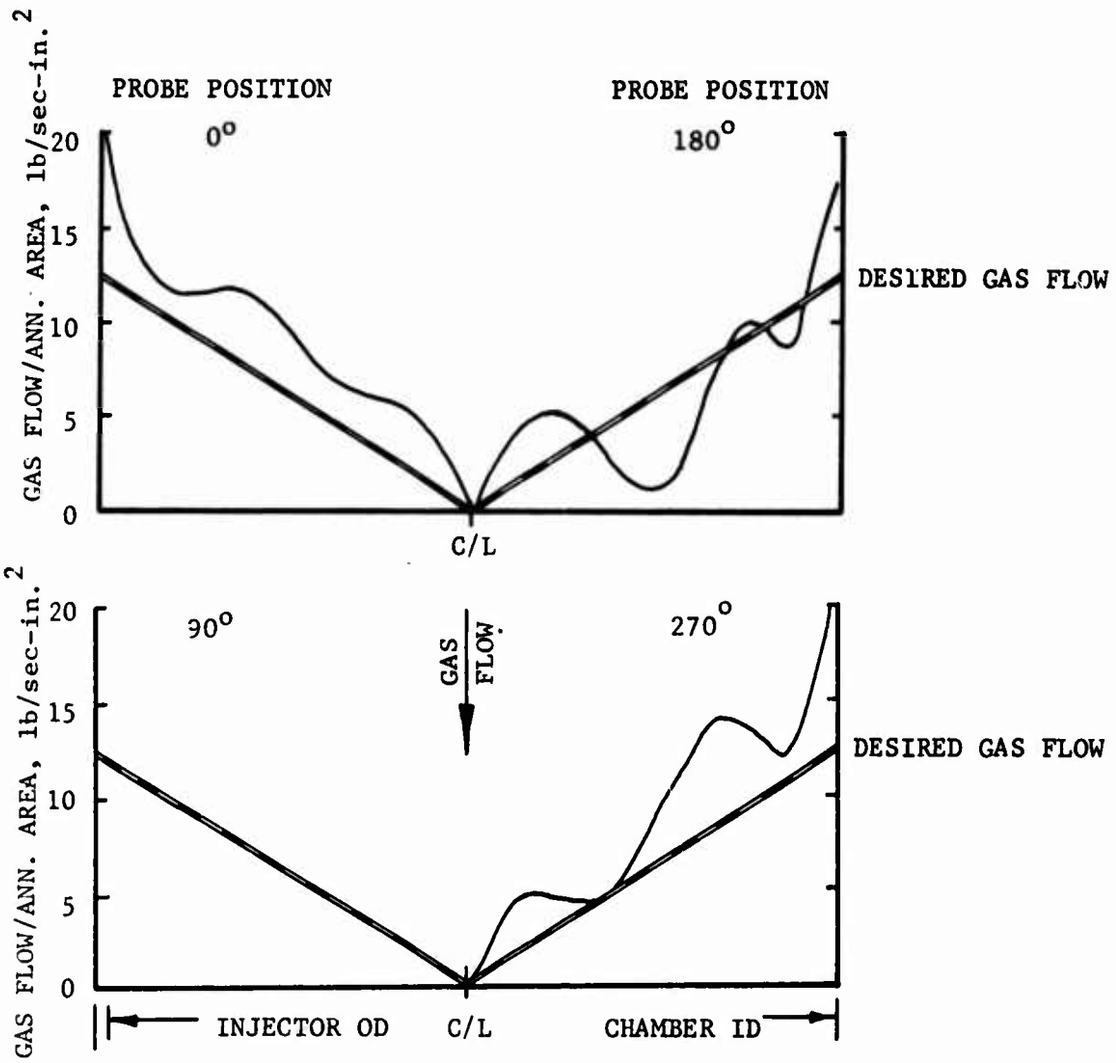

NOTE: "Annular Area" is defined as that area contained in a 1-in.-wide circular annulus having a mean diameter corresponding to any particular diameter across the injector face.

Oxidizer Gas Flow Distribution Warp II Face Plate,
Test 1.2-16-WAM-019 thru -023

Figure VI-107

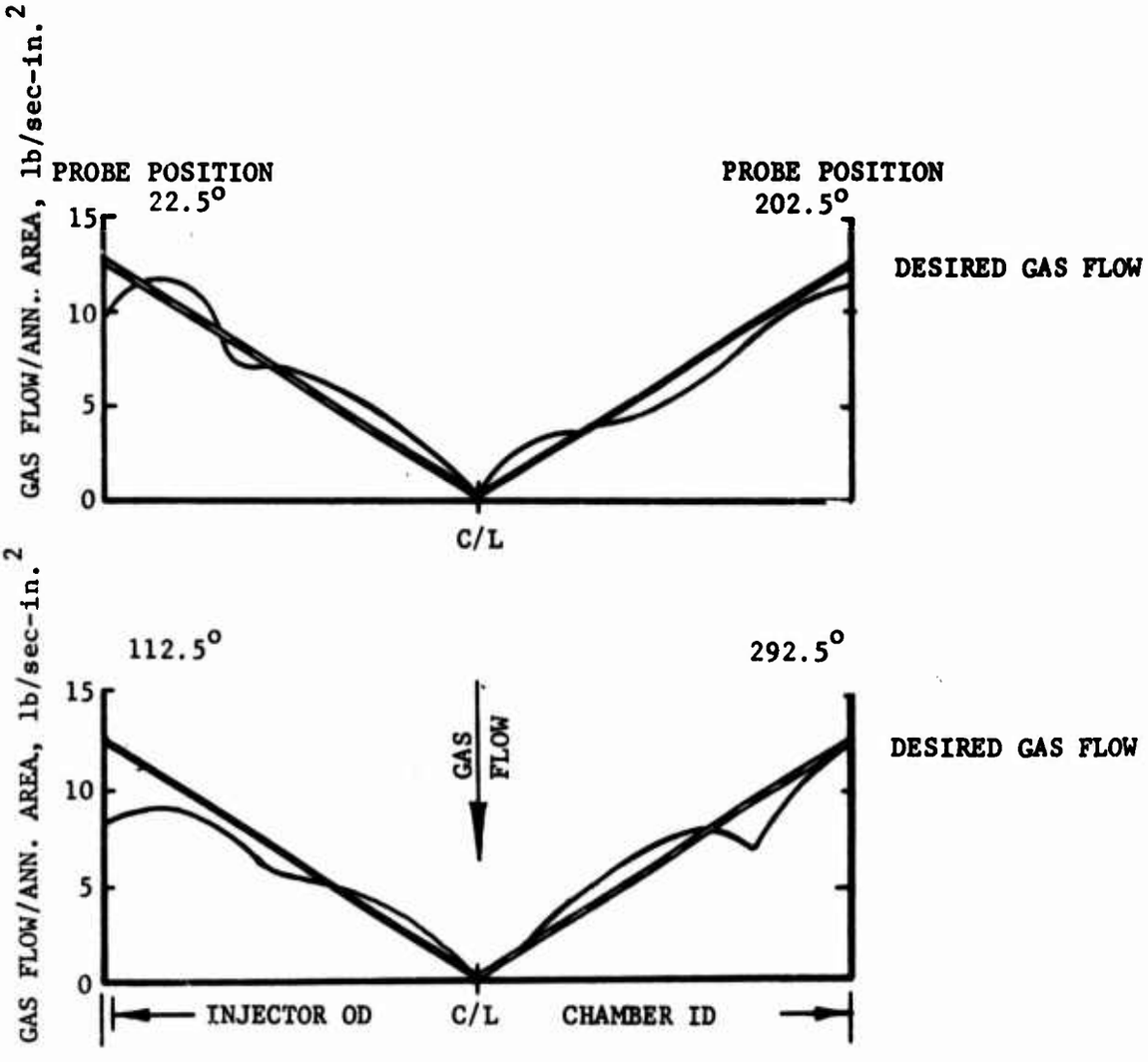

NOTE: "Annular Area" is defined as that area contained in a 1-in.-wide circular annulus having a mean diameter corresponding to any particular diameter across the injector face.

Oxidizer Gas Flow Distribution 712 Drilled Hole Plate
Test 1.2-16-WAM-024 thru -026
1.2-16-WAM-003 thru -051

Figure VI-108

APPENDIX I
HEAT TRANSFER MODEL

I. INTRODUCTION

(U) The cooling action of the ARES cooled surface can be considered to be composed of two separate mechanisms. The first of these is what can be called internal cooling, or the transfer of heat between the platelets and coolant inside the wall itself. The second mechanism is film cooling, which is the suppression of heat flux to the wall as a result of the coolants being injected into the boundary layer after they leave the wall. These two mechanisms are coupled since the film cooling effect which is obtained depends upon the temperature of the coolant as it leaves the wall. Similarly, the heat flux into the wall and the temperature of the coolant as it leaves the surface depend upon the film cooling effectiveness.

(U) The approach which will be taken here is to derive separately the equations governing each of the two mechanisms. Once these equations are obtained the computational procedure which couples them will be outlined.

II. INTERNAL COOLING

(U) The thermal model for the internal cooling is shown in Figure 1. The wall is considered to be composed of platelets which are "2t" thick and having coolant channels between which are "D" deep. The coolant enters the channels at X=0 at a temperature $T_{c,o}$ and at a rate G per unit cooled wall surface area. At the end of the platelets, at X=L, the platelets are exposed to a hot gas at temperature T_g with a surface film coefficient h_g.

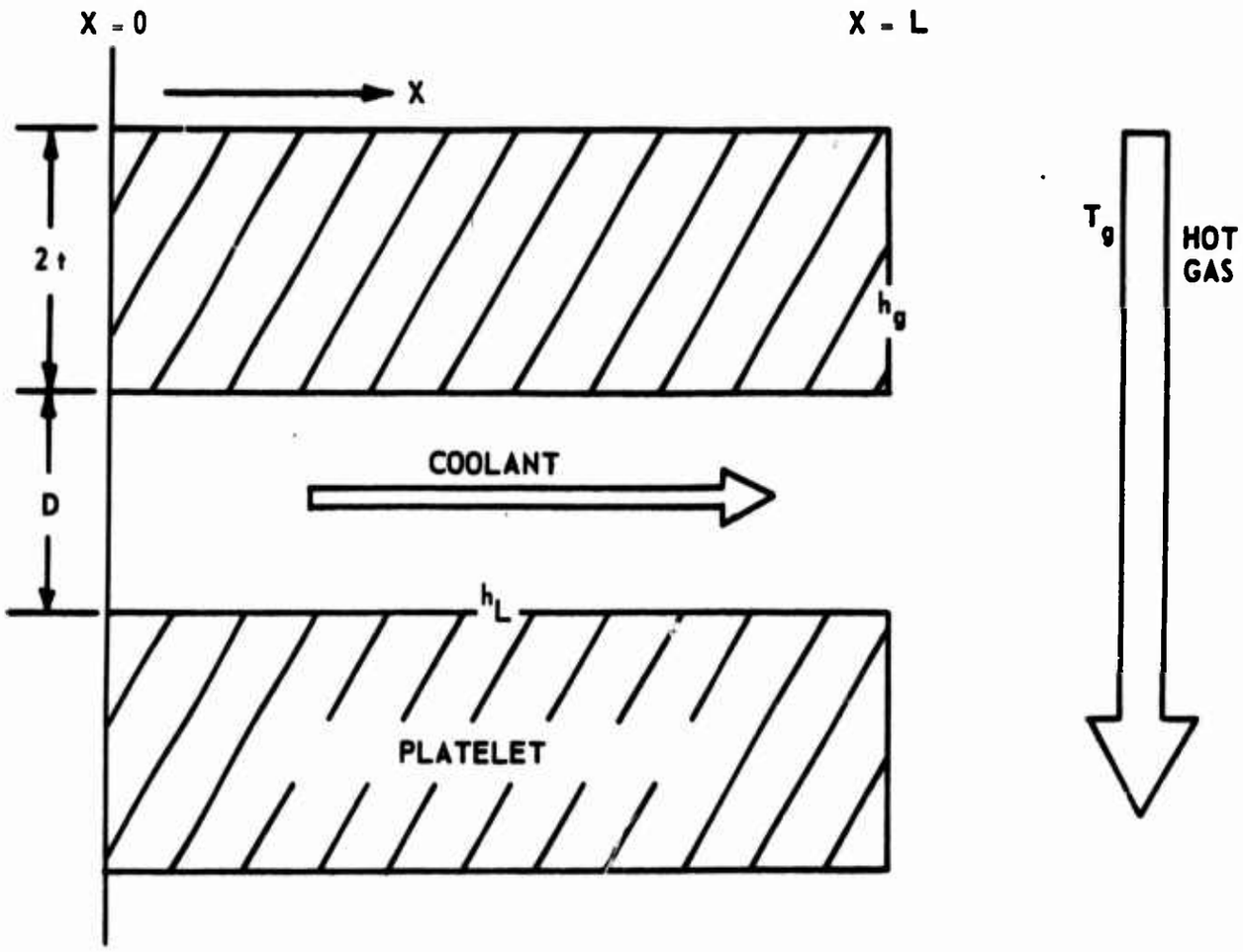

Figure 1

Appendix I

(U) It will be assumed that the heat conduction in the platelets is one-dimensional* and that the platelet material and coolant properties are not temperature dependent.

(U) The differential equation governing conduction in the platelet is:

$$K_m \, t \, \frac{d^2T}{dX^2} = h_L \, (T - T_c) \qquad (1)$$

where K_m = platelet conductivity
h_L = film coefficient between the platelet and coolant
T = platelet temperature at X
T_c = coolant temperature at X
t = platelet half thickness
X = distance from coolant inlet

(U) If X-direction conduction in the coolant is assumed to be negligible the differential equation describing the coolant temperature is:

$$G \, C_{p,c} \, t \, \frac{dT_c}{dX} = h_L \, (T - T_c) \qquad (2)$$

where $C_{p,c}$ = coolant specific heat
G = coolant weight flow rate per unit of cooled wall surface area

Combining equations (1) and (2)

$$\frac{d^3T}{dX^3} + A \, \frac{d^2T}{dX^2} - B \, \frac{dT}{dX} = 0 \qquad (3)$$

*Early in the program a two-dimensional numerical analysis of the platelet conduction showed that the one-dimensional approach is valid for thin platelets.

where $A = h_L/G\ C_{p,c}\ t$

$B = h_L/K_m\ t$

Using differential operator notation equation (3) can be written as:

$$(D^3 + AD^2 - BD)\ T = 0 \tag{3a}$$

The solution of equation (3a) is:

$$T = C_1\ e^{r_1 X} + C_2\ e^{r_2 X} + C_3 \tag{4}$$

$$r_1 = -A/2 + \sqrt{\frac{A}{4}^2 + B} \tag{5}$$

$$r_2 = -A/2 - \sqrt{\frac{A}{4}^2 + B} \tag{6}$$

(U) Three boundary conditions are required for the evaluation of the constants C_1, C_2, and C_3. At the platelet edge (X=L) the conduction into the platelet must equal the convective heat input from the hot gas stream.

$$\text{at } X=L,\ h_g\ (T_g - T) = K_m \frac{dT}{dX} \tag{7}$$

where h_g = surface (gas) film coefficient

T_g = hot gas temperature

(U) It will be assumed that the coolant inlet (or entrance to the thermal influence zone) is an adiabatic surface. This gives;

$$\text{at } X = 0,\ \frac{dT}{dX} = 0 \tag{8}$$

$$k_m\, t\, \frac{d^2T}{dX^2} = h_L\, (T - T_{c,o}) \tag{9}$$

where $T_{c,o}$ = coolant inlet temperature

(U) Evaluating C_1, C_2, and C_3 through the use of equations (7), (8), and (9), and rearranging produces

$$\frac{T - T_{c,o}}{T_g - T_{c,o}} = \frac{e^{r_1 X} - \left(\frac{r_1}{r_2}\right) e^{r_2 X}}{e^{r_1 L}\left[- \left(\frac{r_1}{r_2}\right) e^{(r_2 L)} + \left(\frac{K_m}{h_g}\right) r_1 \left(e^{r_1 L} - e^{r_2 L}\right)\right]} \tag{10}$$

where L = distance from coolant inlet to wall surface (platelet edge)

(U) It can be shown that for the range of values of interest

$$\left| e^{r_1 X} \right| >> \left| \frac{r_1}{r_2}\, e^{r_2 X} \right| \tag{11}$$

$$\left| e^{r_1 L} \right| >> \left| \frac{r_1}{r_2}\, e^{r_2 L} \right| \tag{12}$$

Employing equations (11) and (12) for simplifying equation (10) yields

$$\frac{T - T_{c,o}}{T_g - T_{c,o}} = \frac{e^{r_1 (X-L)}}{1 + \frac{K_m\, r_1}{h_g}} \tag{13}$$

(U) Equation (13) relates the temperatures existing at all points in the platelets to the properties of the coolant, the coolant flow rate, the platelet material properties and thickness, and the conditions at the hot gas boundary. This equation is the key equation used in the design and evaluation of the ARES platelets.

(U) The film coefficient "h_L" which exists between the coolant and the platelets can be evaluated using the expression for fully developed laminar flow between parallel plates.[1]

$$h_L = \frac{4\ K_c}{D} \tag{14}$$

where D = depth of coolant channel

K_c = coolant thermal conductivity

This value, when used in design, is on the conservative side since it is the minimum value which h_L can possibly have. Such things as entrance effects and phase changes can only act to increase h_L.

III. FILM COOLING

(U) The analysis of the film cooling effect achieved by the coolant after it leaves the wall will be somewhat different from the type of analysis used with the more conventional transpiration cooling systems. Normally in the analysis of transpiration cooling systems the assumption is made that the coolant is injected uniformly over the entire surface. This assumption will not be made in the present analysis. Rather, the analysis will treat the problem as one of highly refined multiple slot film cooling. There is a twofold reason for doing this. First, and most important, highly refined multiple slot film cooling is a more accurate description of the actual physical system

which the model is representing. The second reason for taking a multiple slot approach is that with the results of this approach it will be possible to account for the effect of platelet thickness on the film cooling effectiveness. Obviously, this cannot be done if the model assumes uniformly distributed coolant injection.

(U) The basic approach taken is similar to that of Stollery and El-Ehwany[2] except for some modifications to make the range of flows over which it is applicable somewhat broader. It is assumed that at each injection point the boundary layer begins to develop anew, and that the mass of gas in the boundary layer is composed of injected coolant plus enough entrained free-stream gas to give the total boundary layer gas flow. There is experimental justification for this approach. In work performed on film cooling with injection through a porous section[3] it was noted that the injected coolant appears to simply lift the existing boundary layer off the wall. Downstream of the point of injection the coolant and hot gas begin to mix, with the growth of the velocity profile in the coolant layer on the hot gas - coolant boundary not being too much unlike that of a turbulent boundary layer on a flat plate.

(U) The derivation will begin by assuming that the total mass flow rate in the boundary layer is composed of injected coolant plus enough entrained freestream gas to give the total boundary layer flow rate.

$$\dot{m}_{BL} = \dot{m}_c + \dot{m}_\infty \qquad \dot{m}_{BL} \geq \dot{m}_c$$

$\dot{m}_{BL}$ = boundary layer flow rate
$\dot{m}_c$ = coolant flow rate
$\dot{m}_\infty$ = flow rate of entrained freestream gases

Appendix I

The temperature of the boundary layer "T_{BL}" can be given by

$$T_{BL} = \frac{h_{BL}}{\dot{m}_{BL}\, C_{p,BL}} = \frac{(\dot{m}_{BL} - \dot{m}_c)\, C_{p,\infty}\, T_\infty + \dot{m}_c\, T_c\, C_{p,c}}{(\dot{m}_{BL} - \dot{m}_c)\, C_{p,\infty} + \dot{m}_c\, C_{p,c}} \tag{16}$$

$C_{p,\infty}$ = freestream specific heat
T_∞ = freestream total temperature
T_c = temperature of coolant as it leaves the wall
$C_{p,c}$ = coolant specific heat
$C_{p,BL}$ = boundary layer specific heat
h_{BL} = boundary layer film coefficient

The only unknown in eq. (16) is $\dot{m}_{BL}$. In general,

$$\dot{m}_{BL} = \int_0^\delta \rho\, u\, dy \tag{17}$$

δ = boundary layer thickness
u = local velocity
ρ = local density
y = normal distance from surface

(U) If it is assumed that similar velocity profiles exist in the boundary layer as it develops from the point of injection and that this profile is only a function of the freestream conditions then

$$u = u_\infty \left(\frac{y}{\delta}\right)^{1/n} \tag{18}$$

n = a function of the freestream Reynolds number
u_∞ = freestream velocity

(U) Further assuming that a uniform density exists across the boundary layer and that this is equal to the freestream density "ρ_∞" (a reasonably good assumption in both the chamber and throat).

$$\rho = \rho_\infty \tag{19}$$

$$\dot{m}_{BL} = \int_0^\delta \rho_\infty \mu_\infty \left(\frac{y}{\delta}\right)^{1/n} dy = \frac{n}{n+1} \rho_\infty u_\infty \delta \tag{20}$$

(U) It can be shown that for a developing boundary layer the boundary layer thickness can be expressed

$$\delta = Z^{\frac{n+1}{n+3}} \left[\frac{n \quad (C_n)^{\frac{2n}{n+1}}}{(n+2)(n+3)} \left(\frac{\rho_\infty \mu_\infty}{\mu_\infty}\right)^{\frac{2}{n+1}} \right]^{-\frac{n+1}{n+3}} \tag{21}$$

Z = distance over which the boundary layer has been developing

C_n = a function of n, values of which are given on Page 507 of Ref. (4).

μ_∞ = free stream viscosity

Combining equation (20) and (21)

$$\dot{m}_{BL} = \left(\frac{n}{n+1}\right) \left[\frac{n}{(n+2)} \frac{(C_n)^{\frac{2n}{n+1}}}{(n+3)} \right]^{-\frac{n+1}{n+3}} (\mu_\infty)^{\frac{2}{n+3}} (\rho_\infty u_\infty)^{\frac{n+1}{n+3}} Z^{\frac{n+1}{n+3}} \tag{22}$$

Let: $$R_Z = \alpha \left(\dot{m}_{BL}/\dot{m}_c\right) \tag{23}$$

Appendix I

(U) Based on the data presented by Stollery and El-Ehwany the value of "n" should be somewhere between .80 and .85, for the conditions encountered with the TRANSPIRE designs. This constant compensates to a certain extent for some of the assumptions made earlier, particularly as regards the temperature distribution across the boundary layer.

(U) The effective local boundary layer temperature can now be obtained by combining equations (16), (22), and (23).

$$T_{BL} = T_c \text{ for } 0 < \frac{\dot{m}_{BL}}{\dot{m}_c} < 1.0 \tag{24}$$

$$T_{BL} = \frac{(R_Z - 1)\,\dfrac{C_{p,\infty}}{C_{p,c}}\,T_{o,\infty} + T_c}{(R_Z - 1)\,\dfrac{C_{p,\infty}}{C_{p,c}} + 1}, \quad \frac{\dot{m}_{BL}}{\dot{m}_c} > 1.0 \tag{25}$$

where $T_{o,\infty}$ = freestream stagnation temperature

$$R_Z = \frac{0.82}{\dot{m}_c}\left(\frac{n}{n+1}\right)\left[\frac{n}{(n+2)}\,\frac{(C_n)^{\frac{2n}{n+1}}}{(n+3)}\right]^{-\frac{n+1}{n+3}} (\mu_\infty)^{\frac{2}{n+3}} (\rho_\infty u_\infty)^{\frac{n+1}{n+3}} Z^{\frac{n+1}{n+3}} \tag{26}$$

(U) In order to combine the film cooling equations with the internal cooling equations, to calculate the cooling operation of the TRANSPIRE wall, it is necessary that several additional operations be performed. The gas temperature "T_g" in equation (13), and the boundary layer temperature "T_{BL}" in equations (24) and (25) are in essence the same quantity. These two temperatures are not strictly equivalent, however, since T_g refers to an average driving temperature existing over the end of the platelet while T_{BL} is a local temperature which varies in the direction of stream flow. The relationship between these two temperatures is given by

$$T_g = \frac{\int_D^{D+2t} T_{BL}\, dZ}{2t} \qquad (27)$$

It should also be noted that the flow rates G of eq. (13) and $\dot{m}_c$ of eq. (24) and (26) are not the same. The relationship between them is

$$\dot{m}_c = \frac{G\ (2t+D)}{\pi d} \qquad (28)$$

where d = local chamber diameter

(U) The general calculational procedure in the use of these equations is to first select a platelet thickness, material, coolant flow channel depth, and design surface temperature. A coolant flow rate G and coolant temperature as it leaves the wall ($T_{c,L}$) are assumed. With these values and the use of equations (24), (25), (27), and (28), a value of T_g is found. With this T_g (the platelet surface temperature T_L and the use of equation (13) and equation (29)) the originally assumed coolant temperature $T_{c,L}$ can be checked by

$$(T_{c,L} - T_{c,L})\ G\ C_{p,c} = h_g\ (T_g - T_L) \qquad (29)$$

where $T_{c,L}$ = coolant temperature as it leaves wall
T_L = platelet surface temperature

If the assumed and calculated values of $T_{c,L}$ are considerably different a new value of $T_{c,L}$ should be assumed and the calculation procedure repeated. If the assumed and calculated values are very nearly equal the platelet surface temperature T_L is checked to see how it compares with the desired design value. If it is either too high or too low the coolant flow rate is increased or decreased and the procedure repeated. If the calculated surface temperature is about equal to the desired value the design is finished at this point.

(U) There is a comment which should be made relative to the evaluation of equations (25) and (27). As they now stand they tacitly assume that once the coolant in the boundary layer has traveled the thickness of one platelet, it is lost to the cooling system and no more cooling benefit is derived from it. This lack of film cooling carryover from one platelet to the next can be compensated for by assuming that the freestream gas feeding the boundary layer is composed of the boundary layer coming off the preceding platelets.

(U) The entire design procedure given above has been programmed on a digital computer. Film cooling carryover from the two platelets upstream of the one being analyzed has also been included.

IV. PLATELET HYDRAULIC EQUATIONS

(U) The coolant flow in the platelet flow control channels is laminar. The pressure drop - flow relationship employed for these channels is the equation for fully developed laminar flow in rectangular passages.

$$Q = \frac{aD^3}{16\mu}\left(\frac{\Delta P}{\Delta L}\right)\left(\frac{4}{3} - 0.836\,\frac{D}{a}\right) \qquad (30)$$

Q = volumetric flow rate
a = channel width
D = channel depth
μ = coolant viscosity
$\frac{\Delta P}{\Delta L}$ = pressure gradient in the channel

(U) The validity of this equation for these small passages has been proven in numerous flow tests of both the test units used in this program and other programs.

(U) Entrance and exit losses although generally very small are also taken into consideration.

REFERENCES APPENDIX I

1. W. M. Rohsenow, and H. Choi, Heat Mass and Momentum Transfer, Prentice-Hall, Inc., 1961, p. 141, Unclassified.

2. J. A. Stollery, A. A.M. El Ehwany, "A Note on the Use of a Boundary-Layer Model for Correlating Film Cooling Data," Int. J. Heat and Mass Transfer, Vol. 8, pp 55-65, 1965, Unclassified.

3. R. J. Goldstein, G. Shavit, T. S. Chen, "Film Cooling Effectiveness With Injection Through a Porous Section," J. Heat Transfer, Trans. ASME, Series C, August 1965, Unclassified.

4. H. Schlicting, Boundary Layer Theory, McGraw-Hill Book Company, Inc., 1960, Unclassified.

Unclassified

Security Classification

DOCUMENT CONTROL DATA · R&D

(Security classification of title, body of abstract and indexing annotation must be entered when the overall report is classified)

1 ORIGINATING ACTIVITY (Corporate author)
Advanced Storable Engine Program Division
Liquid Rocket Operations
Sacramento, California

2a REPORT SECURITY CLASSIFICATION
Confidential

2b GROUP
4

3 REPORT TITLE
Advanced Rocket Engine--Storable

4 DESCRIPTIVE NOTES (Type of report and inclusive dates)
Final Report Phase 1, 1 July 1965 through 1 February 1968

5 AUTHOR(S) (Last name, first name, initial)
R. Beichel, J. A. Gibb, R. A. Hankins, et al.

6 REPORT DATE	7a TOTAL NO OF PAGES	7b NO OF REFS
May 1968	323	12

8a CONTRACT OR GRANT NO	9a ORIGINATOR'S REPORT NUMBER(S)
AF 04(611)-10830 b PROJECT NO	10830-F-1, Phase I, Supplement 1
c	9b OTHER REPORT NO(S) (Any other numbers that may be assigned this report) AFRPL-TR-68-70
d	

10 AVAILABILITY/LIMITATION NOTICES
[redacted]

11 SUPPLEMENTARY NOTES	12 SPONSORING MILITARY ACTIVITY
	AFRPL, Air Force Systems Command Edwards, California

13 ABSTRACT

See Attached Sheets

DD FORM 1473

Unclassified

Security Classification

Unclassified

Security Classification

14 KEY WORDS	LINK A		LINK B		LINK C	
	ROLE	WT	ROLE	WT	ROLE	WT
High Chamber Pressure Staged Combustion Storable Propellants Forced Deflection Nozzle Gas-Liquid Injection Integrated Turbopump Thrust Chamber Coatings Propellant Lubricated Bearings Transpiration Cooling						

INSTRUCTIONS

1. ORIGINATING ACTIVITY: Enter the name and address of the contractor, subcontractor, grantee, Department of Defense activity or other organization *(corporate author)* issuing the report.

2a. REPORT SECURITY CLASSIFICATION: Enter the overall security classification of the report. Indicate whether "Restricted Data" is included. Marking is to be in accordance with appropriate security regulations.

2b. GROUP Automatic downgrading is specified in DoD Directive 5200.10 and Armed Forces Industrial Manual. Enter the group number. Also, when applicable, show that optional markings have been used for Group 3 and Group 4 as authorized.

3. REPORT TITLE: Enter the complete report title in all capital letters. Titles in all cases should be unclassified. If a meaningful title cannot be selected without classification, show title classification in all capitals in parenthesis immediately following the title.

4. DESCRIPTIVE NOTES: If appropriate, enter the type of report, e.g., interim, progress, summary, annual, or final. Give the inclusive dates when a specific reporting period is covered.

5. AUTHOR(S): Enter the name(s) of author(s) as shown on or in the report. Enter last name, first name, middle initial. If military, show rank and branch of service. The name of the principal author is an absolute minimum requirement.

6. REPORT DATE: Enter the date of the report as day, month, year, or month, year. If more than one date appears on the report, use date of publication.

7a. TOTAL NUMBER OF PAGES: The total page count should follow normal pagination procedures, i.e., enter the number of pages containing information.

7b. NUMBER OF REFERENCES: Enter the total number of references cited in the report.

8a. CONTRACT OR GRANT NUMBER: If appropriate, enter the applicable number of the contract or grant under which the report was written.

8b, 8c, & 8d. PROJECT NUMBER: Enter the appropriate military department identification, such as project number, subproject number, system numbers, task number, etc.

9a. ORIGINATOR'S REPORT NUMBER(S): Enter the official report number by which the document will be identified and controlled by the originating activity. This number must be unique to this report.

9b. OTHER REPORT NUMBER(S): If the report has been assigned any other report numbers *(either by the originator or by the sponsor)*, also enter this number(s).

10. AVAILABILITY/LIMITATION NOTICES: Enter any limitations on further dissemination of the report, other than those imposed by security classification, using standard statements such as:

(1) "Qualified requesters may obtain copies of this report from DDC."

(2) "Foreign announcement and dissemination of this report by DDC is not authorized."

(3) "U. S. Government agencies may obtain copies of this report directly from DDC. Other qualified DDC users shall request through _____."

(4) "U. S. military agencies may obtain copies of this report directly from DDC. Other qualified users shall request through _____."

(5) "All distribution of this report is controlled. Qualified DDC users shall request through _____."

If the report has been furnished to the Office of Technical Services, Department of Commerce, for sale to the public, indicate this fact and enter the price, if known.

11. SUPPLEMENTARY NOTES: Use for additional explanatory notes.

12. SPONSORING MILITARY ACTIVITY: Enter the name of the departmental project office or laboratory sponsoring *(paying for)* the research and development. Include address.

13 ABSTRACT: Enter an abstract giving a brief and factual summary of the document indicative of the report, even though it may also appear elsewhere in the body of the technical report. If additional space is required, a continuation sheet shall be attached.

It is highly desirable that the abstract of classified reports be unclassified. Each paragraph of the abstract shall end with an indication of the military security classification of the information in the paragraph, represented as *(TS), (S), (C), or (U)*

There is no limitation on the length of the abstract. However, the suggested length is from 150 to 225 words.

14 KEY WORDS: Key words are technically meaningful terms or short phrases that characterize a report and may be used as index entries for cataloging the report. Key words must be selected so that no security classification is required. Identifiers, such as equipment model designation, trade name, military project code name, geographic location, may be used as key words but will be followed by an indication of technical context. The assignment of links, rules, and weights is optional.

Unclassified

Security Classification

UNCLASSIFIED ABSTRACT

(U) This report summarizes the Phase I work of ARES Program, Contract AF 04(611)-10830. The period of performance was from 1 July 1965 through 31 January 1968.

(U) The objective of this program was to demonstrate the engineering practicality and performance characteristics of a high chamber pressure, staged combustion engine. The program was to be conducted in two phases. Phase I was to demonstrate critical engine features by component testing. Demonstration of the assembled engine system was to be accomplished in Phase II.

(U) Phase I is now completed and all critical engine features have been demonstrated. This engine concept is ready to proceed into the Phase II program. Specific accomplishments of the Phase I program are as follows:

(1) Master layouts for two engine designs were established. One uses a turbopump with the shaft axis oriented perpendicular to the thrust axis, while the other uses a turbopump with the shaft axis oriented in line with the thrust axis.

(2) A master layout was established for a propulsion system utilizing 20 engine modules in a cluster, with all modules exhausting into a single large forced-deflection nozzle.

(3) Detail designs for all the engine components tested in this program were prepared.

(4) The primary injector and combustion chamber for production of the turbine drive gas were demonstrated.

(5) Performance and durability of the cooled thrust chamber and secondary injector combination were demonstrated.

DD Form 1473

UNCLASSIFIED ABSTRACT (Cont.)

(6) The feasibility of lubricating turbopump bearings with the storable propellants used in the engine was demonstrated.

(7) Pump wear ring designs that permit high pump efficiency operation without need for high tolerances and with no risk of explosion hazard from pump rub were demonstrated.

(8) The weight and practicality of two types of multipurpose housings for the turbopump and primary combustion chamber assembly were demonstrated.

(9) Propellant flow control components and shutoff valves for the engine were demonstrated.

(10) A layout design of the engine evolved from the testing effort was prepared.

(11) Several supporting studies were completed that provide additional design criteria in such areas as nozzle aerodynamics, low-frequency stability, fluid flow characteristics of propellant and turbine drive-gas passages, and design changes required for conversion to advanced storable propellants.

DD Form 1473